

INVEST. BUILD. GROW.

# MANITOBA



## GEOSCIENTIFIC REPORT GR2021-2

GEOLOGY OF THE  
WUSKWATIM–GRANVILLE  
LAKES CORRIDOR,  
KISSEYNEW DOMAIN,  
MANITOBA (PARTS OF NTS  
63O, P, 64A–C)

Manitoba Geological Survey





---

**Geoscientific Report GR2021-2**

**Geology of the Wuskwatim–Granville lakes corridor,  
Kisseynew domain, Manitoba  
(parts of NTS 63O, P, 64A–C)**

**by L.A. Murphy and H.V. Zwanzig  
Manitoba Geological Survey  
Winnipeg, 2021**

---

©Queen's Printer for Manitoba, 2021

Every possible effort is made to ensure the accuracy of the information contained in this report, but Manitoba Agriculture and Resource Development does not assume any liability for errors that may occur. Source references are included in the report and users should verify critical information.

Any third party digital data and software accompanying this publication are supplied on the understanding that they are for the sole use of the licensee, and will not be redistributed in any form, in whole or in part. Any references to proprietary software in the documentation and/or any use of proprietary data formats in this release do not constitute endorsement by Manitoba Agriculture and Resource Development of any manufacturer's product.

When using information from this publication in other publications or presentations, due acknowledgment should be given to the Manitoba Geological Survey. The following reference format is recommended:

Murphy, L.A. and Zwanzig, H.V. 2021: Geology of the Wuskwatim–Granville lakes corridor, Kiseynew domain, Manitoba (parts of NTS 63O, P, 64A–C); Manitoba Agriculture and Resource Development, Manitoba Geological Survey, Geoscientific Report GR2021-2, 94 p.

**NTS grid:** 63O, P, 64A, B, C

**External author contacts:**

Linda Murphy, P.Geo.  
E-mail: [lnrmurphy@gmail.com](mailto:lnrmurphy@gmail.com)

Herman Zwanzig  
E-mail: [hvzwanzig@shaw.ca](mailto:hvzwanzig@shaw.ca)

**Published by:**

Manitoba Agriculture and Resource Development  
Manitoba Geological Survey  
360–1395 Ellice Avenue  
Winnipeg, Manitoba  
R3G 3P2 Canada

Telephone: 1-800-223-5215 (General Enquiry)  
204-945-6569 (Publication Sales)

Fax: 204-945-8427

E-mail: [minesinfo@gov.mb.ca](mailto:minesinfo@gov.mb.ca)

Website: [manitoba.ca/minerals](http://manitoba.ca/minerals)

**ISBN:** 978-0-7711-1627-8

This publication is available to download free of charge at [manitoba.ca/minerals](http://manitoba.ca/minerals).

**Cover illustration:** F<sub>3</sub> fold in the Granville complex at Notigi Lake.

## Disclaimer

The content of this report is solely of the authors' opinion and interpretation. This publication did not undergo external, technical editing.

## Avis de non responsabilité

Le contenu du présent rapport reflète uniquement l'opinion et l'interprétation des auteurs. Cette publication n'a pas fait l'objet d'une révision technique externe.

---

## Abstract

This report covers parts of two geological domains in the Paleoproterozoic Trans-Hudson orogen: the northeastern part of the Kisseynew domain (KD) and the south margin of the Leaf Rapids domain (LRD). These domains are located northwest of Thompson in north-central Manitoba, 700 km north-northeast of Winnipeg. They abut the Thompson nickel belt (TNB) and extend from Thompson 300 km northwest into Saskatchewan, along the LRD, which forms the northern boundary of the KD. This broad aerial and reconnaissance fieldwork carried out by the Manitoba Geological Survey (MGS) from 2006 to 2009 produced five geoscientific maps (MAP2019-1 to MAP2019-5) and an aeromagnetic compilation map (MAP2019-6). The mapping by the MGS and J.A. Percival and J.B. Whalen of the Geological Survey of Canada (GSC), along with a compilation of previous data, was supported by high-resolution aeromagnetic surveys and geochronology by the GSC. The mapping offered the ideal opportunity to clarify and correlate the stratigraphy along the project corridor. A new structural analysis using stereoplots of fabrics and minor structures guides down-plunge projections of map units for cross-sections and three-dimensional analysis. This provides a regional correlation of the polyphase deformation. The implied crustal architectural and tectonic interpretations may serve as a guide to mineral exploration. The new work and interpretation of previous work in the western part of the Trans-Hudson orogen support a tectonic model with further economic implications.

The parts of the KD described in this report include the Kisseynew north flank and the Northeast Kisseynew subdomain. The bedrock of the north flank of the KD comprises abundant Paleoproterozoic, ca. 1.85–1.83 Ga metasedimentary rocks (the Burntwood group metaturbidite and the Sickle group subaerial to shallow-water metasedimentation). New interpretations of the sedimentary stratigraphic units, a volcano-sedimentary complex (Granville complex) inferred to be older and a suite of sills with unique geochemistry (Blacktrout diorite) in the Sickle group are traced along the north flank. The Sickle group lies locally on top of the Burntwood group with conformity or a gradation and, based on detrital zircon ages, is considered coeval with upper parts of the Burntwood group elsewhere. Regional sedimentary-facies changes, geochemistry, isotopic work and geochronology indicate that sediments were derived mainly from the volcanic-arc domain to the northwest, and prograded into the KD. The Granville complex

features a major Paleoproterozoic suture zone (Levesque Bay–Granville Lake suture zone) with remnants of ocean floor and younger, but pre-Burntwood, metasedimentary rocks. This is soled by a fault zone, a proposed megathrust (Burntwood megathrust) that generally lies between the Granville complex and the Burntwood group. The zone is exposed for 300 km across Manitoba. Its interpretation as a suture is confirmed by the presence of a northerly dipping crustal break seen in a seismic reflection profile. Due to nappe tectonics during continental collision, the units in the suture zone extend south up to 60 km into the KD.

In contrast to the north flank, the Northeast Kisseynew subdomain consists of mainly metasedimentary rocks of the Burntwood group and younger granitoid rocks. In addition, there are small slices of Archean basement gneiss exposed, a thin, highly metamorphosed cover succession (Wuskwatim Lake sequence) as well as isotopically evolved pre-Burntwood intrusive rocks (Footprint Lake plutonic suite, FLPS). The Wuskwatim Lake sequence resembles the Ospwagan group in the TNB, the Paleoproterozoic western continental-margin succession of the Superior craton. Similarities include stratigraphy, geochemistry, Sm-Nd isotopic ratios and abundant Archean detrital zircons with a population peak at 2.7 Ga. These shared features suggest a peri-Superior origin of the sequence and its basement.

The south margin of the LRD borders the north flank of the KD and occurs as structural inliers in the KD. The LRD is a long-active (1.91–1.83 Ga) arc massif including the Lynn Lake and Rusty Lake metavolcanic belts and volcanic-arc plutons. Uranium-lead zircon ages indicate mainly pre-Sickle plutons, rarely “early-arc” but mostly juvenile “successor-arc” plutons within the age-range of 1876–1830 Ma in the LRD and also surrounding the KD in the south and west.

Detailed structural studies at Granville, Notigi and Wuskwatim lakes have elucidated the origin of overlapping and interleaving of units. This is consistent with early ( $D_1$ ) south-east-directed (present coordinates) folding and thrusting before complete lithification of the ca. 1.85 to 1.835 Ga Burntwood group. Soft-sediment deformation and dewatering features in thrust faults were apparently initiated in the forearc and trench-slope during subduction that formed the late successor arc at this age. These structures are most evident at high crustal levels but are deduced to exist also at mid-crustal level at high metamorphic grade from Notigi Lake eastward

to the TNB. During terminal collision, by ca. 1.84 Ga, a reversal in vergence occurred. The early recumbent structures ( $F_1$ ) were overturned and inverted within a series of north-verging backfolds ( $F_{2a}$  nappes). A second vergence reversal, evident at Notigi and Wuskwatim lakes, occurred during peak metamorphism, when migmatization and the transfer of crustal melts formed syntectonic intrusions between ca. 1810 and 1807 Ma. Horizontal, melt-assisted transport created another set of folds (southwest-verging  $F_{2b}$  nappes). In addition to high-level interleaving, this change of dominant vergence suggests southerly tectonic wedging of the leading edge of the LRD at deeper level during collision. Final major deformation ( $D_3$ ) produced consistently northeast-trending structures by intracontinental transpression during the 1.78–1.77 Ga peak metamorphism in the TNB. The  $F_3$  crossfolds in the KD, shared with the TNB, were critical in providing structural relief in which both deep structural levels of granulite, and high-level paragneiss are exposed. Structural culminations that contain the Archean basement inliers, their early Paleoproterozoic paragneiss cover and the early (FLPS) intrusions indicate the  $F_3$  antiforms cross nearly recumbent  $F_{2b}$  antiforms. Outliers of the arc plutons from the LRD occur in the north flank of the KD in similar  $F_3$ - $F_{2b}$  culminations. Such culminations in the KD also show the present southern limit of structurally buried nappes containing the Granville complex and Sickle group. In addition, structural basins with inverted KD tectonostratigraphy outline the minimum northern extent of the  $F_{2a}$  nappes in the LRD. Thus the history and crustal architecture of a Paleoproterozoic collisional orogen is provided in the correlation of structures from upper to middle crust. An interpretation of the tectonic history involves magmatism, sedimentation and polyphase deforma-

tion in and around the KD during multiple collisions of Archean cratons with the volcanic arc–back-arc and basinal terranes. This is consistent with oroclinal bending and crustal stacking and interleaving that built up the core of Laurentia in Manitoba and Saskatchewan. Late heating of the upper crust and the geochemistry of plutons suggest that lithospheric/slab collapse with rising asthenosphere lead to the final closure of the KD and deep collision of the surrounding Archean cratons and Paleoproterozoic arc massifs.

Mineral showings along the Wuskwatim–Granville lakes transect have been considered, to date, as uneconomic but may be undervalued. A gold showing in sulphide-facies iron formation at the contact between Granville complex-type basalt/gabbro and the possible base of the Burntwood group, lies along a series of sulphide showings in shears that may represent a gold metallotect. Altered Granville complex basalt and ultramafic rocks feature elevated As, an element associated with Au. A glacial train of As anomalies and trace Au extends across the KD. A trace Cu showing on Notigi Lake may be related to stratiform copper mineralization that has been documented, also in the Sickle group, at Kadeniuk Lake, southwest of Granville Lake.

The stratigraphic resemblance of the Wuskwatim Lake sequence to the lower half of the Oswagan group in the TNB suggest a Ni potential in the KD. Although no “Thompson-type” ultramafic rocks are exposed in the KD, such units are generally covered in the TNB but found through exploration drilling. A wide distribution of the FLPS indicates extensive Archean rocks at depth and, with the probability of Archean subcontinental mantle, could have a potential for diamond-bearing kimberlite pipes.

## Résumé

Le présent rapport traite de certaines parties de deux domaines géologiques situés dans l'orogène trans-hudsonien du Paléoprotérozoïque : la partie nord-est du domaine de Kisseynew (DK) et la limite sud du domaine de Leaf Rapids (DLR). Ces domaines sont situés au nord-ouest de Thompson, dans le centre-nord du Manitoba, à 700 km au nord-nord-est de Winnipeg. Ils sont attenants à la ceinture nickélicifère de Thompson (CNT) et s'étendent de Thompson jusqu'à 300 km en direction du nord-ouest en Saskatchewan, le long du DLR, qui constitue la limite nord du DK. Ces travaux de reconnaissance et de prospection aérienne de vaste portée, exécutés sur le terrain par la Direction des services géologiques du Manitoba (la Direction) de 2006 à 2009, ont permis la production de cinq cartes géoscientifiques (MAP2019-1 à MAP2019-5) et d'une carte de compilation aéromagnétique (MAP2019-6). Le travail cartographique effectué par la Direction et par J.A. Percival et J.B. Whalen, de la Commission géologique du Canada (CGC), accompagné d'une compilation de données antérieures, a été étayé par des activités géochronologiques et des levés aéromagnétiques de haute résolution réalisés par la CGC. Le travail cartographique a été l'occasion idéale de clarifier la stratigraphie et d'en effectuer le rattachement le long du corridor du projet. Une nouvelle analyse de structure reposant sur des minutes de restitution et sur la stéréorestitution de la fabrique et des structures mineures oriente les projections en profondeur des unités cartographiques aux fins des coupes transversales et des analyses tridimensionnelles. On obtient ainsi une corrélation régionale de la déformation polyphasée. Les interprétations implicites tectoniques et architecturales de la croûte peuvent servir de guide pour l'exploration minière. Le travail récent et l'interprétation de travaux antérieurs dans la partie ouest de l'orogène trans-hudsonien soutiennent un modèle tectonique porteur de débouchés économiques supplémentaires.

Les parties du DK décrites dans le présent rapport comprennent le flanc nord de Kisseynew et le sous-domaine nord-est de Kisseynew. Le substratum du flanc nord du DK comprend d'abondantes roches métasédimentaires de la partie du Paléoprotérozoïque allant de 1,85 à 1,83 Ga environ (les métaturbidites du groupe de Burntwood et le métagrès allant de subaérien à formé en eau peu profonde du groupe de Sickle). Selon de nouvelles interprétations des unités stratigraphiques sédimentaires, un complexe volcano-sédimentaire (le complexe de Granville) présumé plus ancien et une série de filons-couches aux caractéristiques géochimiques uniques (diorite de Black Trout) dans le groupe de Sickle sont repérés le long du flanc nord. Le groupe de Sickle s'étend localement au-dessus du groupe de Burntwood, avec un contact concordant ou progressif, et, selon les datations sur zircon détritique, il est considéré comme étant de même âge que les parties supérieures du groupe de Burntwood à d'autres endroits. Les modifications de faciès sédimentaires à l'échelon régional, la géochimie, des recherches isotopiques et la géochronolo-

gie indiquent que les sédiments proviennent principalement du domaine de l'arc volcanique situé plus au nord-ouest et ont subi une progradation dans le DK. Le complexe de Granville comprend une importante zone de suture du Paléoprotérozoïque (zone de suture baie Levesque-lac Granville) avec des restes de plancher océanique et des roches métasédimentaires plus récentes, mais antérieures à Burntwood. La base est constituée d'une zone de failles, un mégacharrriage proposé (le mégacharrriage de Burntwood) qui s'étend globalement entre le complexe de Granville et le groupe de Burntwood. La zone est exposée sur 300 km dans tout le Manitoba. Son interprétation comme zone de suture est confirmée par la présence d'une rupture de la croûte plongeant vers le nord observée dans un profil de réflexion sismique. Du fait de la tectonique de nappes de charriage pendant la collision des continents, les unités comprises dans la zone de suture s'étendent vers le sud dans le DK sur une distance atteignant 60 km.

À la différence du flanc nord, le sous-domaine nord-est de Kisseynew se compose principalement de roches métasédimentaires du groupe de Burntwood et de roches granitoïdes plus récentes. De plus, on observe de fines écailles exposées de substratum gneissique de l'Archéen, une fine succession de couverture très métamorphisée (la séquence du lac Wuskwatim) ainsi que des roches intrusives antérieures à Burntwood évoluées isotopiquement (le cortège plutonique du lac Footprint). La séquence du lac Wuskwatim ressemble au groupe d'Ospwagan dans la CNT, qui est la succession de la marge continentale occidentale du Paléoprotérozoïque du craton du Supérieur. Les similarités sont diverses : stratigraphie, géochimie, rapports isotopiques Sm-Nd et abondants zircons détritiques de l'Archéen avec un pic à 2,7 Ga. Ces caractéristiques communes semblent indiquer que la séquence et son socle proviennent de la périphérie du Supérieur.

La limite sud du DLR longe le flanc nord du DK et se présente sous la forme d'enclaves structurales dans le DK. Le DLR est un massif d'arc qui a été longtemps actif (de 1,91 à 1,83 Ga) et qui comprend les plutons d'arc volcanique et les ceintures métavolcaniques des lacs Lynn et Rusty. La datation des zircons par l'uranium-plomb indique principalement des plutons antérieurs au groupe de Sickle – ils sont dans de rares cas de « l'arc précoce » et pour la plupart des plutons « d'arcs successeurs » juvéniles dans la tranche d'âge de 1876 à 1830 Ma, tant dans le DLR qu'autour du DK au sud et à l'ouest.

Des études structurales détaillées réalisées aux lacs Granville, Notigi et Wuskwatim ont permis d'éclaircir l'origine du chevauchement et de l'entrelacement des unités. Le phénomène correspond au chevauchement et au plissement précoces ( $D_1$ ) en direction du sud-est (selon les coordonnées actuelles) avant la lithification complète du groupe de Burntwood datant de 1,85 à 1,835 Ga environ. Les caractéristiques liées à l'assèchement et la déformation de sédiments mous dans les failles de chevauchement sont apparemment apparues dans l'avant-arc et la pente de la fosse au cours de la subduction qui a formé l'arc successeur tardif à cet âge. Ces

structures sont les plus visibles aux niveaux élevés de la croûte, mais on a déduit qu'elles existaient également au niveau intermédiaire de la croûte au niveau du métamorphisme intense allant du lac Notigi vers l'est jusqu'à la CNT. Pendant la collision terminale, aux environs de 1,84 Ga, une inversion de la vergence s'est produite. Les structures couchées précoces ( $F_1$ ) ont été retournées et renversées dans une série de plis en retour (nappes  $F_{2a}$ ) orientés vers le nord. Une deuxième inversion de la vergence, visible aux lacs Notigi et Wuskwatim, a eu lieu pendant le pic du métamorphisme, lorsque la migmatisation et le transfert des fusions crustales ont formé des intrusions syntectoniques, entre 1810 et 1807 Ma environ. Le déplacement horizontal facilité par la fusion a créé une autre série de plis (nappes  $F_{2b}$  avec vergence sud-ouest). Outre l'entrelacement au niveau supérieur, ce changement de la vergence dominante semble indiquer un amincissement tectonique vers le sud du front du DLR plus en profondeur pendant la collision. La déformation majeure finale ( $D_3$ ) a produit de manière répétée des structures orientées vers le nord-est par transpression intracontinentale pendant le pic du métamorphisme, de 1,78 à 1,77 Ga, dans la CNT. Le pli transverse  $F_3$  dans le DK, également présent dans la CNT, a été essentiel dans la formation d'un relief structural où sont exposés des niveaux structuraux profonds de granulite et du paragneiss de niveau supérieur. Les culminations structurales contenant les enclaves du substratum de l'Archéen, leur couverture de paragneiss du Paléoproterozoïque et les intrusions précoces (cortège plutonique du lac Footprint) indiquent que les antiformes  $F_3$  traversent les antiformes  $F_{2b}$  presque couchées. Des enclaves de plutons de l'arc du DLR sont relevées dans le flanc nord du DK dans des culminations  $F_3$ - $F_{2b}$  similaires. Ces culminations dans le DK montrent également la limite méridionale actuelle des nappes enfouies de manière structurale qui renferment le complexe de Granville et le groupe de Sickle. De plus, des cuvettes structurales ayant une tectonostratigraphie du DK inversée délimitent la portée septentrionale minimale des nappes  $F_{2a}$  dans le DLR. De fait, l'évolution et l'architecture crustale d'un orogène de collision du Paléoproterozoïque sont révélées par la corrélation des structures de la croûte supérieure à la croûte intermédiaire. Une interprétation de l'évolution tectonique s'appuie sur le magmatisme, la sédimentation et la déforma-

tion polyphasée dans le DK et aux alentours pendant les multiples collisions des cratons de l'Archéen avec les terranes de bassin et les arcs-arrière volcaniques. Cela est cohérent avec la flexion de l'oroclinal ainsi qu'avec l'entrelacement et l'empilement crustal qui ont constitué le noyau de la Laurentie au Manitoba et en Saskatchewan. Le réchauffement tardif de la croûte supérieure et les caractéristiques géochimiques des plutons semblent indiquer qu'un effondrement de la plaquette lithosphérique accompagné d'un soulèvement de l'asthénosphère a mené à la fermeture définitive du DK et à une collision profonde des cratons de l'Archéen et des massifs de l'arc du Paléoproterozoïque environnants.

Jusqu'à présent, on a considéré que les indices minéraux relevés le long du transect des lacs Wuskwatim et Granville étaient non rentables, mais ils pourraient avoir été sous-évalués. Un indice aurifère dans la formation de fer à phase sulfurée repérée au point de contact entre le basalte-gabbro de type complexe de Granville et le socle possible du groupe de Burntwood s'étend le long d'une série d'indices sulfurés dans des cisaillements pouvant représenter un métallotecte aurifère. Les roches basaltiques et ultramafiques altérées du complexe de Granville ont une teneur élevée en arsenic (As), un élément associé à l'or. Une traînée glaciaire d'anomalies en As et d'or-trace s'étend dans tout le DK. Un indice de cuivre-trace au lac Notigi pourrait être lié à une minéralisation en cuivre stratiforme qui a été documentée, également dans le groupe de Sickle, au lac Kadeniuk, au sud-ouest du lac Granville.

La ressemblance stratigraphique de la séquence du lac Wuskwatim avec la moitié inférieure du groupe d'Ospwagan dans la CNT semble indiquer un potentiel en Ni dans le DK. Même si aucune roche ultramafique de « type Thompson » n'est exposée dans le DK, il faut noter que de telles unités sont généralement couvertes dans la CNT, mais peuvent être repérées par forage d'exploration. Une distribution vaste du cortège plutonique du lac Footprint indique une présence forte de roches archéennes en profondeur, ce qui, compte tenu de la probabilité d'un manteau sous-continentale de l'Archéen, pourrait receler du potentiel de cheminées kimberlitiques diamantifères.

## TABLE OF CONTENTS

	Page
Disclaimer / Avis de non responsabilité .....	iii
Abstract .....	iii
Résumé.....	v
1. Introduction.....	1
1.1 Previous work .....	3
1.2 Method and scope .....	4
2. Tectonic setting.....	4
2.1 Bounding lithotectonic domains .....	5
2.2 Kisseynew north flank .....	6
2.3 Northeast Kisseynew subdomain.....	6
3. Tectonostratigraphy.....	7
3.1 Archean (Ag, Ai) .....	8
3.2 Paleoproterozoic .....	10
3.2.1 Wuskwatim Lake sequence (W, Wq, Wp, Wi) .....	10
3.2.2 Granville complex (G) .....	11
3.2.2.1 Tod Lake basalt, layered amphibolite and gabbro (Gt, Gta, Gtb, Gg) .....	11
3.2.2.2 Hatchet Lake-type amphibolite and gabbro–melagabbro (Ghb, Ghg) .....	14
3.2.2.3 Mafic–ultramafic rocks (Pickerel Narrows amphibolite, OIB: Gu, Gua, Gub, Guc).....	15
3.2.2.4 Sedimentary rocks (Gs, Gsa, Gsb, Gsc, Gsd, Gse, Gc, Gi) .....	15
3.2.2.5 Iron formation, sulphidic paragneiss (Gi, Gs/Gc) .....	18
3.2.3 Intrusions of known pre-Burntwood, pre-Sickle ages .....	18
3.2.3.1 Enderbite, minor quartz diorite–gabbro (en).....	19
3.2.3.2 Porphyritic quartz monzonite, syenite–granite (qm) .....	19
3.2.3.3 Biotite tonalite, minor diorite–gabbro (tn) .....	19
3.2.3.4 Biotite granite–granodiorite (Rat granite: gn).....	21
3.2.3.5 Notigi monzogranite (mg) and granodiorite (Lgg).....	21
3.2.4 Burntwood group (B).....	21
3.2.4.1 Greywacke–mudstone (B, Ba) .....	22
3.2.4.2 Upper greywacke and conglomerate (Bca, Bcb, Bc).....	22
3.2.4.3 Greywacke–mudstone gneiss and migmatite (Bg, Bm, Bma, Bd, Bda) .....	22
3.2.4.4 Iron formation (Bi) .....	23
3.2.5 Intrusive rocks (unknown age, felsic to mafic) .....	23
3.2.5.1 Biotite granite to granodiorite (gx) .....	23
3.2.5.2 Tonalite (tx) .....	25
3.2.5.3 Gabbro, amphibolite (gb).....	25
3.2.6 Sickle group (K).....	25
3.2.6.1 Arkose (Ks), crossbedded arkose (Ksa) quartzite (Ksc): lower succession, eastern sub-basin .....	26
3.2.6.2 Light grey to reddish metasandstone (Kba): lower succession, eastern sub-basin .....	27
3.2.6.3 Greenish-grey calcsilicate metasandstone (Khb): middle unit, eastern sub-basin.....	27
3.2.6.4 Muscovite-rich meta-arkose±sillimanite (Ks): upper unit, eastern sub-basin.....	27
3.2.6.5 Amphibole-bearing arenite and conglomerate (Kha, Khc): lower units, southern sub-basin .....	27
3.2.6.6 Locally crossbedded meta-arkose (Ksa), conglomerate (Ksd): upper units, southern sub-basin .....	27
3.2.6.7 Biotite gneiss (meta-arenite), Kb .....	27
3.2.6.8 Hornblende-biotite meta-arenite/gneiss (Kh).....	29
3.2.6.9 Sillimanite-bearing arkose-derived gneiss (Ksb, Kse) .....	29

3.2.7 Late intrusive rocks.....	29
3.2.7.1 Gabbro–pyroxenite (1.79 Ga, Lmu).....	30
3.2.7.2 Metagabbro to tonalite, mafic to intermediate porphyry (Lmi, Lgb, Ldt) .....	30
3.2.7.3 Diorite, quartz diorite (Lqd) .....	31
3.2.7.4 Hornblende and biotite granite–granodiorite (Lhg).....	31
3.2.7.5 Leucogranite–pegmatite, granite–tonalite (Llg, Lgg) .....	31
3.2.7.6 Pegmatite, aplite, granite (Lpg).....	32
4. Whole-rock and Sm-Nd isotope geochemistry.....	32
4.1 Sedimentary rocks (W, B, K, Gs), a comparison.....	33
4.2 Granville complex volcanogenic rocks (G, Gh, Gt, Gu).....	39
4.2.1 Hatchet-Lake–type geochemical units (Gh, Ghg, gb).....	39
4.2.2 Tod-Lake–type mafic rocks (Gt, Gta, Gtb, Gg).....	39
4.2.3 Pickerel Narrows amphibolite (Gu, Gua, Gub, Guc).....	41
4.2.4 Amphibolite, intermediate and felsic gneiss .....	41
4.2.5 Origin of the Granville complex mafic–ultramafic rocks.....	43
4.3 Granitoid intrusive rocks.....	43
4.3.1 Footprint Lake plutonic suite (unit qm) .....	45
4.3.2 Volcanic-arc plutons (LRD-type, tn, gn) .....	45
4.3.3 Granitoid rocks of uncertain age and origin (parts of mg, Lgg, gx) .....	45
4.4 Late intrusive rock.....	47
4.4.1 Blacktrout diorite (Lqd) .....	47
4.4.2 Mafic to intermediate intrusions (Lmi, Lgb, Ltd) .....	47
4.4.3 Synmetamorphic granitoid intrusions or leucosome (Lgg, Llg, Lpg).....	47
4.5 Probable origins of the granitoid intrusive rocks .....	49
5. U-Pb zircon-geochronology compilation .....	50
5.1 Results and implications .....	50
5.1.1 Basement and cover .....	50
5.1.2 Footprint Lake plutonic suite.....	53
5.1.3 Early-arc–successor-arc plutons .....	53
5.1.4 Granville complex.....	55
5.1.5 Detrital zircons, Burntwood and Sickle groups.....	56
5.1.6 Metamorphic zircons.....	57
5.1.7 Late mafic–ultramafic rocks.....	57
6. Structural geology .....	57
6.1 High-level structures: Granville Lake.....	59
6.1.1 Synsedimentary early structures and transposition layering ( $S_0$ ).....	59
6.1.2 Early post-Burntwood structures ( $D_1$ and early $D_2$ ) .....	61
6.1.3 Superposed structures .....	63
6.2 Deeper level: Notigi–Wapisu lakes.....	64
6.2.1 Large recumbent/inclined folds and structural interleaving ( $D_2$ ).....	66
6.2.2 Deepest level: Wuskwatim Lake area .....	71
7. Regional and THO-wide correlation and tectonic model.....	75
7.1 Early arc–back-arc magmatism .....	76
7.2 Successor-arc magmatism.....	77
7.3 Syncollisional sedimentation: Partridge Breast, Granville complex (southern belt), Burntwood, Missi, Grass River, Sickle groups .....	80
7.4 Syncollisional periods of deformation.....	81
8. Economic considerations.....	82

8.1 Historical mineral exploration .....	83
8.2 Kiseynew domain north flank.....	83
8.2.1 Granville complex: gold .....	83
8.3 Northeast Kiseynew subdomain.....	83
8.3.1 Wuskwatim Lake sequence: nickel .....	83
8.3.2 Potential mineral occurrences: IOCG, REE.....	84
8.3.3 Archean basement: possible diamond potential.....	85
8.4 Regional economic implications.....	85
8.4.1 Leaf Rapids domain .....	85
8.4.2 Flin Flon–Lynn Lake connection.....	85
Acknowledgments.....	87
References.....	87

## TABLES

Table 1: Compilation legend of the Wuskwatim–Granville lakes corridor .....	3
Table 2: Unit averages of whole-rock, trace-element and Sm-Nd isotope geochemical results .....	34
Table 3: Geochronology compilation of the Northeast Kiseynew subdomain and Kiseynew north flank.....	46
Table 4: Local and regional structural history.....	58
Table 5: Tectonic history of the western Trans-Hudson orogen with Canada-wide correlation .....	75

## FIGURES

Figure 1: Geology of the Kiseynew domain with subdomains and map locations.....	2
Figure 2: Typical local tectonostratigraphic sections .....	8
Figure 3: Field photographs of Archean gneiss and Wuskwatim Lake sequence .....	9
Figure 4: Field photographs of the Granville complex mafic–ultramafic rocks .....	12
Figure 5: Tectonostratigraphic illustration of structure sections at Granville Lake, and Sickle group sub-basins on the Kiseynew north flank .....	13
Figure 6: Field photographs of mafic–ultramafic and sedimentary rocks, Granville complex at southern Granville Lake .....	16
Figure 7: Field photographs of Granville complex sedimentary rocks.....	17
Figure 8: Field photographs of clean outcrops .....	20
Figure 9: Field photographs of Burntwood and Sickle group rocks .....	24
Figure 10: Sickle group, photographs of main units .....	28
Figure 11: Multi-element plots of various paragneiss units are normalized to Paleoproterozoic pelite .....	37
Figure 12: Neodymium-model ages and $\epsilon_{Nd}$ of the Paleoproterozoic sediment-derived gneisses and igneous rocks in the Wuskwatim–Granville lakes corridor .....	38
Figure 13: N-MORB–normalized multi-element plots of Granville complex metavolcanic and related intrusive rocks with N-MORB, BABB and E-MORB patterns .....	40
Figure 14: N-MORB–normalized multi-element plots of OIB-like metavolcanic rocks of the Granville complex, and arc-like or crustally contaminated rocks .....	42
Figure 15: Major, trace- and multi-element diagrams of northern to eastern Kiseynew intrusive suites .....	44
Figure 16: Primitive-mantle–normalized multi-element diagrams of pre- to postcollisional intrusive rocks.....	48
Figure 17: Location of selected U-Pb zircon age sampling sites and selected mineral showings .....	51
Figure 18: Comparison of pre-Burntwood basement, cover and intrusive ages in the KD with Ospwagan group (from TNB) and Southern Indian domain detrital-zircon ages .....	52
Figure 19: Detrital-zircon ages (Southern Indian domain) and crystallization ages of granitoid rocks.....	54
Figure 20: Crystallization and metamorphic ages of granitic LRD apophyses in the KD .....	55

Figure 21: Comparative probability plots of detrital zircons .....	56
Figure 22: Granville Lake area north-south upper crustal sections and fold stages .....	60
Figure 23: Outcrop photographs of early structures .....	61
Figure 24: Minor structures at Notigi Lake .....	65
Figure 25: Structures at Notigi Lake with interpretations .....	67
Figure 26: Structural-map interpretation at Notigi Lake .....	68
Figure 27: Three-dimensional geometry of the main Notigi culmination .....	70
Figure 28: Regionally modelled structure sections and deformation stages, Misinagu–Notigi lakes.....	72
Figure 29: Interpretive structure map and sections, Wuskwatim Lake .....	73
Figure 30: U-Pb zircon-age frequency plots of the Wuskwatim–Granville lakes corridor and surrounding areas of the THO .....	76
Figure 31: Scale-free tectonic model of W-THO internides and surrounding Archean cratons.....	78
Figure 32: Possible correlation between the Wuskwatim Lake sequence and the Ospwagan group.....	84
Figure 33: Mineral deposits in volcanic and sedimentary belts surrounding the Kisseynew domain in Manitoba.....	86

**DIGITAL DATA**

Data Repository Item DRI2021014: Lithogeochemical database, Sm-Nd isotopic data and U-Pb geochronological data for the Wuskwatim–Granville–Laurie lakes corridor, Manitoba (parts of NTS 63O, P, 64A–C)..... GR2021-2.zip

## 1. Introduction

In 2006 the Manitoba Geological Survey (MGS) began a remapping program in the Kiseynew domain (KD) along its eastern and northern margins: along the Thompson nickel belt (TNB) from Tullibee Lake north to Wuskwatim Lake and west along its north flank to Granville Lake. The corridor is nearly 300 km long and up to 40 km wide. All map areas pertaining to this report are marked by boxes in Figure 1. The program was initiated in part by the Geological Survey of Canada's earlier reconnaissance at Granville Lake (Corrigan and Rayner, 2002) and by the discovery of supracrustal rocks at Opegano Lake (Wuskwatim Lake sequence) that contain only Archean detrital zircons (Percival et al., 2005) in what was previously considered to be an entirely juvenile Proterozoic tectonic domain. The work combined outcrop examination, petrology, geochemistry, Sm-Nd isotope work and geochronology of the Paleoproterozoic and Archean high-grade metasedimentary and meta-igneous rocks. The remapping and reconnaissance were carried out in continuing partnership with the Geological Survey of Canada (GSC) as part of the Targeted Geoscience Initiative, Phase 3 (TGI-3) from 2006 to 2009. This national collaborative geoscience program led by the GSC included work in areas around Tullibee, Opegano, Wuskwatim, Threepoint and Wapisu lakes in the Northeast Kiseynew subdomain, as well as at Kawaweyak, Osik, Notigi and Granville lakes along the Kiseynew north flank (Murphy and Zwanzig, 2019a–d; Zwanzig, 2019; Zwanzig et al., 2019).

Aeromagnetic surveys (Coyle and Kiss, 2006; Kiss and Coyle, 2008) were critical in locating and tracing units over long distances. Rock exposure ranges from sparse to variable in the bush to entirely lacking under widespread Quaternary cover and areas of muskeg; therefore, much of the field mapping was done along the shores of larger lakes, where bedrock exposure is best. Due to the general absence of magnetite, the entire KD's aeromagnetic signature provides a strong negative magnetic backdrop, enhancing more magnetic units and allowing them to be traced under the cover. Uranium-lead zircon geochronology (e.g., Percival et al., 2005) has also been invaluable in tracing units.

Maps of four main areas are upgraded: Granville, Notigi, Wuskwatim and Kawaweyak lakes (Murphy and Zwanzig, 2019a–d; Zwanzig, 2019; Zwanzig et al., 2019). Limited work at occurred at Tullibee Lake along with reconnaissance by the GSC at Opegano, Osik and Atik lakes (Figure 1). All maps use a unified legend shown in Table 1. Areas at Notigi, Wapisu, Osik and Kawaweyak lakes, where most of the mapping took place, are located within 100 km west of Thompson, accessible from Provincial Highway 391. The shores and areas around these lakes were remapped during the summers of 2007–2009, at 1:50 000 to 1:10 000 scale, in collaboration with the GSC (Percival et al., 2006; Murphy and Zwanzig, 2007a, b, 2008, 2009; Percival et al., 2007; Murphy, 2008; Whalen et al., 2008; Zwanzig, 2008). The Granville Lake area (Zwanzig, 2019) features well-preserved Granville complex (G) and Burntwood group

(B) with primary and early deformational structures that provide a tectonostratigraphic model for the northern side of the Wuskwatim–Granville lakes corridor. The unconformably overlying Sickle group (K) is divided into five widely traceable stratigraphic units.

The new ages and remapping confirm the presence of a suture zone between two crustal blocks. This “Granville Lake structural zone” (Zwanzig, 1990, 2008; White et al., 2000), herein Levesque Bay–Granville Lake suture zone, straddles the margin of the Leaf Rapids domain (LRD) to the north, the Granville complex in the centre and the margin of the KD to the south. The LRD includes the Lynn Lake and Rusty Lake volcanoplutonic (greenstone) belts as well as dominantly intrusive areas. The Granville complex (Granville Lake assemblage of Zwanzig et al., 1999a) comprises a laterally extensive volcanosedimentary succession that is part of the Amisk tectonic collage, previously termed the Amisk Group (Zwanzig et al., 1999a). The geology in the KD includes metasedimentary rocks (Burntwood and Sickle groups) and late granitic intrusive rocks. The Burntwood group is divided into metagreywacke (a marine turbidite) and its derived migmatite. The Sickle group is made up of nonmarine arkosic to lithic meta-arenite and its derived paragneiss. The Sickle group unconformably overlies parts of the LRD and the Granville complex in much of the Kiseynew north flank, which is bounded by the southern extent of the Sickle group. On the south shore of Granville Lake, the Sickle group lies directly on the Burntwood group. More generally, along the north flank, the highly deformed Granville complex separates the two sedimentary groups. The southern boundary of the Granville complex forms the province-wide Levesque Bay–Granville Lake suture zone (Green et al., 1985; White et al., 2000). East of Granville Lake, where deeper structures are exposed, much of the Granville complex forms a dominantly mafic tectonite. The presence of alteration in the Granville complex with an As anomaly (Section 8.3.1) suggests a potential for further gold exploration as supported by the presence of a gold showing (Barry, 1965) in line with extensive iron-sulphide showings along a stratigraphic/tectonic contact. Arsenic and Au anomalies in till traced across the KD (Kaszycki et al., 1988).

The description of the geology of the entire north and east margins of the KD is updated to follow the unified legend with its new stratigraphic, structural, tectonic and economic implications. Current aeromagnetic data for a large part of the transect is shown in Murphy and Zwanzig (2019d) with outlines of the new maps and simplified units. A local compilation map east of Granville Lake (Murphy and Zwanzig, 2019c) highlights the regional tracing of units. It features a well exposed and easily accessible north-south tectonostratigraphic section across parts of the lithotectonic domains and subdomains described in this report. The section extends from the LRD, in the north (Rat granite), across the north flank of the KD (at Notigi Lake), into the Northeast Kiseynew subdomain (at Wapisu Lake). The detailed Notigi Lake map (Murphy and Zwanzig, 2019a)

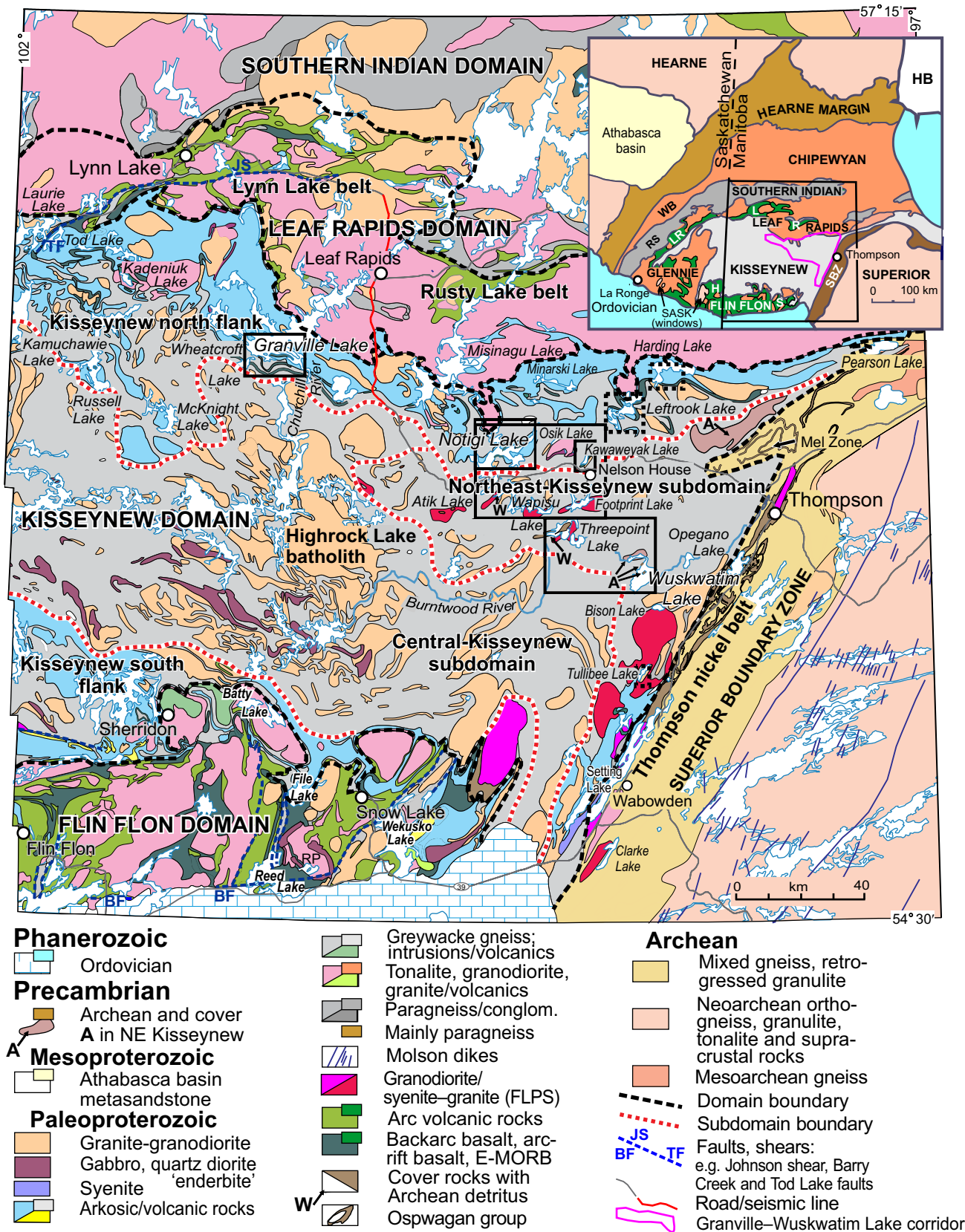


**Figure 1:** Geology of the Kiseynew domain with subdomains and map locations in the north flank at Granville, Notigi, Osik and Kawaweyak lakes, and in the Northeast Kiseynew subdomain at Wapisu, Wuskwatim, Threepoint and Opegano lakes (modified from Zwanzig et al., 2006). The Footprint Lake plutonic suite (FLPS) is shown in red and small Archean inliers (A) with cover rocks (W) containing Archean detrital zircons are indicated by arrows. The outlines highlight the study locations of new mapping as boxes and reconnaissance areas as dotted boxes. Inset: western Trans-Hudson orogen with figure outline; E-MORB, enriched mid-ocean-ridge basalt; H, Hansen Lake domain; HB, Hudson Bay; L, Lynn Lake belt; LR, La Ronge belt; R, Rusty Lake belt; RP, Reed Lake pluton; RS, Rottenstone domain; S, Snow Lake; SBZ, Superior boundary zone; WB, Wathaman batholith.

**Table 1:** Compilation legend of the Wuskwatim–Granville lakes corridor.

<b>Mesoproterozoic</b>		<b>Intrusive rocks (age unknown)</b>	
	M Mackenzie dike, assumed from aeromagnetic pattern	<b>gx</b>	Biotite granite to granodiorite ±any of amphibole, pyroxene, magnetite, K-feldspar porphyroclasts
<b>Paleoproterozoic</b>		<b>tx</b>	Tonalite, local agmatite with granodiorite matrix
<b>Late intrusive rocks (felsic to mafic)</b>		<b>gb</b>	Metagabbro, amphibolite, gabbro-porphyry
<b>Lpg</b>	Pegmatite, aplite, granite	<b>Intrusive rocks (known pre-Burntwood, pre-Sickle age)</b>	
<b>Llg</b>	Leucogranite ±sillimanite, granodiorite, pegmatite	<b>en</b>	Enderbite; minor quartz diorite–gabbro, mafic porphyry (Osik enderbite, 1.89 Ga)
<b>Lgg</b>	Granite–tonalite, mainly leucocratic with biotite ±garnet ±cordierite, local pegmatite	<b>qm</b>	Porphyritic quartz monzonite, syenite–granite (Footprint Lake plutonic suite, 1.88 Ga)
<b>Lhg</b>	Hornblende and biotite granite–granodiorite	<b>tn</b>	Biotite tonalite, minor diorite–gabbro (Osik tonalite, 1.87 Ga)
<b>Lqd</b>	Diorite, quartz diorite (Blacktrout diorite)	<b>mg</b>	Monzogranite (Notigi granite, 1.86 Ga)
<b>Ldt</b>	Diorite–tonalite	<b>gn</b>	Biotite granite–granodiorite (Rat granite, 1.84 Ga)
<b>Lmi</b>	Mafic to intermediate intrusions (gabbro–tonalite)	<b>Granville Complex</b>	
<b>Lgb</b>	Metagabbro, amphibolite	<b>Gs</b>	Metagreywacke, mudstone, semipelitic gneiss
<b>Lmu</b>	Gabbro–pyroxenite (1.79 Ga)	<b>Gsa</b>	Feldspathic metagreywacke, gritstone
<b>K</b>	Sickle Group metasedimentary rocks (undivided)	<b>Gsb</b>	Sillimanite-rich metagreywacke
<b>Ks</b>	Meta-arkose/gneiss +muscovite ±sillimanite knots (upper and lower units)	<b>Gsc</b>	Metagreywacke-breccia, pebbly mudstone/conglomerate
<b>Ksa</b>	Cross-bedded meta-arkose (lower unit)	<b>Gsd</b>	Rhyolitic metaconglomerate/fragmental volcanic, felsic tuff (~1.87 Ga)
<b>Ksb</b>	Sillimanite-bearing gneiss/meta-arkose	<b>Gse</b>	Siliceous meta-arenite and mudstone, chert, minor pelitic gneiss
<b>Ksc</b>	Quartzite	<b>Gi</b>	Meta-iron formation, mainly sulphide facies, local silicate facies and calcsilicate
<b>Ksd</b>	Arkosic metaconglomerate with sillimanite knots		Sulphide showing; gossan
<b>Kse</b>	Sillimanite ±cordierite-bearing gneiss	<b>Gc</b>	Calcareous to siliceous psammite (sandstone–siltstone)
<b>Kb</b>	Biotite gneiss (meta-arenite)	<b>Gg</b>	Metagabbro, amphibolite
<b>Kba</b>	Light grey and reddish metasandstone ±muscovite ±sillimanite	<b>Ghg</b>	Coarse grained diopside-rich melagabbro, ultramafic amphibolite
<b>Kh</b>	Hornblende-biotite meta-arenite/gneiss	<b>Ghb</b>	Layered amphibolite (Hatchet Lake basalt)
<b>Kha</b>	Laminated pink, grey and green metasandstone, minor metamudstone	<b>Gu</b>	Mafic–ultramafic rocks (Pickerel Narrows amphibolite: OIB, fragmental rock, tuff, flows)
<b>Khb</b>	Greenish grey calcsilicate metasandstone	<b>Gua</b>	Mafic–ultramafic pillowed flows, fine grained interlayers of flows or tuff.
<b>Khc</b>	Arkose-pebble metaconglomerate, commonly hornblende	<b>Gub</b>	Layered mafic rock, pillow basalt and gabbro
<b>B</b>	Burntwood Group (Metagreywacke–mudstone turbidite, generally graphitic)	<b>Guc</b>	Calcsilicate rock, carbonate alteration
<b>Ba</b>	Quartz-feldspar-rich arkosic metagreywacke ±sillimanite	<b>Gt</b>	Amphibolite, metabasalt, gabbro (Tod Lake basalt)
<b>Bc</b>	Sandstone-cobble metaconglomerate, local greywacke base or interbeds	<b>Gta</b>	Amphibolite with relict pillow structure, pillowed metabasalt, minor massive basalt, pillow breccia
<b>Bca</b>	Feldspathic metagreywacke ±hornblende, local pebble beds	<b>Gtb</b>	Hornblende-diopside amphibolite, layered ±calcite or massive; intermediate to felsic gneiss
<b>Bcb</b>	Greywacke and pebble metaconglomerate ±sillimanite	<b>w</b>	Wuskwatim Lake sequence (paragneiss, undivided)
<b>Bg</b>	Greywacke–mudstone-derived garnet-biotite±sillimanite gneiss	<b>Wp</b>	Semipelite to pelite, migmatitic garnet-biotite gneiss, meta-iron-formation
<b>Bm</b>	Garnet-biotite±sillimanite migmatite (metatexite, 10–50% leucosome)	<b>Wi(L)</b>	Meta-iron-formation, sulphide facies (su); silicate facies (si); calcsilicate (cs)
<b>Bma</b>	Bm ±cordierite, sillimanite, orthopyroxene, spinel	<b>Wq</b>	Arkosic quartzite, local pelite layers
<b>Bd</b>	Garnet-biotite migmatite (diatexite, 50–90% leucosome)	<b>Archean</b>	
<b>Bda</b>	Bd ±cordierite, sillimanite, orthopyroxene, spinel, ~70% leucosome	<b>Ag</b>	Felsic granulite gneiss (tonalite–granite) and common mafic boudins or dikes (~2.9–2.55 Ga).
<b>Bi</b>	Sulphidic silicate meta-iron formation, Su-rich semipelite/chert	<b>Ai</b>	Intermediate–mafic granulite gneiss (quartz diorite–gabbro) with hornblende, diopside, orthopyroxene, garnet, magnetite

features a new structural interpretation relevant to the entire region. Detailed mapping was enabled by clean shore-line exposures above the Notigi hydro control structure and moss-free outcrops in burnt-over inland areas. The mapping of Frohlinger (1971) at pre-flooding level (in Baldwin et al., 1979) was integrated in the detailed map.

The Kawawayak Lake area (Murphy and Zwanzig, 2019b) features a narrow belt of volcanosedimentary rocks and gabbro tentatively correlated with the type Granville complex. The Threepoint–Wuskwatim lakes area (Zwanzig et al., 2019) features the only known outcrops of Archean gneiss in the KD and the best exposures of the Wuskwatim Lake sequence. Work at Wuskwatim Lake (Zwanzig et al., 2019) has indicated the presence of Archean basement gneiss and its cover, the Wuskwatim Lake sequence (Percival et al., 2006). The basement and cover may occur in domes, or there may be more complex structural interleaving of Archean and various Paleoproterozoic rocks as suggested by the detailed structural mapping at Notigi Lake (elucidated in this report; Zwanzig and Murphy, 2009). Understanding the distribution and structural geometry of the various units is critical for any future nickel exploration in the Northeast Kiseynew subdomain. Most important is linking or separating the Wuskwatim Lake sequence and the Oswagan group, which hosts the nickel sulphide deposits in the

TNB (Percival et al., 2006; Zwanzig et al., 2006). These rocks suggest a previously unknown nickel potential in the KD.

### 1.1 Previous work

Previous mapping of the Notigi–Footprint lakes area by the MGS was carried out by Frohlinger (1971) and Kendrick et al. (1979) during the Burntwood Project. Results are published as part of a set of 1:50 000 scale geological maps (Baldwin et al., 1979). These maps have been incorporated in the new maps for much of the inland exposure. Earlier mapping by the MGS was mainly directly north, in the Leaf Rapids and Southern Indian domains (Figure 1), but extended to Notigi Lake (Elphick, 1972; Schledewitz, 1972). Mapping at Granville Lake included that by Barry (1965), Barry and Gait (1966), Campbell (1972) and Zwanzig and Cameron (2002). Mapping in 1971 by Kendrick (Baldwin et al., 1979) indicated that the Kawawayak Lake area contains greywacke-derived gneiss and migmatite (present Burntwood group) and hornblende–diopside gneiss, pyrite and pyrrhotite-bearing amphibolite gneiss, assigned by them to the Sickle group. The early regional-scale mapping did not recognize the significance of the rocks herein mapped as the Wuskwatim Lake sequence, the Granville complex nor trace out the different units in the Sickle group. Consequently,

the local structure, stratigraphy and mineral potential of this part of the KD remained largely unknown.

## 1.2 Method and scope

This report is a compilation of published Reports of Activities on the Wuskwatim–Granville lakes corridor, combined with earlier work in the area, updated with new interpretations and correlated to areas beyond the transect. Some text is a direct modification of the preliminary reports of the cited authors. Previous work from the Granville Lake area is included, but the rocks were also re-examined and resampled. The report presents a unified stratigraphy under a single legend, as well as a thorough analysis and modelling of structures at outcrop to crustal scales. The main aims of the report are to

- 1) describe the units on the accompanying published geological maps;
- 2) update the understanding and context of the surrounding earlier maps;
- 3) provide new regional structural and tectonic interpretations from the north and east sides of the KD and, with existing regional data and interpretations, to further elucidate the tectonic model of the western Trans-Hudson orogen (W-THO); and
- 4) to provide a guide for any future mineral exploration, particularly for nickel in the Wuskwatim Lake sequence, and gold along the KD north flank.

A key question remaining is whether ultramafic rocks with nickel potential occur in the Wuskwatim Lake sequence. Another challenge is the age of the Granville complex, earlier mapped as part of the Sickie group (e.g., Campbell, 1972), but which is assumed herein to correspond to similar, somewhat poorly dated rocks along strike to the west in Saskatchewan and in the southeast, adjoining the TNB.

Geological investigations, geochronology and Sm-Nd isotopic analyses by the GSC (Percival et al., 2005, 2006, 2007) indicate the presence of Archean-aged zircons in the KD. This discovery led to further sensitive high-resolution ion microprobe (SHRIMP) geochronology and identifying rocks older than the dominant Burntwood group and younger granitoid rocks. The ramifications of this work, including its economic implications, are discussed in this report. Their further study and remapping was prompted by a nickel potential, perhaps as in the TNB.

The exposed rocks in the Granville and Wheatcroft lakes area exhibit the most primary structure, the best preserved tectonostratigraphy and the most representative components of the Granville complex (Cameron, 1981; Zwanzig and Cameron, 1981; Zwanzig, 1990, 2008). The area was thus used as one of the type sections of the regional tectonostratigraphy and early structural style. It was interpreted during preliminary reanalysis as the upper-crustal cover (suprastructure) of the deeper rocks exposed to the east. Units were re-examined and sampled for U-Pb zircon dating, photographed, and more

structural data were collected and analyzed with existing data. Particular attention was given to the belt of mafic- and rare ultramafic rocks with associated metasediments (Granville complex) suggested to be part of the suture zone. This led to developing the tectonostratigraphy for the entire corridor and to further clarifying the regional tectonic history and economic aspects.

The large-scale structure at Notigi Lake was carefully remapped to develop an understanding of the architecture formed deeper in the upper to middle crust. The polyphase Notigi structure has a similar outcrop pattern to the newly discovered Archean inliers with their cover succession. The similar structure of the Archean and related rocks (Zwanzig and Murphy, 2009) provided a new interpretation of their three-dimensional geometry and structural origin. The structural complexity of the Wuskwatim–Granville lakes corridor has prompted multiple approaches using stratigraphy, geochemistry, isotope geology, geochronology and detailed structural analysis to arrive at the most probable inferences.

The report layout uses internal cross-references to numbered sections to enable reading topics separately. Sections and subsections generally start with an introductory summary. This plan allows individual sections of particular interest to be read with access to detailed descriptions and explanations. Sections and subsections are labelled by a dot numbering system that provides short forward and backward cross-references without breaking up fluid reading. The term “unit”, referring to map units, and most metamorphic modifiers are commonly omitted in the following sections. The term “megaunit” is used to combine several units. Map symbols are used as mnemonics of units as on the published set of maps. All units, being metamorphic, are partly described by their mineral assemblage. Mineral contents are given as estimates of their area on thin sections, in many cases as a maximum denoted by “up to” or shortened to the  $\leq$  symbol. The symbol “±[mineral]” designates the occurrence on some outcrops of the hosting unit. The field terms “enderbite” and “charnockite” are retained even where petrography suggests probable metamorphic origins.

## 2. Tectonic setting

The Kisseynew domain forms the large central part of the predominantly juvenile Paleoproterozoic internides (Reindeer zone of the Trans-Hudson orogen (THO), as in Stauffer, 1984; Lewry and Collerson, 1990) in Manitoba and Saskatchewan. It is dominated by metamorphosed greywacke and mudstone of the Burntwood group, whose provenance was from adjacent magmatic-arc terranes, and which was deposited in coalescing turbidite fans (Bailes, 1980a; Zwanzig, 1999). The sedimentary and igneous rocks were metamorphosed to amphibolite- and transitional granulite-facies, generally resulting in migmatization, and were highly deformed. Intrusive bodies include foliated tonalite, granite, diorite and late-stage pegmatite. Synkinematic, relatively late plutons, intrusive sheets and lenses are widespread but most abundant in the core of the KD. At

Granville Lake the Burntwood group is easily recognized as graphitic, deep-water turbidite, like that on the Kiskeynew south flank (e.g., Zwanzig, 1990). The turbidite basin was filled during its opening (e.g., Ansdell et al., 2005; Corrigan et al., 2009) and/or closing (Zwanzig, 1999), coeval with latest (1.85–1.83 Ga) arc magmatism in the W-THO. The Sickle group of highly metamorphosed mainly arenite units, much of it arkosic, was deposited unconformably on the arc massif (Wasekwan collage) including the Granville complex. The sediments were prograded over the Burntwood group during the latest arc magmatism and the onset of continental collision. Large-scale interleaving of units took place before and during ca. 1815–1800 Ma high-grade metamorphism. This established a west to northwest structural trend. Crossfolding on a northeast trend may have occurred during 1790–1770 Ma, coeval with intracontinental transpression (Lucas et al., 1996) and resulting from far-field stresses (Zwanzig and Bailes, 2010).

Early interpretations in the KD featured a simple stratigraphic interpretation of metagreywacke overlain by par amphibolite and, in turn, by arkosic metasandstone, all largely converted to migmatite and anatexitic granite (Baldwin et al., 1979). The standard tectonic model of the KD as a back-arc basin to the Flin Flon volcanic-arc domain was introduced by Ansdell et al. (1995) and has been retained in later publications (e.g., Ansdell, 2005; Corrigan et al., 2005, 2009). This model specified basin opening and filling during the advanced stages of arc magmatism. Paleogeography was implied to largely resemble the present map pattern of the THO, but with belts farther apart. Zwanzig (1999) and Zwanzig and Bailes (2010) proposed a longer-lived and more dynamic evolution in which the present geographic distribution of rocks resulted from crustal-scale overturning and oroclinal bending during continental convergence and collision.

Zwanzig and Bailes (2010) also proposed a subdivision of the KD in Manitoba into subdomains based on rock types (Figure 1). The Kiskeynew north and south flanks are dominated by Paleoproterozoic metasedimentary rocks of the Burntwood and Sickle/Missi groups and late granitoid rocks, all bordering the older volcanic-arc–back-arc domains. The central subdomain comprises Burntwood group migmatite and abundant granitoid rocks. The Northeast Kiskeynew subdomain, which borders the TNB and extends northeast of Thompson, includes Burntwood and Sickle/Grass River groups, Archean basement inliers with their passive-margin–type sedimentary cover (Wuskwatim Lake sequence) and early intrusions (Footprint Lake plutonic suite, FLPS). These subdomains may represent separate structural stacks similar to those proposed in Saskatchewan (Lewry et al., 1990).

## 2.1 Bounding lithotectonic domains

The KD is bounded by the TNB to the east, the Flin Flon volcanoplutonic domain to the south and the Leaf Rapids volcanoplutonic domain (LRD) to the north. Farther north, in the

Southern Indian and Chipewyan domains, some assemblages correlate, at least in timing, with units in the LRD.

The TNB is a northeast-trending belt of Archean migmatitic orthogneiss and unconformably overlying Paleoproterozoic Ospwagan group paragneiss that hosts ultramafic intrusions and associated nickel-sulphide deposits (Bleeker, 1990; Zwanzig et al., 2007). The TNB lies at the northwestern margin of the Archean Superior craton in a collisional zone (Superior boundary zone) with the KD. The TNB was intruded by ca. 1.89–1.82 Ga and probably younger granitoid plutons including two-mica calcalkaline granite and granodiorite throughout but muscovite-free granitoids in the south. The latter have been used to suggest early continental arc magmatism (Zwanzig et al., 2003; Percival et al., 2004, 2005). Alternatively, the oldest suite may be related in part to the largely coeval, alkaline to alkali-calcic FLPS intrusions. Partly coeval (1885–1880 Ma) mafic dikes (Molson dikes; Heaman et al., 2009) and ultramafic sills also occur in the main part of the TNB and the wider Superior boundary zone (Hulbert et al., 2005). The western boundary has a local overlap assemblage, the Grass River group, which is correlative with the Missi and Sickle groups. The Grass River group, Ospwagan group and Archean basement were intruded by 1835 Ma sanukitoid to alkaline (postcollisional) plutons (Zwanzig et al., 2003). Deformation involved thrusting and nappe tectonics followed by ca. 1770 Ma sinistral transpression (Bleeker, 1990; Zwanzig, 2000b) or long-lived “transpression” dominated by an east-side-up component (Gapais et al., 2005), such that the early structural geometry has been largely transposed.

The south flank of the KD and the adjacent margin of the Flin Flon domain have a complex history. This involved final (1.85–1.83 Ga) arc magmatism and deposition of the Burntwood and Missi groups, the latter being an equivalent with the Sickle group but including subaerial arc-volcanic rocks (Zwanzig and Bailes, 2010). The trends of the largest Missi basins follow the margin of the of the greater Flin Flon domain, northerly in the east and westerly in the north. Booth trends are dominated by late structures. West-trending shear zones have sinistral, north-side-up displacement (Zwanzig, 1999), whereas the north trend forms an east-dipping thrust stack (Lewry et al., 1994).

The LRD is underlain in the southeast almost entirely by volcanic-arc granitoid rocks, but is taken herein to include the Lynn Lake and Rusty Lake volcanoplutonic belts because arc magmatism was coeval throughout. Apparently the exposed rocks in the south have experienced greater uplift. These plutonic rocks in the south were considered younger than the Sickle group during early mapping (e.g., Schledewitz, 1972). Basal Sickle conglomerate can be thin, is highly deformed or absent. Basal quartzite is present in some places. New and published U-Pb zircon ages (references and greater detail in Section 5) indicate that the intrusions have the same range of ages (ca. 1.89–1.83 Ga) as magmatic arc plutons and volcanic rocks in the Lynn Lake belt and the rest of the volcanic-arc domains in the Reindeer zone (e.g., Whalen et al., 1999). Thus, most of this terrane is basement to the Sickle group, and

older than the Burntwood group. Only the youngest bodies (1.84–1.83 Ga arc plutons and >1.83 Ga granitoid rocks) may intrude the Sickle group and its equivalents as elsewhere in the THO. The igneous ages in the KD are  $\geq 1.83$  Ga apart from domal LRD inliers and the structurally interleaved FLPS intrusions. The latter are non-arc but related to the Archean basement and subcontinental mantle (Whalen et al., 2008). Narrow belts of Sickle group are structural basins in the LRD. The geology at Notigi Lake has indicated that the south margin of the LRD was involved in the complex deformation of the KD and acted as a crustal wedge (Section 6) with apophyses extending southward into the Kiskeynew north flank. Two of these, the Rat granite and Notigi granite (an inlier), extend into the Notigi Lake area. A granitoid dome or sheath fold at Osik Lake as well as quartz diorite and leucogranodiorite at Leftrook Lake are also from the leading edge of the LRD (Figure 1).

## 2.2 Kiskeynew north flank

On the north side of the Wuskwatim–Granville lakes corridor (Kiskeynew north flank), the Burntwood group and Granville complex are overlain by, and folded with, the Sickle group. This latter metasedimentary rock is generally magnetite-bearing paragneiss rich in quartz and feldspar. At Granville Lake and further north it is recognized as a shallow-water, mainly nonmarine succession of arkosic to lithic meta-arenite (Milligan, 1960; Zwanzig, 1990). The group is locally gradational into the Burntwood group and interpreted as partly coeval (Zwanzig and Cameron, 2002; Zwanzig and Bailes, 2010). The depositional ages of the units on the north flank are approximated from ages of detritus and from correlative units along strike and across the KD. The depositional age for the Burntwood group was constrained by Ansdell and Yang (1995) to be between 1850 and 1840 Ma, and the Sickle group between 1840 and 1835 Ma. Detrital-zircon and intrusive ages in Manitoba (Section 5.1.5) suggest that the Burntwood group may range from as old as ca. 1850 Ma (David et al., 1996) to a minimum age of 1830 Ma of enderbite that intrudes it (Gordon et al., 1990). The two sedimentary groups overlap in age and are the youngest supracrustal rocks in the Wuskwatim–Granville lakes corridor.

In much of the Wuskwatim–Granville lakes corridor, these groups are separated by the volcanosedimentary Granville complex. This composite, predominantly mafic megaunit is herein interpreted as older than the adjacent sedimentary groups and includes remnants of ocean-floor (back-arc tholeiite and ocean-island volcanic rocks) basement to the Burntwood and Sickle groups. The Sickle group unconformably overlies the complex, but the Burntwood group is interpreted as overthrust by the complex and the overlying Sickle group (see Section 6 for details). East of Granville Lake, the Burntwood and Sickle groups are generally separated by the thin, strongly layered unit of mafic and minor felsic tectonite as well as metagabbro and sulphide-facies iron formation.

Areas of best preservation and exposure have allowed their stratigraphic and structural relationships to be extended to establish a regional tectonostratigraphic correlation of units by comparing their composition and geochemistry as well as their relationship to adjacent units. Primary stratigraphic relations and early structures are preserved on Tod Lake and Laurie Lake, southwest of Lynn Lake, where distinctive thrust sheets are evident from structural repetitions (Gilbert et al., 1980; Zwanzig et al., 1999b, Figure 3.1). In each thrust sheet the Sickle group unconformably overlies volcanic and related sedimentary rocks contiguous with rocks in the Lynn Lake belt. The structural stack of volcanics and Sickle group arenite is locally thrust over the Burntwood group at Tod Lake (Zwanzig, 1999, Figure GS-17-2) like farther southeast at Granville Lake (see Section 6.1.1).

In Saskatchewan, the volcanosedimentary assemblage (Granville complex, there called the Levesque Bay assemblage by Corrigan and Rayner, 2002) has been cut by a 1896  $\pm 18$ –16 Ma leucogranite dyke (Corrigan and Rayner, 2002). This  $\sim 1.9$  Ga age is consistent with the relationships and ages of adjoining units in the Lynn Lake belt. At Granville Lake, a probable age of about 1874 Ma has been obtained from rhyolitic tuff or reworked tuff (Corrigan and Rayner, pers. comm., 2008), so that the whole Granville complex or just the tuff and its hosting sedimentary package on the south side of the complex may be younger than the proposed age of the Levesque Bay assemblage. The lack of definitive ages of the Granville complex, however, leaves more than one possibility (Section 5.1.4). It is most likely an amalgam of more than one age of rocks and therefore considered a structural complex.

## 2.3 Northeast Kiskeynew subdomain

The Burntwood group forms the most widely exposed supracrustal rocks in the Northeast Kiskeynew subdomain of the Wuskwatim–Granville lakes corridor. Much of the group is a monotonous, layered, mesosome-dominated migmatite (metatexite) derived from greywacke–mudstone turbidite. It is locally adjacent to the Wuskwatim Lake sequence, the older, heterogeneous paragneiss that was recognized to lie unconformably on Archean basement. Outcrops of the Wuskwatim Lake sequence are very limited and contacts with other units are generally not exposed. Geochemistry, geochronology and Sm-Nd isotope systematics are distinctly different between the Wuskwatim Lake sequence and the Burntwood group (Percival et al., 2005, 2006; Zwanzig et al., 2006). These differences, presented in this report, support an interpretation that there are fault contacts between unrelated units, and repetitions that make the Northeast Kiskeynew subdomain a structural stack.

In the vicinity of Wuskwatim Lake, Archean rocks and their cover, the Wuskwatim Lake sequence (W), occupy an asymmetric domal structure and narrow double-plunging isoclinal. Thin sequences of heterogeneous paragneiss at Threepoint Lake and Wapisu Lake closely resemble W. These small remnants of the Wuskwatim Lake sequence are spatially and isoto-

pically associated with the better exposed FLPS plutons, which are more widespread and define the known extent of the Northeast Kiseynew subdomain. They indicate that Archean rocks, their cover and their intrusions form an important component of the KD, underlying and structurally interleaved with the Burntwood group. It is not immediately apparent how the stacking and interleaving of units took place, nor if Archean gneiss with its cover forms the greatest volume of the crust at depth. The similarity at Wuskwatim Lake to the TNB basement gneiss and the Ospwagan group suggest that they may have belonged to a pericontinental terrane that is contiguous with the Superior craton (Zwanzig and Bailes, 2010). This important issue is further addressed, showing that the ages of detrital zircons in the Wuskwatim Lake sequence do not entirely match those of the Ospwagan group, and that this presents an uncertainty about the relationship of the sequence to the TNB.

Structural relationships at the north end of the TNB suggested that thrusting of the Burntwood group was to the southeast over the Ospwagan group. The structural stack was subsequently folded into southwest-verging nappes and then strongly refolded during northwest transpression (Zwanzig, 2000b; Zwanzig and Böhm, 2002; Burnham et al., 2009). In the southern part of the TNB, rocks of the KD occur in domal structures and the seismic fabric dips northeast (White et al., 1999). The northern exposures of the TNB show a belt-wide increasing pressure gradient towards deeper exposures in the north (Couëslan and Pattison, 2012). This supports the structural stacking of deeper-level rocks from the northeast. The seismic signature and the regional northeasterly plunge with Burntwood group rocks underlying the Ospwagan group in the south suggest that the TNB, there, has overthrust the Trans-Hudson internides. This suggests that the Superior craton forms a middle plate wedged between the KD and the LRD.

### 3. Tectonostratigraphy

Rock units are described in order of decreasing known or inferred age for the entire Wuskwatim–Granville lakes corridor, regardless of their occurrence in different subdomains. Letters within brackets correspond to those in Table 1 and on Geoscientific Map MAP2019-1 to -5 (Murphy and Zwanzig, 2019a–c; Zwanzig, 2019; Zwanzig et al., 2019). Units in the Granville Lake area are metamorphosed to amphibolite facies. Some metagreywacke and meta-arkose contain muscovite+sillimanite, whereas the rock units in the Notigi Lake area and farther southeast are upper-amphibolite- to transitional-granulite facies. Reasonably well-preserved rocks of the Granville Lake area are described first and as separate units or subunits. Higher-grade gneisses, mainly from Notigi, Wapisu and Wuskwatim lakes, derived from the lower-grade rocks, follow as separate units or subunits. Descriptions include mineral estimates, generally done on thin section without point counts, but periodically tested with point counts. They are meant to provide the general range of compositions. Minerals of particular note are those used to define the high met-

amorphic-grade units. The prefix "meta" is generally omitted for brevity where primary rock types are clearly recognized but retained in the legend, titles, generally in opening sentences and where metamorphism is emphasized or has obscured the exact rock type. For the latter, "gneiss" and "schist" may be used.

Composite tectonostratigraphic columns on Figure 2 portray typical sequences separately for the Kiseynew north flank and for the Northeast Kiseynew subdomain. The columns are constructed where units are in stratigraphic or early structural order after inferred early thrust faulting but with major fold repetitions removed. Unit thicknesses in Figure 2 as well as beds are given throughout the text as measured in nearly true sections after deformation, or given as widths on outcrops of steeply dipping rocks. Column a) from Notigi Lake is based on the marked section on MAP2019-3 (Murphy and Zwanzig, 2019a). This column integrates the composite geology and probable lateral sedimentary-facies changes from throughout the Notigi map area to show the general tectonostratigraphic relationships of the units. Tops in the Sickie group are taken from similar, but better preserved successions elsewhere in the Wuskwatim–Granville lakes corridor. Column b) is a composite of the sections interpreted to young south on both sides of the Burntwood River, northwest of Wuskwatim Lake (Zwanzig et al., 2019). The unconformity at the base of the Wuskwatim Lake sequence is confirmed by the detrital-zircon data (Section 5.1.1). The unconformity provides the younging direction of the sequence. The assignment of the calcareous psammite (Gc) to the Granville complex is based on regional correlations. The fault below this unit is based on Sm-Nd isotopic data. Column c) features highly compressed rocks partly cut out by granite (Lgg/gx) at the margin of the FLPS intrusion on the southwest side of Wapisu Lake (Murphy and Zwanzig, 2019c). This succession has unknown facing but it suggests intrusion of the FLPS in the Wuskwatim Lake sequence.

Stratigraphic superposition is recognized in the northwestern part of the Wuskwatim–Granville lakes corridor, where tops are evident from graded bedding or crossbedding very close to formational (unit) contacts. This establishes the position of the Sickie group above the Burntwood group despite large-scale folding and general overturning of the units. A basal quartzite that overlies various units of the Granville complex confirms the unconformity at the base of the Sickie group there. The unconformable relationship is even more prominent in equivalent rocks in the southwest end of the Lynn Lake belt (Zwanzig, 2000a).

Contacts between intrusive and sedimentary rocks of most ages are not exposed or are highly sheared in the Wuskwatim–Granville lakes corridor. Relationships are generally not definitive except for the youngest intrusions. Absolute zircon ages, however, clearly define

- 1) the older (1885–1880 Ma) FLPS (Percival et al., 2005, 2006, 2007) in the Northeast Kiseynew subdomain;

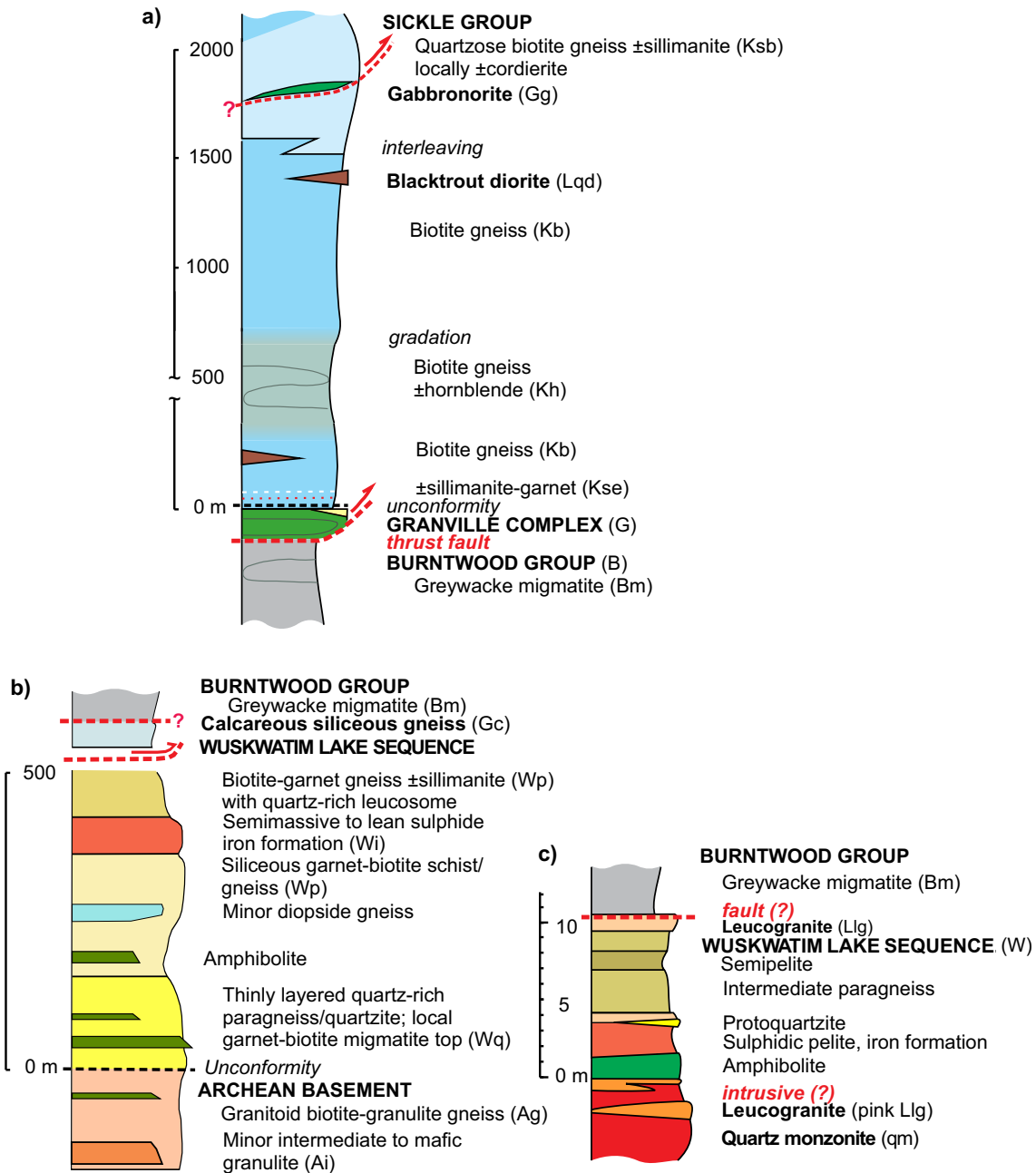


**Figure 2:** Typical local tectonostratigraphic sections with units scaled close to their present (deformed) thickness, and showing the regionally inferred faults between the Burntwood group and the older units: **a)** Kiseynew north flank section as seen in the Notigi structure, also showing the unconformity between the Granville complex and the Sickie group, as well as the Burntwood megathrust and a probable higher thrust fault; **b)** Northeast Kiseynew subdomain composite section as seen near Wuskwatim Lake; **c)** highly appressed section on Wapisi Lake.

- 2) intrusions with a range of ages (ca. 1890–1830 Ma) in the LRD (Section 4.3.2); and
- 3) a suite of intrusions that postdate the Burntwood and Sickie groups and range in age like the metamorphic peak, about 1815–1800 Ma (Growdon et al., 2009; Rayner and Percival, 2007; Murphy et al., 2009).

### 3.1 Archean (Ag, Ai)

Archean multicomponent orthogneiss occurs in the core of several structural culminations exposed northwest of Wuskwatim Lake and on several islands in the lake. Phases of this granulite-facies gneiss are felsic (tonalite to granite, Ag)

and intermediate to mafic enclaves (quartz diorite to gabbro, Ai). Zircon data obtained by SHRIMP suggest crystallization ages of about 2.9–2.55 Ga with probable granulite-facies metamorphism at 2.65–2.55 Ga (Rayner and Percival, 2007). Unit Ag is composed of light brown- or grey-weathering biotite±orthopyroxene-bearing tonalite, “enderbite”, to pink- or brown-weathering granite, “charnockite”. The gneiss contains mafic boudins and local isoclinal, intrafolial folds. It has generally concordant granitic to pegmatitic veins but that locally cut its gneissic layering (Figure 3a). These features are similar to those in TNB basement gneiss, with which it may correlate. Mineral assemblages include quartz, plagioclase,

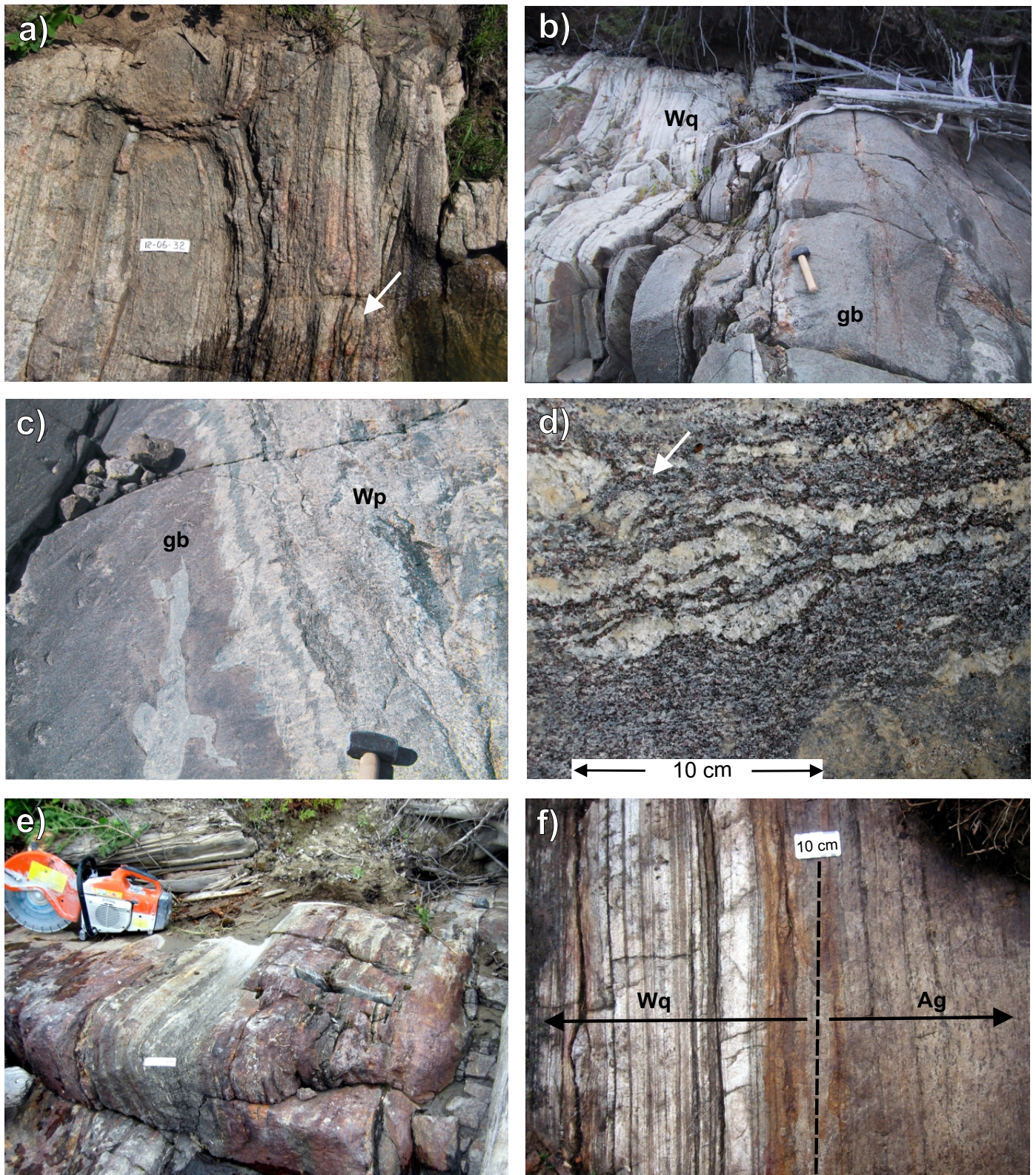


**Figure 3:** Field photographs of Archean gneiss and Wuskwatim Lake sequence: **a)** Archean granulite gneiss (Ag), showing multicomponent biotite-bearing tonalite gneiss, locally with isoclinal intrafolial folds (arrow); **b)** arkosic quartzite (Wq), at the base of the Wuskwatim Lake sequence and yielding only Archean detrital zircons, showing thin layering (left) and mafic dike (gb); **c)** semipelitic migmatite (Wp) with mafic inclusions near contact with mafic sill (left of hammer); **d)** quartz-rich veins in biotite-garnet gneiss formed from Archean detritus; garnets (e.g., at arrow) are deep violet; **e)** lean iron formation (Wi), mainly sulphidic (su), with interlayer of quartz-rich biotite-garnet gneiss (at tape); **f)** unconformity between arkosic quartzite (Wq) and tonalite gneiss (Ag), located at the mouth of the Muskoseu River. Tapes are 10 cm long.

finely perthitic microcline, biotite and magnetite. Mafic and intermediate phases contain any of clinopyroxene, orthopyroxene, garnet, titanite, monazite, zircon, and hornblende. Peak-metamorphic mafic minerals are partly overgrown by biotite and chlorite. Plagioclase is locally antiperthitic and partly sericitized. Orthopyroxene crystals are generally 1 to 2 mm long and may be Paleoproterozoic because they have the same size and habit as those in nearby Burntwood group leucosome. At many sites the entire compositional range from syenogranite (charnockite) to tonalite (enderbite) is interpreted as mesosome with no more than 5% fine-grained mafic minerals, and these occur in thin aggregates or films that are probably melanosomes. Felsic minerals are coarser and granoblastic. Early leucosome, rich in quartz and plagioclase, permeated mafic enclaves only in the Archean orthogneiss.

On the northeast side of the Threepoint Lake pluton, granite gneiss with retrograded mafic minerals resembles unit Ag with its coarse granoblastic texture, similar layering and mafic enclaves. The gneiss may extend around the pluton, under water, along a magnetic anomaly, forming a discontinuous mantle around the pluton along with the Wuskwatim Lake sequence. Its contact with the pluton is generally intruded by biotite granite (gx) and pegmatite to late granite (Lpg). The granite gneiss also extends east beyond the pluton to Kinoshakawa Lake (Zwanzig et al., 2019).

## 3.2 Paleoproterozoic

### 3.2.1 Wuskwatim Lake sequence (W, Wq, Wp, Wi)

The Wuskwatim Lake sequence (W) of heterogeneous paragneiss is exposed at Wuskwatim, Opegano and Threepoint lakes (Percival et al., 2006) and at Wapisu Lake (Percival et al., 2007; Murphy et al., 2009). Composite stratigraphic sections were compiled from shoreline exposures across and along strike of the folded succession of Archean gneiss and Wuskwatim Lake sequence, with details given in Zwanzig et al. (2006). The best composite section is younging southeast as a 500 m thick mantle on Archean orthogneiss, on an island and on the south shore of the flooded Burntwood River (Zwanzig et al., 2019, UTM 524500E, 6162450N to 526250E, 6163700N), northwest of Wuskwatim Lake. The sequence comprises arkosic quartzite (Wq, Figure 3b), migmatitic semipelite (Figure 3c) to pelite (Wp, Figure 3d) with meta-iron formation (Wi, Figure 3e). The basal arkosic quartzite exposed on the island (Zwanzig et al., 2019, UTM 529112E, 6164655N) is interpreted to lie unconformably on the granulite gneiss (Ag, Figure 3f). The sequence is structurally overlain by the Burntwood group (Bm) with one intervening unit of calcareous psammite (Gc) that may be up to 150 m thick (cf. Gc in the Granville complex; Section 3.2.2.4). The Wuskwatim Lake sequence contains prominent mafic sheets and lenses (Figure 3b, c) interpreted as dikes and sills, possibly Molson dikes (not shown on maps).

The unit of arkosic quartzite (Wq) ranges from less than 1 m up to 100 m thick on the Burntwood River. It weathers from

white to pale brown, and is thinly layered (Figure 3b), locally massive or with abundant lenses of gabbro and pegmatite. Biotite-rich partings are common, and thin interbeds of pelite converted to garnet-biotite gneiss occur especially in the upper part of the unit. Detrital zircons yielded (SHRIMP) ages mainly between 3.3 and 2.6 Ga, and Nd-model ages ( $T_{CR}$ ) of 3.77–2.93 Ga (Section 4.1). On Threepoint Lake the arkosic quartzite has 10–30% feldspar, mostly granoblastic K-feldspar. Mafic and aluminous minerals make up less than 5% and include biotite, garnet and rare sillimanite overgrown by muscovite. Layers of semipelite contain more biotite and garnet with abundant K-feldspar±cordierite±sillimanite. Orthopyroxene occurs locally in Wq.

The paragneiss units of semipelite to pelite of the Wuskwatim Lake sequence (Wp) are generally rich in K-feldspar and poor in biotite. Textures include thin segregation of mafic and felsic minerals, suggesting partial melting. Coarser granitoid textures suggest conversion to melt-dominated migmatite (diatexite). The occurrence of orthopyroxene and antiperthite indicates granulite-facies metamorphism. Biotite and hornblende, however, are generally still present in the assemblages. Cordierite rims on garnet in pelite suggest continued high temperatures during decompression. Retrogression to biotite and chlorite and overgrowth of muscovite on sillimanite occur with protomylonitic textures, particularly in zones of late deformation.

The generally migmatitic paragneiss (Wp) comprising semipelite (Figure 3c) to pelite (Figure 3d), with a thin (~ 2 m) interval of interlayered sulphidic schist and iron formation, forms the inferred upper part of the Wuskwatim Lake sequence. This is best exposed on the northwest shore of Wuskwatim Lake, where it comprises rusty- to grey-weathering, siliceous and pelitic, garnet-biotite±sillimanite schist and gneiss with thin primary layering defined by variations in biotite content. The rock has 20–40% quartz-feldspar leucosome and quartz veins. Garnet (generally 10–25%) forms ≤3 mm grains but in iron-rich layers makes up to 50% porphyroblasts ≤8 mm in diameter. Semipelite on Wuskwatim Lake contains up to 50% quartz and subequal K-feldspar and plagioclase, with biotite, garnet, sillimanite and local orthopyroxene and spinel. Pyrrhotite, magnetite, ilmenite and graphite are accessory. Rare pelite exposures on a reef at the south shore of Threepoint Lake contain about 10% biotite and <10% garnet, but contain abundant K-feldspar. Cordierite and sillimanite occur as intergrowths or in clusters in various interlayers. Pyrrhotite, magnetite and graphite are accessory.

Parts of unit Wp are prominently sulphidic and graphitic. Layers of silicate-facies iron formation, Wi(si), in the order of 50 cm thick, are located on the flooded Burntwood River northwest of Wuskwatim Lake. Layers or lenses of calcsilicate rock, Wi(cs), are locally present. Quartz occurs in laminae and as thin veins between layers containing plagioclase, clino- and orthopyroxene, garnet and green amphibole. Some very quartz-rich interlayers are likely derived from impure chert. Sulphide-facies

iron formation, Wi(su), and sulphidic semipelite form prominent rusty-weathering subunits 1 to 3 m thick (Figure 3e). They are highly magnetic, with about 30% pyrrhotite±magnetite. Rocks containing sulphide±magnetite south and northeast of the quartzose rocks at Threepoint Lake have a variety of layers rich in either quartz, plagioclase±clinopyroxene, garnet or K-feldspar and biotite. Aeromagnetic anomalies suggest that pyrrhotite-rich iron formation is covered or under the lake.

At Wapisi Lake, unit W (undivided) forms a thin margin approximately 9 m wide adjacent to the Wapisi porphyritic quartz-monzonite (qm) of the FLPS and younger granite. From west to east the sequence contains

- 1.5 m of layered intermediate gneiss with alternating garnet- and quartz-rich gneiss graphitic garnet-biotite gneiss and calcsilicate gneiss containing magnetite and pyrrhotite;
- 1.6 m of semipelitic gneiss with 2–3 mm garnets;
- 3.5 m of dark grey intermediate gneiss that is cut by leucogranite; 10 cm lens of arkosic quartzite; and
- a 2 m section of rusty-weathering, lean iron formation and semipelite to pelite with 2% pyrrhotite.

The semipelite is rich in K-feldspar. “Lean iron formation” contains clinopyroxene, orthopyroxene, magnetite and 5–6% sulphides. Arkosic quartzite is thinly layered, with local pelite layers that generally contain garnet±sillimanite. This sequence yielded mainly Archean detrital zircons (Section 5.1.1).

### 3.2.2 Granville complex (G)

The Granville complex (G undivided or divided into units described below) is exposed discontinuously along the north side of the Wuskwatim–Granville lakes corridor from Granville Lake to Notigi, Kawaweyak and Leftrook lakes. Geochemically these are back-arc or arc-rift basalt but include slightly altered mid-ocean ridge basalt and related gabbro (Section 4.2). The most distinctive rocks are mafic–ultramafic volcanic units and carbonated equivalents that have an ocean-island–type geochemistry. The type sections of the complex, where primary structures are preserved, occur at Laurie and Granville lakes (called the Granville Lake assemblage in Zwanzig et al., 1999a). Near the top, the volcanic succession at Granville Lake locally contains a thin, conformable, fine-grained sedimentary layer. Throughout most of its extent, the volcanic unit is unconformably overlain by the Sickle group. The volcanic rocks are bounded in the south by a thicker, coarser-grained sedimentary succession (Gs) with local amphibolite. Fault contacts are assumed between the mafic rocks and the southern belt of sedimentary rocks. However, faults are clearly mappable only in rare areas where unit cutoffs, shear zones or mylonites are exposed. Known fault exposures occur south of Pickerel Narrows and on the east side of Muskwanuk Island (Section 7.1; Zwanzig, 2019). The southern sediments

contain felsic rock, possible tuff, which is dated as approximately 1.87 Ga, the only known age in the Granville Lake complex in Manitoba. Near the top of the Burntwood group, south of Granville Lake, a narrow belt of amphibolite units derived from basalt, gabbro and stratabound sulphide may be the base of a thrust slices of the Granville complex. Mafic gneiss and tectonite east of Granville Lake is interpreted as a continuation of the complex as supported by geochemistry,  $\epsilon_{Nd}^{(1)}$  values and an identical tectonostratigraphic position as in the type successions.

#### 3.2.2.1 Tod Lake basalt, layered amphibolite and gabbro (Gt, Gta, Gtb, Gg)

The oldest, thickest and most widespread unit in the Granville complex is the Tod Lake basalt (Zwanzig et al., 1999), which consists of amphibolite, metabasalt and metagabbro (Gt, undivided). The best preserved rocks (Gta) include amphibolite with relic pillow structure, pillowed metabasalt, minor massive basalt, all exposed at Granville and Tod lakes, and pillow breccia with hyaloclastite exposed at Tod Lake. Its tectonite equivalent (Gtb) comprises layered or massive hornblende–diopside amphibolite and local intermediate to felsic gneiss. Subvolcanic gabbro and derived amphibolite (Gg) are widely associated with units Gta and Gtb.

Despite metamorphism at Granville Lake, some of these rocks are well preserved as pillowed basalt (Gta, Figure 4a, b), but more generally they are deformed and metamorphosed to medium grey and dark green to black amphibolite (Gtb) with diopside– and hornblende–plagioclase–rich layers or thin calcsilicate lenses±calcite. This amphibolite unit has local massive layers and layers of intermediate gneiss (Figure 4c–f). The highly metamorphosed volcanic and subvolcanic rocks have been interpreted as the extension of the Tod Lake basalt and gabbro from the southwest end of the Lynn Lake belt south to Kamuchawie Lake (Zwanzig and Wielezyski, 1975; Zwanzig et al., 1999a; Zwanzig, 2000a). From Granville Lake they extend as far east as the TNB. They are key to understanding the Granville Lake structural zone as an ancient suture zone of a destructive plate boundary.

On peninsulas and islands near the south shore of Granville Lake, megaunit Gt (Gta, Gtb and Gg) occupies a major anticline (Pickerel Narrows anticline, Figure 5; Zwanzig, 2019) in which Gt is 350 m thick in the north limb. Gabbro (Gg) and coarse-grained diopside-rich melagabbro (Ghg) form the core of the anticline. High-Mg rocks (Gu) and minor laminated sedimentary rocks (Gse) are intercalated at the top and overlain by the Sickle group. Up to 200 m of layered and massive amphibolite (Gt) exists where the Churchill River enters Granville Lake, as well as in the belts south of the lake, and east on Notigi and Kawaweyak lakes. In most places in the eastern portion of the study area, Gt pinches down to a few tens of metres, a few

<sup>(1)</sup> Epsilon-neodymium values are given as the initial values at the known or estimated age of the rock sample ( $\epsilon_{Nd}$ ), but in the text are simplified to  $\epsilon_{Nd}$ .

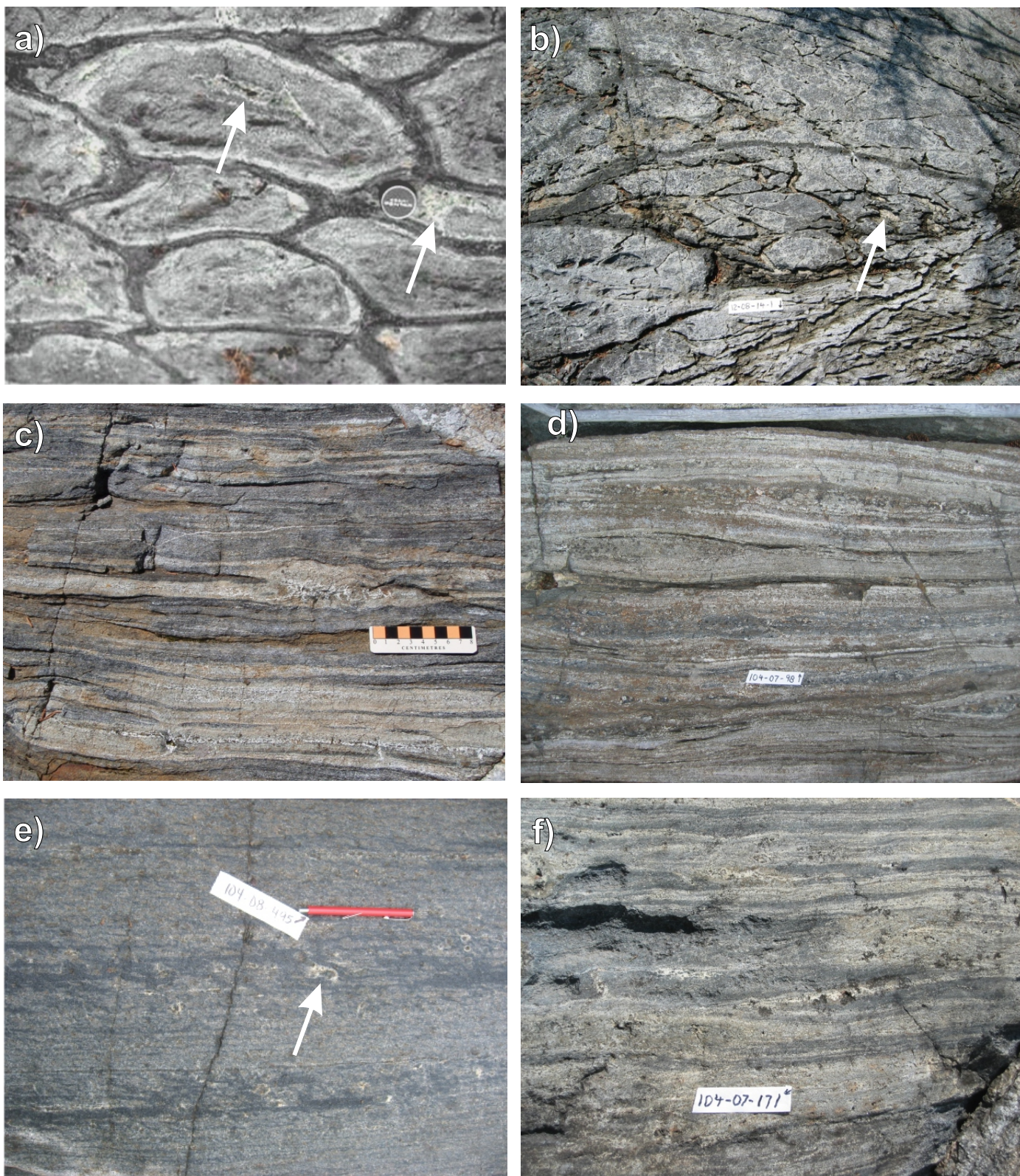


**Figure 4:** Field photographs of the Granville complex mafic–ultramafic rocks: **a)** pillowed Tod Lake basalt in the thick, north-facing limb of the Pickerel Narrows anticline, Granville Lake; alteration to calcisilicate (e.g., at arrows); lens cap is 5 cm; **b)** pillows with metamorphic-hornblende-rich rinds (black) in faulted, south-facing limb of Pickerel Narrows anticline; alteration domains contain calcite (arrow); **c)** layered amphibolite, locally traced into pillowed basalt, Granville Lake; light brown layers are diopside-plagioclase rich; dark grey layers are amphibole rich; **d)** layered amphibolite, Notigi Lake, as in (c); **e)** weakly layered amphibolite, rich in diopside, formed from massive basalt or gabbro, with incipient leucosome around diopside porphyroblasts (arrow); **f)** calcisilicate-rich, layered amphibolite with stretched selvages and alteration domains, Kawaweyak Lake. Tapes are 10 cm long.

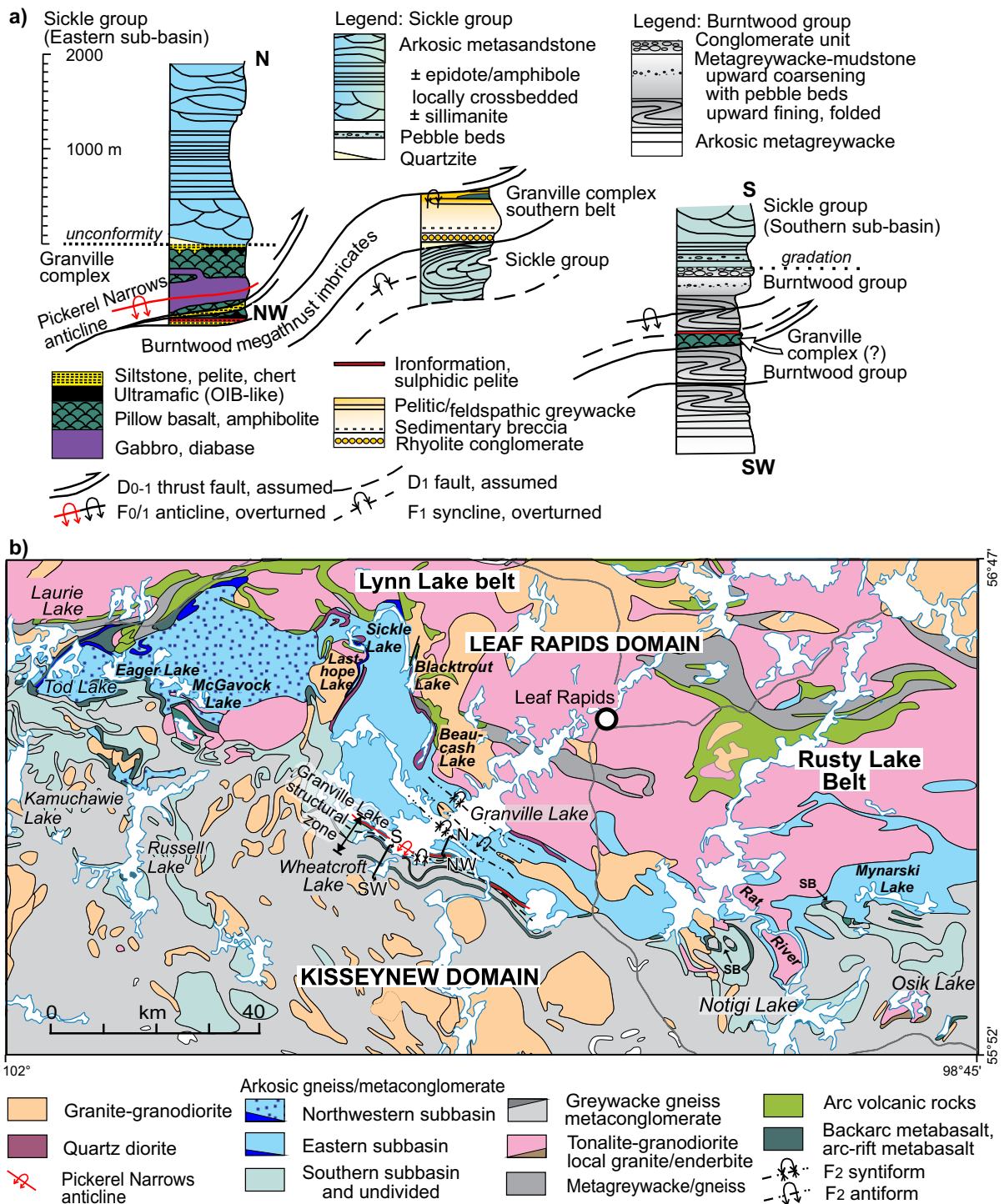


**Figure 5:** Tectonostratigraphic illustration of structure sections at Granville Lake, and Sickie group sub-basins on the Kisseynew north flank, showing: **a)** early structural and stratigraphic relations of the Granville complex, Sickie group and Burntwood group. Columns are restored to the probable style that preceded northerly overturning and compression. Ages of the structures are speculative because of refolding and late reactivation of the early structures. (Figure modified after Zwanzig, 1990); **b)** location of sections and approximate extent of Sickie sub-basins. SB are structural basins with inverted stratigraphy. Abbreviation: OIB, oceanic-island basalt.

metres or pinch out entirely. In these areas, Gt features mainly mafic tectonite that can be interlayered with lesser intermediate to felsic gneiss or iron formation. Major structures cannot be traced in these rocks.

Nearly undeformed-looking, north-younging pillows (Figure 4a) are preserved overlying the melagabbro in the

north limb of the Pickerel Narrows anticline, 5 km east of the settlement of Pickerel Narrows (Figure 5b; Zwanzig, 2019). South-facing pillows occur on Muskwanuk Island, west of the settlement, in the south limb of the anticline (Figure 4b; Zwanzig, 2019). These rocks are aphyric to finely porphyritic and have local preservation of amygdaloidal pillow mar-

gins. The unit (Gta) contains very fine-grained (0.1–0.6 mm) hornblende and plagioclase in subequal proportion, with accessory magnetite±ilmenite. Porphyritic flows have 2 mm long grains of hornblende after pyroxene±plagioclase pseudomorphs containing aggregates of secondary plagioclase. Massive flows contain 0.1–3 mm grains of the same mineral assemblage. Alteration domains and pillow selvages generally contain diopside, calcite and titanite±garnet. Medium- to fine-grained mafic sills (amphibolite, Gg) occur locally in the main section of basalt (Gt, Gta) and form a mantle (≤250 m thick) around the diopside-rich melagabbro (Ghg). The sills contain equal amounts of hornblende and plagioclase with titanite and abundant magnetite±pyrite. Pillowed basalt (Gta) and associated dikes or sills were apparently widespread and locally dominant before deformation because at Granville Lake they extend laterally into highly flattened pillows and onward into the regionally abundant layered amphibolite of unit Gtb.

In the amphibolite unit (Gt, Gta) south of Granville Lake, poorly preserved, partly carbonated pillows occur, and are best exposed on Wheatcroft Lake. The pillows in this location are flattened but preserved. They are on the north side of a long sheet of amphibolite (≤200 m thick) thought to represent part of a structural panel within the Burntwood group. Gabbro (Gg) predominates in the south and sulphide-facies iron formation shown in Zwanzig (2019) as sulphide showings "s" or gossans "g" occurs most commonly at the north contact of the amphibolite megaunit. More than 15 km east of Wheatcroft Lake, the tectonostratigraphy of the panel is still preserved, but the northern member is mainly layered hornblende-diopside amphibolite (Gtb), commonly with garnet in transposed pillow rinds. The sheet of amphibolite is tentatively interpreted to define the base of a north-younging thrust sheet. It is possible that the upper contact is depositional (Burntwood group deposited on iron formation), or that the gabbro may be a younger intrusion belonging to unit Lgb.

At Notigi Lake, unit Gtb consists of dark green to grey hornblende-diopside-plagioclase amphibolite. Its internal structure comprises variously coloured discontinuous layers, pods and lenses showing folding and boudinage (Figure 4d) or straight uniform layers from 1 cm to 1 m thick. Grey layers contain up to 65% ortho- and clinopyroxene with plagioclase and minor titanite and magnetite. Pale grey to green layers and lenses contain diopside and carbonate with ≤5% titanite. Such calcsilicate is interpreted as early alteration of basalt, including epidosite from lower grade rock. Dark green to dark grey, coarser, more uniform amphibolite is interpreted as gabbro or massive flows (Figure 4e). Some darker hornblende-rich layers are interpreted as less altered basalt remnants (Figure 4f). Local, light grey, intermediate to felsic layers are interpreted as intrusive or sedimentary rocks. Transitions along strike at Granville Lake show that thin hornblende-rich layers and lenses ±garnet±biotite are derived from highly strained and recrystallized pillow selvages. Consequently, much of the layered hornblende-diopside amphibolite was part of the mafic volca-

nic succession (Gt, mainly once Gta) that was partly altered, metamorphosed and structurally attenuated.

Massive hornblende-plagioclase amphibolite units (mapped as Gg) at Notigi Lake, locally has 8% magnetite, and are interpreted as a Fe-enriched (fractionated) fine-grained (0.4–1 mm) mafic sills. Iron-rich basalt and gabbro occur characteristically at the top of the Tod Lake basalt in the type section at the southwest end of the Lynn Lake belt (Gilbert et al., 1980; Zwanzig et al., 1999a). Exposures up to 70 m wide of better preserved gabbroic sills (Gg) at Notigi Lake occur on Timew Island, on the mainland shore north of Timew Island and near the northeast end of the lake (Murphy and Zwanzig, 2019a). These intrusive rocks are overlain and underlain by units of the Sickle group, and extending around a fold, appear to join layered amphibolite (Gtb). The sills were interpreted as intruding the Sickle group during mapping; however, chemical analyses (Section 4.2) show them as nearly identical to the Tod Lake basalt (Gta). Consequently, they are tentatively considered part of the Granville complex (i.e., Gg), which requires that they were emplaced as a part of a thrust in the Sickle group (implications in Section 6.2.1). Individual intrusive sheets are up to 20 m thick. They are distinctly coarser-grained and internally more uniform than the layered amphibolite. The sheets are dark green to black and dark grey. Where best exposed, they include four gradational rock types: 1) coarse-grained garnet-biotite rock; 2) hornblende-rich to more leucocratic gabbro; and 3) plagioclase-rich (60%) gabbro overlain by 4) darker amphibolite. Granulite-facies metamorphism is indicated by local orthopyroxene in addition to clinopyroxene, cummingtonite and hornblende.

On Leftrook Lake (Figure 1), concordant sheets of fine- to medium-grained gabbro, coarse-grained melagabbro and anorthositic gabbro (similar to unit Ghg, below) locally overlie mafic tectonite (similar to unit Gtb) interpreted to have formed from basalt. The tectonite has 5–20 mm thick layers rich in hornblende±garnet that are interpreted as sheared pillow selvages. Layers rich in diopside, generally <15 cm thick, are interpreted as highly metamorphosed epidosite (Zwanzig and Böhm, 2002). These rocks occur between the Burntwood and Sickle groups, and are interpreted as a thrust sheet containing units Gg and Gtb; and in which the overlying Sickle group has a basal unit of protoquartzite and is unconformable, similar to the section with the lower unit Ksb on Notigi Lake (Section 3.2.6). Thus the sequence at Leftrook Lake supports the wide continuity of the tectonostratigraphy.

### **3.2.2.2 Hatchet Lake-type amphibolite and gabbro–melagabbro (Ghb, Ghg)**

In the Kawawayak Lake area various layered amphibolite and gabbro units (Ghb, Gg) are interpreted as part of the Granville complex. They form a northeast-trending linear belt less than 150 m wide. They are exposed in several locations on a northern and a southern peninsula and an island in Kawawayak Lake as well as on the east shore of Notakikwaywin Lake

(Murphy and Zwanzig, 2019b). The amphibolite units are up to 20 m wide. They include well-layered, dark-grey to brown hornblende- and diopside-rich amphibolite. They contain more orthopyroxene, pyrrhotite, secondary biotite and calcite in the east than to the west, where layers are 5 mm to 1.5 m thick. These units are chemically similar to unit Ghb (Section 4.2). The amphibolite is interlayered with sulphide-facies iron formation (Gi), the thickest layer ( $\geq 20$  m) lying on the east side of the belt. Most of the amphibolite is bounded by granodiorite (Lgg) and locally includes sheets of granodiorite. Coarse- to medium-grained, dark grey amphibolite (Gg) forms massive, uniform and rare layered sheets up to 4 m wide intruding unit Ghb. Orthopyroxene, locally rimmed by plagioclase, is present in these sheets of unit Gg. Primary magmatic layering is suggested by variable abundances of plagioclase. The sheets intrude the layered amphibolite–iron-formation assemblage along sharp contacts with local chilled margins. Despite the close spatial association with the layered amphibolite, the chemical differences between units Gg and Ghb suggests they are not comagmatic. In contrast, the main intrusion (Ghg) at Granville Lake consists of mostly pale green amphibole ( $\leq 2.5$  mm long) with magnetite and up to 20% diopside and lesser plagioclase.

### **3.2.2.3 Mafic–ultramafic rocks (Pickerel Narrows amphibolite, OIB: Gu, Gua, Gub, Guc)**

Mafic–ultramafic rocks (Gu) are interlayered with mafic rocks (Gt, Gta, Gtb) in the upper part of the succession extending from the settlement of Pickerel Narrows to more than 10 km to the east. These Mg-rich rocks have distinctive trace-element compositions similar to ocean islands (OIB; Section 4.2). They commonly contain up to 20% olivine porphyroblasts (Zwanzig et al., 1999a) suggesting a picrite composition and protolith. Individual layers weather dark green to grass-green and are up to 35 m thick. A prominent part of unit Gu comprises fragmental layers, which are interlayered with massive flows or tuff. Monolithologic fragments and matrix suggest an agglomerate origin for some fragmental layers (Figure 6a), whereas rounded heterolithologic fragments and blocks suggest a conglomerate origin for other beds (Figure 6b). Mafic–ultramafic pillowed flows interlayered with fine-grained flows or tuff (Gua) are rich in calcite or tremolite-actinolite. The pillowed flows are intensely carbonatized. An uppermost layer of unit Gu grades upward into fine-grained siliceous sedimentary rock, probably chert and felsic mudstone (Gse, Figure 6c). Layered, pillowed or massive mafic rocks (Gub, 5–9% MgO, Data Repository Item DRI2021014), identified as oceanic-island basalt (OIB) and gabbro in Section 4.2, occur on Notigi, Leftrook and Granville lakes. Thin layers of green to white and brown calcsilicate rocks (Guc) on Granville (Figure 6d), Notigi and Kawawayak lakes have similar trace-element patterns to the type Pickerel Narrows amphibolite (Section 4.2). These layers have variable contents of plagioclase, diopside, calcite and amphibole  $\pm$  K-feldspar with accessory quartz, titanite, apatite and local scapolite. They

probably represent highly altered and strained mafic–ultramafic volcanic rocks. Those with abundant biotite or quartz and accessory pyrrhotite  $\pm$  graphite were apparently resedimented with the adjacent siliciclastic rocks (Gse).

### **3.2.2.4 Sedimentary rocks (Gs, Gsa, Gsb, Gsc, Gsd, Gse, Gc, Gi)**

Sedimentary rocks (Gs) in the Granville complex are dominated by grey- to white- and brown-weathering metagreywacke to felsic mudstone. More pelitic beds (Gsb) contain abundant small sillimanite knots (faserkiesel, Figure 6e). Sulphide iron formation and siliceous sulphidic rock (Gi, Figure 7c) are exposed in thin sedimentary sections overlying units Gt and Gu in the limbs of the Pickerel Narrows anticline. Sulphidic rock on the north margin of unit Gt south of Granville Lake are marked as sulphide showings. Most greywacke beds (2–10 cm thick) alternate with mudstone (0.2–5 cm thick; Figure 6f). Some of the rocks in the southern belt are highly feldspathic (Gsa), can be very coarse-grained (gritstone), and can contain amphibole. These rocks also contain rare beds of breccia, pebbly mudstone or conglomerate (Gsc), exposed at the south margin of the belt. The rocks are preserved with most of their sedimentary structures intact, but may occur in fault slices. South of the Pickerel Narrows anticline at Granville Lake, they have an aggregate true thickness up to 500 m. Graded bedding shows that this southern succession generally becomes younger toward the Pickerel Narrows anticline to the north and is interpreted to have been overthrust from the northwest by the mainly volcanic rocks in the complex during early deformation (Figure 5a; Section 6.1.1). A high-density turbidite bed, up to 7 m thick, contain intraclasts and exotic blocks below a fine-grained top (Zwanzig, 2008; Figure 7a). Blocks, up to 2 m long, include highly foliated mafic–ultramafic rocks with strong carbonate alteration that preceded their incorporation into the turbidite. A uniform grey bed, probably rhyolite tuff, on strike with rhyolitic conglomerate or fragmental volcanic rock (Gsd, Figure 7b) yielded ca. 1874 Ma zircon grains (Corrigan and Rayner, pers. comm., 2008) that suggest an age intermediate between the mafic rocks (Gt) and the Burntwood group. Thin beds of very fine-grained siliceous meta-arenite (Gse) can contain K-feldspar and only traces of biotite. Other members of unit Gse are graphitic and contain minor pelite, calcareous rocks and probably chert (Figure 6d). Pale gray to white psammite (Gc) is weakly calcareous or siliceous with up to 10 m thick, laminated calcareous layers. The calcareous layers contain calcite, minor amphibole, titanite, epidote, apatite and locally pyrrhotite.

Similar sulphidic layers in cherty beds occur on Notigi Lake (Figure 7d). There, the siliciclastic rocks of the Granville complex include: 1) medium grey to brown siliceous rocks with quartz-plagioclase  $\pm$  hornblende and possible white chert; and 2) grey, green to white calcsilicate rock with variable quartz content and up to 30% diopside (Figure 7d). Calcite (up to 15%) weathers recessively, results in a pitted outcrop surface. The

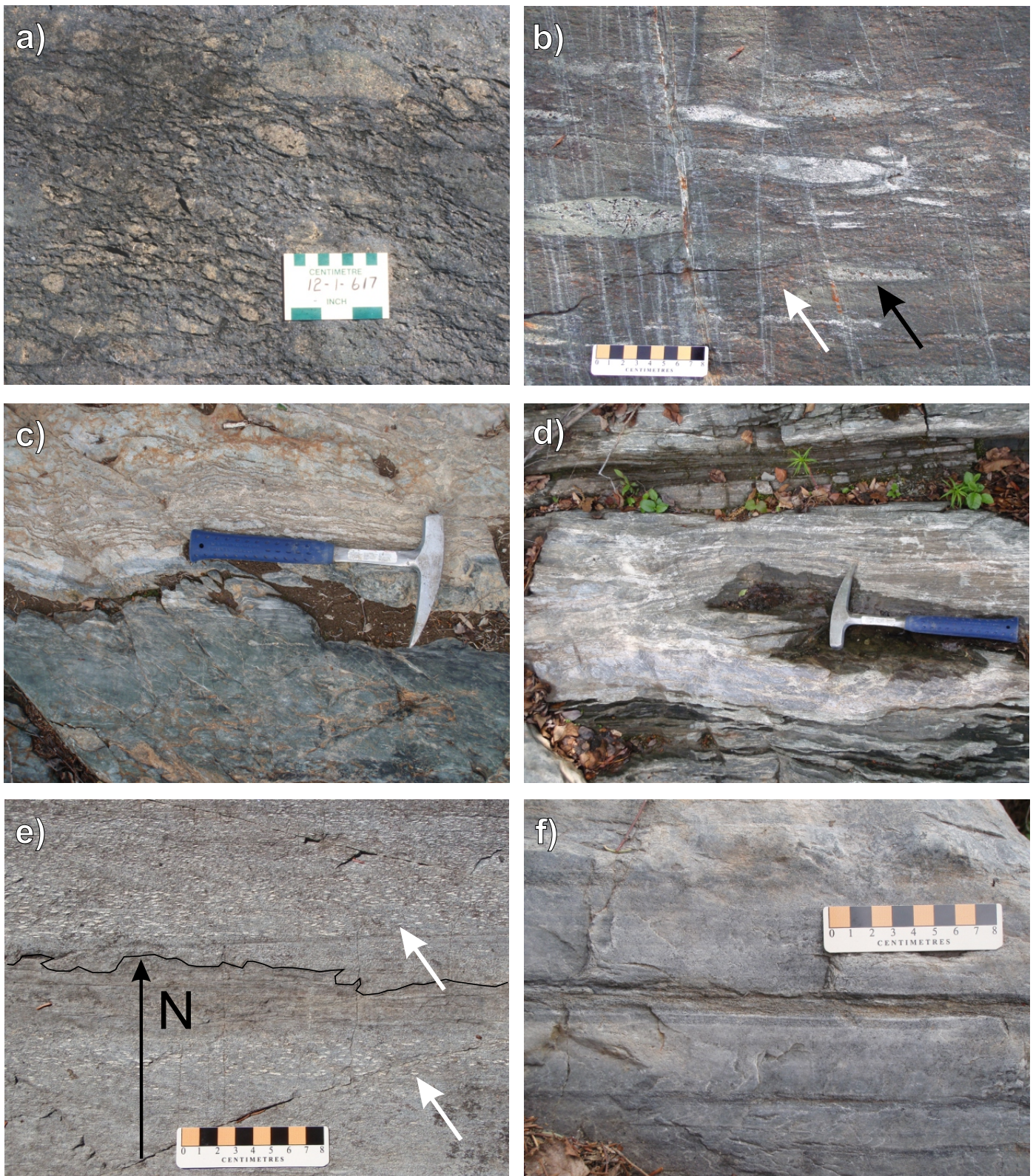


**Figure 6:** Field photographs of mafic-ultramafic and sedimentary rocks, Granville complex at southern Granville Lake: **a)** Pickerel Narrows fragmental mafic-ultramafic rock (Gu) probably formed from agglomerate; **b)** heterolithologic ultramafic fragmental rock (Gu); rusty pits (e.g., at white arrow) are lemmatized olivine porphyroblasts; rounded shapes and dark weathering rind at black arrow suggest a conglomerate origin; **c)** ultramafic mudstone or tuff grading up into chert, siliceous mudstone (Gse) and greywacke; **d)** interlayered chert (under hammer) with calcareous layers (dark recessive layers; Gc) and amphibolite (Gtb) at top; **e)** turbidite divisions (along black arrow) with greywacke (at scale card) grading into sillimanite-rich (white arrows) semipelite (Gsb) and laminated mudstone (middle), overlain by fluted greywacke base (enhanced) of next bed with  $S_2$  at low angle; **f)** rhythmically interbedded quartzose metasandstone and quartzofeldspathic biotite schist/mudstone, probably turbidite (Gse).

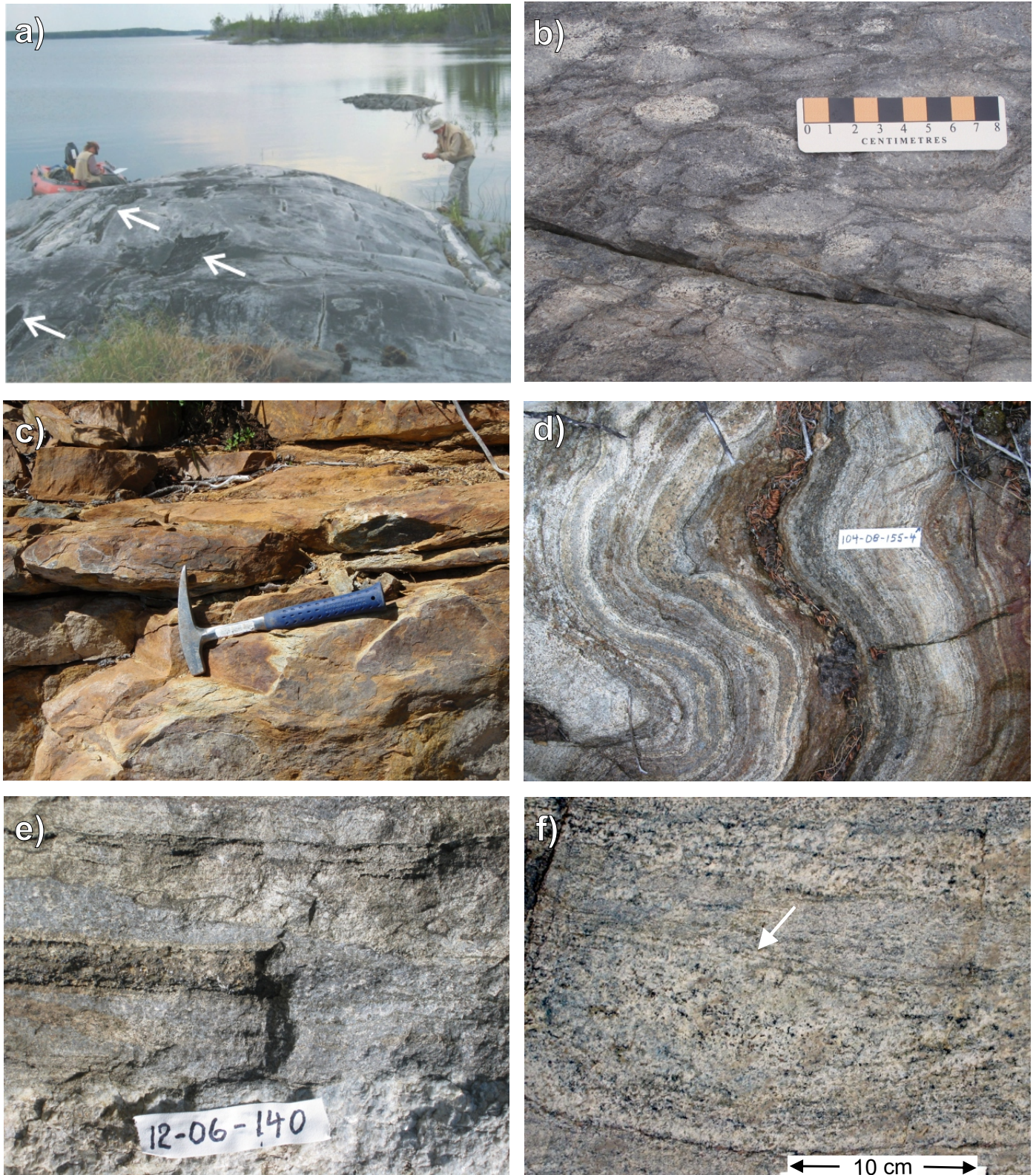


**Figure 7:** Field photographs of Granville complex sedimentary rocks: **a)** ultra-thick bed of feldspathic greywacke-gritstone (*Gsa*) containing exotic blocks (e.g., white arrows) at the base (at boat with assistant) grading through greywacke north (right) into siltstone (near person at right), Granville Lake; **b)** monolithologic rhyolitic conglomerate or fragmental volcanic (*Gsd*) with rounded clasts showing various stages of weathering or alteration but identical populations of plagioclase and mafic phenocrysts in all clasts and matrix, Granville Lake; **c)** quartz-rich sulphidic sediment, Granville Lake; **d)** folded interlayered siliceous and sulphidic beds interlayered within unit *Gtb*, Notigi Lake; **e)** calcareous psammite (in *Gs*, undivided), Kawawayak Lake; **f)** calcareous psammite (*Gc*) with lenses (below arrow) and layers (top) with calcsilicate minerals including calcite, Wuskwatim Lake.

unit contains relatively abundant titanite and apatite, similar to layers in unit Gs at Kawaweyak Lake. Rare gossanous layers containing Fe-sulphide and local patches with a trace of chalcopyrite are found sporadically throughout the assemblage.

In the Kawaweyak Lake area (Murphy and Zwanzig, 2019b), the 120 m wide, northeast-trending belt of unit G is made up of the dominantly volcanogenic rock with lesser sedimentary units. In the southern part of this belt, however, a 70 m succession is dominated by quartzofeldspathic paragneiss (metagreywacke, Gs). Quartz- and plagioclase-rich metagreywacke dominates this section. Most layers have subequal quartz, plagioclase and K-feldspar and only a trace of biotite, but brown members greater than 7 m thick, relatively biotite-rich (~25%), are also featured. Sediments in the east of the main volcanic belt include light-grey to cream-coloured, plagioclase-rich calcareous layers (Gc, Guc). Minerals in these layers include biotite, calcite, diopside, garnet and local titanite and pyrrhotite (Figure 7e). Brown biotite-rich interlayers with local sulphide occur at the centimetre scale in the east. Subunits of grey to patchy brown calcsilicate rock (Guc), up to 8 m thick, have a low quartz content. They are rich in diopside and titanite, some with prominent calcite and scapolite (Figure 7e). Diopside is partly altered to tremolite. These unmapped beds are interpreted as thoroughly carbonatized volcanogenic rock, altered OIB (Section 4.2), possibly tuff reworked as sediment.

On the northwest shore of Wuskwatim Lake, unit Gc comprises 6 m of weakly calcareous semipelite and 8 m of siliceous calcsilicate gneiss (Figure 7f). It separates the upper semipelitic to pelitic part of the Wuskwatim Lake sequence (Wp) from the Burntwood group. The quartz- and plagioclase-rich semipelite weathers light grey, and contains biotite and garnet (~10% each). Pale grey-green calcsilicate interlayers adjacent to the Burntwood group are 10–20 cm thick. These layers are plagioclase-rich and contain calcite, diopside (partly altered to actinolite), relatively abundant titanite and minor pyrrhotite and apatite. Similar rocks occur 2 km to the northwest, adjacent to the main sequence of W (Zwanzig et al., 2019), suggesting that this unit occurs on opposite limbs of a major syncline cored by the Burntwood group where it separates the bodies of the Wuskwatim Lake sequence. The unit (Gc) is interpreted to have formed as fine-grained calcareous sandstone and siltstone with interlayered semipelite to siliceous pelite and marlstone. Calcite may have originated as thin carbonate beds and reworked cement between clastic grains.

### 3.2.2.5 Iron formation, sulphidic paragneiss (Gi, Gs/Gc)

The Granville complex includes rusty, green and grey-brown meta-iron formation (Gi). Sulphide-facies are most abundant; silicate-facies and calcsilicate are local. Thin units of “lean iron formation” grade into, or are interlayered with less sulphidic paragneiss and calcareous to Fe-rich siliclastic rock (Gs, Gc). A 5 m thick sulphidic section, indicated on the map by a pyrite occurrence on the island east of the main

southern peninsula on Granville Lake, grades from quartz- and pyrrhotite-rich layers through 2 m of semi-solid sulphide into rusty psammite overlain by pyritic cherty layers (Figure 7c), greywacke, mudstone and chert (Zwanzig and Cameron, 1981). South of Granville Lake, stratabound sulphide showings and gossans occur commonly on the north side of unit Gt. Sulphidic layers at Notigi Lake are generally thin and interlayered with barren, quartz-rich rocks that are interpreted as chert with siliclastic to calcareous beds (Figure 7d). The sulphidic beds are recessive and contain more biotite than barren beds.

At Kawaweyak Lake, the sulphidic sedimentary rocks are in contact with gabbro (Gg) and layered amphibolite (Ghb). In a nearby amphibolite–sulphidic sediment formation, calcsilicate rocks (Guc) have the OIB-like geochemical signature. Generally, about 1 m is composed of semi-solid iron-sulphide with about 20% quartz. A partly sulphidic section with relatively abundant titanite and graphite has a maximum aggregate thickness of 50 m. It includes paragneiss with orthopyroxene, clinopyroxene and calcite. Quartz-rich laminae alternate with those rich in plagioclase or diopside. Some layers are rich in hornblende. Each type exhibits gradational changes in mineral contents and ranges from 0.3 to 7 m in thickness. They are interpreted to represent sulphidic to calcareous mudstone and chert. The similarity of these sedimentary sections at Kawaweyak and Granville lakes strengthens the lateral correlation of the Granville complex.

### 3.2.3 Intrusions of known pre-Burntwood, pre-Sickle ages

Although no unconformity has been identified between the Burntwood group and older granitoid rocks, the presence of an unconformity between the partly coeval Sickle group and the older intrusions is established in the Lynn Lake belt of the Leaf Rapids domain (Milligan, 1960). Uranium-lead zircon dating in the Wuskwatim–Granville lakes corridor indicates that several plutons are older than the Burntwood group, yet were originally mapped as intruding the sedimentary rocks (details provided in Section 5). Several similar intrusions found along strike are not described in this report but have already been dated. Quartz diorite–tonalite located at Leftrook Lake (Figure 1), on the north margin of the Wuskwatim–Granville lakes corridor, has a crystallization age of  $1890 \pm 2$  Ma (Section 5.1.3). Adjacent leucogranodiorite–trondhjemite with an age of  $1842 \pm 3$  Ma (Section 5.1.3) is interpreted to predate the Sickle group as part of its magmatic-arc basement. Enderbite and tonalite forming the main phases at Osik Lake are dated as  $1885 \pm 7$  and  $1873 \pm 11$  Ma (Section 5.1.3). A reinterpreted emplacement age of monzogranite at Notigi Lake is  $1862 \pm 6$  Ma, and granite north of Notigi Lake has an emplacement age of  $1838 \pm 4$  Ma (Section 5.1.3). These plutons as well as a  $1855 \pm 3$  Ma tonalite and a  $1862 \pm 10$  Ma granodiorite, on the south margin of the LRD north of Thompson, have the same range of ages as the pre-Sickle intrusive suite at Lynn Lake (Beaumont-Smith and Böhm, 2002; Beaumont-Smith et al., 2006). They belong to the

1.89 Ga early arc, 1.878–1.844 Ga early–middle successor-arc and 1.845–1.83 Ga late successor-arc (syn-Missi/Sickle) intrusions that are common throughout the internal zone of the THO (e.g., Whalen et al., 1999).

Porphyritic granitoid rocks, which share Archean Nd-model ages and ca. 1.88 Ga crystallization ages, include the alkaline, alkali-calcic and calcalkaline FLPS (unit *qm*, details below). Similar ca. 1.89–1.88 Ga plutons extend into the TNB (Zwanzig et al., 2003; Percival et al., 2005; Whalen et al., 2008).

### **3.2.3.1 Enderbite, minor quartz diorite–gabbro (*en*)**

At Osik Lake, an “enderbite” suite (*en*) dated as  $1885 \pm 7$  Ma (Section 5.1.3) includes quartz diorite and metre-scale layers of diorite and gabbro. At the map scale, unit *en* varies in thickness from 20 to 1000 m and forms an envelope surrounding the Osik Lake tonalite pluton (*tn*; Section 3.2.3.3) and separating it from the Burntwood paragneiss (Murphy and Zwanzig, 2019c). The suite is mostly medium-grained, homogeneous, and contains hornblende-biotite±orthopyroxene±clinopyroxene (Percival et al., 2007). Foliation intensity varies inversely with the thickness of the unit. Sulphide-rich dioritic layers up to 50 cm thick are exposed in western Osik Lake (Percival et al., 2007). The age of the enderbite older than the closely surrounding Burntwood group indicates a structural emplacement of the intrusion.

### **3.2.3.2 Porphyritic quartz monzonite, syenite–granite (*qm*)**

A distinct suite of K-feldspar–porphyritic plutonic rocks to augen gneiss, defined as the ca. 1885–1880 Ma FLPS (Percival et al., 2007; Whalen et al., 2008), is exposed in the Northeast Kiseynew subdomain. The rocks are dominated by porphyritic quartz monzonite–granite but have been found by Whalen et al. (2008) to range in composition from syenite–monzonite to syenogranite–monzogranite. Work by the GSC in 2007 and 2008 and by the MGS identified seven plutonic bodies: one each at Atik, Wapisu (west), Footprint, Tullibee–Bison lakes and probably Wapisu (east), Threepoint and southwest of Tullibee lakes (Figure 1). The latter three are identified by their typical high magnetic signature (Murphy and Zwanzig, 2019d) and from descriptions by Baldwin et al. (1979). All FLPS plutons are deformed and fairly homogeneous. They contain K-feldspar phenocrysts (up to 4 cm long) as well as hornblende +biotite±pyroxene (Figure 8a). The northern plutons vary from moderately to strongly foliated, to augen gneiss, whereas, in the southeast, cataclastic texture and retrogression of mafic minerals to biotite and chlorite are typical. Contacts with surrounding rocks are generally obscured by granite or pegmatite sheets or overburden. Mafic dikes up to 4 m wide occur within all the plutons. Diffuse enclaves of diorite to gabbro are present in the Atik Lake body.

Geochemical and isotopic data indicate that the FLPS is alkalic to alkali-calcic and contains an Archean melt component. Low-silica intermediate end members are thought to represent low degree partial melts of subduction-modified subcontinental lithospheric mantle (Whalen et al., 2008). Felsic end members are thought to result from mixing with crustal melt. Archean Nd-model ages obtained from the low-silica FLPS samples are interpreted as reflecting their contaminated mantle sources. The unusual and distinctive geochemical and isotopic characteristics of the FLPS make it a potential “marker unit” for identifying the presence of Archean-basement gneiss, mantle and probable cover elsewhere than currently found in the KD of Manitoba and Saskatchewan.

Earlier interpretations were that the FLPS intruded the Burntwood group (Baldwin et al., 1979). However, contacts with the Burntwood group are not exposed. At Wapisu Lake, the 9 m thickness of *W* is separated from a nearby pluton of the FLPS by fine-grained pink leucogranite, which leaves this contact relationship uncertain. The pink leucogranite (*Llg*) may be a marginal phase of the Wapisu Lake pluton or, more likely, a late contaminated melt (Section 4.4.3). The contact relationship is the same as for the partial mantle of *W* and probable basement (*Ag*) and cover gneiss at Threepoint Lake (Section 4.3.3). This very likely makes the FLPS/*W* contact intrusive into *W* and *Ag* (Figure 2c), as confirmed by the U-Pb zircon ages and Nd-model ages.

### **3.2.3.3 Biotite tonalite, minor diorite–gabbro (*tn*)**

Tonalitic rocks underlie most of Osik Lake and have an interpreted emplacement age of  $1873 \pm 11$  Ma (Percival et al., 2007). Several plutonic units in the Osik Lake area correspond directly with rocks previously interpreted as Burntwood or Sickle group (Frohlinger, 1971). The main tonalite phase is medium-grained, homogeneous, moderately foliated and contains 5–10% biotite and 20–30% quartz. It is intruded by a much younger layered mafic–ultramafic complex (*Lmu*; Section 3.2.7.1) and contains sparse enclaves of diorite and gabbro including a distinctive “snowflake-textured” gabbro with poikilitic plagioclase phenocrysts up to 1 cm in diameter (Percival et al., 2007). An older tonalitic phase with sparse orthopyroxene is included as local enclaves, and at least one younger phase of tonalite is present as sheets and dikes cutting the main phase tonalite. The younger tonalite is a homogeneous, medium-grained, hornblende-biotite tonalite with a weak, northeast-striking foliation. The main tonalite at Osik Lake intruded the surrounding  $1885 \pm 7$  Ma (Section 5.1.3) enderbite. The composite intrusive body is interpreted herein as an inlier of the LRD in tectonic contact with the younger Burntwood group.

Tonalite gneiss similar to unit *tn* occurring at Tullibee Lake that yielded four analyses as  $1890 \pm 8$  Ma on a single zircon grain (Section 5.1.3) suggests an important candidate

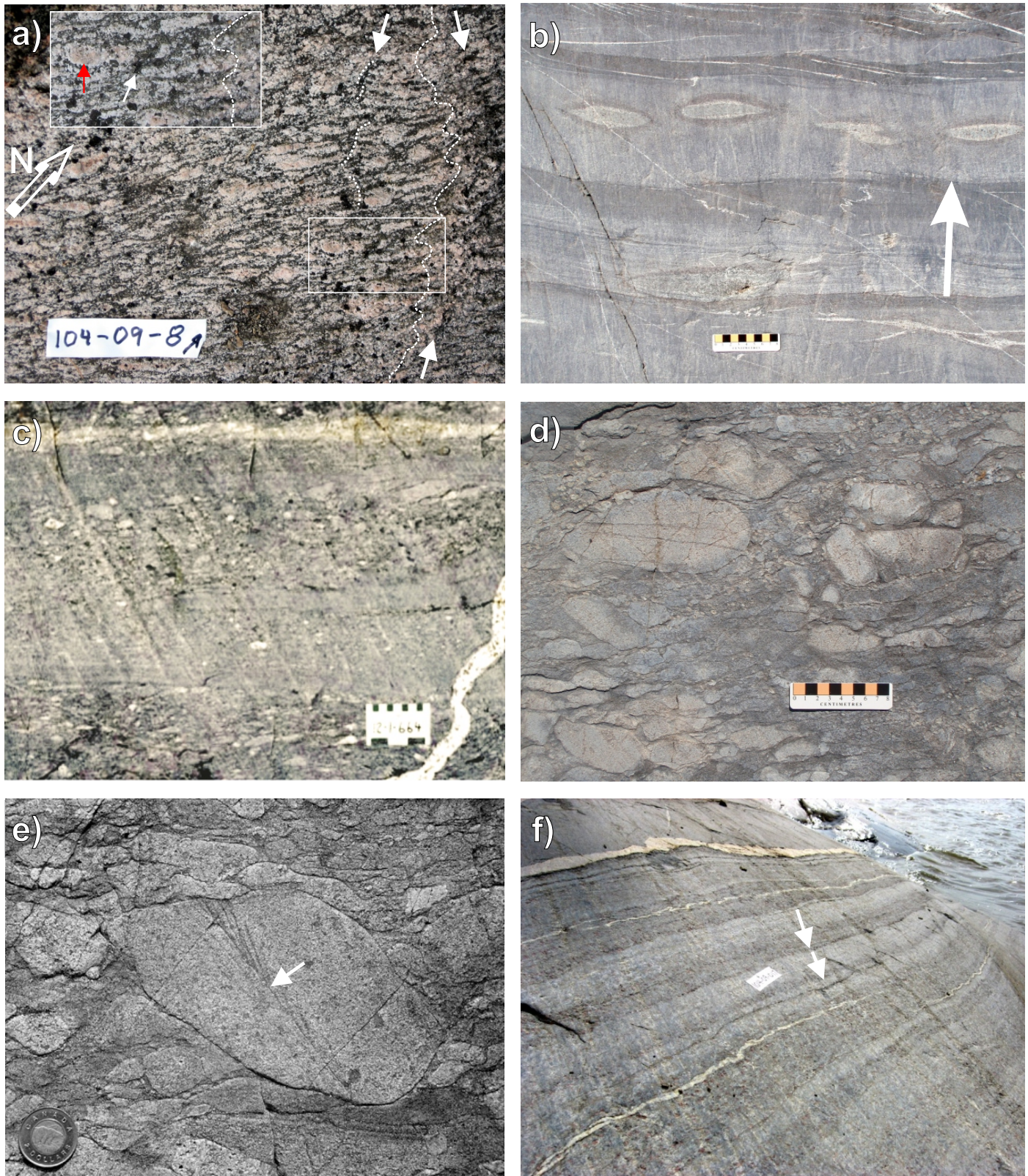


**Figure 8:** Field photographs of clean outcrops: **a)** quartz monzonite (Footprint Lake plutonic suite) with prominent K-feldspar phenocrysts and relatively mafic matrix; main foliation (NE) is  $S_3$ ; spaced foliation (e.g., dotted lines) is remnant with  $D_{2b}$  folding; white arrows mark probable melt-loss channels along  $S_{2a}$ ; increase in mafics and fabric change are to right of continuous dashed line; rounded K-feldspar with rim (red arrow in enlargement), Wapisu Lake; **b-f)** Burntwood group metaturbidite, **b)** showing Bouma bedding divisions with grading at arrow, coarse to fine into a laminated division overlain by a (dark) shaly division. Pale lenses next to arrow are calcisilicate derived from calcareous concretions; **c)** pebbly and laminated beds, near the top of the group grading upward into conglomerate, Granville Lake; **d)** sandstone-cobble conglomerate overlying (c) and grading(?) upward into the Sickie group, Granville Lake; **e)** cobble with crossbedding (arrow) suggesting provenance from shallow water deposit (photo from Corrigan and Rayner, 2002); **f)** turbidite-derived paragneiss with beds grading from metagreywacke (pale) to coarsely garnetiferous metamudstone (darker) and tops shown as arrows, Wapisu Lake. Tapes are 10 cm long.

for early arc magmatism along the TNB boundary (Rayner and Percival, 2007) with important connotations for the local tectonic history.

#### **3.2.3.4 Biotite granite–granodiorite (Rat granite: gn)**

The Rat granite (gn) is located along the Rat River, 5 km north of Notigi Lake, at the south margin of the LRD, where it forms an asymmetric dome mantled by the Sickle group. This biotite granite is foliated, pinkish-grey and medium grained. It contains subequal amounts of quartz, plagioclase and potassium feldspar with about 5% biotite and accessory magnetite, apatite, monazite and zircon. Equant grains up to 4 mm in diameter suggest an igneous texture with development of dynamo-thermal metamorphic subgrains and local myrmekite along grain boundaries. The granite has a crystallization age of ca. 1838 ±4 Ma (Section 5.1.3) indicating that it was emplaced relatively shortly before or during the deposition of the oldest units in the Sickle group but probably later remobilized. The Rat granite, like similar-aged trondhjemite farther east, at Leftrook Lake (Section 5.1.3), forms a structural apophysis at the south margin of the LRD.

#### **3.2.3.5 Notigi monzogranite (mg) and granodiorite (Lgg)**

At Notigi Lake, north of Timew Island, a composite pluton of monzogranite (mg) and younger granodiorite (Lgg) occurs near the core of the northeastern culmination of the Notigi structure. Unit Lgg has intruded biotite gneiss (Kb) and sillimanite-bearing gneiss (Ksb) of the Sickle group. The southern contact of the ca. 1862 Ma monzogranite appears to truncate the layered amphibolite of the Granville complex. Outcrops of presumably an oval, post-Sickle granodiorite in the west and the elongate, pre-Sickle monzogranite in the east are separated by low ground with no exposures (Murphy and Zwanzig, 2019a). The monzogranite (mg) is leucocratic, commonly pink, with foliation defined by <5% mafic grains. It contains about 35% quartz, 30% each of micropertite and plagioclase and minor amounts of biotite, hornblende, ilmenite and tourmaline. The presence of minor hornblende and significant ilmenite in thin seams of melanosome in the leucocratic monzogranite suggests low-temperature partial melting of this rock. The monzogranite has a medium-grained metamorphic texture with abundant myrmekite and replacement textures of K-feldspar after plagioclase, biotite after hornblende, and leucosome after ilmenite. It was affected by the adjacent granodiorite or by metamorphic fluids. These textures and its contact relations with sheared sidewalls are interpreted to be the result of structural emplacement during high-grade metamorphism.

The western body (Lgg; Murphy and Zwanzig, 2019d), which intrudes the Sickle group, has a strong aeromagnetic signature and has magnetite- and cordierite-bearing schlieren presumably entrained from the Sickle group. It has different

trace-element contents to the granodiorite, and higher alumina to alkali ratio (A/CNK) that indicate a component of sediment-derived melt (Section 4.4.3).

#### **3.2.4 Burntwood group (B)**

The Burntwood group forms the dominant map unit in the Wuskwatim–Granville lakes corridor and the rest of the KD (Zwanzig, 1990, 1999). It consists mainly of folded, faulted and metamorphosed greywacke–mudstone turbidite. It is structurally imbricated to the south with the Flin Flon domain (Bailes, 1980a; Zwanzig and Bailes, 2010) as well as to the east with the TNB (Zwanzig et al., 2007). Within the Wuskwatim–Granville lakes corridor, greywacke–mudstone (B) and quartz-feldspar-rich arkosic metagreywacke (Ba) are well preserved south of Granville Lake. East, towards Footprint Lake, upper amphibolite-facies garnet-biotite gneiss (Bg) derived from unit B has restricted exposure; graded bedding is only locally preserved in Bg. Most eastern areas are underlain by metatexite (Bm), a layered garnet-biotite±sillimanite migmatite, and in some places by melt-dominated migmatite (diatexite, Bd), a garnet-biotite migmatite that is coarse-grained and homogenized with more than 50% leucosome. Southeast, at Wuskwatim Lake, cordierite and sillimanite are most common in Burntwood group migmatite. Orthopyroxene±spinel occur in some layers of high-grade metatexite (Bma) and diatexite (Bda).

Iron formation or sulphidic paragneiss (Bi) occurs as local interlayers in the Notigi–Wapisu lakes area. In an inferred fault-slices south of Granville Lake, the stratabound sulphide showings may occur above a footwall thrust, possibly at the stratigraphic base of the Burntwood group overlying back-arc basalt and gabbro (Gt). Similarly, southeast of Reed Lake, in the Flin Flon domain, graphitic pelite and sulphide-facies iron formation at the lowest exposed part of the Burntwood group also occur in thrust-contact with ocean-floor basalt (unit F1 in Gagné, 2017) and in the hangingwall of an adjacent imbricate. A similar contact with ocean-floor basalt occurs north of Reed Lake and extends toward the KD (Gagné et al., 2017). Faulting in the Flin Flon belt and south of Granville Lake is indicated by cutoffs and contacts with various units but may represent a detachment exploiting incompetent rock at the unconformable base of the Burntwood group. At Wuskwatim Lake, the Burntwood group lies on the thin unit of siliceous calcareous psammite (Gc) that is nearly identical in appearance and composition to Gc at Granville Lake. This unexposed contact is also interpreted as a thrust fault. At Notigi Lake, the Burntwood–Granville-complex contact is indicated by local biotite schist, considered to represent a fault.

The top of the Burntwood group is exposed along the south shore of Granville Lake, where it grades upward into the Sickle group. This local section lies above the folded and thrust-faulted stack with thick north-younging limbs and thrust-panels. The succession is estimated to be a minimum of 1100 m thick after inverted limbs are removed but potential

thrusts ignored. The stratigraphic top of this succession coarsens upward from deep-water graphitic turbidite into a unit of sandstone-cobble conglomerate (Bc) that ranges up to 300 m thick or, along strike, into feldspathic greywacke with metamorphic amphibole (Bca). Upward coarsening also occurs in a 100 m thick lens of feldspathic greywacke (Bcb) that contains progressively coarsening and thickening interbeds of pebble conglomerate. Similar interbedding of greywacke and pebble conglomerate in transition to arkosic rocks (Missi group) occurs also on the south flank of the KD (Zwanzig and Bailes, 2010).

The mafic minerals in the best preserved Burntwood group south of Granville Lake are biotite±garnet and include iron sulphide at the top. In contrast, the arenite and pebble conglomerate of the overlying Sickie group generally contain hornblende and magnetite. The local base of the Sickie group is defined by the first appearance of pink- and green-weathering beds with K-feldspar, abundant magnetite and lacking sulphide. This represents a change in deposition from a reducing (deeper water) to an oxidizing (shallower water) environment.

#### **3.2.4.1 Greywacke–mudstone (B, Ba)**

Exposures of unit B, south of Granville Lake to the middle of Wheatcroft Lake, contain turbidite bed forms that grade upward from light-grey–weathering greywacke into darker, locally laminated mudstone (Figure 8b). Median bed thickness ranges from 5 to 20 cm but beds can locally reach 1 m. Mudstone makes up ≤35% of the turbidite beds and is most prominent in the upper part of the succession. Original grains (≤1.5 mm) are rarely preserved, but the change from greywacke to mudstone is marked by an increase in biotite content from about 10% to 35%. There is a sporadic, but generally concomitant, increase in graphite content from a trace to more than 5%. Minor minerals also include apatite, tourmaline, monazite and zircon. K-feldspar, sillimanite and late muscovite occur locally. The restriction of garnet (≤1.5 mm in diameter) to only a few of the most shaly beds at Granville Lake is unusual for the Burntwood group compared to the rest of the KD, where the rock is more coarsely recrystallized and probably more pelitic. Lenses with calcsilicate minerals are interpreted as calcareous concretions. Local late-synsedimentary folds and thrusts may indicate that deformation occurred prior to complete dewatering and lithification (see Section 6.1.1). Early asymmetric structures suggest southeast mass transport. An unusual bed of intermediate fragmental rocks occurs within unit B near the top of the succession.

Light grey to tan arkosic greywacke (Ba) exposed farther south of Granville Lake commonly has graded beds up to 60 cm thick and locally up to 2 m massive beds with ≤2.5 mm clasts. Dark grey mudstone, 0.5–2 cm thick, caps many beds. Scour structures and rip-ups occur at the base of some beds. Unit Ba has more quartz and less biotite (median of 15%) than unit B. There is K-feldspar (≤25%) and muscovite in more than half the samples, and sporadic sillimanite and graphite throughout.

Garnet is rarely present and the graphite (≤5%) occurs in irregularly scattered beds.

The arkosic greywacke (Ba) has virtually the same major and trace-element composition as the muscovite- and/or sillimanite-bearing meta-arkose in the upper part of the Sickie group (unit Ks; Section 4.1). Unit Ba occurs low in the Burntwood structural section, and was likely deposited relatively distant from shore but was overrun by more proximal facies, and may be coeval with the lower part of the Sickie succession of equivalent composition.

#### **3.2.4.2 Upper greywacke and conglomerate (Bca, Bcb, Bc)**

High in the Burntwood section the greywacke has interbedded pebbly horizons and feldspathic or sillimanite-bearing horizons (combined in unit Bcb, Figure 8c). This unit also contains thick local beds of coarse-grained sandstone, some with deep basal scours and crossbedding indicative of shallow-water deposition. These may have formed in an upper-fan setting. Interbeds are similar to units B and Ba. An upward decrease in biotite content in this part of the section is consistent with a decrease of mudstone and general upward coarsening. Groups of beds are variable in composition; most contain late muscovite and some have K-feldspar and abundant sillimanite (faserkiesel). Graphite appears to be lacking, but minor Fe-sulphide is present. Pebble beds are either matrix supported or clast supported. Some show normal grading with reverse-graded bottoms.

The conformably overlying conglomerate unit (Bc) is more than 10 km long and up to 300 m thick and consists of clast-supported cobbles and pebbles of sandstone (Figure 8d). The cobbles have biotite-rich bedding-plane partings and rare internal crossbedding (Figure 8e) not generally found in the stratigraphically underlying Burntwood group rocks (B). At one location, a quartz vein is confined to a single clast. These structures suggest a provenance from older, well-lithified, shallow-water sandstone, perhaps an ephemeral precursor to the Burntwood and Sickie groups. The lens shape of the conglomerate unit suggests that it may have been a broad feeder channel to younger distal parts of the Burntwood group to the south. As the conglomerate tapers toward the east, it grades into the upper, feldspathic greywacke (Bca). This unit (Bca) contains local hornblende and has poorly preserved bedding. It is only a few tens of metres thick and appears to form the local gradation between the Burntwood group and the Sickie group.

#### **3.2.4.3 Greywacke–mudstone gneiss and migmatite (Bg, Bm, Bma, Bd, Bda)**

The Burntwood group occurs as garnet-biotite±sillimanite gneiss (Bg) preserved in limited localities southeast of Granville Lake. It has remnant bedding and minor to moderate veining by leucosome (e.g., Figure 8f). Parts of unit Bm in remapped areas were previously mapped as unit Bg with up to 25% granitoid “segregation”, although, bedding is preserved in many

places and locally shows grading. Unit Bg at Wapisi Lake and near Threepoint Lake generally has about 10% plagioclase- and quartz-cored boudins of leucosome with only minor mafic minerals (Figure 9a). Where studied in detail (Zwanzig, 1999) these are the earliest leucosome veins, and may have resulted from in situ fluid-present melting of quartz and plagioclase (Zwanzig and Bailes, 2010) or subsolidus segregation (Sawyer and Barnes, 1988). At high structural levels, such as at Granville Lake or in some structural basins farther southeast, metagreywacke (B) or greywacke-gneiss (Bg) is intruded by pegmatite (Lpg) or granite (Llg, Lgg) with sharp, locally crosscutting contacts (Section 3.2.7). Unit Bg commonly has about 15% garnet porphyroblasts (1.0–2.5 mm in diameter) with the larger grains occurring in the upper, more pelitic parts of beds. Biotite content is variable; in some layers sillimanite forms small faserkiesel with sillimanite plus quartz or plagioclase. Cordierite is also locally developed. Accessory minerals include graphite, monazite and zircon. Biotite is strongly aligned with the transposed bedding, although metamorphic layering (gneissosity) is weak.

Most of the Burntwood group southeast of Granville Lake occurs as garnet-biotite±sillimanite migmatite, commonly as metatexite (Bm) with 10–50% leucosome (Figure 9a–c) or lesser diatexite (Bd) with disrupted primary structure (Figure 9d) and more uniform partial melting or granite injection with up to 90% neosome or leucosome. About 5–25% early, quartz-rich leucosome occurs in layers and lenses up to 15 cm thick in the metatexite. Thicker sheets of leucogranite occur in a wide range of proportions in various outcrops and may be intrusive. The migmatite at Wapisi Lake generally has 10–65% leucosome that occurs in three locally crosscutting generations. Leucosome layers are up to 50 cm thick and most have the same composition as adjacent larger granitoid units (Lgg, Llg and Lpg). Rafts and schlieren of Burntwood group unit Bm are incorporated in the late granitoid components. Although slightly more coarsely recrystallized at Threepoint and Wuskwatim lakes, with garnet up to 20 mm in diameter and cordierite up to 30 mm long, leucosome is generally less than 10–15 cm thick. It has less sharply defined contacts suggesting in situ melting, whereas sharp-walled granite veins and sheets farther west are considered intrusive (Figure 9b). The latter suggest transfer of melt from deeper structural levels.

The mineralogy of the Burntwood group greywacke–mudstone-derived metatexite (Bm) at Notigi Lake includes quartz, plagioclase, garnet, biotite, cordierite, tourmaline, locally graphite and rare orthopyroxene. Small (ca. 5 mm) garnets are ubiquitous in psammite and larger garnets (≤20 mm) in pelite. In places, tourmaline was replaced by chlorite during retrograde metamorphism; cordierite was pinitized and garnet was partly chloritized. At Wapisi Lake the unit contains abundant biotite, up to 15% garnet and, in places, cordierite. At Wuskwatim and Threepoint lakes, by comparison, neosome of the metatexite (Bma) commonly contains more garnet (ca. 20%), up to 30 mm in diameter, and occurs with sillimanite, cordierite and local orthopyroxene, apparently in aluminous layers.

Diatexite derived from unit B has two end members, both mapped as unit Bd. One is highly injected by leucogranitoid rock in veins and sheets that commonly contain sieve-textured garnet±cordierite±sillimanite and up to 25% greywacke mesosome in rafts or melanosome in schlieren. The other is relatively uniform but coarsely recrystallized neosome with large porphyroblasts of feldspar, garnet (≤30 mm) and cordierite±sillimanite. At the highest grade, mainly coarse-grained diatexite (Bda), such as exposed on the south shore of Wuskwatim Lake, contains antiperthitic plagioclase. K-feldspar-garnet-cordierite-sillimanite coexist, and rare orthopyroxene is present.

#### **3.2.4.4 Iron formation (Bi)**

Sulphidic silicate-facies iron formation (Bi) forms local grey to brown concordant layers and pods typically 1.5 m in thickness, alternating with layers of greywacke and thinly layered chert that contains pyrrhotite, magnetite and rare chalcopyrite. At two locations at the southwest end of Notigi Lake (Murphy and Zwanzig, 2019c) concordant pegmatite and granitic rocks intrude along the contact between iron formation and greywacke.

#### **3.2.5 Intrusive rocks (unknown age, felsic to mafic)**

The relative and absolute ages of a wide variety of intrusions along the north flank of the KD and the Northeast Kiskeynew subdomain are uncertain because contacts are covered or highly strained, and/or U-Pb geochronology was either unsuccessful or not attempted. Most of the intrusive rocks are strongly recrystallized, strained internally and folded with the supracrustal rocks. Sills/dikes of syenogranite to granodiorite (gx) occur at Wapisi Lake. In the southeast the tonalite and gabbro units (tx, gb) contain abundant clinopyroxene and local orthopyroxene. Charnockite is not part of these intrusions of uncertain Paleoproterozoic age. The intrusive rocks that extend south across Bison and Tullibee lakes show various degrees of cataclasis and mineral retrogression after lower granulite-facies metamorphism. These bodies were transposed into parallelism with the adjacent TNB during late-stage deformation.

##### **3.2.5.1 Biotite granite to granodiorite (gx)**

At Threepoint Lake, a large pink-weathering intrusion of heterogeneous biotite granite to granodiorite forms part of an east-west-trending chain of poorly exposed plutons that are identified on the basis of their prominent magnetic signatures. The Threepoint Lake pluton is strongly foliated and occupies the core of a large northeast-trending antiform that crosses the east-west-trending chain. Thin belts of the Wuskwatim Lake sequence form a local mantle and extend east and west, suggesting that the pluton represents a culmination of older rocks in the KD. One of the few exposures near the center of the pluton is a pale pink-weathering granite (gx) with about 30% quartz, 40% K-feldspar and 20% plagioclase, with

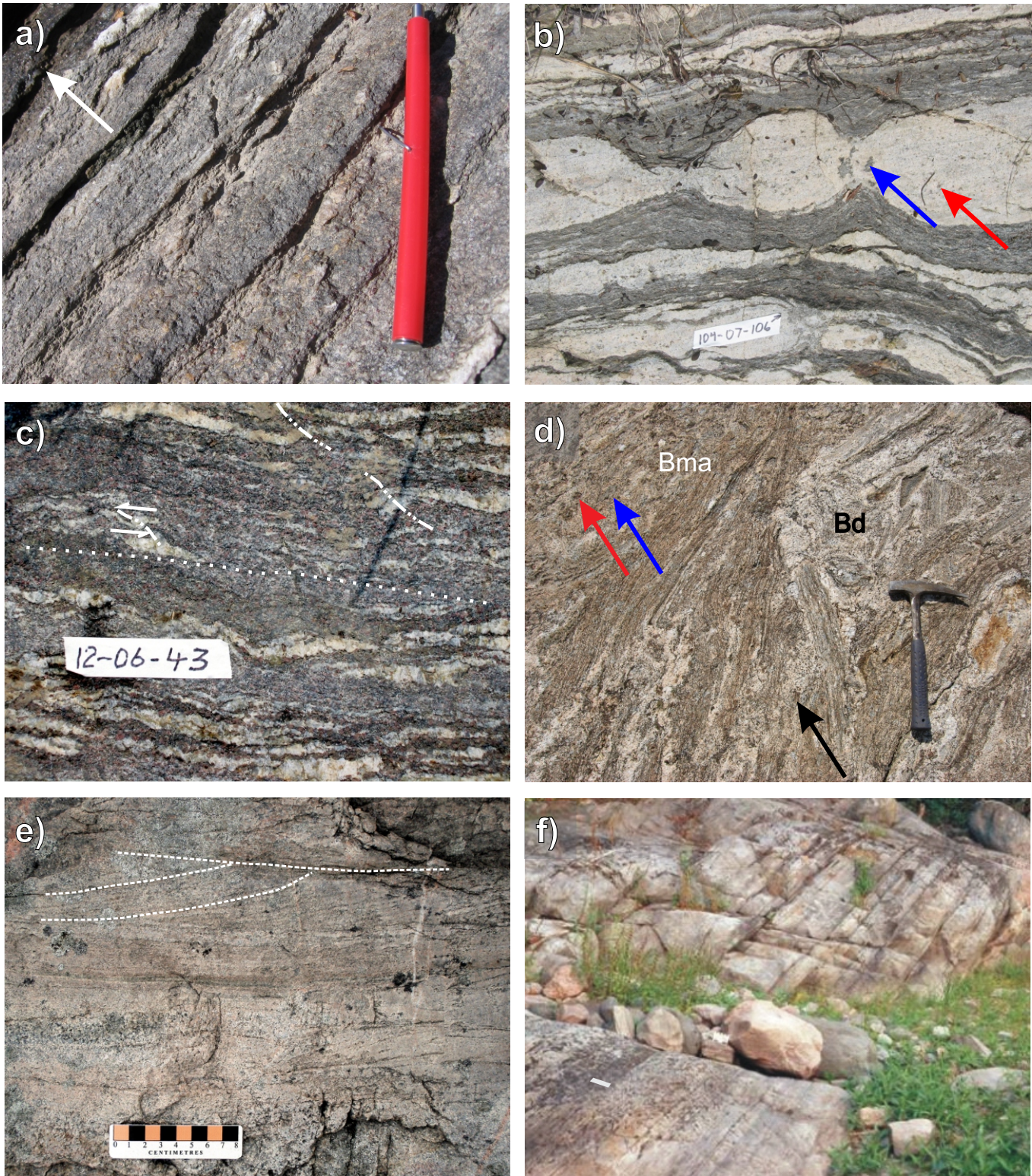


**Figure 9:** Field photographs of Burntwood and Sickle group rocks: **a–d)** greywacke–mudstone-derived gneiss and migmatite; **a)** garnet-biotite gneiss (Bg) showing compositionally graded bedding from quartz-plagioclase-rich psammite with small sparse garnet (e.g., base of arrow) through semipelite with more biotite producing foliation (arrow centre) up to recessive biotite schist with larger, more abundant garnet (arrow head), white lenses are early quartz-vein boudins with rims and tails of quartz-plagioclase leucosome; **b)** early wispy trondhjemitic in situ veins in garnet-rich melanosome indicating melt loss; also late injected granite sheets (with pinch-and-swell structure) indicating open-system metamorphism and high strain; cordierite (blue arrow) and garnet (red arrow) in granite, unit Bm, Notigi Lake; **c)** garnet-rich metatexite (Bm) with  $\leq 50\%$  garnet in melanosome (below tape), and consistent intrafolial S folds with axial planes (lines)  $\sim 45^\circ$  to sinistrally flowing foliation and small shear (dotted line), Wuskwatim Lake; **d)** highly mobilized migmatite (Bma), after melt loss, and diatexite (Bd), all with abundant garnet, cordierite and orthopyroxene (red, blue and black arrows), partly retrogressed to biotite and chlorite; **e, f)** Sickle group basal units, northern succession, Granville Lake; **e)** lower, crossbedded meta-arkose (Ksa); **f)** basal quartzite (Ksc) unconformably on Granville complex (to left, off photo). Note overturning. Magnet and tapes are 10 cm long.

5% biotite±hornblende partly altered to chlorite. Scattered orthopyroxene±cordierite, also altered, occurs in this rock and in pegmatitic mobilizate. Magnetite, pyrrhotite, apatite and zircon are present in the granite. Now-submerged outcrops also featured K-feldspar porphyroclasts (Baldwin et al., 1979) in a possible phase of unit qm (FLPS).

The origin and age of unit gx is uncertain. Based on its mineralogy, geochemistry (Section 4.3.3), positive magnetic anomaly and previous mapping of an abundant porphyritic phase, it is most likely associated with the FLPS. It may represent a late phenocryst-free phase or a younger phase that has assimilated FLPS rock. A sample of Llg from this body has an Archean Nd-model age (2.54 Ga; DRI2021014). This is consistent with either of the above origins but most likely with young assimilation. It was intruded by still younger leucogranite (Llg) and local pegmatite.

Somewhat similar looking pink granitoid sheets (gx/Llg) at Wapisi Lake occur at the margin and center of the western FLPS intrusion; another occurs in the main part of the lake. They have a lower quartz content and more feldspar and mafic minerals than the granite at Threepoint Lake. The sheets include fine-grained syenogranite, monzogranite, and granodiorite. A sheet of similar granodiorite (mapped as gx) at Wapisi Lake borders multiphase gabbro/gabbro-porphyry (gb; Section 3.2.5.3). This sheet contains 20% quartz, 6–8% each of garnet and clinopyroxene with 5% biotite, some in aggregates that may be pseudomorphs after orthopyroxene.

Large bodies of granite south of Bison Lake (Figure 1) surrounded by the Burntwood group may also be associated with the FLPS. They weather pink with moderate to high K-feldspar contents and mainly biotite as mafic phase. Magnetite is ubiquitous and results in a prominent aeromagnetic signature (Murphy and Zwanzig, 2019d). All bodies are strongly foliated to gneissic. Textures range from granular to porphyritic. Close to Setting Lake, to its west (Figure 1), smaller bodies with similar lithology yielded old Nd-model ages typical of the FLPS, and a poorly defined U-Pb zircon age of about 1.87 Ga (Zwanzig et al., 2003). Much of the rock in the larger bodies where these seem to contact and apparently intrude the Burntwood group, however, may be younger than the FLPS.

### 3.2.5.2 Tonalite (tx)

Sheets of foliated tonalite exposed along the Burntwood River, southeast of Threepoint Lake, adjoin probable Archean basement gneiss (Ag), and granite (gx) of uncertain age. The tonalite has elongate intermediate inclusions and in places appears to contain orthoamphibole largely replaced by biotite. Its main phase is rich in plagioclase with about 25% quartz and 10–20% biotite as well as chlorite and relatively abundant magnetite and titanite. Local agmatite that consists of tonalite enclaves and a granite or granodiorite matrix, east of Threepoint Lake, is also included in unit tx. Rare agmatitic tonalite is also exposed in the Wuskwatim Lake area.

### 3.2.5.3 Gabbro, amphibolite (gb)

Gabbro sheets and lenses (gb) occur locally in the older plutons (qm, tn). These are too small to depict at the mapping scale and have an unknown absolute age. Dikes and boudins of strongly recrystallized migmatitic gabbro (gb) are locally abundant in the Wuskwatim Lake sequence and its Archean basement, and likewise have an unknown age. The scarcity of similar rocks in the surrounding Burntwood group suggests that they may be older, at least in part. They have aphyric and rare plagioclase-phyric textures, similar thickness and locally complex contact relationships (Figure 3b, c), comparable to the ca. 1.88 Ga dikes in the TNB. Migmatitic amphibolite domains in the Archean basement are included in units Ag, Ai.

A composite gabbro, gabbro-porphyry and granodiorite intrusion (gb, gx) about 20 m wide is exposed along the west shore of Wapisi Lake, surrounded by the Burntwood group. It comprises from north to south:

- 1) mafic plagioclase-hornblende porphyry;
- 2) plagioclase-diopside gneiss;
- 3) hornblende-diopside gneiss;
- 4) plagioclase porphyry that appears to grade from coarse- to fine-grained over a distance of 9 m; and
- 5) locally hypersthene-bearing granodiorite (gx), interpreted as the youngest phase.

Phases 1 and 3 are geochemically similar to the Hatchet Lake gabbro (Section 4.2), but the intrusion has an unknown age. The intermediate phase has 5% magnetite and conspicuous apatite and, in addition, contains clinopyroxene±cummingtonite±orthopyroxene similar to intrusions into the Burntwood group south of Granville Lake. Mafic to intermediate sheets (gb) that occur directly to the northwest of the composite gabbro have an uncertain affinity. In addition to hornblende-diopside amphibolite with biotite and magnetite, these contain quartz-diopside-calcite layers and diopside-calcite-titanite±tremolite layers that may be tectonized correlatives of unit Gtb. In this case, the amphibolite may be part of a sliver thrust into the Burntwood group.

### 3.2.6 Sickie group (K)

The Sickie group consists of mainly nonmarine arkosic and lithic meta-arenite and derived magnetite-bearing quartz-feldspathic gneiss in locally traceable stratigraphic units. These units are interpreted to represent different depositional facies defined by field characteristics or, in the highest-grade rocks, mainly by metamorphic mineralogy resulting from bulk compositions. These define a unique stratigraphic sequence mainly in the Granville Lake area but vary across high-amplitude major folds and for tens of kilometres along strike farther east. Units likely reflect both stratigraphic and lateral changes in depositional facies as well as structural repetition. Allowing for stratigraphic pinchout of some units and the overstepping of others, the Sickie group has a broadly consistent stratigraphy from the

west end of the Lynn Lake belt to the TNB, much like the correlative Grass River group.

Large structures at Granville Lake feature somewhat different stratigraphic successions. One occupies a narrow syncline at the south shore; another succession forms the very thick, dominantly north-facing limb of a synclinorium north of the Granville Lake structural zone (Figure 5; Zwanzig and Corrigan, 2005), which differs slightly from the north limb. These differ, in turn, from the northwest area around McGavock and Tod lakes. The successions are interpreted to have occupied different sub-basins that may have been fed by different point sources and/or were partly separated by barriers. Apparently, they started to be filled and may have formed in a northwest-southeast progression. The Sickle group from Notigi Lake eastward is characterized by attenuated units and abrupt mineralogical changes (reflecting bulk composition) that occur for 50–500 m across strike. Gneissic units are mapped continuously for 5 km or more and are defined largely by the presence or absence of amphibole, sillimanite and locally cordierite. The highest grade rocks in the eastern part of the Wuskwatim–Granville lakes corridor have characteristics of the eastern and southern sequences. The presence of intraformational conglomerate within the Sickle group at McGavock Lake and the cut-outs of lower units in the southeast suggest that there are low-angle unconformities in the group.

The sedimentary succession of Sickle group in a north-western sub-basin and the north side of an eastern sub-basin lie in high-angle unconformity on (arc) volcanic and plutonic rocks (Milligan, 1960), whereas those on the south side of the eastern sub-basin lie in low-angle unconformity on the Granville complex. The southern succession is interpreted to lie conformably on the Burntwood group in the south and is faulted in the north. It occupies a southern sub-basin, generally south of the Granville complex. The changes in contact relationships and sedimentary facies have important tectonic and paleogeographic implications. The two sub-basin successions recognized at Granville Lake extend along the length of the Kiskeynew north flank (Figure 5b).

Previous mapping indicated that the Sickle group close to the Lynn Lake belt comprises more than 3000 m of fluvial-alluvial arenite including coarse pebbly sandstone that overlies up to 800 m of polymictic pebble and cobble conglomerate at the base of the group (Milligan, 1960; Syme, 1977; Zwanzig, 1979). Some abrupt facies changes at the edge of granitoid-basement highs suggest deposition in fault-bounded sub-basins (Zwanzig and Corrigan, 2005). Wedges of basal conglomerate with interfingering crossbedded arkose are up to 1000 m in the north and taper to the south (Zwanzig, 1981). A middle unit of ca. 1000 m laminated to massive pink-, grey- and green-weathering sandstone to mudstone with minor carbonate overlies the basal units at Lasthope Lake (Figure 5). In the southeast, this unit is characterized by containing metamorphic amphibole, epidote±calcite but has locally preserved mudcracks (Zwanzig, 1981). As remapped at the south shore of Granville Lake, the facies of the middle

unit overlies the Burntwood group with only pebble interbeds at the base. More than 1000 m of reddish, crossbedded, muscovite-rich meta-arkose overlies the middle unit in the north. This uppermost unit is grey and ripple laminated farther southeast. It grades from coarse-grained meta-arkose in the north to finer-grained, quartz-rich lithic arenite with metamorphic biotite, muscovite±sillimanite on Granville Lake.

The transition between sedimentary rocks with preserved primary features and entirely recrystallized metamorphic rocks is crucial to interpreting the highest-grade metamorphic rocks and their stratigraphy in the Wuskwatim–Granville lakes corridor. The rocks in the northwest also establish a regional fining and consequent sediment-transport direction to the southeast. This lateral change continues along the Granville–Wuskwatim corridor with basal quartzite or conglomerate in the northwest (Section 3.2.6.1) and protoquartzite to psammite (containing garnet and sillimanite) in the Leftrook–Harding lakes area in the east (Zwanzig and Böhm, 2002, Figure 1). The tapering direction of the lower units, and the changes from basal conglomerate to basal quartzite and southward to conformity with the largely coeval Burntwood group are all to the southeast (Figure 5a; Zwanzig, 2019). This prompts the interpretation that the orogenic, oxidized sediments of the Sickle group and unknown forerunners prograded into the deeper Kiskeynew turbidite basin, where they became graphitic and were mapped as the Burntwood group. These stratigraphic and structural relations are consistent with the very similar age distributions of detrital zircons in the two apparently partly coeval groups (Section 5.1.5). The relations also suggest that the inception of the proposed Burntwood megathrust was coeval with sedimentation such that the Sickle group may be interpreted as an overlap assemblage.

### **3.2.6.1 Arkose (Ks), crossbedded arkose (Ksa) quartzite (Ksc): lower succession, eastern sub-basin**

Arkosic rocks occur at high and low stratigraphic levels in the Sickle group throughout the north flank of the KD. These rocks generally have higher quartz and K-feldspar contents than other units and may contain large quartz-sillimanite knots (faserkiesel). At the low stratigraphic level of the eastern sub-basin, at Granville Lake, meta-arkose (Ksa) with muscovite and local faserkiesel has retained local crossbedding (Figure 9e). This unit is stratigraphically underlain by up to 20 m of coarse-grained (≥3 mm) quartzite (Ksc) that has been traced for 2 km unconformably overlying the Granville complex. The base of unit Ksc is white- to grey-weathering quartzite with a red or green cast and grades upward into arkosic quartzite (Figure 9f). The overlying unit is finer, buff-weathering meta-arkose (Ks) with muscovite and faserkiesel. Quartz-rich arkose in lower sections contains more plagioclase than K-feldspar but has increasing K-feldspar content higher in the section. Biotite and muscovite generally make up less than 5%; quartz-sillimanite faserkiesel are widespread in more micaceous layers. Faserkiesel are 1–2 cm long and have a sillimanite-rich core surrounded

by quartz and generally rimmed by late muscovite. Fresh metamorphic K-feldspar occurs in the granoblastic matrix and was not observed in contact with sillimanite. Magnetite is ubiquitous and, in many places, concentrated in bedding partings or placers in crossbedding.

### **3.2.6.2 Light grey to reddish metasandstone (Kba): lower succession, eastern sub-basin**

Thick-bedded ( $\leq 100$  cm) grey and reddish-grey metasandstone (Kba) occurs locally above unit Ksa, below and interlayered with unit Khb at Granville Lake. It contains subequal parts of quartz and plagioclase with lesser K-feldspar and 1–2% biotite and magnetite. Large-scale ( $>25$  cm thick) crossbedding indicates the younging directions. One crossbedded interval has K-feldspar in excess of quartz and plagioclase, about 10–15% biotite, accessory magnetite and apatite.

### **3.2.6.3 Greenish-grey calcsilicate metasandstone (Khb): middle unit, eastern sub-basin**

The central unit (Khb) in the northern succession at Granville Lake is a hard, fine-grained greenish-grey to pink rock with thin calcsilicate layers (Figure 10a). Grey and pale pink beds (2–40 cm thick) vary from quartz rich with only plagioclase, to K-feldspar rich with less quartz. Most beds contain less than 5% biotite and late muscovite. Magnetite ranges up to 3% and is partly altered to hematite or locally pyrrhotite. Apatite and tourmaline are accessory. Epidote occurs locally in the fine-grained layers. The nearly ubiquitous 1 to 5 cm thick, green calcsilicate layers that typify the unit are rich in epidote and amphibole. Their origin is uncertain but may be related to lacustrine carbonate deposition and cementation.

### **3.2.6.4 Muscovite-rich meta-arkose $\pm$ sillimanite (Ks): upper unit, eastern sub-basin**

The upper stratigraphic level of meta-arkose at Granville Lake, which extends from the south shore into the central part of the lake, is rich in muscovite (ca. 15%) and K-feldspar, and locally includes minor sillimanite-bearing beds. It is mapped as unit Ks similar to the lower unit because east of the lake the upper and lower sections cannot always be distinguished due to complex folding, high-grade metamorphism and subtle sedimentary facies changes. In the less coarsely recrystallized rocks, in the upper section at Granville Lake, quartz and plagioclase are generally abundant but K-feldspar content locally exceeds that of quartz. Biotite measures less than 5%. Muscovite is late; magnetite, apatite and tourmaline are accessory. Beds are uniform, reddish- and greenish-grey, generally 5–10 cm thick to laminated, and locally with thin calcsilicate seams. In the north, higher in the section, beds are 10–20 cm thick. In the uppermost exposed part of the section, the beds are up to 50 cm thick, locally weakly graded and have muscovite-rich laminated tops (Figure 10b). Rip-ups of more biotite-rich argillite occur in some of these bedding bases, suggesting deposition by flash floods in

the vegetation-free, desert-like environment of the Paleoproterozoic.

### **3.2.6.5 Amphibole-bearing arenite and conglomerate (Kha, Khc): lower units, southern sub-basin**

The southern sub-basin of the Sickie group at Granville Lake has a lower hornblende-bearing unit (Kha) of pink-, grey- and green-weathering metasandstone, up to 160 m thick. The unit includes clast-supported pebble conglomerate (Khc), up to 40 m thick, at or near the base, but this tapers out toward the east. Clasts consist mainly of pink and grey arkosic rocks. The conglomerate matrix has abundant epidote and several types of amphibole. The lower contact of this succession is conformable, possibly gradational into sandstone-cobble conglomerate (Bc) or conformable on hornblende-bearing greywacke (Bca) of the Burntwood group.

The metasandstone (Kha, Figure 10c) contains subequal parts of quartz and plagioclase with successively less K-feldspar, green amphibole, biotite, titanite, epidote, magnetite, calcite and apatite. Some beds contain only biotite and magnetite as mafic phases and have thin layers rich in K-feldspar. These can have selvages with coarse biotite and magnetite around small lenses of incipient granitoid leucosome. They contain chlorite, muscovite and calcite, probably as secondary minerals. Some granite veins cut across the layering. Other beds are laminated and rich in epidote and amphibole (total  $\leq 40\%$ ). Despite the metamorphic grade and structural flattening, some areas show bedding-plane partings interpreted as trough-crossbedding (Figure 10).

Unit Kha is the stratigraphically lowest magnetite-bearing (oxidized) unit of original redbeds in the southern basin. It is considered to be a fluvial-alluvial unit lying on the iron-sulphide-bearing (reduced; i.e., marine) conglomerate (Bc) assigned to the Burntwood group.

### **3.2.6.6 Locally crossbedded meta-arkose (Ksa), conglomerate (Ksd): upper units, southern sub-basin**

Meta-arkose (Ksa) in the long narrow syncline on the south shore of Granville Lake (southern sub-basin) lying stratigraphically above the basal hornblende-bearing metasandstone or conglomerate (units Kha, Khc) contains muscovite  $\pm$  sillimanite and has locally preserved crossbedding. Trough-crossbedded rocks high in this section are darker, lack sillimanite and compositionally resemble unit Kba. The arkosic section tapers out to the east (see above) and may form the basal unit on the north limb of the syncline as suggested by a local conglomerate lens (Ksd) at the northern contact. Reliable tops from crossbedding are generally absent in the northern exposure of this unit, and part of the contact is a fault.

### **3.2.6.7 Biotite gneiss (meta-arenite), Kb**

Arenite-derived biotite gneiss (Kb) is abundant at Notigi Lake. It appears to occur at various stratigraphic levels, often

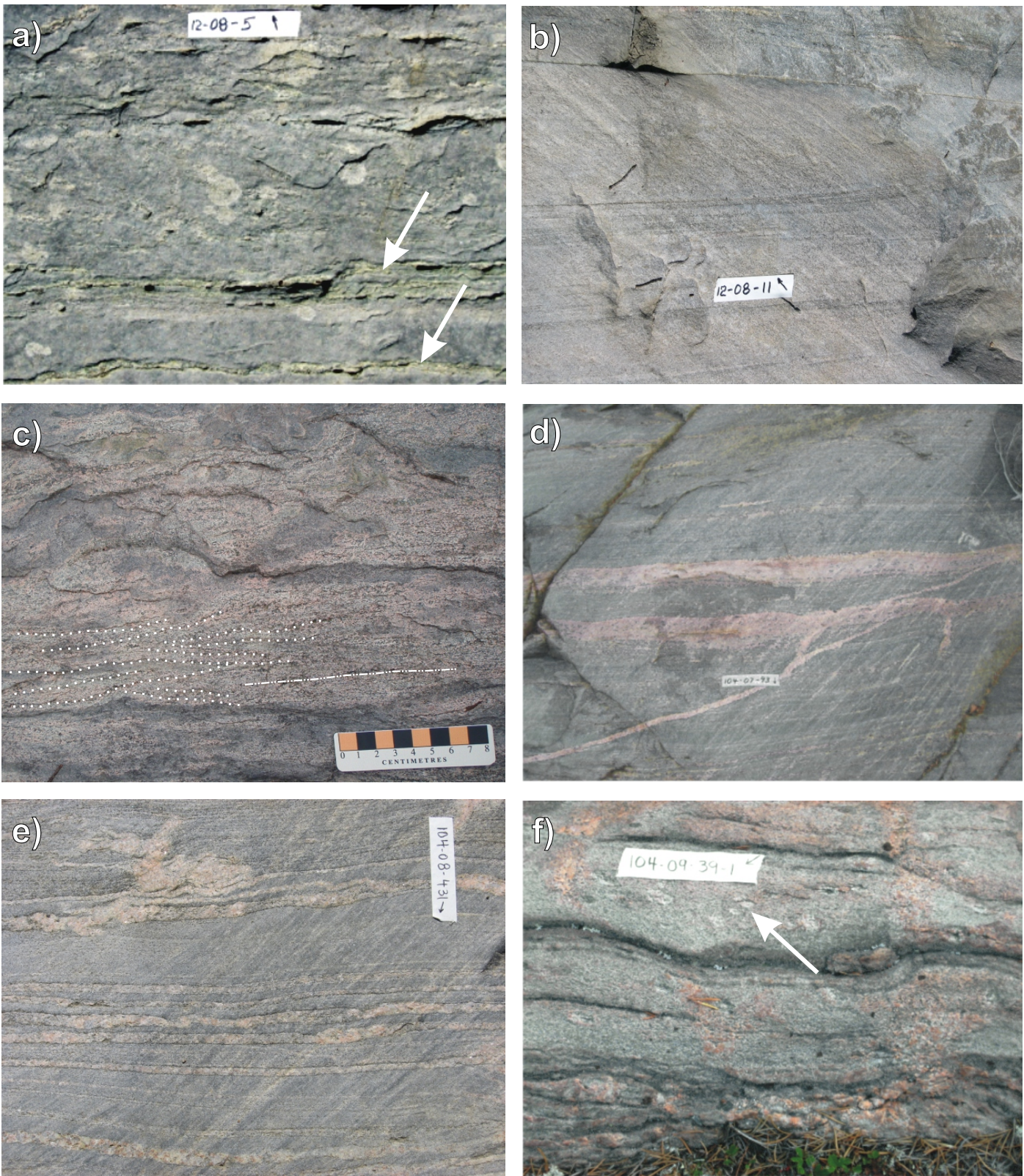


**Figure 10:** Sickie group, photographs of main units: **a)** fine-grained, greenish-grey calcisilicate metasandstone±amphibole with epidote-rich calcisilicate horizons along bedding planes (arrows), central unit in northern section, Granville Lake; dots are lichen; **b)** muscovite-biotite-bearing meta-arkose with rare sillimanite; some beds showing weak grading with laminated tops and may have been deposited by flash floods; **c)** hornblende-bearing meta-arenite (Kh), basal unit on Burntwood group, south shore of Granville Lake (southern sub-basin); outlined bedding-plane partings suggesting trough-crossbedding flattened in  $S_2$ ; **d)** hornblende-biotite-bearing psammitic gneiss on Notigi Lake ranging from laminated (photo) to massive and correlates with (c); **e)** biotite-bearing migmatitic meta-arenite (Kb), Notigi Lake; **f)** sillimanite-bearing gneiss (Ksb) forming the upper unit at Notigi Lake and farther east. It may correlate with (b) but at higher metamorphic grade with muscovite consumed and having quartz-sillimanite knots (faserkiesel, e.g., at arrow). Fresh K-feldspar from the reaction occurs outside the knots. Tapes are 10 cm long.

interleaved with Kh. The unit weathers from light to medium grey and brown to reddish brown. It may have pink to reddish leucosome, very locally up to 60% but on average less than 20% (Figure 10e). The gneiss also varies from a very fine-grained, uniform arenite to thin-bedded (at cm scale) more coarsely recrystallized paragneiss. The mineral content of Kb includes quartz and feldspar, generally with biotite and magnetite as the only mafic minerals. Locally there is also cordierite, tourmaline, garnet, epidote, diopside, muscovite, sillimanite, hematite and rare malachite. Magnetite is generally present (<5%) as subhedral crystals that range up to 3 cm in diameter and may occur in 10 cm clusters. Closer to the core of the northeastern Notigi culmination, Kb may contain up to 10% pink to red leucosome or, rarely, up to 80% of injected granite. Closest to the core, Kb is interlayered with the sillimanite-bearing gneiss (Ksb).

#### **3.2.6.8 Hornblende-biotite meta-arenite/gneiss (Kh)**

Paragneiss (Kh) at Notigi Lake containing hornblende and biotite was derived from sandstone similar to units Kha and Khb and weathers greenish-grey to pink (Figure 10d). Unit Kh is typically interlayered with hornblende-free biotite gneiss and more rarely grades into a biotite-free hornblende gneiss. Massive grey and locally laminated varieties with a green and pink paleosome generally contain up to 15% pink granite leucosome. Uniform beds of unit Kh, up to 2 m thick, tend to be fine-grained, whereas thinly layered (0.5–10 cm) Kh is more coarsely recrystallized. The unit contains quartz, plagioclase, K-feldspar, hornblende, diopside, tourmaline with less magnetite than other Sickie group subunits. Amphibole is present in both the paleosome and leucosome, being much coarser in the latter. Diopside is abundant in certain layers and within cores of hornblende-rich lenses that sporadically occur in the leucosome. The lenses are in part boudinaged melanosome, which may have formed from thin calcsilicate layers found in unit Khb in the west.

#### **3.2.6.9 Sillimanite-bearing arkose-derived gneiss (Ksb, Kse)**

Arkose-derived gneiss of the Sickie group on Notigi Lake (Ksb) generally contains sillimanite knots (faserkiesel) or layers with sillimanite knots. Unit Ksb is interpreted to occur at two stratigraphic levels. It denotes a sedimentary facies rather than two formations. A thin unit of this rock type with abundant quartz lies locally at the base of the group and probably high in the structural stack. A thicker succession occurs in the upper part of the Sickie group from Notigi to Leftrook lakes and beyond. Unit Ksb weathers light grey to grey and pink with up to 40% pink leucosome. Where present, layering occurs at a centimetre scale with millimetre-scale biotite-rich laminae possibly representing transposed bedding or bedding-plane parting. Sillimanite occurs as fibrolite in the faserkiesel that are variably flattened and stretched, most strongly along the

attenuated limbs of the Notigi Lake structure. Some faserkiesel have a magnetite core.

Although these high-grade rocks have unreliable tops, the sequence of units is similar to the northward-younging succession at Granville Lake in which the lower and upper units of Ks would become Ksb after the complete reaction of muscovite to sillimanite. A similar upper unit is exposed 75 km west of Granville Lake in the Sickie group at Kamuchawie Lake (Zwanzig and Wielezynski, 1975). Unit Ksb also correlates with a very similar sillimanite-bearing, crossbedded unit at the top of the Grass River group along the TNB (Zwanzig et al., 2007).

The lower succession of Ksb at Notigi Lake is exposed close to the Granville complex. It has rare sillimanite but common retrograde muscovite that is interpreted as derived from sillimanite. Retrograde metamorphism is also evident as chloritization of biotite. On the mainland extending north and northeast of Timew Island (Murphy and Zwanzig, 2019a), rare cordierite occurs locally in the lower succession or in interlayers mapped as Kse (below). This lower succession of Ksb is tentatively correlated with basal Sickie group quartzite at Granville Lake and quartzose orthogneiss at Leftrook Lake. Lower unit Ksb is magnetite bearing and contains about 50–70% quartz, 3–10% biotite,  $\pm 1\%$  garnet ( $\leq 8$  mm, rarely  $\leq 30$  mm) and faserkiesel ( $\leq 20$  mm) in beds of aluminous composition. The rock has biotite-rich laminations and local concentrations of magnetite, interpreted as bedding-plane partings with placer minerals in crossbedding (Zwanzig and Böhm, 2002).

On the north shore of Timew Island and on the mainland farther northeast, unit Ksb is generally rich in quartz and feldspar and locally interbedded with light grey protoquartzite. It is derived from coarse-grained arkose with locally preserved crossbedding, and probably more argillaceous rocks with abundant faserkiesel ( $\geq 2$  cm; Figure 10f). The sillimanite-rich layers reflect local concentrations of alumina, probably from an original clay component. These rocks were not distinguished during mapping from the rest of the sillimanite-bearing unit elsewhere, but they overlie gabbro (interpreted as Gg), which suggests an early thrust fault at the base of Gg (Section 6.1.1). The local Ksb may be part of the lower succession lying unconformably on Gg, hence the presence of quartzite beds as with the basal unit (Ksc) at Granville Lake but more distal where true quartzite petered out.

Local exposures of quartzofeldspathic paragneiss within Ksb contain sillimanite and porphyroblasts of cordierite. This rock is designated as Kse but has not been traced along strike to form a mappable unit. It is interpreted to have formed in originally more magnesium-rich pelite-bearing beds, possibly with biotite breakdown.

#### **3.2.7 Late intrusive rocks**

Intrusions into the Sickie and Burntwood groups are considered younger than 1840 Ma, the presumed earliest age of

deposition of the sedimentary rocks. These intrusions range from mafic–ultramafic composition to leucogranite. Only their youngest members (Llg, Lpg, Lmu and possibly Lgg) are dated (ca. 1815–1800 Ma), either directly (DRI2021014), from adjacent areas (Baldwin et al., 1987; Gordon et al., 1990; Beaumont-Smith and Böhm, 2002) or indirectly by having formed from crustal melts during peak metamorphism and migmatization (Growdon et al., 2009). The oldest members are mafic to intermediate intrusions (Lmi, Lqd) that have not yielded useful zircons but have a composition similar to ca. 1830 Ma bodies elsewhere in the KD (Zwanzig and Bailes, 2010). The intrusions are described in order of composition from mafic to felsic.

### **3.2.7.1 Gabbro–pyroxenite (1.79 Ga, Lmu)**

A layered gabbro–pyroxenite body at least 15 m thick and 100 m long is exposed at one location in Osik Lake (UTM 501693E, 6200559N; Percival et al., 2007). It yielded a crystallization age of 1791 ±1 Ma (Rayner and Percival, pers. comm., 2007). Rhythmic centimetre-scale layers in gabbro give way to anorthositic gabbro, pegmatitic gabbro and pyroxenite. Garnet is abundant in some layers. The body occurs in the vicinity of ultramafic cobbles noted in overburden by DiLabio and Kaszycki (1988), with an aeromagnetic anomaly beneath the lake, and about 100 m west of a drillhole that intersected peridotite containing 0.22% nickel (Figure GS-7-2 in Percival et al., 2007).

### **3.2.7.2 Metagabbro to tonalite, mafic to intermediate porphyry (Lmi, Lgb, Ldt)**

Sheets of gabbro to tonalite occur in the northern part of the Burntwood group, the southern (mainly sedimentary) part of the Granville complex and within the Sickie group. Their intrusive relationship into the Burntwood and Sickie groups indicates their relatively young age (but see unit gb; Section 3.2.5.3). Those at Granville Lake are generally complex sills with multiple intrusive phases and cognate xenoliths. They are recrystallized to hornblende and plagioclase±pyroxene with variable biotite and quartz contents. Magnetite and apatite are typically relatively abundant in the intermediate phases and in some mafic phases. Two major types are present: 1) gabbro to melagabbro and fine-grained amphibolite/diabase (Lgb), and 2) diorite or leucogabbro to tonalite (Ldt). Where these types are undivided they are mapped as unit Lmi. They are interpreted to have formed from early-syntectonic tholeiitic magma that has undergone crystal fractionation and crustal contamination (Section 4.4.2).

Gabbro and uniform nearly black-weathering amphibolite form prominent intrusive sheets south of Granville Lake. These are associated with diorite to tonalite (Ldt) with relatively abundant magnetite and apatite. Parts of some mafic sills contain centimetre-scale inclusions of mafic rock. Northward gradations to less mafic compositions as well as crosscutting relations and local gradational boundaries indicate that the various

phases originated by crystal fractionation, magma mixing and apparently crustal contamination (Section 4.4.2). Mafic minerals in unit Ldt are hornblende (20–50%) and biotite (0–20%) with plagioclase (45–70%) and quartz (trace to 30%). Accessory minerals are magnetite (≤2%) and apatite (≤1%). At lower-granulite facies on Wuskwatim Lake, local mafic sheets in the Burntwood group are rich in clinopyroxene±orthopyroxene.

Gabbro to quartz diorite, porphyry and minor tonalite form a differentiated sill and narrow laccolith (Lmi) at the base of the central unit (Khb) of the Sickie group on Granville Lake. The base of the sill is melagabbro (ca. 65% mafic minerals, up to 60% as biotite) to gabbro (hornblende ≈plagioclase) with abundant xenoliths containing mostly pale green amphibole. The leucogabbro top contains 60–65% plagioclase with about 12% biotite and 20% hornblende including that in pseudomorphed mafic phenocrysts up to 5 mm long. Quartz and K-feldspar are minor phases; titanite is relatively abundant and accessory minerals include apatite and pyrite. Tonalite is a separate minor intrusive phase at the top of the sill.

An intermediate, 600 m thick laccolith (Ldt) emerges out of a 6 km long gabbro sill (Lgb) emplaced near the top of the Burntwood group south of Granville Lake. It grades inward from a diorite margin (45% mafic minerals) through quartz diorite (35% mafic minerals, ≤20% quartz) into tonalite (25% mafic minerals, 30% quartz) in the upper part of its core. The intrusion has multiple crosscutting phases that are partly intermingled or present as large and small cognate xenoliths, some partly digested. Some phases occur as dikes or dismembered dikes. The complex intrusive structure of the laccolith indicates multiple injection, magma mixing and assimilation. This provides an important clue for the late (post-arc) origin of the suite of Lmi. The high content of apatite is also typical of late intrusions in the KD. The quartz diorite phase has yielded no datable zircons, but the range of compositions and magmatic structures are similar to the ca. 1830 Ma enderbite in the Central Kisseynew subdomain (Gordon et al., 1990). The sill at the base of the laccolith contains medium- and fine-grained gabbro and probable diorite. Very similar compositional ranges and hybrid structures occur on the northeastern (fractionated and/or contaminated) side of a sill that extends across the Laurie River to the shore of Granville Lake. Although petrologically related, the two phases represent discrete intrusions that are separated by a wedge of Burntwood group southeast of the Laurie River. A similar but less evolved (≤7% quartz) sheet intruded the southern part of the Granville complex.

At Tullibee Lake, a 10 m thick sill of layered gabbro–pyroxenite occurs within Burntwood paragneiss (Percival et al., 2006). The gabbroic rocks contain 30% clinopyroxene; layered gabbro also contains amphibole and grades into layered tonalite with abundant quartz, ca. 15% hornblende and minor K-feldspar. These rocks generally contain biotite and magnetite. They are tentatively correlated with unit Lmi.

A possible correlation between unit Lmi and the sheared and higher metamorphic grade quartz diorite and intermediate gneiss (part of Gtb at Notigi Lake) is indicated by

- 1) the proportions of mafic minerals ( $\leq 70\%$  with  $\leq 1/3$  as biotite);
- 2) the abundance of accessory magnetite and apatite;
- 3) the abundance of quartz (up to 20%) in the most felsic phase; and
- 4) evidence of fractionation in the form of local compositional grading.

### **3.2.7.3 Diorite, quartz diorite (Lqd)**

Blacktrout diorite (Lqd) forms widely distributed sills of diorite to quartz diorite in the Sickie group along the north flank of the KD. Blacktrout diorite was described by Milligan (1960) from areas southeast of Lynn Lake (Zwanzig and Cameron, 2002) and is currently traced from Granville Lake to Notigi Lake and east to the TNB. A complete absence of zircon in tested samples did not allow dating this unit. A sill of similar composition, however, intruded after early deformation in the Southern Indian domain, northwest of Lynn Lake, yielded a ca. 1832 Ma crystallization age from zircon (Manitoba Geological Survey, 2018). In addition, an “undeformed” monzodiorite from Southern Indian Lake yielded an U-Pb thermal ionization mass spectrometry (TIMS) zircon age of 1829  $\pm$  5/–2 Ma (Rayner and Corrigan, 2004). This is consistent with an age of unit Lqd shortly after the deposition of the Sickie group.

A weakly differentiated 8 m thick sill on Granville Lake occurs at the base of the upper unit (Ks) in the Sickie group. It is fine- to medium-grained with chilled margins. It contains about 50% plagioclase that typically weathers orange. Other main minerals are quartz (4–10%), green hornblende (generally 10–25%) and biotite (8–15%, but  $\leq 30\%$  in the upper chill zone). Minor minerals are relatively abundant: 2–5% magnetite, 3–5% titanite and generally 2.5% apatite. Large ( $\leq 1.5$  mm) grains of magnetite and 4% apatite ( $\leq 1$  mm long) near the base suggest crystal settling of these minerals. Quartz-free diorite in unit Lqd occurs only at the exposure north of the TNB and was reported from north of the type area at Blacktrout Lake (Figure 5b) by Milligan (1960).

Sills of unit Lqd at Notigi Lake are also up to 8 m thick. They generally occur within the biotite gneiss (Kb) of the Sickie group, either stratigraphically below or above unit Kh. Exposures of Lqd were visited on the west side of the Rat River channel, southwest of Timew Island, at several sites north of the lake, and along the southeast side of the northeastern Notigi culmination. The quartz diorite in these sills is uniformly medium-grained, dark grey to black with orange-weathering feldspar. It is strongly magnetic. As elsewhere, these sills are typically rich in plagioclase, contain equal parts hornblende and biotite, relatively abundant magnetite and apatite but less quartz than elsewhere. Titanite is present as remnants and ilmenite becomes prominent at higher metamorphic grades.

The continuity of the sills from an area 20 km southeast of Lynn Lake for more than 200 km to the TNB, and their absence to the south and west, where the Sickie group stratigraphy differs, indicates that the Lqd intrusions are restricted to the eastern Sickie sub-basin. Apparently, only this sub-basin had access to the unusually volatile-rich magma with elevated trace-element contents that made up unit Lqd (Section 4.4.1). Deep access for Lqd magma may have been from the inferred boundary (suture) between the volcanic-arc massif (LRD) and the Granville complex, the back-arc ophiolite-type basement to the Sickie group. This is predicated by the different assemblages under the north and south Sickie unconformities. The deep crustal break may be important for gold exploration. The northwestern sub-basin contains no Blacktrout diorite, whereas the southern sub-basin contains only subalkaline, intermediate intrusions (Lmi). These differences have important implications concerning the crustal history of the basement rocks underlying the Sickie group, as well as the type of mantle accessed under the various sub-basins.

### **3.2.7.4 Hornblende and biotite granite–granodiorite (Lhg)**

Hornblende and biotite granite–granodiorite occurs in the high-relief terrain of the northern part of the Granville Lake map area. The rock is homogeneous, weathers buff–grey to grey–pink and has grey fresh surfaces. The unit is medium-grained with coarse-grained to pegmatitic phases. The ratio of hornblende to biotite is locally variable although the total mafic content is mostly constant. The unit contains magnetite in significant proportions, which allows it to be distinguished on the basis of its moderate to high-intensity geophysical response (description taken from unpublished Burntwood Project notes of Baldwin et al., 1979).

### **3.2.7.5 Leucogranite–pegmatite, granite–tonalite (Llg, Lgg)**

The youngest granitoid rocks intruded the Burntwood and Sickie groups as well as the Granville complex. They range from pale pink or white leucogranite, granite to granodiorite and pegmatite (Llg); and white, plagioclase-rich tonalite to granite (Lgg). Grain size in both units varies from fine to coarse and ranges to pegmatitic. The rocks are rare in the migmatite-free area at Granville Lake but abundant to the east and south. Leucogranite to leucotonalite (Llg) has the lowest content of mafic minerals ( $\leq 5\%$ ). These granitoids occur most consistently in thin sheets and veins in Burntwood group gneiss (Bg) and migmatite (Bm) but occur also in larger bodies. Minor minerals of note in both leucogranite and pegmatite (Llg) include biotite and may include sillimanite, cordierite, garnet and muscovite or hornblende, also tourmaline and magnetite or graphite. Retrograde metamorphism is identified by garnet replaced by biotite, and cordierite and biotite replaced by chlorite. Granitoid rocks with  $>5\%$  mafic minerals (Lgg) occur more commonly

in larger bodies, often containing Burntwood group inclusions or schlieren. Unit Lgg has a similar mineral suite as unit Llg, but plagioclase, biotite and, locally, hornblende are more abundant in Lgg. Pink varieties of Llg and Lgg generally containing magnetite are mainly associated with the Sickie group or the FLPS. Thus a close relation with the youngest supracrustal rocks and close similarity to their leucosomal vein network as well as crosscutting field relations, indicate the young age of these intrusions. The bodies are massive to strongly foliated, generally at least with a weak foliation or foliated margins. These textures suggest syn- to late-tectonic intrusions. The maximum age of intrusions, as related to migmatization, is estimated as ca. 1817 ±5 Ma, the oldest monazite age from metamorphism in the central KD (Gordon et al., 1990). A minimum age of such intrusions may be ca. 1785–1750 Ma. (Beaumont-Smith and Böhm, 2002), the time of early development of S<sub>3</sub> foliation with ubiquitous northeast trend and best seen in the late igneous rocks.

At Wapisi Lake, the young leucogranite to tonalite phases (Llg) are white, medium grey to brown. A white, fine-grained to pegmatitic tonalite phase forms a series of thin sheets alternating within Bg/Bm intruded by younger granite and pegmatite. Leucogranite at Wapisi Lake contains local garnet±sillimanite with K-feldspar in excess of plagioclase and less than 5% biotite. The tonalite or granodiorite (Lgg) is buff to light grey and occurs as discreet sheets containing up to 1 m rafts and schlieren of differing rock types including a quartz-rich garnet-bearing gneiss and layered psammitic to semipelitic rocks of the Burntwood group.

At Kawawayak Lake, unit Lgg weathers cream to grey-brown and is generally equigranular with local grain size ranging from medium to coarse, and texture ranging from foliated to massive. The unit is injected by younger pegmatite and finer-grained granitic veins. Unit Lgg is composed of quartz, feldspar and generally biotite, but it may also contain garnet, sillimanite and cordierite. Commonly, the unit contains inclusions of the Burntwood group host rock, which affect its content of minor minerals. Granodiorite margins adjoining amphibolite contain mafic inclusions. These margins contain hornblende±diopside ±magnetite±pyrrhotite. These minor-mineral contents reflecting the adjacent country rock and inclusions suggest a crustal source for the late granitoid rocks, or strong contamination.

At Notigi Lake and along the Rat River north of the lake, granodiorite, sillimanite-bearing leucogranitoid rock (Llg) and pegmatitic equivalents intrude the Burntwood group. These granitoid rocks are light grey, often rich in quartz and plagioclase, and contain up to 2% sillimanite-quartz faserkiesel. The melt may have assimilated pelite of the Burntwood group, producing igneous muscovite that reacted to form sillimanite during subsequent metamorphism. A metamorphic, rather than igneous, origin of the sillimanite suggests that metamorphism outlasted much of the late granitoid rock intrusion.

The leucocratic intrusive bodies occur as in-source veins and sheets, dykes, sills, laccoliths and larger ovoid intrusions.

These are pervasive in the Burntwood and Sickie groups at mid- to upper-crustal levels. Intrusive bodies can occupy some higher levels in or near unit Bg that is nearly free of small veins. Abundant, commonly boudinaged trondhjemite veins, often with quartz cores, apparent have lost most of their melt (e.g., Vanderhaeghe, 2001), which formed higher-level intrusions. Diatexite rich in plagioclase, garnet, cordierite±sillimanite ±orthopyroxene (Bda) is also expected to have lost melt.

#### 3.2.7.6 Pegmatite, aplite, granite (Lpg)

Mappable bodies of granite pegmatite are not abundant in most areas except on Granville Lake and to its south. These coarse-grained bodies up to 2 km long are generally somewhat crosscutting of the stratigraphy; some intruded along late east-northeast-trending faults. Others occur in the outer limbs of north-northeast-trending folds where north-south extension has taken place.

## 4. Whole-rock and Sm-Nd isotope geochemistry

New and published geochemical data are used to typify the various sedimentary, volcanic and intrusive rocks in the Wuskwatim–Granville lakes corridor. Despite alteration, whole-rock analysis is a useful tool for correlating metamorphic units using unique patterns on various normalized-element plots. This is supported by Sm-Nd-isotope geochemistry. Although stratigraphy remains the prime mapping tool, correlation of rocks that have lost all primary features, in some cases, are recognized only from chemical and isotopic analyses. Geochemistry is particularly useful for correlating the highest-grade metamorphic rocks with those that retain more features that are primary. Neodymium-model ages or initial  $\epsilon_{Nd}$  values generally support the chemical fingerprinting by falling into a similar limited range of values. With geochemistry, they facilitate correlations and inferences about tectonic origins and provenance.

Sampling techniques and data treatment followed those of Zwanzig and Bailes (2010). Work focused on the least mobile, least fluid-soluble elements, including rare-earth elements (REE) and high field-strength elements (HFSE: Nb, Zr, Hf and Ti). This avoided much of the effect of alteration caused by metamorphism. The main consideration is given to these conservative elements for the mafic to ultramafic rocks. Some more fluid-mobile elements are also used for the granitoid and sedimentary rocks. Where these elements occur in higher concentrations, patterns can still be discerned among the scatter. Such fluid-mobile compounds and elements as Na<sub>2</sub>O, K<sub>2</sub>O, Rb, Ba, Sr, P and U are often necessary to assess tectonic origins or possible correlations. Where tight patterns occur from widespread samples, limited alteration of the original rocks is generally indicated. In order to minimize erroneous conclusions, the ratios of various groups of compounds/elements are considered.

The grouping of the igneous rocks is facilitated by comparing ratios of REE and minor elements such as Ti, P, Cr and Ni

(DRI2021014). An initial comparison and correlation of samples was made using La/Sm and Gd/Yb for the ratios of light REE (LREE) and heavy REE (HREE). Alkali elements and silica were used with caution. Multi-element plots were normalized to normal mid-ocean-ridge basalt (N-MORB) with values after Sun and McDonough (1989) or primitive mantle (Sun, 1982). These, and selected ratio plots were used in a final iteration to determine geochemical types and tectonic origins of the analyzed rocks. The results are used in assessing tectonic environments with their metallogeny and the economic mineral potential for various subdomains in the study area and wider regions.

Whole-rock major- and trace-element analyses were carried out by Activation Laboratories Ltd. (Ancaster, Ontario) using methods described in DRI2021014. Niodymium-Sm-isotopic data were provided by the Crustal Re-Os Geochronology Laboratory (University of Alberta). These data, most of which were previously published (Zwanzig et al., 1999a; Zwanzig, 2000a; Zwanzig et al., 2006; Murphy and Zwanzig, 2007a), are presented here in summary diagrams. Previously published data from outside the study area and data from established tectonic environments are used as fields for comparison and correlation. A compiled list of published and new geochemical data and Sm-Nd isotopic data are given in DRI2021014, and unit averages of the major, minor and trace-element analyses and Sm-Nd isotopic results are summarized in Table 2.

Many of the volcanogenic rocks at Granville Lake are inferred to be altered, and all rock types are altered to some degree in the rest of the study area. Epidotization and carbonatization are most abundant, probably due to seafloor alteration. Carbonate was locally concentrated as thin layers and lenses in mafic tectonites. Partial melting and granite injection strongly altered the Burntwood group migmatite and to a lesser extent the Sickle group. These rocks were affected mainly by alkali element (Na, K, Rb, Cs, Sr and Ba) mobility during metamorphism, melt extraction and back-reaction by fluids from crystallizing melts. Those intrusive rocks that were not affected by partial remelting or veining appear to have undergone nearly isochemical recrystallization. Where possible, only non-veined and non-migmatitic samples were collected. The more detailed study of similar high-grade metamorphic rocks (Zwanzig and Bailes, 2010) indicated that primary trends produced by fractionation, fractional melting, crustal contamination and composition of the melt source(s) are surprisingly resilient for many elements.

#### **4.1 Sedimentary rocks (W, B, K, Gs), a comparison**

In addition to outcrop colour, mineral content, grain size, texture, layer thickness and rock associations, Zwanzig et al. (2007) and Böhm et al. (2007) have shown that the Ospwagan and Burntwood groups along the TNB-KD boundary are clearly distinguished by geochemical and Sm-Nd isotopic data. Even different units that formed similar-looking garnet-biotite-bearing paragneiss have unique multi-element profiles and  $\epsilon_{Nd}$

values. Consequently, the approach of using Sm-Nd isotopes and geochemistry has been applied to the Wuskwatim–Granville lakes corridor to provide clearly distinguishing criteria. This work further benefits from detrital-zircon data (Percival et al., 2005, 2006, 2007; Rayner and Percival, 2007; Zwanzig et al., 2006). The geochemical and isotopic distinctions were also applied more widely. They are critical for mapping purposes in areas where isolated outcrops of highly recrystallized rocks occur, and where units are structurally interleaved.

Multi-element profiles of Burntwood Group sedimentary rocks normalized to the local average Paleoproterozoic pelite (P2 member of the Pipe Formation in the TNB; Zwanzig et al., 2007; Figure 11a) have distinctive patterns with slightly positive slopes and prominent enrichments in U and P, and depletions in Th, K, Zr and Ti. Considering the variable pelite content and metamorphic grade of these rocks, the profiles are remarkably similar for 9 out of 14 samples. This is attributed to taking samples from vein-free areas of paragneiss or paleosome. The other five samples show progressively greater scatter toward less pelitic, fluid mobilized or melt-injected rock. Sickle group rocks have similar multi-element profiles with positive slopes and enrichments and depletions that compare well with the samples from the Burntwood group (Figure 11b), consistent with similar sources of detritus.

In units Ksc and Kse of the Sickle group, quartz- or plagioclase-rich samples have profiles with slightly negative slopes and depletions in the heavy REE (Figure 11c), consistent with a somewhat different detrital source or simply a scarcity of mafic minerals. The coarse-grained, thick-bedded arkosic greywacke (Ba) has a very similar geochemical pattern to the more impure arkosic rocks (lithic arenite?) unit Kb, in the Sickle group. A minor difference in unit Kb is a flatter overall P2-normalized slope than in unit Ba (Figure 11a, b).

Neodymium data from the Burntwood, Sickle, Ospwagan and Wuskwatim groups were treated in the manner of Böhm et al. (2007) to distinguish the average age of crustal residence ( $T_{CR}$ ) of their detritus. These data show that Nd-model ages from the Sickle group are nearly the same as those from the Burntwood group (Figure 12a, b), including its southeastern equivalent, the Grass River group. The Paleoproterozoic model ages coupled with the geochemical signatures confirm a similar provenance for these groups and are consistent with a provenance in the mainly juvenile arc terranes surrounding the KD.

The multi-element profiles of semipelitic gneiss from the Wuskwatim Lake sequence at Wapisu and Threepoint lakes and west of the Mel zone (Figure 1), normalized to the P2 member of the Ospwagan group (Zwanzig et al., 2007), are nearly identical to that of P2 (Figure 11d). The probable correlation of the Wuskwatim Lake sequence with the Ospwagan group in the TNB may suggest an unrecognized potential for nickel-sulphide mineralization also exists in the KD.

**Table 2:** Unit averages of whole-rock, trace-element and Sm-Nd isotope geochemical results.

	Burnt-wood Group	Muscovite/sillimanite arkose	Biotite arkose	Hornblende arkose	Sillimanite arkose	Quartzose arenite	Granville Lake sediments	Wuskwatim Lake sequence semipelite	Wuskwatim Lake sequence quartzite	Hatchet Lake basalt (Lynn Lake belt)	Kawaweyak Lake layered amphibolite
Unit	B	Ks	Kb	Kh	Ksa	Ks/c,e	Gs	Wp	Wq	Gh	Ghb
SiO <sub>2</sub>	63.84	67.88	65.87	63.29	77.31	79.39	68.93	64.51	75.89	49.43	48.55
Al <sub>2</sub> O <sub>3</sub>	16.02	14.83	15.29	15.54	11.66	10.72	13.98	16.75	11.71	14.98	15.10
Fe <sub>2</sub> O <sub>3</sub>	8.27	5.36	5.93	5.49	2.27	1.87	2.15	6.88	2.37	13.37	10.86
MnO	0.10	0.07	0.07	0.07	0.02	0.01	0.04	0.14	0.02	0.19	0.17
MgO	3.00	2.04	2.46	2.98	0.50	0.46	1.43	1.83	1.92	8.22	8.10
CaO	2.40	1.72	2.42	3.59	0.43	1.21	7.52	1.28	3.79	10.19	13.35
Na <sub>2</sub> O	2.82	3.05	3.77	4.29	2.50	1.82	4.02	3.14	2.83	2.23	2.40
K <sub>2</sub> O	2.58	4.29	3.45	4.03	4.96	4.12	1.45	4.85	1.11	0.18	0.91
TiO <sub>2</sub>	0.83	0.60	0.59	0.54	0.27	0.35	0.37	0.59	0.24	1.12	0.51
P <sub>2</sub> O <sub>5</sub>	0.15	0.16	0.15	0.18	0.09	0.05	0.10	0.05	0.09	0.10	0.05
Mg#	46	45	32	46	34	36	58	38	64	58	62
La/Yb	12.2	13.4	17.0	19.5	20.4	22.3	18.1	24.8	40.0	1.1	0.8
La/Sm	5.22	6.17	6.47	6.33	8.59	5.60	3.97	8.53	10.19	1.11	1.30
Gd/Yb	1.76	1.60	2.03	1.93	1.60	2.13	1.79	2.13	3.23	1.25	0.88
V	160	92	87	83	39	36	53	87	44	354	203
Cr	156	94	74	77	40	61	45	85		256	490
Ba	553	1159	863	693	925	1480	424	811	287	36	102
Rb	92	142	118	110	127	66	22	151	2	2	12
Sr	237	222	253	303	201	267	265	209	212	131	155
Y	26	24	32	23	11	10	6	15	6	24	16
Ni	62	41	33	47			20	45		108	200
Zr	170	226	225	176	156	160	122	174	126	54	22
Nb	9.1	13	15.5	11.7	6.5	5	5.0	10.0	4.5	3.6	1.7
La	30.7	37.8	54.3	42.7	30.5	17.6	11.8	41.8	26.1	2.9	1.4
Ce	61.1	76.1	105.2	85.8	59.7	33.5	24.1	71.0	43.7	10.5	3.7
Pr	7.43	9.31	12.39	10.21	7.07	4.24	2.77	8.46	4.56	1.40	0.52
Nd	28.25	31.02	42.81	34.98	20.40	15.40	9.85	30.00	16.60	7.23	2.96
Sm	5.66	6.11	8.28	6.84	3.55	3.16	1.95	4.90	2.75	2.59	1.04
Eu	1.35	1.26	1.23	1.18	0.75	1.05	0.55	1.13	0.60	1.01	0.51
Gd	4.96	4.97	6.56	5.34	2.55	2.47	1.60	3.60	2.15	3.27	1.53
Tb	0.82	0.78	1.04	0.79	0.40	0.34	0.25	0.55	0.30	0.65	0.32
Dy	4.71	4.52	5.92	4.31	2.40	1.80	1.35	2.75	1.45	4.13	2.22
Ho	0.9	1.0	1.2	0.8	0.5	0.4	0.3	0.6	0.3	0.9	0.5
Er	2.79	2.86	3.43	2.50	1.55	0.93	0.70	1.65	0.70	2.59	1.73
Tm	0.42	0.44	0.52	0.37	0.23	0.13	0.11	0.26	0.11	0.39	0.27
Yb	2.69	2.83	3.33	2.32	1.50	0.86	0.65	1.70	0.65	2.61	1.73
Lu	0.41	0.42	0.52	0.35	0.23	0.14	0.10	0.26	0.10	0.40	0.27
Hf	4.86	6.62	6.35	5.15	4.65	4.30	3.35	4.80	3.35	1.79	0.70
Ta	0.7	1.0	1.0	1.0	0.8	0.2	0.5	0.7	0.4	0.6	0.1
Th	7.9	12.2	17.1	14.2	11.8	3.8	2.6	16.0	10.0	0.3	0.1
U	2.9	2.6	2.6	2.1	2.5	0.6	1.1	1.7	3.5	0.3	0.2
n	14	3	6	8	2	2	2	2	2	9	2
εNd <sub>T</sub>	+0.35	-1.65	-1.38	-1.55		+3.55	+3.06	-9.56	-11.6	+3.50	+3.65
T <sub>CR</sub>	2.32	2.41	2.42	2.43		2.04	2.23	2.95	3.16		

*Italic:* Uncertain origin-type source

Units: Weight percent (SiO<sub>2</sub>-P<sub>2</sub>O<sub>5</sub>), parts per million (V-U)

**Table 2 (continued):** Unit averages of whole-rock, trace-element and Sm-Nd isotope geochemical results.

	Tod Lake basalt	Kawawayak Lake metagabbro	Notigi Lake mafic calc- silicate	Kawawayak Lake mafic calcsilicate	Pickereel Narrows amphib.	Wheat- croft Lake amphib.	Granville frag. (alt.)	Intermediate gneiss Lmi in Gtb	Laurie Lake amphib. high Mg	Laurie Lake schist	Laurie Lake intrusion
Unit	Gta	Gg	Guc	Guc	Gua	Gt	Gu	Gtb	<i>Ra</i>	<i>Rb</i>	<i>Ru</i>
SiO <sub>2</sub>	52.33	48.00	44.67	49.06	43.04	45.66	54.20	55.68	52.44	<i>49.64</i>	<i>48.55</i>
Al <sub>2</sub> O <sub>3</sub>	14.90	13.34	9.56	17.53	8.45	14.57	3.93	13.70	16.26	<i>11.27</i>	<i>6.25</i>
Fe <sub>2</sub> O <sub>3</sub>	12.87	16.68	8.39	4.85	16.04	15.78	9.15	15.02	7.59	<i>9.97</i>	<i>12.41</i>
MnO	0.20	0.25	0.14	0.08	0.22	0.24	0.16	0.23	0.13	<i>0.17</i>	<i>0.20</i>
MgO	4.80	6.48	5.07	4.97	17.90	8.77	20.87	3.31	9.63	<i>15.17</i>	<i>20.51</i>
CaO	9.15	10.07	28.18	17.51	10.84	11.87	11.03	6.71	9.98	<i>11.01</i>	<i>10.95</i>
Na <sub>2</sub> O	3.41	2.03	1.99	1.94	0.47	1.35	0.44	2.09	2.93	<i>1.64</i>	<i>0.55</i>
K <sub>2</sub> O	0.55	0.85	0.81	1.53	0.28	0.13	0.14	1.12	0.32	<i>0.38</i>	<i>0.14</i>
TiO <sub>2</sub>	1.59	2.07	1.04	2.27	2.49	1.39	0.06	1.69	0.63	<i>0.60</i>	<i>0.32</i>
P <sub>2</sub> O <sub>5</sub>	0.19	0.23	0.14	0.26	0.26	0.25	0.03	0.45	0.09	<i>0.14</i>	<i>0.11</i>
Mg#	46	47	58	68	72	56	84	33	74	<i>78</i>	<i>78</i>
La/Yb	2.2	2.0	5.4	6.7	19.8	3.3	5.1	3.2	4.0	<i>6.5</i>	<i>5.6</i>
La/Sm	2.01	1.67	2.49	3.43	4.21	3.18	2.94	2.46	2.42	<i>3.04</i>	<i>2.98</i>
Gd/Yb	1.22	1.52	2.25	2.02	4.33	1.31	1.86	1.58	1.57	<i>1.94</i>	<i>1.93</i>
V	352	433	220	282	282	337	77	282	146	<i>166</i>	<i>141</i>
Cr	62	100	2607	830	1110	577	5490	35	430	<i>894</i>	<i>2330</i>
Ba	200	50	321	364	40	15	9	233	104	<i>50</i>	<i>56</i>
Rb	8	19	8	36	3	3	28	21	16	<i>9</i>	
Sr	162	101	297	278	168	196	25	219	421	<i>238</i>	<i>175</i>
Y	32	40	13	28	20	33	3	49	12	<i>11</i>	<i>7</i>
Ni	40	75	519	230	654	202	2195	40	156	<i>373</i>	<i>861</i>
Zr	82	133	66	112	157	74	9	158	43	<i>40</i>	<i>20</i>
Nb	5.7	7	6.4	21.5	27.5	16.8	4.9	6.5	3.3	<i>3.5</i>	<i>1.1</i>
La	7.7	8.0	6.1	17.7	27.8	10.5	1.4	17.4	5.0	<i>7.3</i>	<i>3.3</i>
Ce	22.7	21.5	14.4	40.2	60.9	22.9	2.8	41.5	16.0	<i>22.1</i>	<i>7.4</i>
Pr	2.60	2.98	1.91	4.97	7.36	2.79	0.37	6.14	1.75	<i>2.34</i>	<i>0.98</i>
Nd	11.94	15.39	8.97	21.40	31.91	12.34	1.70	26.40	7.70	<i>9.77</i>	<i>4.61</i>
Sm	3.73	4.84	2.44	5.15	6.83	3.47	0.49	7.12	2.07	<i>2.39</i>	<i>1.10</i>
Eu	1.24	1.63	0.83	2.14	2.12	1.27	0.57	2.08	0.73	<i>0.73</i>	<i>0.35</i>
Gd	4.29	5.87	2.64	5.30	6.24	4.43	0.54	8.53	1.99	<i>2.18</i>	<i>1.14</i>
Tb	0.84	1.09	0.43	0.85	0.84	0.82	0.12	1.44	0.35	<i>0.35</i>	<i>0.17</i>
Dy	5.51	6.81	2.52	5.10	4.49	5.31	0.52	8.96	2.20	<i>2.07</i>	<i>1.01</i>
Ho	1.2	1.4	0.5	1.0	0.8	1.2	0.1	1.9	0.4	<i>0.4</i>	<i>0.2</i>
Er	3.30	4.37	1.45	3.00	1.97	3.46	0.30	5.87	1.23	<i>1.15</i>	<i>0.64</i>
Tm	0.52	0.64	0.21	0.43	0.25	0.53	0.06	0.88	0.18	<i>0.17</i>	<i>0.10</i>
Yb	3.49	3.78	1.22	2.60	1.44	3.38	0.29	5.63	1.27	<i>1.12</i>	<i>0.59</i>
Lu	0.53	0.56	0.18	0.38	0.17	0.53	0.05	0.86	0.18	<i>0.17</i>	<i>0.10</i>
Hf	2.55	3.60	1.49	3.30	3.89	2.12		4.60	1.40	<i>1.30</i>	<i>0.40</i>
Ta	0.7	0.5	0.8	1.8	2.8	1.5	0.4	0.5	0.7	<i>0.5</i>	
Th	1.5	0.5	0.8	1.7	2.9	1.6		2.6	0.8	<i>1.4</i>	<i>0.6</i>
U	0.6	0.4	1.0	1.2	0.7	0.4		1.3	0.4	<i>0.7</i>	<i>0.4</i>
n	6	2	3	2	6	3	2	3	4	<i>4</i>	<i>2</i>
εNd <sub>t</sub>	+2.30	+3.39	+2.35	+4.12							

Abbreviations: alt., altered; amphib., amphibolite; frag., fragmental rock.

*Italic:* Uncertain origin-type source

Units: Weight percent (SiO<sub>2</sub>-P<sub>2</sub>O<sub>5</sub>), parts per million (V-U)

**Table 2 (continued):** Unit averages of whole-rock, trace-element and Sm-Nd isotope geochemical results.

	Quartz monzonite	Footprint Lake granodiorite	LRD arc granitoids	Quartz diorite	Tullibee gabbro	Fe-quartz diorite	Granite/ granodiorite	Granite/ granodiorite	Leucogranite, low Yb	Leucogranite
Unit	qm	qm	gn/tn	Lqd	Lgb?	Lmi	Lgg	gx	Llg	Llg
SiO <sub>2</sub>	61.43	67.89	63.70	55.13	51.88	54.82	72.20	64.42	72.50	74.25
Al <sub>2</sub> O <sub>3</sub>	17.61	15.09	16.65	13.84	15.38	12.77	13.80	18.07	15.70	14.32
Fe <sub>2</sub> O <sub>3</sub>	5.41	4.25	5.75	11.92	11.12	15.63	2.61	3.20	0.90	1.05
MnO	0.07	0.05	0.10	0.17	0.15	0.23	0.03	0.04	0.01	0.02
MgO	1.95	1.61	2.19	3.28	9.26	3.11	0.78	0.75	0.18	0.14
CaO	3.36	2.54	5.56	5.90	9.20	6.12	1.56	1.82	1.14	0.85
Na <sub>2</sub> O	3.74	3.40	4.04	3.04	1.69	3.46	2.90	4.50	4.36	3.07
K <sub>2</sub> O	5.15	4.20	1.49	2.70	0.71	1.15	5.56	6.40	5.09	6.17
TiO <sub>2</sub>	0.93	0.73	0.41	2.65	0.52	2.12	0.40	0.65	0.10	0.05
P <sub>2</sub> O <sub>5</sub>	0.36	0.25	0.21	1.38	0.08	0.59	0.16	0.14	0.02	0.08
Mg#	45	46	45	37	66	30	41	35	30	23
La/Yb	96.4	82.6	11.3	27.5	6.4	2.7	83.7	63.6	36.0	26.7
La/Sm	11.06	12.59	4.19	6.62	4.60	2.13	11.85	8.41	6.13	9.24
Gd/Yb	4.96	3.97	2.10	2.53	1.41	1.72	4.09	4.34	6.00	1.83
V	92	65	78	216	221	207	33	41	7	
Cr	23	20		70	350		30			
Ba	2272	1087	446	1623	144	397	1469	1107	961	482
Rb	113	102	25	94	19	24	186	118	80	150
Sr	970	467	437	591	227	187	478	586	527	122
Y	20	16	13	60	23	67	12	31	2	8
Ni	11	14	50	30	125	37				
Zr	667	382	81	515	46	201	294	634	60	66
Nb	20.1	18.0	3.4	33.7	2.4	8.5	15.0	31.5	2.5	6.0
La	131.1	93.2	13.3	133.1	8.4	18.1	76.6	151.5	6.5	20.8
Ce	234.3	164.5	27.2	267.1	18.5	44.6	135.8	300.5	9.9	34.7
Pr	26.04	16.90	3.39	34.02	2.29	7.08	13.90	35.55	1.22	3.72
Nd	86.32	53.20	13.0	119.1	9.75	31.03	46.66	118.2	4.30	12.20
Sm	12.14	7.40	2.75	20.38	2.28	8.28	6.56	17.85	1.00	2.30
Eu	2.49	1.42	0.83	4.63	0.73	2.58	1.19	2.31	0.42	0.44
Gd	7.46	4.50	2.56	16.53	2.39	10.38	4.14	10.15	0.80	1.60
Tb	0.88	0.60	0.38	2.12	0.40	1.78	0.56	1.35	0.10	0.25
Dy	4.16	2.90	2.20	10.62	2.48	11.18	2.64	6.90	0.50	1.40
Ho	0.7	0.5	0.5	2.1	0.5	2.4	0.5	1.2		
Er	1.97	1.40	1.35	5.80	1.54	7.28	1.26	3.25	0.15	0.85
Tm	0.26	0.18	0.21	0.80	0.23	1.07	0.16	0.42		
Yb	1.55	1.15	1.32	4.83	1.54	6.58	0.96	2.40	0.10	0.80
Lu	0.21	0.16	0.20	0.69	0.23	0.99	0.14	0.34		
Hf	15.11	9.50	2.28	11.38	1.45	6.05	7.46	15.50	2.00	2.50
Ta	1.1	0.8	0.3	1.8	0.2	0.5	0.8	2.4	0.2	0.2
Th	18.5	19.9	1.2	7.0	0.5	2.7	36.5	19.7	2.8	14.0
U	1.4	0.7	0.2	1.4	0.5	1.4	5.3	2.7	4.7	4.5
n	10	2	3	9	2	4	5	3	2	2
εNd <sub>T</sub>	-10.2	-9.31	+3.84	-4.1		+2.88	+1.09		-2.52	-3.22
T <sub>CR</sub>	2.90	2.80	2.01	2.58			2.13		2.54	2.66

Units: Weight percent (SiO<sub>2</sub>-P<sub>2</sub>O<sub>5</sub>), parts per million (V-U)

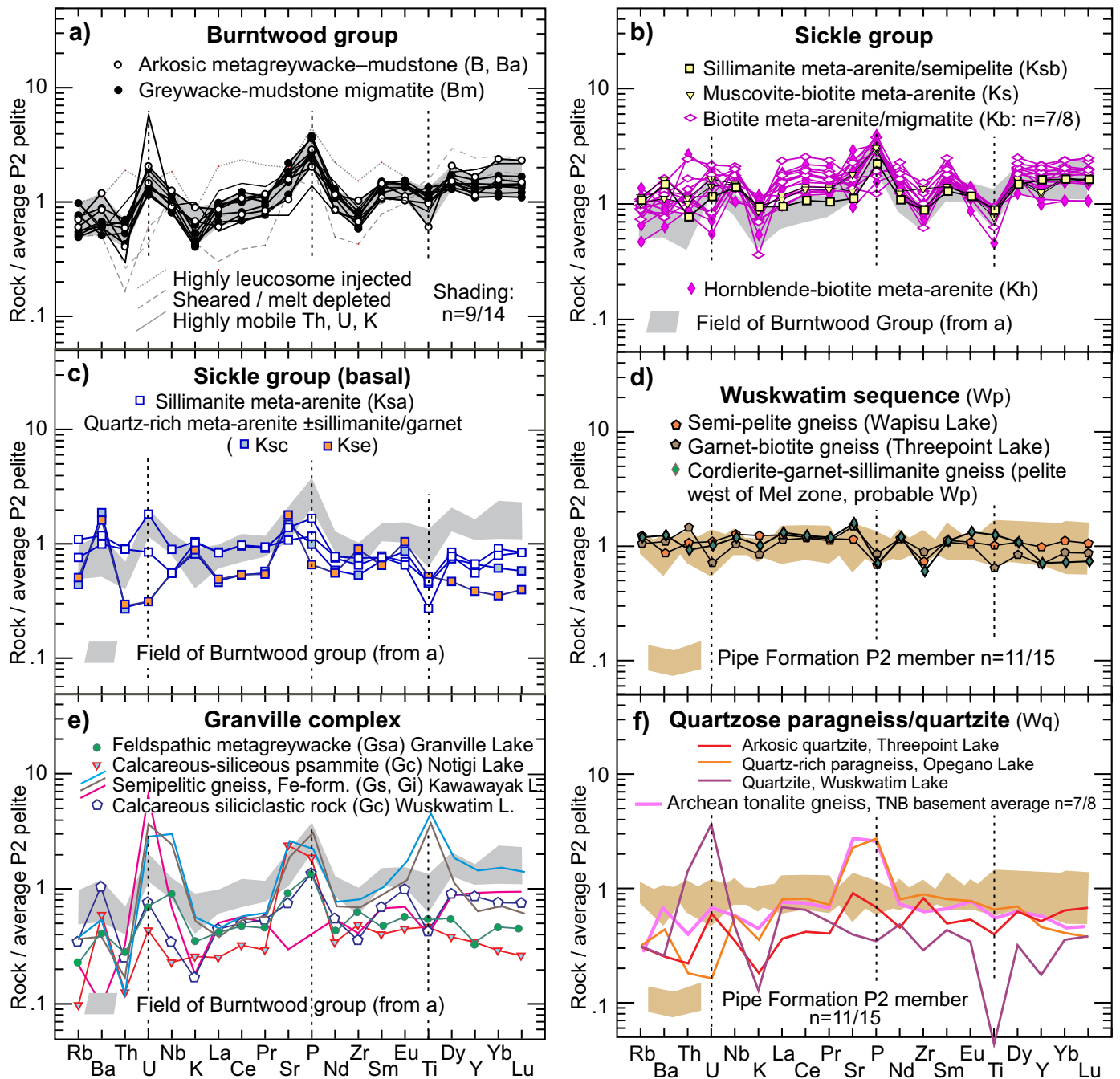


**Figure 11:** Multi-element plots of various paragneiss units are normalized to Paleoproterozoic pelite (average Pipe Formation P2 member, in the Thompson nickel belt, Manitoba after Zwanzig et al., 2007). Three elements (U, P and Ti) are marked with dashed lines: **a)** characteristic pattern of peaks and troughs with a slight positive slope of Burntwood group metagreywacke–mudstone (grey field) is used to compare with **b)** the main part of the Sickle group, which is similar, but not **c)** the quartz-rich basal units. Samples in **d)** of the Wuskwatim Lake sequence at Wapisi and Threepoint lakes and a likely Wp sample west of the Mel zone indicate that the chemistry of the semipelite–pelite is nearly identical to P2. **e)** A sample of Granville Lake metagreywacke is relatively depleted in the selected elements, with prominently lower HREE, a pattern similar to calcareous psammite and the quartzose basal Sickle group. The sulphidic metapelite plots show elevated U, Nb and Ti; sulphide iron formation is enriched in U; in **f)** paragneiss/quartzite (Wq) scatter is high and average values are low due to dilution by quartz. P2 data from Zwanzig et al. (2007). Abbreviation: Fe-form, iron formation.

The same peaks of 2.95 Ga and spreads of 3.3–2.8 Ga in Nd-model ages of the Wuskwatim Lake sequence and Ospwagan group support their correlation (Figure 12c, d). Ranges of younger model-ages from similar-looking rocks in the Burntwood group indicate a different provenance (Figure 12a, b). Detritus in unit W with average crustal residence ages older

than 3.6 Ga (Figure 12c) suggest an additional provenance from Mesoproterozoic crust, perhaps comparable to the Assean Lake crustal complex (Böhm et al., 2003) or a more exotic source in the THO.

The multi-element profiles of five widely separated samples of felsic sedimentary rocks in the Granville com-

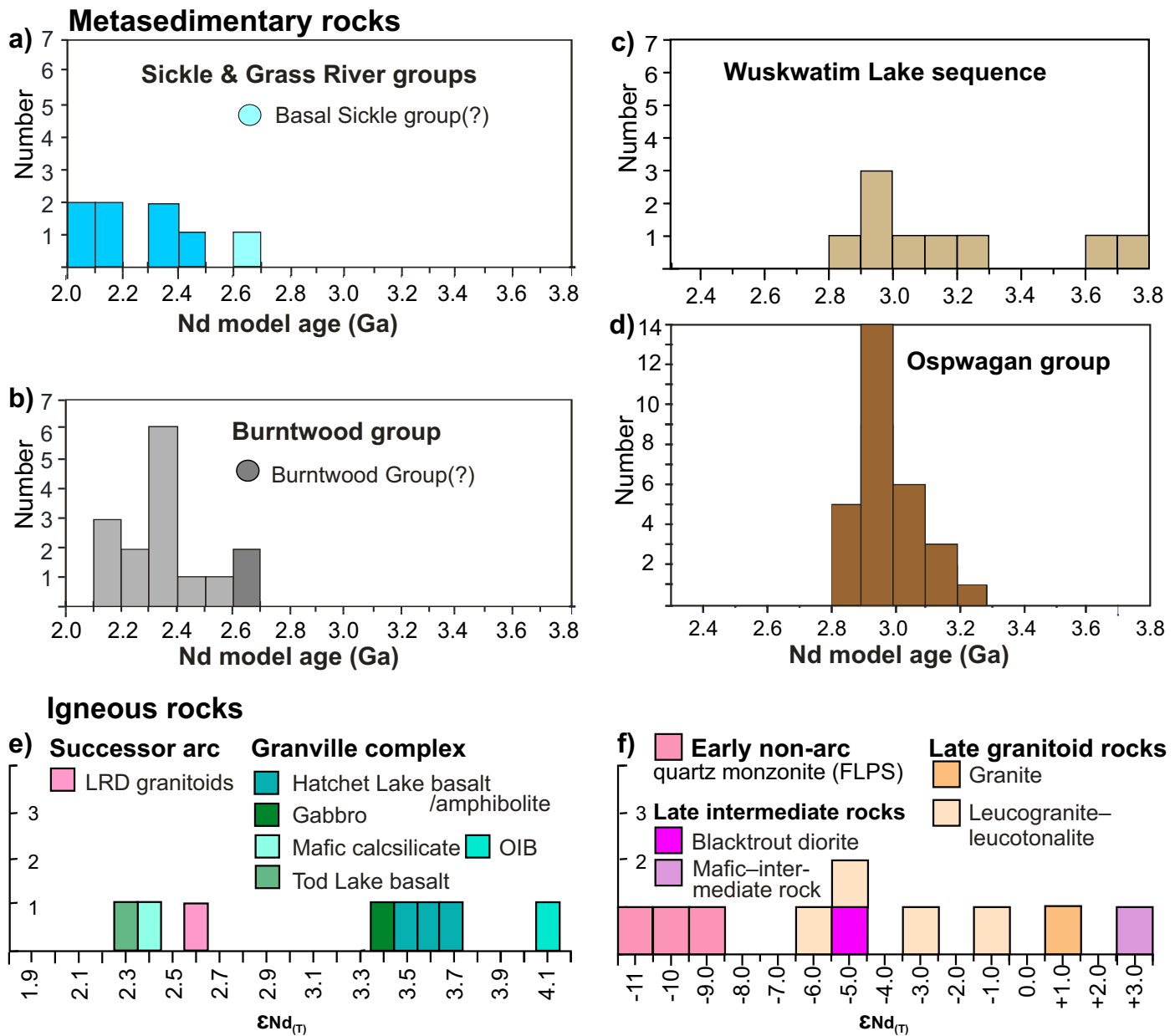


**Figure 12:** Neodymium-model ages ( $T_{cr}$ ) and  $\epsilon Nd_{(T)}$  of the Paleoproterozoic sediment-derived gneisses and igneous rocks in the Wuskwatim–Granville lakes corridor are compared with those in the Thompson nickel belt (TNB). **a, b** The similarity between the Sickle group (Kisseynew north flank) Grass River group (adjoining the TNB) and the Burntwood group (from the same areas) confirms their provenance in the same terrane. The rare samples with older model ages have a less certain origin but may simply be injected by leucosome with an Archean melt component. **c, d** The correlation between the Wuskwatim Lake sequence (in the corridor) and the Ospwagan group (in the TNB) is supported by their identical peak model ages. The older ages in the former indicate detritus from Mesoarchean rocks such as in the Assean Lake crustal complex (Böhm et al., 2003). **e, f** Epsilon-neodymium values of igneous rocks: **e** Leaf Rapids domain margin (successor-arc) and Granville complex (back-arc); **f** early and late, non-arc, mafic to felsic rocks. Data are from DRI2021014 and from Böhm et al. (2007). Age calculation is after Goldstein et al. (1984).

plex are somewhat similar to the Burntwood group but have lower trace-element contents. They show depletion of HREE like other quartz- and feldspar-rich units (Figure 11e). Fine-grained, sulphidic samples show great scatter of mobile elements and Ti. The calcareous siliciclastic rock (Gc) between the Burntwood group and the Wuskwatim Lake sequence at Wuskwatim Lake has a similar pattern to the Burntwood group, but trace-element values are slightly lower. This suggests a similar provenance from an arc terrane, which is also indicated by its Paleoproterozoic Nd-model age of 2.38 Ga. The calcare-

ous sample (Gc) from Notigi Lake is even more depleted and is probably unrelated to the Burntwood group but similar to the feldspathic greywacke in the Granville complex.

Samples of arkosic quartzite and quartz-rich paragneiss (Wq) from the base of the Wuskwatim Lake sequence have highly irregular profiles, but that from Opegano Lake, closest to the TNB, has a least-mobile–element profile nearly identical to an average of seven samples of tonalite basement gneiss in the TNB (Figure 11f). Neodymium-model ages (3.77–2.99 Ga) indi-

cate an Archean provenance (DRI2021014). Figure 12c suggests that unit Wq has a component of Mesoarchean detritus. The quartz-rich paragneiss from Opegano Lake and TNB basement tonalite gneiss have somewhat similar Mesoarchean model ages (3.77 and 3.40 Ga; TNB data is from Zwanzig et al., 2007).

## 4.2 Granville complex volcanogenic rocks (G, Gh, Gt, Gu)

Geochemical and Sm-Nd isotopic data are critical in defining units and assessing their tectonic origin in the Granville complex. Geochemical data from the Wuskwatim–Granville lakes corridor are compiled in DRI2021014. This includes

- 1) previously published data from volcanic and subvolcanic rocks in the Tod–Laurie lakes area at the southwest end of the Lynn Lake belt (Zwanzig et al., 1999a);
- 2) unpublished data from the adjacent Kisseynew north flank, summarized in Zwanzig (2000b), and
- 3) data obtained from the study area during this project.

Multi-element plots normalized to N-MORB are shown on Figures 13 and 14. Widely separated samples from units in the same tectonostratigraphic assemblage with similarly shaped profiles are correlated and probably stem from the same volcanic terrane. The relatively little-altered rocks in the northwest are compared with more altered and higher-grade metamorphic rocks in the southeast to test potential correlations. The analyses are subdivided into groups by location and degree of REE fractionation using ratios of La/Yb, La/Sm and Gd/Yb (DRI2021014). They are generally plotted with increasing ratios in Figures 13 and 14. Unit averages as shown in Table 2 were used to identify outlying values, and to remove these from the average in making final assignments of the chemical types and a final iteration of their averages. All analyzed samples, however, are shown in the figures. Major elements (e.g., 3.0–11.5% MgO) and pertinent trace elements (V=92–553 ppm, Cr=32–500 ppm, Zr=40–150 ppm, Y=17–65 ppm; DRI2021014) of the Granville complex basalts (Gh, Gta, Gtb) fall into the field of back-arc–basin basalt (BABB) as compiled by Furnes et al. (2012).

Because of strong local alteration and possible regional alteration, plots were constructed (not shown but available from the authors) using various proxy elements that are not fluid mobile as well as some major elements. Regression analysis of their ratios show distinctive trends for the various units identified in Figures 13 and 14. The test value,  $r^2$ , shows the fit of the regression line, which is good for values  $>0.5$ . In general  $r^2$  is much greater than 0.5 with few outlying values, and indicates that alteration was not a significant factor in establishing geochemical subdivisions from the selected elements.

### 4.2.1 Hatchet-Lake–type geochemical units (Gh, Ghg, gb)

Hatchet Lake basalt (Gh) with interlayered gabbro (Ghg) was found where the Granville complex occurs in the Hatchet–

Laurie lakes area, southwest end of the Lynn Lake belt. These mafic units are part of the Wasekwan tectonic collage, previously Wasekwan group (Zwanzig et al., 1999). The rocks have yielded a juvenile  $\epsilon_{Nd}$  value of +3.5 (Beaumont-Smith and Böhm, 2002) indicating they are uncontaminated by Archean or old Paleoproterozoic crust. The preferred interpretation is that Hatchet Lake basalt and gabbro represent distal ocean floor (MORB). The basalt and high-Mg gabbro (Ghg) have relatively flat N-MORB–normalized multi-element patterns and no Nb or Ti anomalies beyond scatter presumably produced by alteration (Figure 13a). With their slightly fractionated LREE they are comparable to modern BABB distant from the arc (i.e., similar to N-MORB). Normal-Mg gabbro-porphyry at Wapisi Lake (gb, age and origin unknown) has slightly more fractionated LREE than unit Ghg.

Comparisons are made of Hatchet Lake basalt and gabbro (Gh, Ghg) in the Laurie Lake area, as well as mafic porphyry and gabbro (gb) at Wapisi Lake, with layered high-grade amphibolite (Ghb) at Kawawayak Lake (Figure 13a, b) and with depleted high-Mg basalt and gabbro/melagabbro (Figure 13c). The layered amphibolite may represent altered, depleted mid-ocean–ridge basalt (MORB) as suggested by its low contents of middle REE and HFSE and lack of significant Nb anomaly with high  $\epsilon_{Nd}$  of +3.6 and +3.7 (DRI2021014). Enrichment in Th and LREE is probably from crustal fluid or melt, as part of back-arc volcanism and/or high-grade metamorphism. Both samples of Ghb have elevated Ni—one has CaO substitution for some MgO—the other has elevated  $K_2O$  (DRI2021014). Unit Ghb is therefore considered as a possible altered version of the high-Mg unit Gh (Figure 13c). The gabbro to porphyry (gb) at Wapisi Lake is chemically similar to type-Ghg gabbro but may be unrelated and younger than the “hosting” Burntwood group. One interlayer of unaltered, depleted pillowed basalt (La/Yb=0.4; Figure 13c) occurs within unit Gh on Laurie Lake (UTM 325072E, 6274411N). An interlayer (at UTM 325315E, 6274449N) of a fine-grained felsic rock with flat elevated REE and strong negative Eu-Ti anomalies (Figure 13c) has the geochemistry of sodic rhyolite that suggests a mid-ocean–ridge granite composition fractionated from a mafic parent probably associated with Gh.

The coarse melagabbro (Ghg) with its fine-grained margin (Gg), in the core of the major anticline on Granville Lake, is strongly depleted and has a positive slope in N-MORB–normalized space (La/Yb=0.4 to 0.5; Figure 13c) similar to the high-Mg basalt on Laurie Lake (La/Yb=0.4). The gabbro intrudes Tod Lake basalt (below) and is therefore younger.

### 4.2.2 Tod-Lake–type mafic rocks (Gt, Gta, Gtb, Gg)

Tod Lake basalt (Gt), the main megaunit in the Granville complex and an important geochemical marker, is exposed along the Wuskwatim–Granville lakes corridor as well as at the margin of the Lynn Lake belt. It represents a crystal-fractionated tholeiite with up to 15% total iron oxide as  $Fe_2O_3$  (Mg-numbers 58–31; DRI2021014). The type samples of pillowed basalt (Gta,

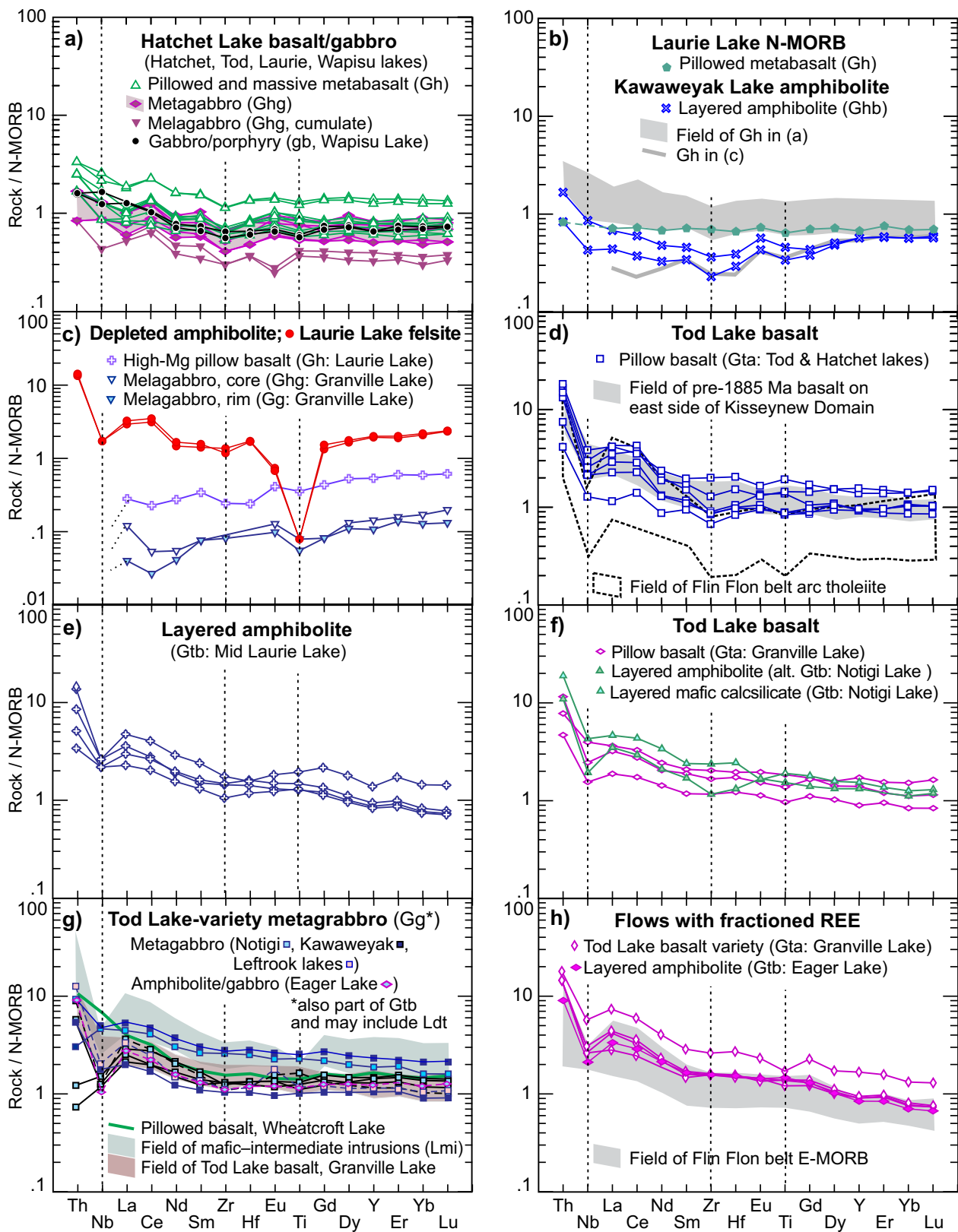


**Figure 13:** N-MORB-normalized multi-element plots of Granville complex metavolcanic and related intrusive rocks with N-MORB, BABB and E-MORB patterns are shown from the Kisseynew north flank and Lynn Lake belt southwest margin. Three HFSE are marked with dashed lines for readability; fields after Zwanzig (2005) and Syme, pers. comm. (1996). Patterns range from a–b) flat, N-MORB-like with minor peaks and troughs to c) depleted tholeiite with Th and Nb below detection, plus related Na-rhyolite. Plots d–f) of Tod Lake basalt, amphibolite and gabbro having identical weak arc-like characteristics including LREE enrichment with local negative HFSE anomalies; these may be arc-rift, subduction-fluid enriched or crustally contaminated back-arc basalts. g) Metagabbro/amphibolite has the same chemistry as Tod Lake basalt, but samples with dashed lines have more fractionated LREE and more crustal signature. h) Some interlayered units show slightly greater overall fractionation, similar to E-MORB. Abbreviation: alt., altered.

at Tod Lake) have slightly elevated LREE and enriched Th but no consistent Ti anomaly and only weakly depleted Nb contents. The middle and heavy REE are the same as typical N-MORB (Figure 13d). The weak but distinct crustal signature of Gta is supported by  $\epsilon_{Nd}$  of +2.3, slightly lower than most N-MORB in the THO.

Layered amphibolite from a structural belt farther southwest, on Laurie Lake, shows a similar pattern (Figure 13e) but with slightly more fractionated HREE (higher Gd/Yb, Table 2). The scatter in Th contents suggests mobility or variable crustal contamination of that element in this higher-grade amphibolite in the south. Type-Tod Lake pillowed basalt (Gta) at Tod Lake (Figure 13d), as well as pillowed basalt mapped as Gta at Granville Lake and altered layered amphibolite in unit Gtb at the Rat River, northwest of Notigi Lake (Figure 13f) generally have very similar trace-element profiles. These units all lie below the Sickle group unconformity and tectonostratigraphically above the Burntwood group, thus strengthening their correlation.

Gabbro units (Gg) at Notigi and Kawaweyak lakes also have geochemistry with moderate ratios of Gd/Yb (1.5–2.9) similar to the types in the west (Figure 13g). Gabbro (Gg) and local amphibolite (Gtb) units at Notigi, Leftrook and Eager lakes have negative Nb anomalies and slightly more fractionated LREE (dashed lines, Figure 13g). These features suggest crustal contamination. All individual patterns are relatively smooth and subparallel, shifted to higher values by fractionation (higher REE contents at lower Mg-numbers). They suggest limited alteration and limited crustal sources of the immobile elements. Values of Th are highly scattered however in samples collected near the transition to granulite in the southeast. Gabbro from Kawaweyak Lake has  $\epsilon_{Nd}$  of +3.4, a value that falls close to Hatchet Lake basalt (Figure 12e).

One group of samples of mainly pillowed basalt from Granville Lake has somewhat more fractionated REE (average La/Yb=4.1) versus other samples from Granville Lake and those from Tod Lake (average La/Yb=2.15). Because these flows are stratigraphically interlayered with OIB-like rocks (see below), they are interpreted to have an enrichment component of plume-derived melt. These light-REE-enriched samples of Tod Lake basalt are comparable to E-MORB (enriched mid-ocean-ridge basalt) in the Flin Flon domain (Figure 13h). However, they are also chemically similar to the late mafic–intermediate intrusions (Lmi, Figure 13g). Thus, some or all of these rocks may not correlate with Tod Lake basalt.

Implications of Figure 13g and the large error (+18/–19 Ma) on the age of the dike cutting the correlated Levesque Bay assemblage, as well as lack of clear contact relations between the Burntwood group and Lmi, shed some doubt on the old age (>1880 Ma) inferred for the basalts in Saskatchewan and Manitoba. The similarity and scatter of Th and Nb in the units compared in Figure 13g permits an interpretation that Tod Lake basalt is comagmatic and coeval with, or only slightly older than, unit Lmi intrusions into the Burntwood group. The

lower content of REE and less consistent negative HFSE anomalies may be a result of less crustal contamination in Gt than in megaunit Lmi. Nevertheless, the Levesque Bay assemblage is clearly cut by a dyke of tonalite dated as  $1867 \pm 3$  Ma (Corrigan et al., 2001a), and thus making the Granville complex older than the Burntwood group, while most data support an ~1.90 Ga age of the Tod-Lake–type basalt.

#### 4.2.3 Pickerel Narrows amphibolite (Gu, Gua, Gub, Guc)

Pickerel Narrows amphibolite has unique geochemical characteristics useful for regional correlation. This mafic–ultramafic amphibolite is found at Granville, Notigi and Kawaweyak lakes in unit Gu, partly fragmental volcanic rocks; unit Gua, pillowed flows; fine-grained interlayers of flows or tuff; unit Gub, layered mafic rock, and gabbro; and unit Guc, low-SiO<sub>2</sub>–calcsilicate rock (mafic–ultramafic carbonate alteration). These units have variably steep negative slopes on an N-MORB–normalized plot, similar to OIB found in conglomerate cobbles in the Flin Flon domain (Figure 14a). Titanium is slightly elevated in the most fractionated members. Olivine-porphyroblastic fragmental and massive units (Gu) at Granville Lake include chemically relatively well-preserved olivine basalt and picrite. Their plots have steep negative slopes showing elevated Ti and Gd and slightly elevated Eu contents, typical of OIB (Figure 14b). Unit Guc and parts of Gua are interpreted as carbonatized and depleted in MgO because they contain calcite, have elevated CaO (average 24%) and average Cr (2140 ppm). In comparison, less altered ultramafic rocks have average MgO=18.5%, CaO=10.1%, Cr=1167 ppm. Nickel content is elevated and highly variable in both Gua and Guc. The grey-weathering calcsilicate gneiss (included in undivided units Gtb and Gs on Notigi and Kawaweyak lakes) locally has geochemical patterns typical of Pickerel Narrows amphibolite (Guc) and is plotted as such on Figure 14a. Samples of Guc have yielded  $\epsilon_{Nd}$  of +2.35 and +4.12, similar to Tod and Hatchet lakes basalts ( $\epsilon_{Nd}$ =+2.30 to +3.65, Figure 12e), indicating minimal interaction with evolved crustal materials. Alteration is interpreted as generally low-temperature hydrothermal and early—on the sea floor—as suggested by altered pillow interstices. Two samples of silicified ultramafic fragmental rock (Pickerel Narrow amphibolite, Gu) from Granville Lake (averages of SiO<sub>2</sub>=54.2%, MgO=20.9%) are depleted in TiO<sub>2</sub> and REE but have strong, positive Eu anomalies, and one has a Nb anomaly (Figure 14d). These profiles and anomalously elevated arsenic support hydrothermal alteration. The mobility of Eu in the absence of elevated Ca (DRI2021014) and lack of cumulate plagioclase in unit Gu may indicate high-temperature alteration in these rocks.

#### 4.2.4 Amphibolite, intermediate and felsic gneiss

Multi-element profiles of local amphibolite megaunit (Gt) bounded by the Burntwood group south of Granville Lake, and sampled on Wheatcroft Lake, are characterized by

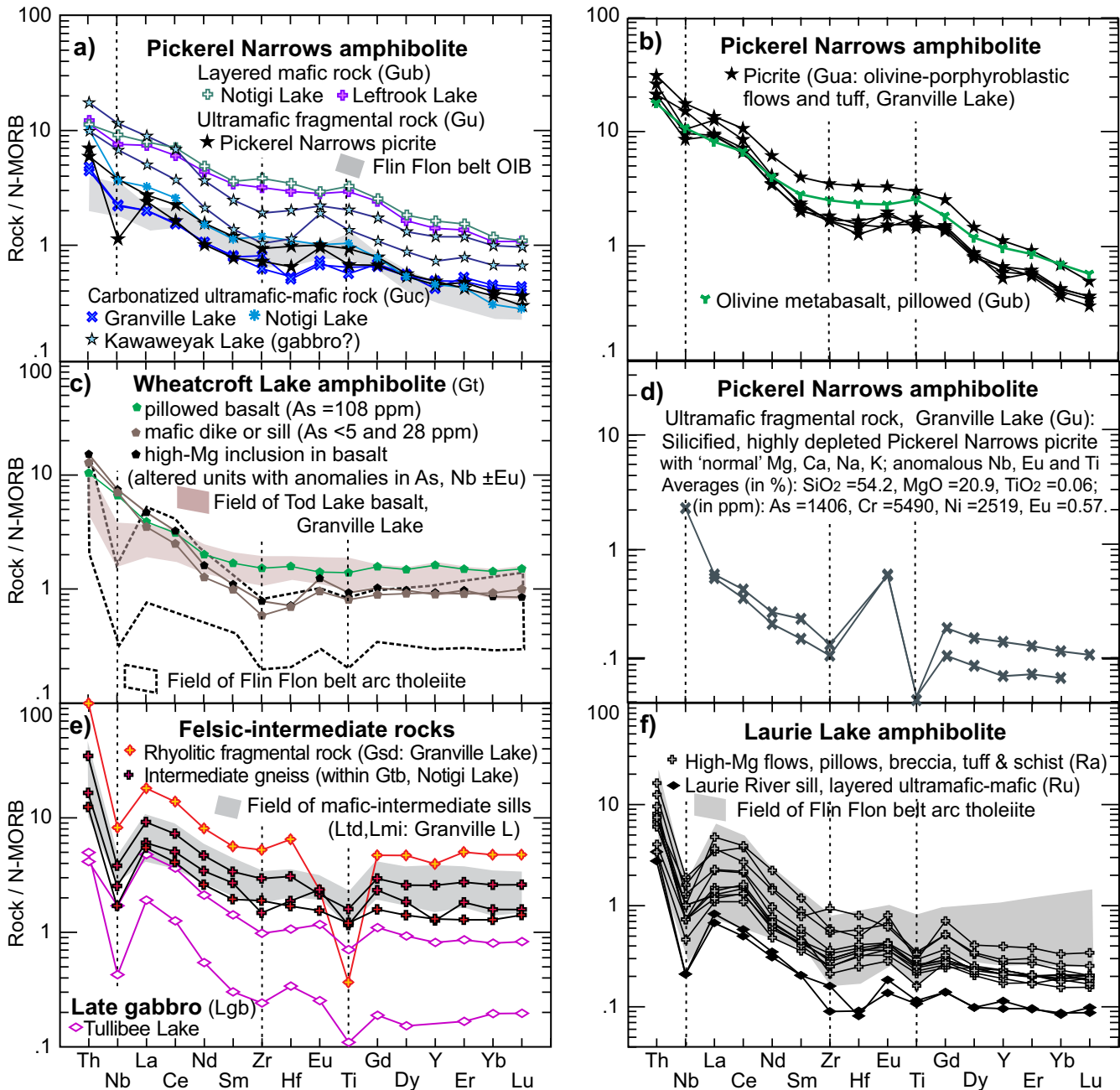


**Figure 14:** N-MORB-normalized multi-element plots of OIB-like metavolcanic rocks of the Granville complex, and arc-like or crustally contaminated rocks are shown from the Kisseynew north flank. Patterns range from **a–b)** strong negative slopes including HREE and no consistently negative HFSE anomaly, indicating a non-arc origin with ocean-island affinity. The field of OIB is after Syme, pers. comm. (1996). Fractionated LREE with flat HREE and no HFSE anomalies in **c)** have possible alteration or an admixture of OIB. Carbonatization appears to have had little effect on the selected elements that are fluid-insoluble, but strong alteration in **d)** has lowered total REE and affected Eu. Gabbro at Tullibee Lake in **e)** shows an arc signature. Intermediate gneiss at Notigi Lake has only slightly more fractionated REE than the field of the mafic-intermediate sill (Ltd, Lmi) that intruded the Burntwood group and the megaunit Gs at Granville Lake. Felsic-intermediate rocks lie within the Granville complex. The Laurie Lake amphibolite in **f)** from a northeastern thrust sheet, have calcalkaline geochemistry with highly fractionated LREE and prominent negative HFSE anomalies. They are clearly distinguished from the back-arc/arc-rift and OIB-like units of the Granville complex by their strong negative HFSE anomalies. Three HFSE are marked by dashed lines for readability.

flat HREE like Tod Lake basalt, and fractionated LREE like arc tholeiite, but have elevated Nb (16–18 ppm) rather than a negative Nb anomaly (Figure 14c) as expected in arc tholeiite.

Intermediate gneiss mapped as part of the Granville complex (Gtb) at Notigi Lake has the multi-element profile of the

mafic to intermediate sills south of Granville Lake (Ltd, Lmi, Figure 14e). The gneiss at Notigi Lake may occur as metasediments (Gs) or sheared quartz diorite sills (Lmi) that had intruded the mafic parts of unit Gtb.

The rhyolitic fragmental rock (conglomerate/agglomerate, Gsd) in the southern sedimentary part of the Granville com-

plex shows a similar profile to the sills but is more enriched in all plotted elements with the exception of Eu and Ti (Figure 14e). This pattern is expected from crystal fractionation of the parent magma of units Ltd, Lmi. The felsic to mafic rocks in Figure 14e show a strong resemblance to a volcanic arc pattern (cf. Figure 14f). The rhyolitic fragmental rock in the Granville complex lies along strike of the ca. 1874 Ma rhyolitic tuff and is considered to be related to it, and apparently fractionated from arc tholeiite.

#### 4.2.5 Origin of the Granville complex mafic–ultramafic rocks

The geochemical characteristics of the Granville complex mafic rocks are comparable to modern and Paleoproterozoic back-arc or arc-rift basalt, suggesting a similar petrogenesis involving adiabatic partial melting of a metasomatized, previously-depleted mantle wedge as occurs in back-arc environments (Pearce and Peate, 1995; Stern et al., 1995; Lucas et al., 1996; Syme et al., 1999). The Tod Lake basalt has been considered part of a ca. 1.9 Ga back-arc or arc-rift sequence (Zwanzig et al., 1999a), which is supported herein. The identical trace-element pattern characterizes an amphibolite unit that is intruded by an  $1891 \pm 5$  Ma (Percival et al., 2004) pluton at the KD margin of the TNB and suggests that the old rocks of the Granville complex also extend along the KD-TNB boundary. A similar thin succession of fine-grained clastic rocks and chert within the upper part of the Tod Lake basalt and the OIB-type rocks at Granville Lake is also present locally along the KD-TNB boundary. The complex may be interpreted as ocean floor (partial suprasubduction ophiolite) that probably formed throughout an early Kiseynew basin. It is stratigraphically overlain by the Sickie group but structurally came to overlie the Burntwood group during early thrusting (Section 6.1.1).

The variably positive values of  $\epsilon_{Nd}$  (+2.3 to +4.1, Table 2) in the mafic rocks of the Granville complex are consistent with juvenile mafic–ultramafic rocks with only local contamination by older crust as in the Wasekwan tectonic collage in the Lynn Lake belt (Beaumont-Smith and Böhm, 2002). Such older Paleoproterozoic or Archean crust must have underlain limited parts of the arc terranes.

In comparison to the mafic–ultramafic rocks in the Granville complex, some normal- to high-MgO (6.75–17.6%) metavolcanic rocks (Laurie Lake amphibolite and schist of Zwanzig et al., 1999a: geochemical units Ra and Rb; DRI2021014) show little fractionation of heavy- to middle-REE (average Gd/Yb=1.52–2.36). They have strongly fractionated LREE (average La/Sm=2.42–3.41) and prominent negative HFSE anomalies on an N-MORB–normalized plot (Figure 14f), all providing evidence of volcanic-arc affinity. These rocks are restricted to the margin of the Lynn Lake belt, where they form a separate thrust sheet together with the unconformably overlying conglomerate of the Sickie group. They are considered part of a major calcalkaline arc assemblage in the Wasekwan tectonic collage (Zwanzig et al., 1999a).

The thin but widespread layers of OIB-type rocks along the north flank of the KD indicate the presence of ocean islands within the floor of the early KD. The geochemistry of the early volcanic rocks on the Kiseynew north flank is consistent with the model (Zwanzig and Bailes, 2010) that an early back-arc basin between an arc terrane in the THO internal zone and the TNB expanded into a significant oceanic tract large enough to contain MORB (i.e., Hatchet Lake basalt) and ocean islands that influenced much of its preserved floor.

#### 4.3 Granitoid intrusive rocks

The Wuskwatim–Granville lakes corridor and the adjoining margin of the LRD experienced about 200 m.y. of Paleoproterozoic granitoid magmatic activity. Each domain or subdomain has a unique suite of intrusions as shown by common field relations, petrography, geochemistry and, where available, U–Pb zircon ages (Section 5.1). Geochemical analyses from widely spaced samples plot in overlapping but consistent fields and patterns on modern tectonic diagrams. Eight intrusive suites considered to be younger than the gabbroic rocks in the Granville complex are tested for consistent geochemistry and proposed for separate origins.

Although the use of tectonic diagrams formed with modern data has been discouraged for use in older rocks (e.g., Pearce et al., 1984), the body of work in the Flin Flon domain (Lucas et al., 1996; Stern et al., 1995; Syme et al., 1999; Whalen et al., 1999) indicates that plate tectonics was active in the THO, and that the geochemistry of the igneous rocks matches that of modern rocks. We infer that comparisons of Phanerozoic igneous rocks with the igneous units, including granitoid rocks in the study area, are indeed valid. Nevertheless, the groups separated by several criteria are tested on the modern tectonic diagrams primarily for consistent geochemistry to identify related suites without tectonic inference and only secondarily for a proposed tectonic origin. In some cases more than one possible origin is presented for consideration. Zwanzig and Bailes (2010) suggested that the granitoid rocks that were deemed to be postcollisional based on their age, distribution and rock associations were broadly similar to those intruded as part of the volcanic arc. They indicated recycling of, or mingling with major crustal components of melts from the existing rocks of the arc, back-arc and probably upper mantle.

The alkali-silica contents of the granitoid rocks plot in overlapping but elongate to compact fields (Figure 15a). Suites analyzed for chemistry (Figure 15a–f) but first determined by lithology and field relations (Sections 3.2.2–3.2.7) comprise the following in order of average age: Footprint Lake plutonic suite (qm); pre-Sickie (LRD-type) quartz diorite to granite (tn, gn); Blacktrout diorite (Lqd); mafic–intermediate suite (Lmi, including Lgb and Ldt); granite–granodiorite (Lgg) and leucogranite (Llg). Granite/granodiorite (gx) is of uncertain age and the Notigi composite granite has several possible ages and origins. Many suites fall into the field of postcollisional intrusions according to geochemistry as determined by Aldanmaz et al.

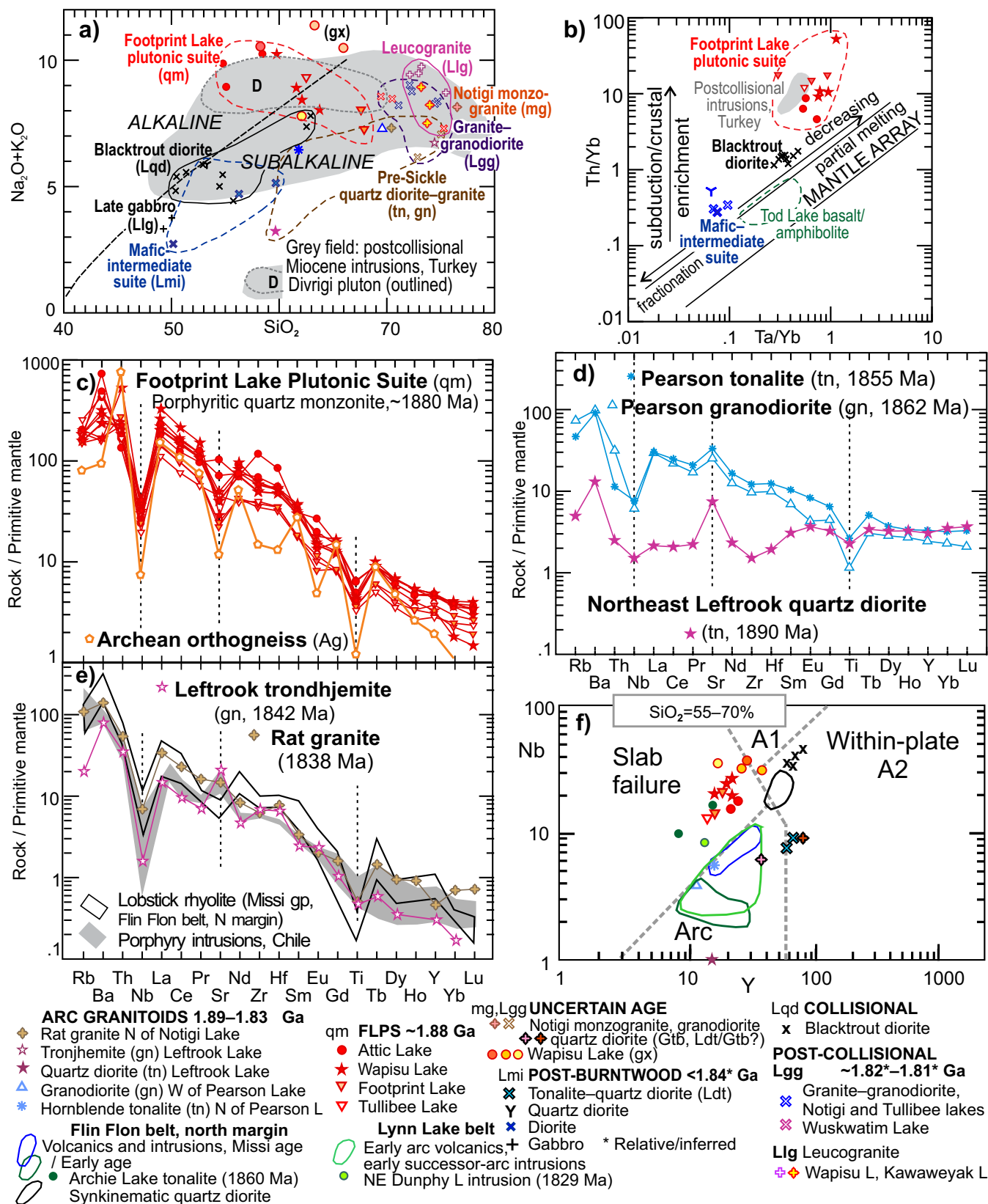


**Figure 15:** Major-, trace- and multi-element diagrams of northern to eastern Kiseynew intrusive suites: **a)** alkalis vs. silica diagram, also showing fields of Early and Middle Miocene postcollisional volcanics, western Turkey (main grey field after Aldanmaz et al., 2000; Divrigi pluton, D, after Kuşçu et al., 2013), with alkaline boundary (dashed); **b)** Th/Yb vs. Ta/Yb diagram for mafic–intermediate rocks suggesting variable partial melting and range of crustal components (after Pearce, 1983) with postcollisional field of mafic–intermediate rocks from Turkish data as in a) and field of Tod Lake basalt including all samples from Granville Lake to Leftrook Lake; **c)** FLPS includes alkaline syenite and quartz monzonite to granite (qm). **d, e)** early arc to late successor-arc intrusions (fields after Zwanzig and Bailes, 2010; Richards, 2003); **f)** volcanic-arc vs. slab-failure and within-plate granitoid diagram of Whalen and Hildebrand (2019) filtered to 55–70% SiO<sub>2</sub>. Flin Flon domain data (Zwanzig and Bailes, 2010), Lynn Lake belt data after X.M. Yang, pers. comm. (2020). Abbreviation: gp, group.

(2000) for the eastern Mediterranean collision in Turkey. The wide field of pre-Sickle intrusions shows the typical fractionation trend of arc intrusions, central in the subalkaline space but overlapping the postcollisional suites, especially at high silica values, where the trends merge. Therefore lithology and field-relations were used primarily to separate felsic intrusive suites, whereas geochemistry was more important for mafic–intermediate compositions ( $\text{SiO}_2=50\text{--}70\%$ ). Multi-element plots were used to better subdivide these suites of intrusive rocks. Those data are normalized with primitive-mantle values using relatively immobile elements plus Rb, Ba and Sr. The latter elements show similar profiles with limited scatter within individual suites despite their higher fluid solubility. Their greater abundance in the granitoid rocks, and a coarser grain size of these rocks apparently allowed them to retain primary geochemical characteristics (Whalen et al., 1999).

#### 4.3.1 Footprint Lake plutonic suite (unit qm)

Chemical analyses and plots of Whalen et al. (2008) indicate that the ca. 1880–1885 Ma FLPS (unit qm) ranges from low- $\text{SiO}_2$  (syenite and monzonite) to highly potassic syenogranite. The crossover from magnesian alkalic compositions to high- $\text{SiO}_2$  subalkaline (Figure 15a) is consistent with magma mixing from multiple sources of subcontinental mantle and middle to upper crust as suggested by Whalen et al. (2008). Trace-element ratios suggest small-fraction partial melting of Th-enriched sources with low available Yb (Figure 15b). Normalized extended element plots from Whalen et al. (2008) and herein indicate strong enrichment of large-ion lithophile elements (LILE), LREE, Zr, Hf and Th, but with depletion of HREE and negative Nb, Sr and Ti anomalies (Figure 15c). The low HREE suggest that garnet remained in the residuum of the melt, and elevated LREE, Rb and Ba indicate a fertile or crustal-source fraction.

#### 4.3.2 Volcanic-arc plutons (LRD-type, tn, gn)

The LRD features plutons with the same range of ages as early volcanic-arc and successor-arc magmatism in the Lynn Lake belt and the rest of the volcanoplutonic domains surrounding the KD. Their origin is confirmed to be in a volcanic arc, as for example shown by their Nb–Y geochemistry of plutons with  $\text{SiO}_2$  of 55–70% (Figure 15f) and flat HREE with negative HFSE anomalies (Figure 15d). Six U–Pb zircon ages from these plutons provide a range of 1890–1838 Ma (Table 3; Section 5). Samples fall into three sets with successively decreasing ages corresponding to “early arc”, “early to middle successor arc” and “late successor arc” of Whalen et al. (1999) in the Flin Flon domain. A similar set of igneous ages occurs in the Lynn Lake belt (Beaumont-Smith and Böhm, 2002) as well as in the Southern Indian domain (Martins et al., 2019). Two unpublished analyses directly from the south margin of the LRD near Pearson Lake, north of the TNB, are also included. Three of the dated plutons extend into

the study corridor in the Kiskeynew north flank: quartz diorite and trondhjemite (as defined by Barker et al., 1974) at Leftrook Lake, and granite on the Rat River, north of Notigi Lake. Other LRD-type plutons occur in structural culminations as at Osik Lake and possibly at Notigi Lake. All but one of the dated plutons have ages that are herein considered as older than the Sickle group.

Whole-rock analyses of the LRD-type intrusions (tn and gn) occupy a distinct field following a typical subalkaline fractionation trend (brown dashed outline in Figure 15a). The field is similar to that of calcalkaline volcanic-arc plutons in the Flin Flon domain (Whalen et al., 1999). However, at  $\text{SiO}_2 > 70\%$  the field of the LRD-type intrusions overlaps the fields of younger granites. Trace-element geochemical patterns of plutons with middle-successor–arc ages, shown on the multi-element plot (Figure 15d), have a flat HREE pattern and moderately fractionated or flat LREE and negative Nb and Ti anomalies. They are therefore arc-like. Leftrook trondhjemite and Rat granite, however, have highly fractionated REE (Figure 15e), probably from melting of mafic and felsic crust, leaving garnet in the residuum. These samples show negative Nb and Ti anomalies and spikes of Ba and Sr. Fractionation of REE increases with younging of volcanic-arc plutons (Figure 15d, e) as it does on the north margin of the Flin Flon domain (Zwanzig and Bailes, 2010).

The Rat granite and Leftrook trondhjemite, being at the south margin of the LRD, have the same trace-element geochemistry as Lobstick rhyolite in the 1845–1832 Ma Missi group at the north margin of the Flin Flon domain. They also match typical porphyry intrusions at the Andean active continental-arc margin in Chile (Figure 15e; Richards, 2003). As suggested for the Andean granitoid intrusions, this can be interpreted to result from the interaction of mafic (normal) arc magma with the (early-arc) crust in a melting, assimilation, storage and hybridization process, but which is questioned by Hildebrand and Whalen (2014) and reinterpreted as formed resulting from slab failure. The latter interpretation is supported in the northeast KD by the similarity of the multi-element patterns in Figure 15c and e. Of the sampled plutons with 55–70%  $\text{SiO}_2$  in the northeast KD, the Flin Flon domain north margin (Zwanzig and Bailes, 2010) and in the Lynn Lake belt (X.M. Yang, pers. comm., 2020). Those dated as 1880, 1860 and 1829 Ma respectively (Figure 15f), scatter in the field of “slab failure” of Whalen and Hildebrand (2019).

Moderately positive values of  $\epsilon_{\text{Nd}}$  (+2.2 for the Leftrook trondhjemite, and +2.6 from granitoids near Pearson Lake) suggest an isotopically slightly Archean-contaminated magma from a mainly juvenile Paleoproterozoic source of melts.

#### 4.3.3 Granitoid rocks of uncertain age and origin (parts of mg, Lgg, gx)

The two phases of the composite Notigi monzogranite/granodiorite (mg/Lgg) lie in the high-silica end (>70%) of chem-

**Table 3:** Geochronology compilation of the Northeast Kisseynew subdomain and Kisseynew north flank.

Site <sup>1</sup>	Sample	Location	UTM-E	UTM-N	Rock type	Unit	U-Pb age Ga/Ma	Type	Interpretation	Lab.	Reference
1	WX04-T050	Wuskwatim Lake	530394	6158874	Charnockite	Ag	<sup>1</sup> 2.64–2.66, 3.24	1	Detrital peaks	GSC	Rayner and Percival, 2007
2	PBA04-16A	Burntwood River	527644	6163534	Quartzite	Wq	<sup>1</sup> 2.7, 3.15, 3.3	1	Detrital peaks	GSC	Zwanzig et al., 2006
3	PBA06-26A	Muskoseu River	528812	6164543	Tonalite	Ag	<sup>1</sup> 2.5–2.55, 2.7–3.0	1	Detrital peaks	GSC	Rayner and Percival, 2007
4	PBA07-1278B	Wapisu Lake	479114	6184062	Quartzite	Wq	<sup>1</sup> 2.65–2.7, 2.85–2.9, 3.1–3.3	1	Detrital peaks	GSC	Murphy et al., 2009
5	PBA06-26B	Muskoseu River	528812	6164543	Quartzite	Wq	2.2–2.4, <sup>1</sup> 2.5–2.7, 2.9	1	Detrital peaks	GSC	Rayner and Percival, 2007
5	PBA06-26B	Muskoseu River	528812	6164543	Quartzite	Wq	1806 ±5	1	Metamorphic	GSC	Rayner and Percival, 2007
6	PBA03-35	Pipe 2 Mine	553442	6149738	Pelite	P2	<sup>2</sup> ~1.97, <sup>1</sup> 2.65–2.75	1	Detrital peak	GSC	Figure 18f; Rayner et al., 2006
7	12-4-4461	Setting Lake	526268	6098883	Greywacke	S	<sup>1</sup> 2.7, 2.9, 3.0	3	Detrital peaks	U Alb.	Figure 18g; Couëslan, 2016
8	25-71-412	Atik Lake	463212	6179568	Quartz monzonite	qm	1879 ±13	1	Igneous	GSC	Percival et al., 2007
9	PBA07-1278A	Wapisu Lake	479114	6184062	Quartz monzonite	qm	<sup>3</sup> 1872 ±9 min.	1	Igneous min.	GSC	Murphy et al., 2009
10	25-71-328	Footprint Lake	511677	6183356	Quartz monzonite	qm	1882 ±10	1	Igneous	GSC	Percival et al., 2007
11	12-02-783	Leftrook Lake	524879	6218839	Quartz diorite	tn	1890 ±>1	2	Igneous	U Alb.	DRI2021014; Figure 23c <sup>4</sup>
12	12-02-7909	Leftrook Lake	523272	6217434	Tronhjemite	gn	1842 ±3	2	Igneous	U Alb.	DRI2021014; Figure 23d <sup>4</sup>
12	12-02-7909	Leftrook Lake	523272	6217434	Tronhjemite	gn	1807 ±19	2	Metamorphic	U Alb.	DRI2021014; Figure 23d <sup>4</sup>
13	12-05-4606	Pearson Lake	604586	6244456	Hornblende tonalite	tn	1855 ±3	3	Igneous	U Alb.	DRI2021014; Figure 23e <sup>4</sup>
14	12-05-4605	West of Pearson Lake	582218	6231955	Granodiorite	gn	1862 ±10	3	Igneous	U Alb.	DRI2021014; Figure 24f <sup>4</sup>
15	104-04-446	Rat River	477164	6205837	Granite	gn	1838 ±4	3	Igneous	U Alb.	DRI2021014; Figure 24a <sup>4</sup>
15	104-04-446	Rat River	477164	6205837	Granite	gn	~1807	3	Metamorphic	U Alb.	DRI2021014; Figure 24b <sup>4</sup>
16	104-07-242	Notigi Lake	485429	6201971	Monzogranite	mg	1862 ±6	1	Igneous	GSC	Murphy et al., 2009
16	104-07-242	Notigi Lake	485429	6201971	Monzogranite	mg	1805 ±3	1	Metamorphic	GSC	Murphy et al., 2009
17	PBA07-1034	Osik Lake	504806	6200250	Enderbite	en	1885 ±7	1	Igneous	GSC	Rayner and Percival, 2007 <sup>5</sup>
18	PBA07-1024	Osik Lake	504056	6201805	Tonalite	tn	1873 ±11	1	Igneous	GSC	Rayner and Percival, 2007 <sup>5</sup>
19	CXA-02-D20	Granville Lake	401203	6232613	Felsic tuff(?)	Gsd	~1874	1	Igneous?	GSC	Corrigan and Rayner, 2002 <sup>5</sup>
20	CXA-02-N4	Granville Lake	395600	6232600	Conglomerate	Bc	<sup>1</sup> 1860, 2.32, 2.57	1	Detrital peaks	GSC	Corrigan and Rayner, 2002 <sup>5</sup>
21	CXA-02-N1	Wheatcroft Lake	461415	6259422	Greywacke	Ba	<sup>1</sup> 1850, 2.4, 2.54	1	Detrital peaks	GSC	Corrigan and Rayner, 2002 <sup>5</sup>
22	PBA04-3	Wabowden	499800	6060800	Greywacke	Bg	1850–1875	1	Detrital peak	GSC	Percival et al., 2005
23	CB01-09	Southwest Lynn Lake	359934	6288436	Pebbly arkose	Ksa	1.83, <sup>1</sup> 1.87, 2.54	3	Detrital peaks	U Alb.	Beaumont-Smith and Böhm, 2002
24	12-08-11	Granville Lake	406804	6235918	Arkose	Ks	<sup>1</sup> 1855, 2.53–2.57	3	Detrital peaks	U Alb.	Figure 25c <sup>4</sup>
25	WX04-T035	Setting Lake	524500	6101350	Arkose	Ks	<sup>1</sup> 1864, 2.5–2.7	1	Detrital peaks	GSC	Percival et al., 2005
26	PBA06-91	Tullibee Lake	528247	6124396	Tonalite gneiss	Lmi	1890 ±8	1	Igneous	GSC	Rayner and Percival, 2007
26	PBA06-92	Tullibee Lake	528247	6124396	Tonalite gneiss	Lmi	1809 ±4	1	Metamorphic	GSC	Rayner and Percival, 2007
27	PBA07-1028	Osik Lake	501693	6200559	Ultramafic rock	Lmu	1791 ±1	1	Igneous	GSC	Rayner and Percival, 2007 <sup>5</sup>

<sup>1</sup> Main peak<sup>2</sup> Single grain<sup>3</sup> Includes metamorphic grains<sup>4</sup> This report<sup>5</sup> Personal communication*Italic:* UTM ±100 m

Analysis type: 1-SHRIMP; 2-TIMS; 3-Laser-ablation, multicollector, inductively coupled plasma–mass spectrometry (LA-MC-ICP-MS).

See Figure 17 for site locations.

Abbreviations: Lab., laboratory; min., minimum; U Alb., University of Alberta.

ically overlapping varieties of intrusions (Figure 15a). Notigi monzogranite yielded two zircon ages (SHRIMP): 1862 ±6 Ma (large cores) and 1806 ±3 Ma (subhedral rims; Section 5.1.3). This leaves the possibilities of

- 1) an older monzogranite intruded by a younger granodiorite during migmatization and regional late-granite intrusion as assumed in the regional legend;
- 2) two nearly coeval phases and a metamorphic age typical of the study area; and
- 3) two younger plutons with an inherited age (e.g., Murphy et al., 2009).

Whole-rock geochemical data of the compositions of the relatively high-silica monzogranite (mg) and granodiorite (Lgg) lie on the successor-arc fractionation trend and on the lower-alkali end of the late granites (Figure 15a). Primitive-mantle-normalized trace-element data show moderately fractionated LREE and high contents of LILE for both bodies (Figure 16a). Both show flat HREE and strong negative anomalies of Nb and Ti typical of volcanic-arc plutons. Negative anomalies also suggest loss of Sr, Eu by fractionation of plagioclase. The Notigi Lake monzogranite is less mafic, has a lower alumina to alkali ratio ( $A/CNK=1.01$ , cf. 1.03 and 1.06 of the granodiorite, DRI2021014). The monzogranite also has slightly less fractionated REE than the granodiorite. Although tentatively mapped as unit Lgg, the granodiorite has a trace-element profile that is unrelated to rocks mapped as Lgg elsewhere but matches the monzogranite.

Distinctive pink varieties of fine-grained, alkaline biotite-granite (gx, Llg) occur as sheets at the margin of and interlayered in qm of the FLPS intrusion in the southwestern Wapisi Lake area or that adjoining gabbro (gb) of uncertain origin farther north (UTM 483276E, 6187566N). Like unit qm, the sheets have a prominent magnetic signature. Major-element contents extend to higher alkali contents than qm (Figure 15a). Extended-element patterns of gx have a similar primitive-mantle-normalized profile to qm but with slightly less fractionated REE (i.e., overlapping LREE but with higher HREE; Figure 16b). In Nb/Y space, unit gx plots into the field of slab failure of Whalen and Hildebrand (2019) as on Figure 15f. The alkaline biotite-granite sheets (gx, Llg) at southwest Wapisi have a similar trace-element profile to unit Lgg and may belong to this younger suite, but combined geochemistry and the close association with unit qm, unit gx is also probably a candidate for a phase of the FLPS. Late leucogranite (Llg) directly adjacent to one of the sheets of gx and unit W (UTM 479158E, 6184024N) has an  $\epsilon_{Nd}$  value of -4.47 and  $A/CNK=1.06$ , indicating contamination (partial melting) from one of the older units.

#### 4.4 Late intrusive rocks

##### 4.4.1 Blacktrout diorite (Lqd)

The Sickie group covering the margin of the LRD and Sickie inliers in the KD uniquely contain sills of Blacktrout diorite (Lqd). These sills are distinguished by their high contents of magnetite, apatite and titanite, and therefore contain high contents of  $TiO_2$ , and  $P_2O_5$  as well as total REE (Table 2). They have elevated contents of  $K_2O$ ,  $Na_2O$  with  $SiO_2$  at 50–63%, placing a few low- $SiO_2$  samples in the alkaline field (Figure 15a). On a multi-element plot, samples of Lqd shows a unique pattern (Figure 16c) identical from the type area at Beaucage Lake to all along the Kisseynew north margin. Blacktrout diorite has high contents of REE (average concentration of La and Yb of 133 and 4.8 ppm,  $La/Yb=27.5$ ). Negative  $\epsilon_{Nd}$  values (-4.98, DRI2021014; -4.8, Corrigan and Rayner, 2002) indicate that the Blacktrout diorite has an Archean component from either crust or mantle. Moderately low-fraction melting (Figure 15b) of old mantle plus crustal contamination could produce a quartz diorite with elevated  $K_2O$  and  $P_2O_5$ , and negative  $\epsilon_{Nd}$ . In Nb/Y space, Lqd plots as “within-plate” granitoids along with similar synkinematic quartz diorite, also with negative  $\epsilon_{Nd}$  on the Flin Flon domain north margin (Figure 15f).

##### 4.4.2 Mafic to intermediate intrusions (Lmi, Lgb, Ltd)

A distinctive intermediate to mafic intrusive suite (Lmi with phases Lgb, Ltd) of subalkaline gabbro and quartz diorite to tonalite sills (Figure 15a) intruded the Granville complex and Burntwood group in the southern Granville Lake area. Based on their intrusion as sills and a laccolith that are fractionated and give younging like the hosting Burntwood group (Zwanzig, 2019), and the involvement, at least, in early  $D_2$  deformation, these intrusions are considered to be early post-Burntwood in age. Based on similar geochemistry and intrusion into unit G, they are tentatively correlated with intermediate gneiss at Notigi Lake (Figure 14e), suggesting a wide distribution. The units are distinctly different from Blacktrout diorite in their minimal fractionation of REE (Figure 16d) as opposed to the strong fractionation in Lqd (Figure 16c).

##### 4.4.3 Synmetamorphic granitoid intrusions or leucosome (Lgg, Llg, Lpg)

Small synmetamorphic, synkinematic granitoid intrusions including prominent leucosomal veins and sheets occur from Notigi Lake to the TNB boundary in the study area. They are weakly peraluminous (alumina index,  $A/CNK=0.99–1.08$ ) and generally relatively rich in  $K_2O$  but low in mafic elements (DRI2021014). Inclusions and schlieren of Burntwood group (average  $A/CNK=1.36$ ) indicate some assimilation or flux of partial melt. Granite and granodiorite (Lgg, Figure 16e) are commonly similar to the abundant larger intrusions in the Central Kisseynew subdomain south of the Highrock Lake batholith (Figure 1; i.e., Flatrock Lake granite in Zwanzig and Bailes [2010]). Most samples, however, show slightly greater fractionation of REE and LILE than those in the south. A granite (Sample 104-07-085-2) from the south side Notigi Lake is juvenile ( $T_{CR}=2.13$  Ma).

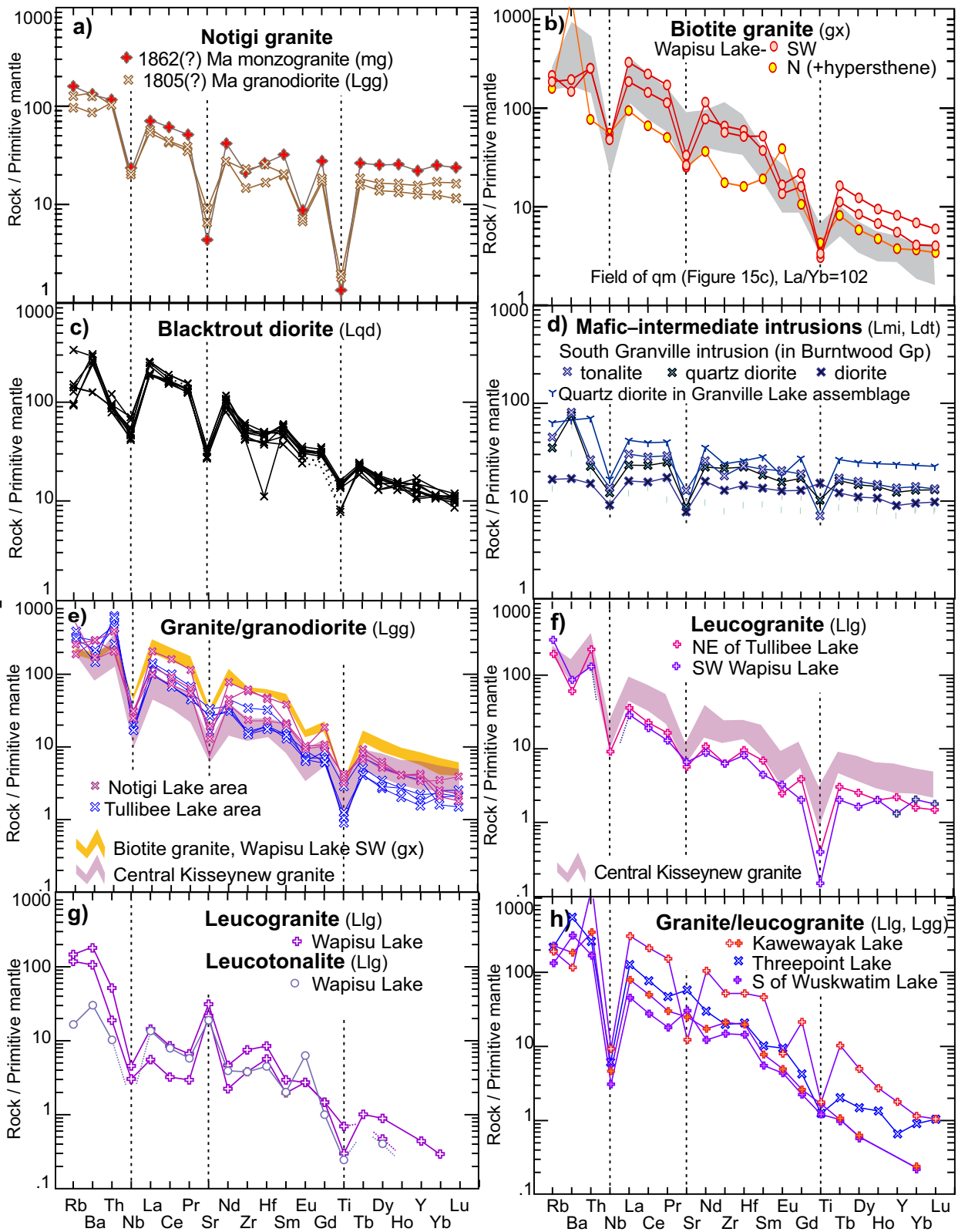


**Figure 16:** Primitive-mantle-normalized multi-element diagrams of pre- to postcollisional intrusive rocks: **a)** two phases or plutons of Notigi granite (mg) and granodiorite (Lgg); **b)** granite to granodiorite similar to large intrusions in the central Kisseynew, and alkali-rich granite similar to the FLPS but of unknown age; **c)** quartz diorite with elevated alkalis, intruding the Sickie group bordering the Leaf Rapids domain and within the Notigi inlier; **d)** postcollisional sills intruding the Granville complex, Burntwood and Missi groups, Kisseynew north flank, south of the main suture; **e)** leucogranite with typical pattern of central Kisseynew intrusions but slightly more fractionated; **f)** leucogranite, as e) but lower REE; **g)** leucogranite sills and a trondhjemite leucosome vein at Wapisu Lake with low concentration of REE and positive Sr and Eu anomalies, possibly due to granite-melt escape with resulting plagioclase accumulation (Aldanmaz et al., 2000); **h)** leucogranite with strong REE fractionation. Field of central Kisseynew granite after Zwanzig and Bailes (2010).

Leucogranite to leucotonalite sheets, veins and lenses (Llg) that make up the migmatitic leucosomes have  $A/CNK=1.06$ – $1.08$ . Samples from small leucosome intrusions (anatectite) at Wapisi Lake and northeast of Tullibee Lake have less fractionated REE and less LILE than the granite-granodiorite (Figure 16f, g). Niobium and Ti are depleted, and Nd-model-ages ( $T_{RC}$ ) range from 2.28 to 2.79 Ma, suggesting a variety of felsic sources of melts locally including Archean sources. The earliest veins have low REE contents, particularly HREE (average  $La \leq 10$ ,  $Yb \leq 0.1$  ppm) with positive anomalies of Ba and Sr (Figure 16g). A sample (12-09-11-1B) of leucotonalite leucosome in the Burntwood group (Bm) at Wapisi Lake has the Nd-model age of 2.28 Ga similar to the average of the Burntwood group (2.30 Ga). A sample (12-09-23-1B) from the margin of the FLPS at western Wapisi Lake, however, has the Nd-model age of 2.79, similar to the average FLPS (2.85 Ga). Samples from Kawawayak, Threepoint and south of Wuskwatim lakes have extreme fractionation of REE (average  $La/Yb=393$ ), higher than the FLPS (average  $La/Yb=96.4$ ). This is possibly caused by melting of biotite with inclusions of minerals with high contents of LREE. A sample of leucogranite in the Threepoint Lake pluton has  $T_{RC}=2.53$  Ga, showing some Archean contamination from the main intrusion.

#### 4.5 Probable origins of the granitoid intrusive rocks

The FLPS could be derived in large part from a subcontinental lithospheric mantle source that had been previously modified during subduction. Whalen et al. (2008) based this conclusion on major and trace-element geochemistry in the less felsic members, in analogy to a similar younger plutonic suite of Tibetan potassic lava (data from Williams et al., 2004). Further analogues are in western Turkey (Figure 15a; data from Aldanmaz et al., 2000, and Kuşcu et al., 2013). It is probable that the 2.8–2.9 Ga Nd-model ages and highly negative  $\epsilon_{Nd}$  of the FLPS (DRI2021014) are characteristics of the mantle source. Crustal melt addition and mixing would produce granite end members with only slight changes in Nd-isotopic composition (Whalen et al., 2008).

Hildebrand and Whalen (2014) have argued, based on work on Sierra Nevada plutons, that intrusions with e.g. high  $La/Yb$  and Ba concentrations, and low concentrations of Y and Nb like the FLPS formed in uplifted volcano-plutonic terranes after a collisional event as a results of slab failure (breakoff) and rising, hot, fertile asthenosphere. Whalen and Hildebrand (2019) have developed element-ratio diagrams of geochemical features of such rocks, which are similar to the FLPS intrusions. Leftrook trondhjemite and Rat granite, with similar trace-element patterns as the FLPS, are also possible candidates of slab-failure origins (Figure 15e), but with respectively  $>70\%$  and  $\approx 70\%$   $SiO_2$  do not fit or are marginal to the criteria set for Figure 15f.

Biotite granite (unit gx), although free of feldspar phenocrysts and undated, may be part of the FLPS (Figure 15f). These fine-grained granite sheets may represent a late melt

fraction during crystal fractionation, possibly filter pressing, of the main FLPS intrusion in the western Wapisi Lake area. The variation of  $\{Na_2O+K_2O\}$  at 7.2–10.2% and  $Al_2O_3$  at 2.8–3.3% (DRI2021014) suggests K-feldspar fractionation in the FLPS that may have formed a gx residual melt that intruded the crystallized part of the pluton and its hosting Wuskwatim Lake sequence.

The Blacktrout diorite (unit Lqd) and the mafic–intermediate sills (units in Lmi) occur on opposite sides of the crustal suture, with the former on the side of the LRD (upper plate). Both units plot at the margin of “within plate” intrusions in Nb/Y space as type A2 ( $SiO_2$ -saturated, Figure 15f). Such rocks are herein considered to postdate arc magmatism. Low-fraction melting (Figure 15b) and a deep source of Lqd from a high melt column in the north, extending through crust and mantle, could help to explain the higher content alkalis and highly fractionated trace elements being from multiple sources. The negative values of  $\epsilon_{Nd}$  indicate that the melt column has encountered Archean mantle and/or crust.

Leucogranite to leucotonalite sheets (Llg) that share their geochemistry with leucosomes are interpreted to be the result of melt withdrawal, at least in part, from the migmatitic Burntwood group because of both their occurrence mainly within it and their peraluminous compositions. Geochemical signatures such as in Figure 16g are found in leucosome formed by fluid-present crustal melting of quartz and feldspar in metagreywacke and metapelite at near granulite-facies conditions (Cruciani et al., 2008). Such melts with low REE and strong positive Sr and Eu anomalies (Figure 16g), formed by fluid-present melting of quartz and feldspar, are relatively immobile and remain in, or near, the source rocks (Fornelli et al., 2002). The very low HREE contents indicate that garnet remained behind in the source rock and became enriched in the melanosome and mesosome. It may explain the increase in garnet content in the Burntwood group from directly south of Granville Lake (unit B) to the migmatite (units Bg, Bm and Bd) farther south and east. Nevertheless, the quartz-rich veins may have formed by subsolidus segregation (Sawyer and Barnes, 1988). Quartz cores with trondhjemite rims of early veins and boudins suggest protracted development from subsolidus state to melt segregation and loss.

The granites with highly fractionated REE are probably melts from the top of the granulite metamorphic zone where biotite is partitioned into melt and hypersthene with release of its trace elements and that of its inclusions (e.g., LREE), but HREE-bearing minerals (e.g., garnet) remaining in the restite. A high heat source is required.

Neodymium-model ages of the late granites (2.13 to 2.79 Ga) and a wide range of  $\epsilon_{Nd}$  (–5.5 to +1.09, Figure 12f) indicate a small variable addition of Archean melt component, consistent with postcollisional granites in a largely juvenile terrane (KD) but with local exposures of Archean gneiss, and intrusions and sediments from Archean sources.

## 5. U-Pb zircon-geochronology compilation

Absolute ages of zircon, either magmatic, detrital, inherited or metamorphic, provide critical information to constrain the geological evolution of the Wuskwatim–Granville lakes corridor and tie it into the rest of the W-THO. This section is a compilation and re-evaluation of U-Pb zircon-age data from the following sources:

- 1) collected and analyzed by the GSC
- 2) from archived MGS samples, analyzed at the GSC
- 3) collected by the MGS (the authors or Beaumont-Smith and Böhm, 2002, 2003, 2004) and analyzed at the Radiogenic Isotope Facility, University of Alberta (Edmonton, Alberta)
- 4) comparative data from the TNB. Analytical methods include SHRIMP and laser-ablation, multicollector, inductively coupled plasma–mass spectrometry (LA-MC-ICPMS) as well as TIMS

Methods, laboratories and results are given in DRI2021014. All sample locations are shown on Figure 17. Up to 20 kg of representative rock for each sample were collected using hammers or rock saw; weathered surfaces, veins and alteration inhomogeneities were trimmed away in the field on the source rock.

The work by the GSC was focused on the oldest rocks: the basement gneiss and basal quartzite of the Wuskwatim Lake sequence as well as the FLPS. For the purpose of comparison some ages of rocks in the TNB similar to those in the KD are included in Table 3. Samples of the Sickie group were collected to facilitate comparisons with the Burntwood group and in order to supplement GSC data from Granville Lake (Corrigan and Rayner, pers. comm., 2008). Feldspathic greywacke (Gsa) of the Granville complex was also sampled but yielded no useful grains. Similarly, various intrusions into the Burntwood group also yielded no useful results.

In order to better understand the timing and relationship of successor-arc intrusions juxtaposed across the Leaf Rapids–Kisseynew domain boundary, in relation to orogenic history, plutonic samples from the Rat River and Notigi Lake area were collected and processed for U-Pb zircon dating. The biotite granite (Rat granite, gn, sample 104-08-446) was collected from an apophysis of the LRD on the Rat River, and the monzogranite (Notigi granite, mg, sample 104-07-644) was collected at Notigi Lake, in the KD. Samples collected for dating by Zwanzig and Böhm from the south margin of the LRD, and the sample from the Rat River were processed at the University of Alberta; the sample from Notigi Lake was sent for processing to the GSC. Using SHRIMP, the GSC successfully obtained U-Pb ages also from enderbite, tonalite and ultramafic rock in the Osik Lake plutonic inlier in the KD.

The University of Alberta's Radiogenic Isotope Facility carried out the U-Pb geochronology for most samples using LA-MC-ICPMS. Zircon-grain separation and analysis followed similar procedures as outlined by Anderson (2008) using the methodology of Simonetti et al. (2005). The internal features of the zircons in the Rat River sample 104-08-446 are described

from cathodoluminescence imagery provided by the University of Alberta.

The GSC carried out the U-Pb geochronology using SHRIMP. Results were previously released for unit mg in Rayner (2009). Other data sources are given in Table 3. The SHRIMP analytical procedures followed those described by Stern (1997), with standards and U-Pb calibration methods following Stern and Amelin (2003). The internal features of the zircons (such as zoning, structures, alteration, etc.) were characterized in backscattered electron mode using a Zeiss Evo® 50 scanning electron microscope. Analytical conditions and calibration parameters are listed in DRI2021014. Analyses of secondary standard z1242 were interspersed through the analytical sessions and the measured  $^{207}\text{Pb}/^{206}\text{Pb}$  age was compared with the accepted age determined by TIMS (2679.7 Ma; B. Davis, pers. comm., 2009).

Isoplot v. 3.00 (Ludwig, 2003) was used to generate concordia plots and calculate weighted means. All errors reported in the text are given at the  $2\sigma$  uncertainty level. References for all geochronology discussed in this report, including previously published Data Repository Items, are compiled in Table 3.

### 5.1 Results and implications

Work in the Northeast Kisseynew subdomain by the GSC from 2005 to 2008 led to the discovery of Archean gneiss with Archean-sourced supracrustal cover (Wuskwatim Lake sequence; Percival et al., 2005). In addition, a suite of distinctive K-feldspar–porphyritic plutonic rocks (FLPS) within the juvenile Paleoproterozoic sedimentary rocks of the KD yielded a surprisingly early age (ca. 1.88 Ga) with Nd-model ages of ca. 2.8 Ga derived from Archean mantle (Percival et al., 2007; Whalen et al., 2008). Paleoproterozoic ages determined from intrusive rocks match the range of ages of volcanic-arc plutonic ages surrounding the KD. Detrital zircons further yielded the age range of the detritus in the sediments that formed the main units in the KD.

#### 5.1.1 Basement and cover

The GSC SHRIMP data in Figure 18 of charnockite and tonalite, intrusive phases of the basement gneiss (part of unit Ag), are compared with the overlying arkosic quartzite (Wq) of the Wuskwatim Lake sequence from three localities, and with the Ospwagan group metasedimentary rocks from the TNB. The data show that each unit has Archean zircon populations with prominent peaks with similarities and differences for the basement rocks and their cover in the Northeast Kisseynew subdomain.

Charnockite (part of unit Ag) has a peak of ages between 2.55 and 2.8 Ga as well as Mesoarchean peaks between 3.1 and 3.25 Ga (Figure 18a). Muskoseu tonalite (part of unit Ag, Figure 18b) yielded zircon ages with a general spread mostly overlapping that of the charnockite but with an older peak at 2875 Ma. The peaks in the basement rocks may have several inter-

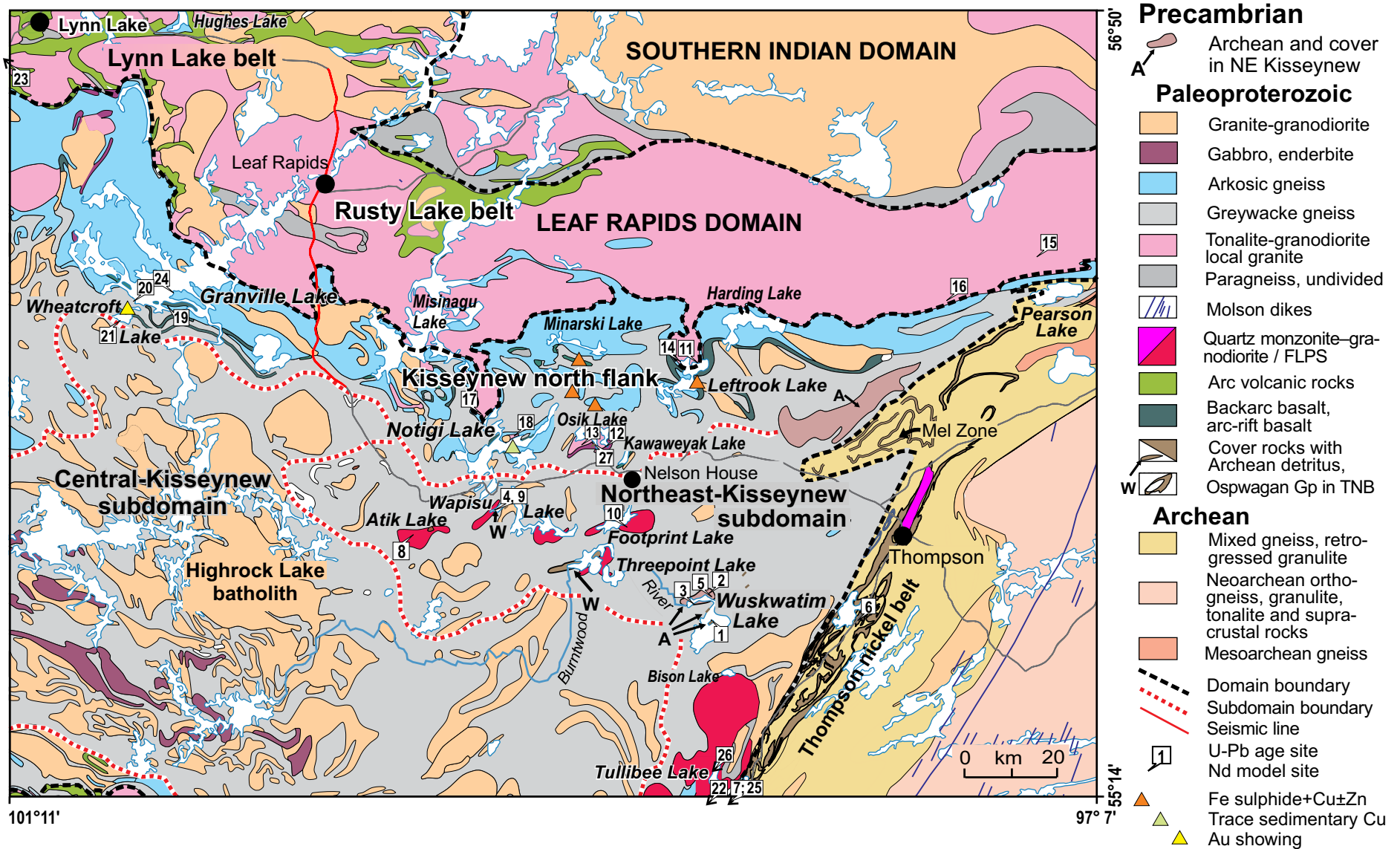
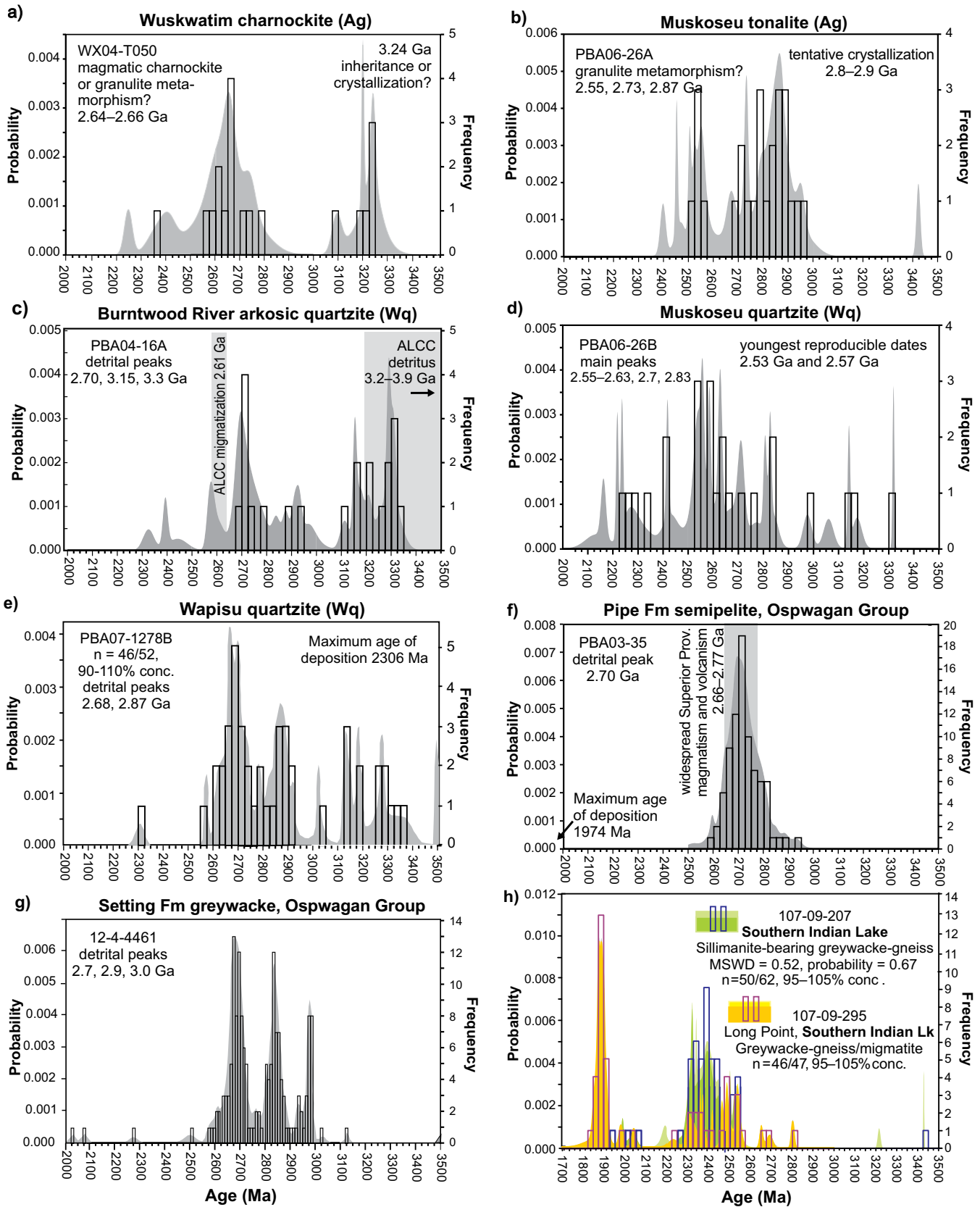


Figure 17: Location of selected U-Pb zircon age sampling sites and selected mineral showings: Fe sulphide + Cu ± Zn, trace sedimentary Cu and Au. Details are described in Section 8. Age data are given in Table 3.



**Figure 18:** Comparison of pre-Burntwood basement, cover and intrusive ages in the KD with Oswagan group (from TNB) and Southern Indian domain detrital-zircon ages: **a-g)** pericontinental detrital zircons probably from the Superior craton, but also older exotic ages; probability density curves illustrate the entire dataset, including replicate analyses and >5% discordant results; overlaid histograms do not include replicate analyses or discordant results; data from Rayner and Percival (2007); Percival et al. (2005); Murphy et al. (2009); maximum age of Oswagan group deposition data from Hamilton and Bleeker (2002); widespread Superior-craton magmatism data from Corfu and Davis (1992); **h)** detrital-zircon data from Southern Indian Lake metagreywacke, after Martins et al. (2019). Abbreviation: ALCC, Assean Lake crustal complex (data from Böhm et al., 2003). Abbreviation: conc., concordant.

pretations including ages of crystallization, zircon inheritance and granulite metamorphism (Rayner and Percival, 2007).

Uranium-lead ages of detrital zircons in the arkosic-quartzite samples (Wq) on the Burntwood River and Wapisi Lake area have prominent peaks at or near 2.7 Ga with minor younger and significant older peaks (Figure 18c, d). The 2.7 Ga peak is the same as in the Ospwagan group sedimentary rocks in the TNB (Figure 18f) from semipelitic detritus eroded from the Superior craton. A significant abundance of zircons in Wq older than 2.7 Ga (Figure 18c–e) may come from the local basement (Figure 18a, b) or, possibly, from exotic crust such as the Assean Lake crustal complex, northwest Superior craton (Böhm et al., 2003). The two main peaks for quartzite on Wapisi Lake (Figure 18e) are like those of the Setting Lake Formation, near the top of the Ospwagan group (Figure 18g). Young ages with 2.30–2.55 Ga peaks overlap those from greywacke-gneiss in the Southern Indian domain (Figures 18h and 19a) or the margin of the Hearne craton (Martins et al., 2019).

### 5.1.2 Footprint Lake plutonic suite

The distinctive FLPS of porphyritic quartz monzonite and syenite–granite (qm) yielded SHRIMP ages of about 1880 Ma (Percival et al., 2007; Whalen et al., 2008). The rocks represent a rare alkalic to alkali-calcic suite that predates the Burntwood group and contains an Archean melt component (Percival et al., 2007) including subduction-modified mantle (Whalen et al., 2008). The bodies at Atik and Footprint lakes (Sites 8 and 10, Figure 17) yielded crystallization ages of  $1879 \pm 13$  Ma and  $1882 \pm 10$  Ma from 23 and 24 SHRIMP analyses, respectively (Percival et al., 2007). The high error is ascribed to low U contents of the zircons and high-grade metamorphism. A slightly younger age, within error of the older, has been obtained from a sample at Wapisi Lake ( $1872 \pm 9$  Ma; Murphy et al., 2009). Those data show scatter that includes the age of regional metamorphism (Figure 19b). Despite the highly negative  $\epsilon_{Nd}$  of the rocks (Section 4.3.1; Percival et al., 2006) no inherited zircons were found.

### 5.1.3 Early-arc–successor-arc plutons

Uranium-lead dating shows that granitoid rocks along the south margin of the LRD range in age from 1.89 to 1.84 Ga, similar to early arc and early to late successor-arc plutons in the rest of the THO internides (1.89–1.83 Ga, e.g., in the Lynn Lake belt; Zwanzig et al., 1985; Baldwin et al., 1987; Turek et al., 2000; Beaumont-Smith and Böhm, 2002; Beaumont-Smith et al., 2006; in the Flin Flon domain, e.g., Whalen et al., 1999; in the Southern Indian domain, Martins et al., 2019). Foliated quartz diorite (unit tn), north of Leftrook Lake, from the margin of a large trondhjemite pluton (unit gn), yielded a three-point concordia age of  $1890 \pm 2$  Ma (Figure 19c; UPB-12-2-783, DRI2021014). Although no contacts are exposed, it is considered to be one of the oldest components of the LRD volcanic arc massif. The main body of the pluton (composed of trond-

hjemite, unit gn, Site 14, Figure 17) yielded a crystallization age of  $1842 \pm 3$  Ma (Figure 19d; UPB-12-2-7909, DRI2021014), indicating that it is a younger body intruded into the quartz diorite. The two-point selected discordia of five analyses is anchored at 0 Ma, thus providing a minimum age of emplacement. The three remaining grains yielded an age of  $1807 \pm 19$  Ma (Table 3) interpreted to represent metamorphism, this being one of the most common ages of recrystallization and migmatization in the THO internides (e.g., Manitoba Geological Survey, 2018).

Age determinations by LA-MC-ICPMS on granitoid rocks of the Livingston plutonic belt on the south side of the LRD (Lenton and Corkery, 1981; Corkery and Lenton, 1990) north and west of Pearson Lake (Sites 15 and 16, Figure 17) include  $1856 \pm 3$  Ma from hornblende tonalite (Figure 19e; UPB-12-5-4604, DRI2021014). Granodiorite yielded a mean  $^{206}\text{Pb}/^{207}\text{Pb}$  age of  $1862 \pm 10$  Ma from zircons, which is interpreted as the time of crystallization (Figure 19f; UPB-12-5-4605, DRI2021014).

Zircon grains in the Rat granite (gn) at the south margin of the LRD (Site 17, Figure 17) are a mixture of mostly prismatic and euhedral to slightly rounded, partly resorbed grains. They vary from clear and colourless to slightly red-brown and fractured. Cathodoluminescence images of the grains show oscillatory magmatic zoning and rare metamorphic overgrowths. The corresponding age data, interpreted as evidence of late successor-arc plutonism, are also relatively complex, indicating  $1838 \pm 4$  Ma crystallization and ca. 1807 Ma metamorphism (Figure 20a, b; UPB-104-08-446, DRI2021014). Although the local age range of sedimentation is uncertain, the Rat pluton may be slightly younger than the base of the Sickie group, and older than the final sediment deposition (see below).

The SHRIMP ages on part of the composite pluton containing the Notigi monzogranite and granodiorite also indicate two distinct stages of zircon growth with older cores ( $1862 \pm 6$  Ma) and younger rims ( $1806 \pm 3$  Ma) that are thick and euhedral (Figure 20c, d). The rims were originally interpreted as yielding the crystallization age of the pluton, with the cores representing inherited grains (Murphy et al., 2009). This was supported by the intrusive contact relationship of the granodiorite that is interpreted as into the upper part of the Sickie group. A back-scattered electron image displaying selected zircons (Figure 20d), however, indicates an apparent resorption of large, euhedral cores. Faint oscillatory zoning indicates changes in the magmatic environment that affected the zircon growth. The cores are herein interpreted as yielding the crystallization age of the monzogranite as  $1862 \pm 6$  Ma, placing it within the range of successor-arc intrusions in the LRD. Assimilation of magnetite-bearing arkosic gneiss of the Sickie group may have occurred in the granodiorite as illustrated in the local aeromagnetic high (Murphy and Zwanzig, 2019a), thus suggesting a younger age than that of the monzogranite. This western pluton, which is undated, may have formed entirely from widely derived, ca. 1805–1809 Ma synmetamorphic melt, but its geochemistry suggests an arc origin with only contamination by the Sickie group. This would indicate an age of crystallization

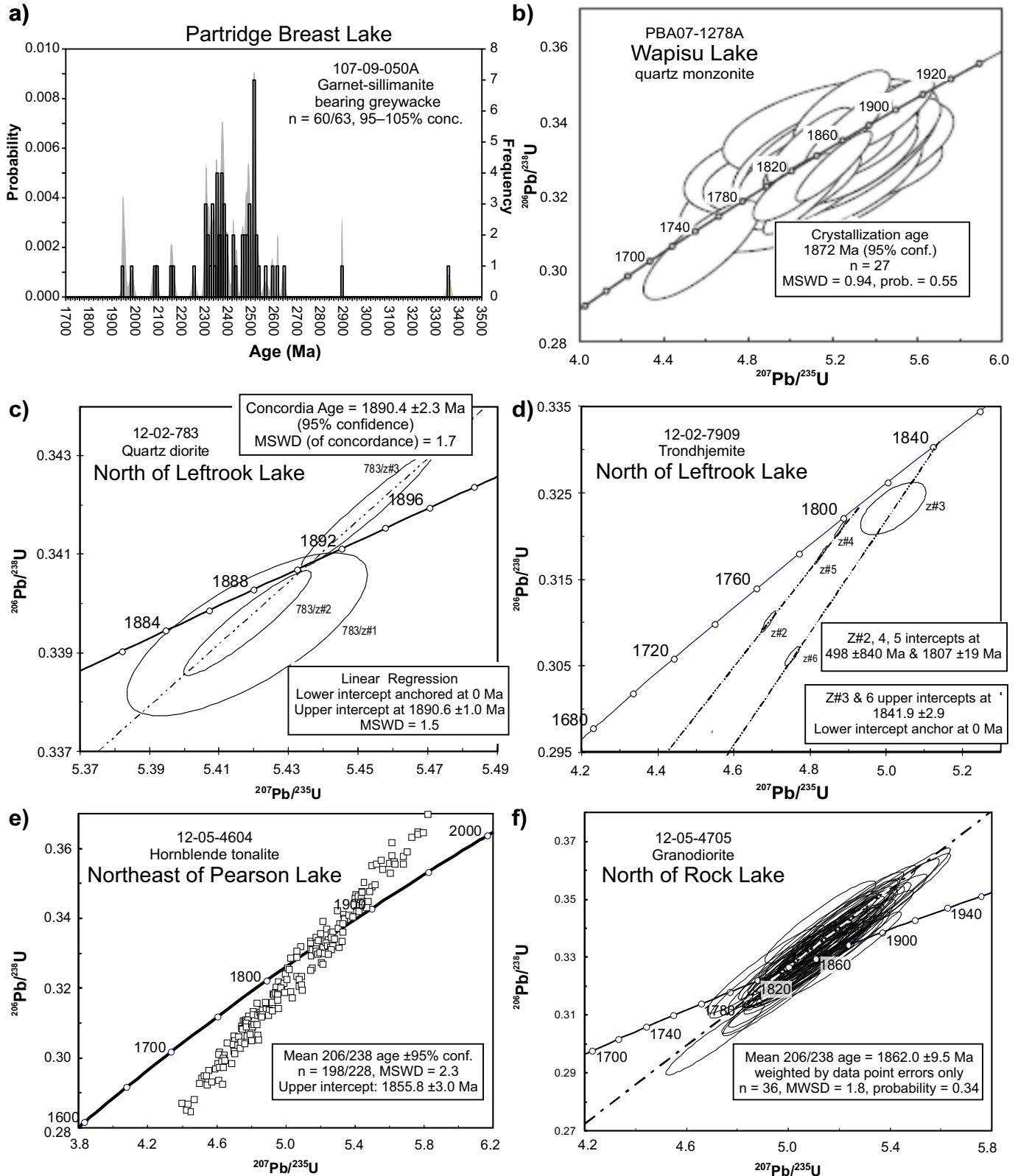


**Figure 19:** Detrital-zircon ages (Southern Indian domain) and crystallization ages of granitoid rocks (KD and south margin of LRD): **a)** SHRIMP age from Partridge Breast greywacke-gneiss; **b)** Wapisi Lake quartz monzonite (Böhm et al., 2003); **c)** quartz diorite, north of Leftrook Lake; **d)** trondhjemite showing discordia of the interpreted approximate crystallization age and a four-point metamorphic age; **e)** LA-MC-ICPMS ages of 1856 ± 3 Ma hornblende tonalite, north of Pearson Lake; **f)** granodiorite showing a concordia plot with selected points approximating a crystallization age of 1862 ± 10 Ma and a metamorphic age of ca. 1810 Ma. Concordia-plot ages are in Table 3, data in DRI2021014. Abbreviation: conc., concordant.

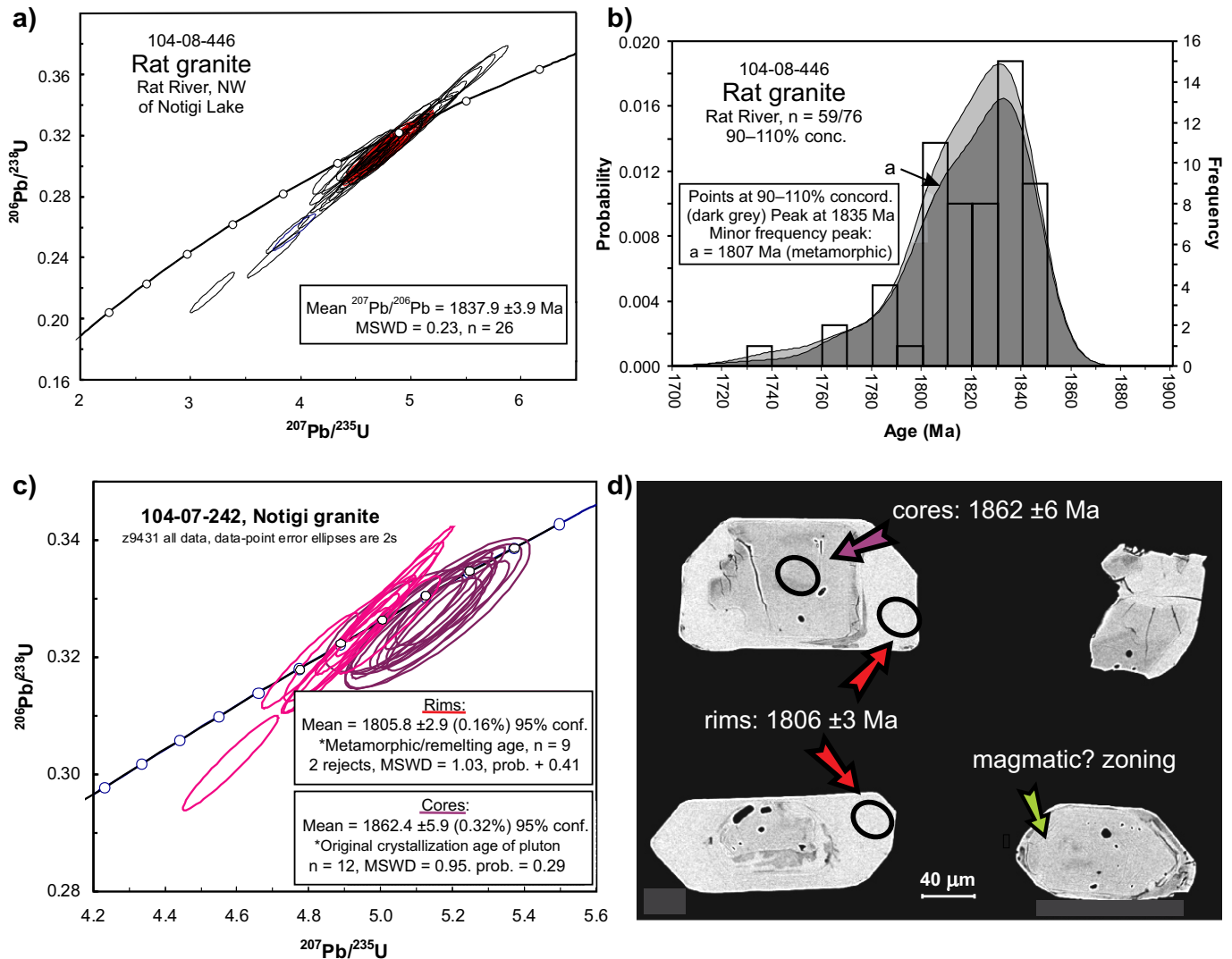


**Figure 20:** Crystallization and metamorphic ages of granitic LRD apophyses in the KD: **a, b)** LA-MC-ICPMS ages of Rat granite, Rat River, northwest of Notigi Lake, interpreted as  $1838 \pm 4$  Ma crystallization from a concordia plot (a), and metamorphism at ca. 1807 Ma from a minor peak of a frequency plot (b); **c)** SHRIMP ages of the Notigi granite (after Murphy et al., 2009) showing the reinterpretation as  $1806 \pm 3$  Ma rims and  $1862 \pm 6$  Ma igneous cores consistent with metamorphic textures and regional considerations (see text); **d)** zircon photomicrograph showing the resorption of euhedral (igneous) zircons, and at the green arrow, faint oscillatory zoning; euhedral rims reinterpreted as migmatitic products. Abbreviation: prob., probability.

between 1830 and 1840 Ma. The younger age obtained from the monzogranite would consequently represent metamorphism with partial melting.

Tonalitic rocks (tn) at Osik Lake were previously mapped (Baldwin et al., 1979) as intruding the Burntwood group (Murphy and Zwanzig, 2019c; Percival et al., 2007). The main tonalite at Osik Lake is dated as  $1873 \pm 11$  Ma (Table 3) and is therefore interpreted as an inlier of the LRD in the KD, having intruded the  $1885 \pm 7$  Ma enderbite that mantles the tonalite, but not intruding the Burntwood group.

Four analyses were done on a single zircon grain with a distinctive habit among the mainly metamorphic grains ( $1809 \pm 4$  Ma) in the tonalite gneiss at Tullibee Lake, and the three oldest analyses yielded a weighted mean  $^{207}\text{Pb}/^{206}\text{Pb}$  age of

$1890 \pm 8$  Ma to suggest early arc magmatism at the margin of the TNB (Rayner and Percival, 2007).

#### 5.1.4 Granville complex

The Tod Lake basalt or derived amphibolite (Gta/Gtb) in the Granville complex is not dated at the type sections. The age of ca. 1.9 Ga is assumed because it is likely correlated with the Levesque Bay assemblage in Saskatchewan (Section 2.2; but see Section 4.2.2). The only direct age was obtained from the felsic unit interpreted as tuff (Corrigan and Rayner, pers. comm., 2008) in the sedimentary megaunit (Gs) that forms the southern belt in the complex. If the dated unit was reworked in the sedimentary environment of the surrounding rocks, however, the obtained age may be a maximum age of it and the associated sediments. Arkosic sandstone in the Levesque

Bay assemblage, which is cut by  $1867 \pm 3$  Ma tonalite (Corrigan et al., 2001), is probably equivalent to quartz-rich metasediments (Gse) in the southern belt of megaunit Gs at Granville Lake, and lends credence to the ca. 1874 Ma age of the sedimentary package. Nevertheless, the lack of definitive ages of the Granville complex leaves more than one possibility: the complex may be an amalgam of more than one age of rocks that include ca. 1.9 Ga basalt and younger sediments, both older than the Burntwood group (Section 5.1.5) and certainly older than the Sickle group; alternatively, but less likely, the complex has the same age as the lower part of the Burntwood group. A structural interpretation (Section 6.1.1) is that of an early in-sequence thrust stack that included successively older overlying units. This would be consistent with the sediments in the southern belt of the Granville complex as older than the Burntwood group, the mafic rocks as the oldest and the unconformably overlying Sickle group the youngest but partly coeval with the Burntwood group. Regardless of absolute ages, these relationships are assumed to extend for the length of the Kisseynew north flank. The Burntwood megathrust is inferred to occur at the base of the complex (Section 6.1). This thrust is interpreted as the upper-crustal expression of a full crustal break that is prominent on a seismic profile (Section 6). The

fault is fundamental to the interpretation of the tectonostratigraphy, relative ages and structure presented in this report.

### 5.1.5 Detrital zircons, Burntwood and Sickle groups

Detrital-zircon ages (by LA-MC-ICPMS) define prominent, overlapping peaks on probability plots for the Burntwood group (1870–1850 Ma), Sickle and Grass River groups (1865–1845 Ga) and, additionally, similar Archean scatter in the two groups sampled across a wide area (Figure 21; Corrigan and Rayner, pers. comm., 2005). The plots indicate that the Burntwood and Sickle group sediments were eroded from the same (arc) terrane. Probability peaks of samples from the southeast corner of the KD indicate ages between 1870 and 1850 Ma with the youngest grain at  $1831 \pm 25$  Ma (Percival et al., 2005). This is the same range of ages as that of successor-arc plutons in the THO internides (Table 3). General southeasterly fining of the Sickle group (Section 3.2.6) indicates a provenance in the LRD and probably the 1862–1850 Ma (Meyer et al., 1992) main phases of the Wathaman-Chipewyan–batholithic domain. Older zircons in both groups scatter to 2.75–2.85 Ga with minor peaks between 2.3 and 2.6 Ga like the main range of ages of Partridge Breast greywacke (Figure 19a; Martins et al., 2019). The data suggest a subsidiary provenance from parts of the

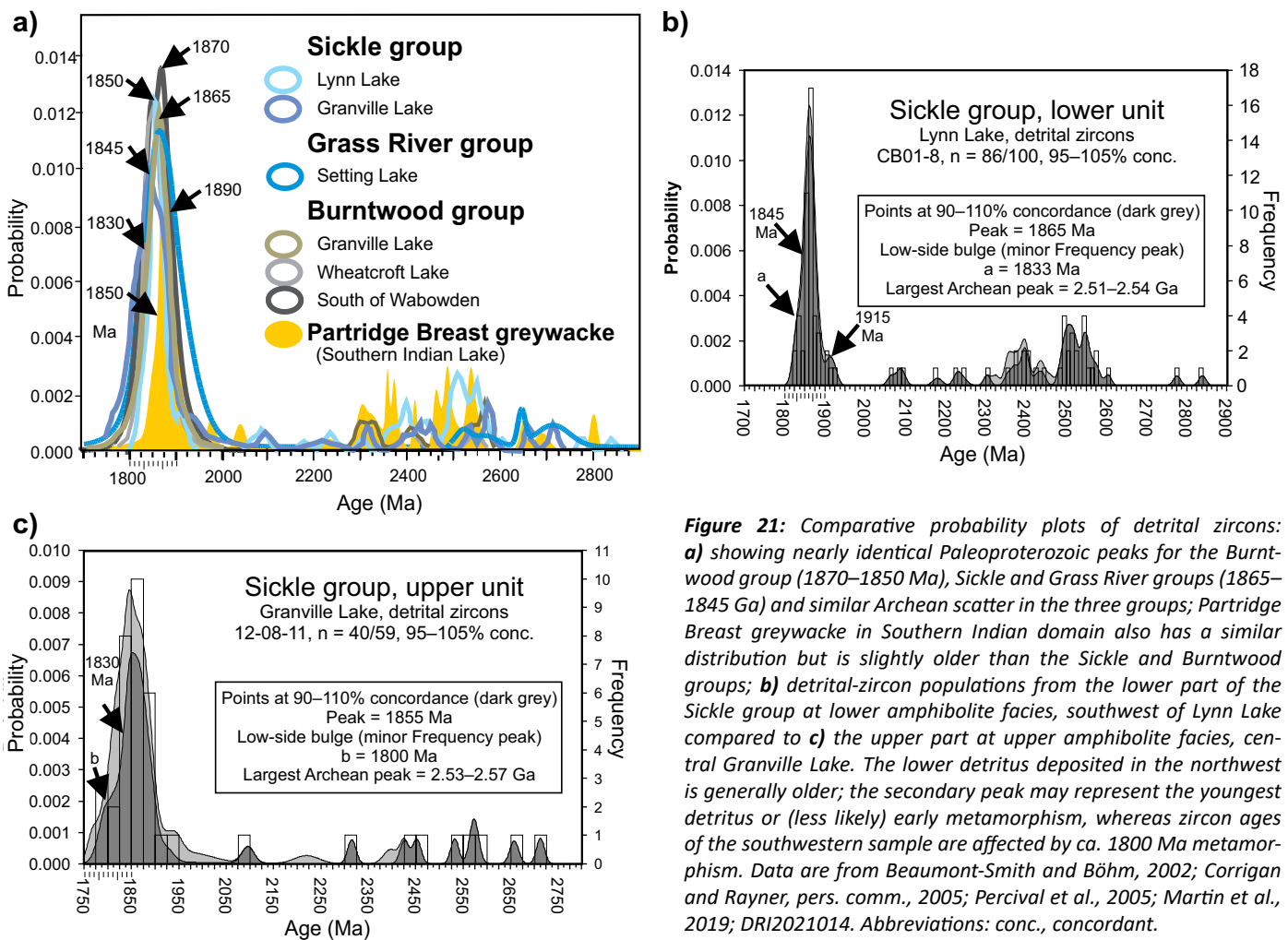


**Figure 21:** Comparative probability plots of detrital zircons: **a)** showing nearly identical Paleoproterozoic peaks for the Burntwood group (1870–1850 Ma), Sickle and Grass River groups (1865–1845 Ga) and similar Archean scatter in the three groups; Partridge Breast greywacke in Southern Indian domain also has a similar distribution but is slightly older than the Sickle and Burntwood groups; **b)** detrital-zircon populations from the lower part of the Sickle group at lower amphibolite facies, southwest of Lynn Lake compared to **c)** the upper part at upper amphibolite facies, central Granville Lake. The lower detritus deposited in the northwest is generally older; the secondary peak may represent the youngest detritus or (less likely) early metamorphism, whereas zircon ages of the southwestern sample are affected by ca. 1800 Ma metamorphism. Data are from Beaumont-Smith and Böhm, 2002; Corrigan and Rayner, pers. comm., 2005; Percival et al., 2005; Martin et al., 2019; DRI2021014. Abbreviations: conc., concordant.

Southern Indian domain or possibly the Hearne craton margin. The abrupt decreases in the abundance of detrital-zircon ages through the 1845–1830 Ma interval (Figure 21a; Percival et al., 2005) suggests this age range to be close to the time of deposition for the Burntwood and Sickle groups. In marginal basins on active margins, such a decrease coincides with the known age of deposition because of the provenance from active volcanoes and rapidly exposed plutons (Cawood and Hawkesworth, 2014; McKenzie et al., 2014). Enderbite, dated in Manitoba as 1830 +11/–5 Ma (Gordon et al., 1990) and in Saskatchewan as 1830 ± 2 (Ashton et al., 1999), intruded the Burntwood group in the southern part of the KD, and provides a local minimum age of deposition. The small difference in ages between the Burntwood and Sickle groups is consistent with the interpretation that the groups represent lateral marine and terrestrial facies (Zwanzig and Bailes, 2010).

### 5.1.6 Metamorphic zircons

The ca. 1810–1800 Ma timeframe for metamorphic monazite and zircon is widespread in the KD (Hunt and Zwanzig, 1993; Parent et al., 1999; Machado et al., 1999). High-grade metamorphism apparently lasting about 10 m.y. was synchronous throughout the KD. In the Wuskwatim–Granville lakes corridor, metamorphic ages found in the Sickle group and intrusive rocks range from 1806 ± 5 to 1809 ± 4 Ma (Table 3). This probably represents the metamorphic peak.

### 5.1.7 Late mafic–ultramafic rocks

The small body of layered gabbro–pyroxenite (Lmu) at Osik Lake yielded a zircon crystallization age of 1791 ± 1 (Table 3). The age is significant as it may date the late tholeiitic mantle-derived magmatism reported by Zwanzig and Bailes (2010) from the north margin of the Flin Flon domain and a possibly coeval mafic dike that cuts migmatitic leucosome on the south-east margin of the KD, west of Setting Lake (location in Figure 1).

## 6. Structural geology

Structural analysis was carried out with data collected during the local mapping and from previous work (Kendrick et al., 1979), supported by the use of equal-area stereoplots of sub-areas of consistent structure. The data were supplemented by measuring structural symbols shown on the existing maps of Baldwin et al. (1979), and including these data in the analysis. The progressing work was published as Reports of Activities (Percival et al., 2006; Murphy and Zwanzig, 2007a, 2008; Zwanzig and Murphy, 2009). A more detailed structural analysis in this report has attempted to resolve the origin of the complex interference structures and their significance in the Wuskwatim–Granville lakes corridor, and relate them to structures encompassing a wide region of the THO. Of particular interest is an attempt at unravelling the refolded, large-scale nappes (e.g., the Russell Lake structure; Lenton, 1981) that produced

crustal interleaving. The results presented here support a tectonic model of the THO in Manitoba proposed by Zwanzig and Bailes (2010), and that model is expanded (Section 7) and used to provide suggestions for future mineral exploration (Section 8).

Deformation stages are presented in their inferred chronological order based on overprinted fabrics where possible, but more widely by analyzing the geometry of interfering large-scale folds and apparent changes in structural transport direction (vergence) in thrusts and regionally asymmetric first-order folds. Foliation in various ages of rocks, planar or folded, and such markers as flattened faserkiesel helped to provide a relative time-scheme for stages of deformation. Isotopic ages of zircon crystallized during high-grade metamorphism and migmatization that can be matched with certain structures provide an approximate absolute timeline. For consistency with the structural history described from the east margin of the KD and overlapping the TNB (Burnham et al., 2009), the structural history of the Wuskwatim–Granville lakes corridor is described in four generations:  $D_1$  to  $D_4$  (Table 4). Any earlier structures were generally transposed into layering, designated as  $S_0$ .

In summary, after the development of the earliest structures, restricted to the Granville Lake complex (megaunit G), isoclinal folding and southeast-verging thrusting ( $D_1$ ) occurred in the Burntwood group during overthrusting by G. This deformation was followed by  $D_2$  northerly overturning with the development of large nearly recumbent north-verging folds or fold-nappes ( $F_{2a}$ ) during high-grade metamorphism. These nappes were refolded at depth by southwest-verging inclined to recumbent folds ( $F_{2b}$ ). The refolded crust was then overprinted by northeast-trending upright folds ( $F_3$ ) and final, less penetrative  $D_4$  north- and east-trending structures. Similar phases of deformation were recognized on the KD south flank by Zwanzig, 1999 (Table 4). They also correspond to stages in the TNB (the polyphase model in Burnham et al., 2009).

The corridor of structural analysis extends from the highest crustal level preserved at Granville Lake through mainly Paleoproterozoic paragneiss uplifted from deep burial in the Northeast Kiseynew subdomain, and the moderately uplifted Ospwagan group covering the Archean basement gneiss of the Superior craton in the TNB (Couëslan and Pattison, 2012). The depths that these areas attained is reflected in their structural style, relative age of the dominant deformation, the character of intrusive rocks and metamorphic assemblages with increasing grade toward areas near the TNB.

At Granville Lake the folded and thrust-stacked succession involving the Granville complex, Burntwood and Sickle groups (Granville Lake structural zone in Figure 5b) is mainly north younging. The oldest rocks, the mafic–ultramafic volcanics, occupy the Pickerel Narrows anticline in the north (Figure 5). Syntectonic sediments (Gs) form a wedge-shaped southern thrust belt in the complex. The Burntwood and Sickle groups south of the complex are separated from it by the structural discontinuity interpreted as the Burntwood megathrust, the

**Table 4:** Local and regional structural history.

Kisseynew north flank				Kisseynew south flank–Flin Flon belt margins <sup>4</sup>				Lynn Lake belt <sup>5</sup>		U-Pb age <sup>5</sup> (Ga.)	
Notigi Lake	Stage <sup>1</sup>	Granville Lake <sup>2</sup>	McKnight Lake <sup>3</sup>		Arc assembly, folding		D <sub>1</sub>	Upright folding in TNB <sup>6,7</sup>	D <sub>1</sub>	Assembly; folding	>1.87
Earliest structures transposed into layering (S <sub>0</sub> )			Foliation, folding, thrusting (S <sub>0</sub> ) in megaunit G								
Thrusting: Granville Lake complex and Sickie group over Burntwood group; F <sub>1</sub> folding, development of S <sub>1</sub> schistosity (rare preservation)	D <sub>1</sub>	Development of SE-verging fold-and-thrust belt, late-synsedimentary, coeval with deposition of parts of Burntwood and Sickie groups			D <sub>1</sub>	Final assembly; development of NE-verging fold-and-thrust belt (present orientation)	Early D <sub>2</sub>	SE-directed thrusting of Burntwood group over northern TNB <sup>6</sup>		Upright folding, dextral transposition and shear sense	
Northerly overturning of the Sickie and Burntwood groups: Granville Lake thrust stack in the under limb of an early D <sub>2</sub> recumbent fold, syncline closing at Timew Island, curved around culmination; probably tight major folding, now on the east side of the culmination	D <sub>2</sub>	Northerly overturning and flattening of D <sub>1</sub> structures, north-verging back folding; development of weak southerly dipping S <sub>2</sub>	D <sub>1</sub>	Isoclinal nappe-like folding, producing inversion of sections	D <sub>2</sub>	W-verging upright to recumbent folding to small nappes	Late D <sub>2</sub>	Recumbent SW-verging folding, overturning and flattening of D <sub>1</sub> structures and 1.87 Ga Molson dikes; placing Burntwood group under the TNB in the south; dextral transpression; underthrusting of the Superior craton to north(?)	D <sub>2</sub>	Development of shear zones	~1.835–1.80
Late reclined southwest-verging refolding of D <sub>1,2</sub> structures (i.e., F <sub>2</sub> antiforms and saddle in Notigi culmination); vertical flattening, horizontal flow		Northerly-dipping seismic reflectors in crust below Granville Lake	D <sub>2</sub>	NW-trending sub-horizontal isoclinal folding, axial surfaces with moderate dip to E and NE	D <sub>3</sub>	SW-verging recumbent folding				Reverse faulting	
Axial planar S <sub>2</sub> schistosity						Sinistral shear zones					
Upright F <sub>3</sub> flexural– to flexural-flow–folding, forming the Notigi culmination as F <sub>2</sub> –F <sub>3</sub> interference with gently northeast-plunging sheath folds in the core	D <sub>3</sub>	NNE–ENE–trending folding with SE plunge; dextral transpression on the easterly trend; open northerly trending folding with ESE plunge; some box shapes	D <sub>3</sub>	NE-trending folds of irregular form, plunging E at 30°, axial traces curved and bifurcated	D <sub>4</sub>	NNE-trending upright flexure folding	D <sub>3</sub>	Tight NNE-trending upright folding of D <sub>1</sub> and D <sub>2</sub> structures, and sinistral transpression on the NNE trend	D <sub>3</sub>	Open S folding	1.785–1.775
S <sub>2</sub> –S <sub>3</sub> composite foliation transposing migmatite layering, as well as S <sub>1</sub> and bedding; local S <sub>3</sub> foliation; rodding at S <sub>0,2</sub> –S <sub>3</sub>									D <sub>4</sub>	Open Z folding	1.765–1.750
Open northerly trending folding with north to northeast plunge	D <sub>4</sub>	NNE- and E-trending faulting	D <sub>4</sub>	NW-trending brittle deformation	D <sub>5</sub>	Northerly-trending E-side-up faulting	D <sub>4</sub>	Northerly sinistral faulting, dextral ENE-trending, faulting	D <sub>5</sub>	Kink folding with box shapes	~1.73
Northerly and easterly trending faulting			D <sub>5</sub>	NE-trending faulting and shearing					D <sub>6</sub>	Sinistral shearing	~1.71

<sup>1</sup> This report; <sup>2</sup> Modified after Zwanzig (1990); <sup>3</sup> Lenton (1981); <sup>4</sup> Zwanzig (1999); <sup>5</sup> Modified with ages after Beaumont-Smith and Bohm (2002); <sup>6</sup> Predates Molson dikes, Burnham et al. (2009); <sup>7</sup> Zwanzig and Böhm (2002).

main structure in the Levesque Bay–Granville Lake suture zone. Along the south shore of Granville Lake, in the footwall of the megathrust, the Sickle group that lies conformably on the Burntwood group, and occupies a narrow syncline. The full tectonostratigraphic succession is shown as a schematic reconstruction as it may have been after  $D_1$  (N to SW, Figure 5a). Toward the east the megathrust cuts out: first the northern unit Ks/Ksa in the Sickle group, and then the entire group as well as the southern sediment belt. Thus, in the east mainly mafic rocks of the Granville complex are interpreted to have been thrust directly over the Burntwood group (Figure 2a).

Uranium-lead Zr geochronology, including that of distant correlated units (section 5.1.5), indicates that the lower units above each major fault are successively older to the north. In the Burntwood group these faults are determined to be part of  $D_1$  southeast-verging thrusting and folding. The earliest structures within the Granville complex, however, are deemed older than the Burntwood group as suggested by the lack of interleaving of the group with the rocks internal to the complex and by the presence of sedimentary breccia, conglomerate, mylonite and blocks in the lower part of the ca. 1874 Ma sedimentary panel (Section 6.1).

The fold-thrust stack at Granville Lake dips moderately south, making it face downward, and indicating large-scale overturning after a reversal of vergence to northerly during early- $D_2$  folding. This stage of deformation south of Granville Lake is considered to be synmetamorphic and related to a rare, weakly crosscutting foliation with biotite alignment. The higher-grade metamorphic rock with migmatization south and east of the lake are determined to have two sets of  $D_2$  folds. These are termed  $F_{2a}$  and  $F_{2b}$  with respective northerly and southwest vergence. They occur as large, nearly recumbent folds or inclined folds with highly overturned common limbs and strong down-dip linear structures. A final set of major folds and faults, assigned to  $D_3$ , comprises northeast-trending upright structures.

The structural geometry and local history of the high-grade rocks at Notigi Lake are of particular interest because they are well exposed and appear to be comparable in other areas in the eastern part of the corridor. They are taken to be representative of the regional structural style and history formed at a deeper level, dominated by late stage  $D_2$  structures and by tight upright folds formed during  $D_3$ . Such large-scale geometry southeast of Notigi Lake exposes the Archean basement and its cover rocks, the Wuskwatim Lake sequence.

The crustal architecture of the study area with its sutures (Granville Lake structural zone and Superior boundary) was investigated by seismic reflection experiments (White et al., 2000, 2002). A schematic crustal section at Granville Lake, used to illustrate the local geometry and structural history, is interpreted from a down-plunge view (Figure 22), and a parallel seismic section extending across strike east of the lake (White et al., 2000). At the deeper structural level, east of the lake, the seismic fabric shows that structures have a

northerly apparent dip (Figure 22d) with a true dip to the north-northeast (Clowes and Roy, 2020). Together with the south-dipping high-level structure at Granville Lake, this reveals the architecture of the Wuskwatim–Granville lakes corridor to include a crustal-scale, south-tapering wedge. The structure of the rocks at surface along with the deep structure explain the complex geometry and polyphase nature of the deformation related to terminal continental collision in the THO as modelled in the context of plate tectonics in Section 7.

## 6.1 High-level structures: Granville Lake

From the southern half of Granville Lake to the south shore of Wheatcroft Lake (Figure 5; Zwanzig, 2019), primary sedimentary and volcanic structures are preserved. Consequently the earliest diastrophic structures must also still be present. These are termed “high-level structures” because of the preservation, lower metamorphic grade and lack of migmatite compared to structures farther east. The early structures include bedding in megaunit Gs that suggests transport of blocks and sheets in the southern belt of the Granville complex. In the north belt, pillows are preserved or locally transposed into layering or tectonite ( $S_0$ ). The most prominent early structures are large isoclinal  $F_{1-2}$  folds and locally observed thrusts in the Burntwood group. Their overprinting by the younger structures ( $D_3$ – $D_4$ ) had only a moderate effect. This makes the structural geometry and history at Granville Lake critical to understanding the tightly refolded structures in the rest of the corridor to the east.

### 6.1.1 Synsedimentary early structures and transposition layering ( $S_0$ )

Tectonic and sedimentary structures in the southern belt of the Granville complex include large sheet-like lenses of mafic–ultramafic rocks within the sedimentary succession (Zwanzig, 2019) and a variety of blocks in a thick turbidite bed (Section 3.2.2). Sedimentary breccia of pelite fragments in greywacke, intraformational greywacke conglomerate and mylonite are locally observed. These structures suggest large-scale transport (olistostromes and olistoliths) during the deposition of megaunit Gs. The proposed age of ca. 1874 Ma (Section 5.1.4; Corrigan and Rayner, pers. comm., 2008) of the rhyolitic member (Gsd) would suggest that deformation occurred in this early sedimentary environment before deposition of the Burntwood group. Apparently, these earliest structures formed in the Levesque Bay–Granville Lake suture zone, which was active as a destructive plate boundary (Section 7.2) by 1870 Ma (Section 4.5), and so subject to sedimentation during deformation.

The large Pickerel Narrows anticline, along the southern peninsula of Granville Lake (Figure 5; Zwanzig, 2019), has a north limb with well-preserved primary structures (e.g., Figure 4a), whereas the south limb is faulted (Figure 23a) and more strongly foliated (e.g., Figure 4b). This structural style



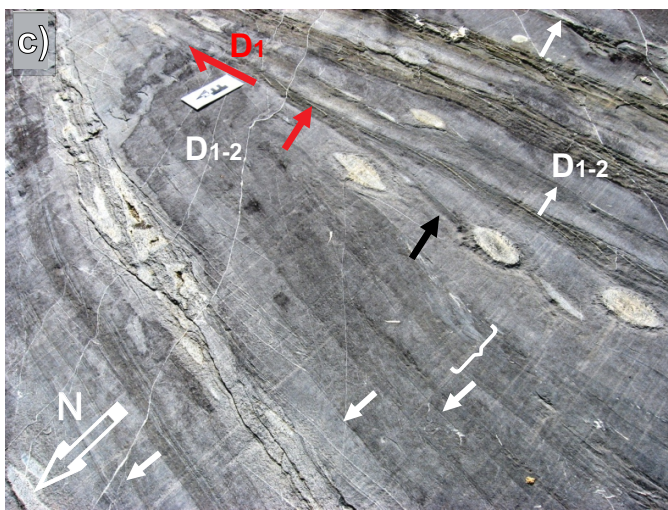
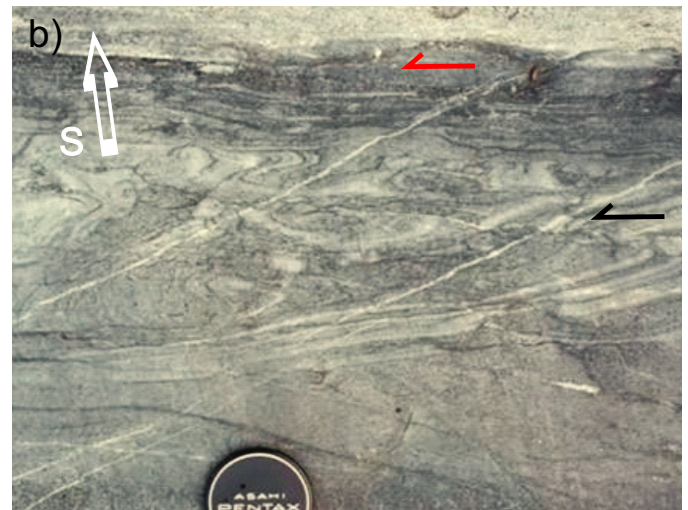


**Figure 23:** Outcrop photographs of early structures; **a)** faults (heavy dashed lines) bounding greywacke, sulphidic pelite (brown) and chert (white) between south-younging (arrows) panels of Tod Lake pillowed basalt in the south limb of the Pickerel Narrows anticline in the Granville complex, Muskwanuk Island, Granville Lake. Bedding is disrupted into lenses with the small thrust below T. Layering is truncated at  $S_{0-1}$ . Younger foliation ( $S_2$ ) cuts the fault. Late cross faults (e.g., short dashes) with dextral apparent offset are probably part of  $D_3$ . Hammer (in yellow circle). **b)** Pre-lithification  $F_1$  deformation in Burntwood group turbidite with an easterly component of transport (black arrow) and the main detachment (red arrow) in a pelite and with a calcisilicate-filled fault (pale top layer), Granville Lake area. Early-metamorphic quartz veins trend normal to the quadrant of extension for continued apparent south-side-east shear. The lens cap is 5 cm; **c)** Early isoclinal fold ( $F_1$ ) and thrust in the turbidite on Wheatcroft Lake has younging shown at the white arrows. Bedding disruption (bracket) probably preceded complete lithification as suggested by shale injection (black arrow) from shale detachment layer (at red arrows). Truncations extend beyond the 15 cm long scale card. Apparent thrust displacement of the northern limb (originally upright) was to the east. Post-thrusting quartz veins, normal to field of extension in continued upper-limb eastward motion, show rotation due to shear and attenuation of incompetent beds.

suggests southerly overturning of the south limb and a southerly vergence (present coordinates) during the formation of the anticline. On the south side of the fold, at the east shore of Muskwanuk Island, a thin panel of sedimentary rocks (Gs, Gse) has layering truncated along one contact with amphibolite (Gta, Gtb), and quartz veining along the other contact. The sedimentary panel may be a sheared thrust-imbriate from the sedimentary rocks to the south. It may postdate structural overriding of the southern belt by the volcanic rocks in the north. Disrupted bedding and small sinistral thrusts occur in the sedimentary panel. A reversal in younging direction in graded bedding in the southern-belt sediments (Gs) implies the presence of a tight syncline originally below the Pickerel Narrows anticline. Although the age of this fold is uncertain, the presence of a footwall syncline in Gs is consistent with an early onset age of folding and thrusting below the Pickerel Narrows anticline. Widespread post-Burntwood deformation, including

thrusting of the Granville complex over the Sickie group and later overturning of the complex, indicates protracted deformation extending from the formation of the Pickerel narrows anticline into the  $D_1$  and  $D_2$  periods.

### 6.1.2 Early post-Burntwood structures ( $D_1$ and early $D_2$ )

Despite indications of pre-Burntwood (and –Sickle) deformation, the northern limb of the Pickerel Narrows anticline is overlain by the Sickie Group with only a low-angle unconformity. A fault at the south margin of the complex truncates the Sickie group in a footwall syncline (Zwanzig, 2019) and is interpreted as active during  $D_1$  deformation wherein the composite thrust stack (Granville complex) was transported over the 1850–1835 Ma Burntwood group of basinal turbidite as well as over the Sickie group.

The faults north and east of Muskwa Bay, which bound the mainly sedimentary panel (Zwanzig, 2019), locally truncated sedimentary units and amphibolite. The fault panel is up to 500 m in true thickness but tapers out to the east. Mylonite horizons mark the southern fault at the shore about 1.3 km southwest of the settlement of Pickerel Narrows. The local cutoffs within Gs and the reversal in younging at its structural base confirm that the basal contact of the Granville complex is a fault rather than an unconformity. This is interpreted as part of the sole thrust of the Granville complex. East of Muskwa Bay the southern fault forms the contact with the Sickle group in the narrow syncline. This fold also has an attenuated south-younging limb and a north-younging limb with preserved primary structures (Zwanzig, 2019). It suggests an  $F_1$  age of its formation below a thrust that was still active during  $D_1$ , after the deposition of the Sickle group. It indicates a prolonged history of displacements along the Burntwood megathrust.

The Burntwood turbidites also formed a fold-thrust complex, possibly with an imbricate panel including part of the Granville complex. Directly south of Granville Lake the Burntwood group features early ( $D_1$ ) thrusts and folds. The folds are isoclinal with large amplitude and axial surfaces averaging about 25 m apart, widening further in the thick-bedded greywacke to the south and tighter in the greywacke–mudstone to the north (Zwanzig, 2019). Their early age is indicated by soft-sediment deformation and slump structures in partly fluidized beds, mudstone injected into thrusts, and calcsilicate developed in faults subparallel to bedding and above internally mobilized bedding (Zwanzig, 2008; Figure 23b, c).

The  $F_1$  isoclinal folds in the Burntwood group south of Granville Lake presently lie in a moderately south-dipping plane. North- and south-younging limbs of the folds have nearly the same orientation as shown by tight clustering of poles to bedding in stereogram  $D_{1-2}$  (Figure 22c). A  $\beta$  axis is weakly defined by the slightly different median orientations of the north- and south-younging limbs and supported by a linear structure and minor fold axis. These suggest a southerly (down-dip) plunge of the folds that would make them east-verging, inclined neural folds. Schistosity, defined mainly by biotite alignment, is developed subparallel to bedding but cuts across a small isocline at a low angle. The foliation is a metamorphic fabric that apparently postdates the  $F_1$  folds. Its association with thin quartz veins parallel to and crosscutting the bedding (Figure 23a–c) suggests development during early pro-grade metamorphism during late  $D_1$  or early  $D_2$ . The  $F_1$  fold axes were apparently rotated toward the lineation during  $D_2$  down-dip stretching. The present geometry is therefore a product of  $D_1$  and  $D_2$ .

North-younging  $F_1$  fold limbs in the Burntwood group are thicker and generally better preserved than south-younging limbs. The Burntwood metagreywacke in the former shows little or no foliation but has preserved bedding and other sedimentary structures. The south-younging limbs are more atten-

uated and commonly contain strike-subparallel, well-foliated fault zones with calcsilicate alteration (Figure 23c). The difference in structural style between the limbs is the reverse of that expected in the fold-thrust stack with its present dip. In a stack of in-sequence folds, the common limbs are expected to be overturned and the long limbs to be upward younging (Ramsay and Huber, 1987). Thrusting and shearing is generally in the common limbs, and structural transport is in the direction of their rotation with regard to the long limbs. In the Granville Lake area the dip is reversed and requires large-scale northerly overturning that followed  $D_1$  folding and thrusting. When the present orientations of the median plane of the  $F_{1-2}$  fold limbs is restored to having the north-younging limbs as horizontal and upright, and the hinge trending northeast, the common limbs acquire a shallow northwest dip and downward younging after the same restoring rotation ( $D_{1-2}$  in Figure 22c). The early northeast plunge is indicated by the present regional plunge along the KD north flank (Figure 14 in Zwanzig, 1990). This geometry confirms southeast-vergent  $D_1$  folding.

Fault rocks are foliated, and some of the early faults contain calcsilicate horizons, probably marking dewatering surfaces (Figure 23b, c). Thin  $D_{1-2}$  early synmetamorphic quartz veins show folding or rotation due to compression of incompetent (shaly) beds. Reactivation of early  $D_1$  structures and the metamorphism associated with  $D_2$  structures indicate long-lived ( $D_1$ – $D_2$ ) or polyphase deformation consistent with rotation, attenuation and reactivation of the locally earliest structures.

Folding and thrusting is gravity driven by a downward slope in the topography of the deforming pile. The folds became progressively younger forward, “in sequence”, as the structural wedge grew at its tip. Older rocks that generally carry younger rocks “piggyback” are thus transported over the younger rocks at the deformation front. These kinematics are consistent with the  $D_1$  structure south of Granville Lake with most younging of the Burntwood group beds toward the stratigraphically overlying Sickle group. Beds with younging criteria in this north-facing fold-thrust stack include those adjacent to unit contacts. They provide the regional stratigraphic succession. The most apparent change imposed by subsequent deformation during metamorphism at this level appears to involve the inversion of the early ( $F_1$ ) folds, with further attenuation along the weakly crosscutting biotite foliation.

The southerly dip that resulted from overturning of the  $F_1$  fold-thrust package is parallel to the average axial plane of  $F_2$  folds measured in the Sickle group northeast of Pickerel Narrows (Figure 22c, plots  $D_{1-2}$  and  $D_{2,3}$ ). The median dip of bedding in the isoclines south of Granville Lake is south at  $40^\circ$ , and the axial plane of the pair of step-like folds (close inclined folds) is estimated at  $43^\circ$  in the regionally overturned Sickle group north of Pickerel Narrows, on Mistuhe Island (Figure 22a, b; Zwanzig, 2019). The  $F_2$  folds in the Sickle group have caused further overall shallowing and northerly transport with local ramping of the previously inverted section (Figure 22a).

They are second-order folds ramping the inverted limb of the main syncline in the Sickie group. They indicate the vergence of the early  $D_2$  folding ( $F_{2a}$  folding described in Section 6.2), and fully involve the bedding but to a lesser degree the foliation. The driver for the reversal in vergence is interpreted to be the upward-diverging  $F_2$  fan structure (Zwanzig, 1990) in the central KD. At deeper structural levels the  $F_{2a}$  northerly verging folds are refolded by southwest-verging  $F_{2b}$  folds (Section 6.2). Both generations are synmetamorphic structures with similar styles, and were refolded in  $F_3$  structures.

In areas east of Granville Lake the Granville complex is in structural contact almost everywhere with the Burntwood group but is still stratigraphically overlain by the Sickie group. Its southern sedimentary belt is missing and assumed to be cut out by the proposed Burntwood megathrust at its base. This thrust is interpreted as the surface expression of the major crustal break indicated in the seismic profile (Figure 22d; White et al., 2000). The break has a lateral extent of hundreds of kilometres as traced in the tectonostratigraphy and structure encompassing the Granville complex at surface. It provides evidence of the importance of this fault. Eighty kilometres northwest of Granville Lake, between Laurie and Tod lakes (Gilbert et al., 1980; Zwanzig et al., 1999b), the Granville complex occurs in well-defined thrust sheets over the Sickie group, but also locally over the Burntwood group. As at Granville Lake, the faults were subsequently reactivated, but in that area, steepened by transpression. The faults presently have minor structures of dextral shear zones (Beaumont-Smith and Böhm, 2004). Their early fabric of thrusting may be preserved in their down-dip stretching lineations that later became axes of rotation. The stacking of the fault-panels above the Burntwood and Sickie groups is consistent with a  $D_1$  age and south-east vergence of the main fault development.

The wide extent of the thrust zone, for hundreds of kilometres along strike and tens of kilometres across strike, is marked by the presence at, or near, the base of the stack of highly deformed and faulted rocks of the Granville complex. These tectonites with their overlying Sickie group formed an early nappe that reached far into the KD. This  $D_1$  thrust nappe is interpreted as rooted in the Levesque Bay–Granville Lake suture zone between the KD and the LRD (Section 7). The farthest known southern extent of tectonostratigraphy as at Granville Lake occurs at Russell Lake and McKnight Lake (locations in Figure 1) in structural culminations (e.g., Russell Lake structure of Lenton, 1981; Martins and Couëslan, 2019). At Russell Lake, an upright section of the Granville complex is unconformably overlain by the Sickie group at a basal polymictic conglomerate like at Tod Lake, 50 km to the north. Geochemical data of amphibolite (Lenton, 1981; T. Martins and C.G. Couëslan, pers. comm., 2020) indicate that both Tod Lake-type and Hatchet Lake-type volcanic and intrusive rocks occur at Russell Lake. Lenton (1981) showed this section to overlie granodiorite in the core of a refolded recumbent fold that contains amphibolite in both the lower and upper limbs. The presence of thrusts

at the base of the complex at Tod and Granville lakes suggests that the granodiorite at Russell Lake intruded this thrust. The contact with the Burntwood group in the upper (inverted) limb is also interpreted as a thrust like at Tod and Granville lakes. The Granville complex and its basal thrust lies consistently on younger rocks and is folded with them in  $F_2$  recumbent structures. The wide extent of a sole-thrust (Burntwood megathrust) indicates the presence of a  $D_1$  thrust-nappe, herein called the Russell nappe.

The Sickie group and Granville complex are illustrated in Figure 22a to extend south in the subsurface under the Burntwood group (but not shown to scale or full extent in the figure). Such structural overlap is evident at a number of localities in the KD where structural culminations with inverted stratigraphy occur in areas of the Burntwood group. This includes the culminations in the southwest, at Russell and McKnight lakes. The area of overturned stratigraphy and early structures is evidently the lower limb of an  $F_2$  northerly verging antiformal fold-nappe that inverted much of the  $D_1$  southerly verging Russell thrust-nappe. Similar overturned tectonostratigraphy at a deeper structural level in the east, between Notigi and Minarski lakes and between Leftrook and Harding lakes, suggest that the  $D_2$  nappe and an underlying recumbent syncline extend for 200 km along strike. Outliers (structural basins) forming the northern limit of the inverted section at Minarski Lake suggest that the proposed  $D_2$  nappe closes nearby in the north. The  $D_2$  nappe is herein called the Minarski nappe. The underlying recumbent syncline involving the Granville complex and Sickie group closes in the south. This geometry indicates a large component of  $D_2$  northerly transport with crustal-scale interleaving on the north side of the KD.

The distribution of the Sickie group exposures on the KD north flank and the northern boundary of the Central Kisseynew subdomain suggest that both the  $D_1$  and  $D_2$  nappes consisted of a series of lobes (Figure 1) that comprise large allochthons. However, such local shapes have not been mapped out fully or investigated in detail. The present distribution of Sickie inliers (Figure 1) suggests the formation of two major lobes: one extending southeast of Russell Lake and the other from Notigi to Leftrook lakes.

### 6.1.3 Superposed structures

Because of the inversion of bedding in long  $F_1$  fold limbs and the anomalous upright younging of the isoclinal common limbs, the  $F_2$  folds that caused the overturning are considered to have been recumbent. Analogous folds, considered to be  $F_2$ , are prominent east of Granville Lake. The structures in the east are inferred to have formed at deeper structural levels than in the west. They formed in rocks that reached higher metamorphic grade, and were more attenuated and gneissic to migmatitic. Their plunge is northeast, lying in the plane of the deep seismic structures. Their main style is that of interference structures between three separate phases:  $F_{2a}$  and  $F_{2b}$  on

which  $F_3$  folds are superposed. The  $F_3$  folds, which are open at Granville Lake but tightly closed from Notigi Lake eastward, form a main phase in the TNB (Bleeker, 1990). They are upright and maintain their northeast trend, allowing correlation along the Wuskwatim–Granville lakes corridor, west into the TNB and south into the central KD. Zwanzig (1990) showed that the northeast-trending, superposed structures ( $F_3$ ) are prominent in the northeastern part of the KD and that the older, northwest-trending, recumbent/inclined folds are preserved at a deep structural level along the south flank of the KD. Zwanzig (1990) further proposed that the entire array of upright ( $F_3$ ) folds is detached from the deeper-level recumbent structures.

The highest-level  $F_3$  folds have variable north-northeast to east-northeast–trending axial traces, depending on their maturation during progressive northwest compression and clockwise rotation. The most northerly trending folds are open, whereas the most easterly trending folds are tight (Zwanzig, 2019). Thick lenses of competent supracrustal rocks of the Granville complex or intrusive bodies lie in some hinge zones. These bodies are interpreted to have caused a flexural instability during  $F_3$  fold nucleation.

Open  $F_3$  crossfolds that are outlined by amphibolite megacunit (Gt) and mafic–intermediate intrusions (Lmi) surrounded by Burntwood group (B) are prominent south of Granville Lake (Zwanzig, 2019).  $F_3$  folds, suggested by folded  $S_2$  foliation, are nearly co-axial with the  $F_2$  folds ( $\pi_3$  in stereoplots  $D_{2,3}$  and  $D_3$  in Figure 22c). They are large, open flexures with north- to northeast-trending axial traces and shallow southeast plunging axes. Some are box-shaped folds (with two hinges) developed in the interlayered units of different competence. They die out in the uniformly sedimentary rocks to the north and south. The  $F_3$  folds have moderately to steeply southeast-dipping axial surfaces with steeper west-dipping layering and foliation in the west limb than southeast dip in east limbs of anticlines. They have rare axial planar  $S_3$  foliation that dips approximately 60° southeast (e.g., 4.5 km SW of Pickerel Narrows in Zwanzig, 2019). That asymmetry suggests southeast-over-northwest  $D_3$  tectonic transport with northwest-southeast shortening. Some of the northerly trending limbs of box folds are faulted or refolded into a Z shape with an east-northeast-trending axial plane and shallow east-southeast plunge. These may be late  $F_3$  or  $F_4$ . One of these folds ( $D_{3-4}$  in Figure 22a) has a dextral north-northwest-side-down sense of rotation, coaxial with  $F_2$  but with the opposite sense of upper-limb transport.

The  $F_3$  folds extend north through the Pickerel Narrows anticline (Figure 22b; Zwanzig, 2019) and deform the Granville complex into large, open flexures that have S asymmetry. Long limbs are slightly steeper (~60°SW) and have narrower exposure than the shallower dipping (~36°SE) common limb. Good preservation of pillow shapes suggests that folding was flexural, and the true thickness of limbs represents  $D_2$ , with little compression in  $D_3$ . The true thickness of the common limb, which has a competent intrusive core, is two times the true thickness of the eastern long limb. The synform (eastern

bend) has a southeast plunge (plot  $D_3$  in Figure 22c). It was superposed on the early anticline that was already overturned during  $D_2$ . The  $F_3$  limbs lie close to the  $F_2$  axial plane (shown for reference in plot  $D_3$ ), thus consistent with their  $D_2$  overturned attitude. Short dispersions of poles to foliation across the main girdle have poorly defined, moderately west-plunging and shallow southwest-plunging axes ( $\pi_3$ ), respectively for the long and common  $F_3$  limbs. These short-girdle axes may give the positions of the  $F_1$  fold axis of the tight Pickerel Narrows anticline as rotated in the  $F_3$  fold limbs. If so, the foliation in the Granville complex, the oldest rocks in the area, is the oldest recognized local fabric, and predates the structures locally designated as  $D_1$ .

## 6.2 Deeper level: Notigi–Wapisiu lakes

Throughout the deeper levels, in the southeastern part of the Wuskwatim–Granville lakes corridor, much early fabric is interpreted to have been obliterated during metamorphic annealing, overprinting, late high strain and migmatization. These produced the present strong planar fabrics:  $S_2$  and  $S_3$  or mostly composite  $S_{2-3}$  foliation. Three locally recognizable generations of minor folds are represented as  $F_{2a}$ ,  $F_{2b}$  and  $F_3$  (Figure 24). Most difficult to identify at the deeper crustal level is the early major thrust between the Burntwood group and the Granville complex. At one site at Notigi Lake the contact has a thin layer of schist but is involved in a step fold with a shallow-dipping axial surface (Figure 24a). The fold is typical of  $F_2$  and makes the schist layer at the contact a  $D_1$  or early  $D_2$  shear zone in the position of the Burntwood megathrust. The proposed thrust was intruded by pegmatite that is also sheared and indicates reactivation of the thrust apparently during  $F_{2b}$  folding. The presence of the early fault is also evident from truncations of units against the Burntwood group on the east side of the Notigi structure (Murphy and Zwanzig, 2019a). Individual panels within the Granville complex (forming part of the Burntwood megathrust at Granville Lake) were not recognized in the deeper structural level, nor could the fold-thrust stack be mapped in the migmatized Burntwood group. The Granville complex, however, is largely a tectonite as seen in transposed pillowed basalt (Figure 4d). Some contacts of the associated sedimentary rocks that form layered gneiss may be thrusts.

A prominent feature in the Sickle group at Notigi Lake is axial-planar foliation ( $S_2$ ) with biotite±amphibole segregations and parallel granitoid veins (Figure 24b). In the limbs of isoclinal  $F_2$  folds, bedding ( $S_0$ ) and foliation ( $S_2$ ) are subparallel. This strong anisotropy has acted as detachment to much of the  $D_3$  structures. The  $F_3$  folds commonly terminate against it (Figure 24c). The  $F_3$  folds strike consistently northeast with a steeply dipping axial plane (Figure 24c, d, f). Where the  $F_3$  folds are tight, all planar structures are subparallel, commonly forming  $S_{2-3}$  gneissosity.

Crosscutting fabrics that show sequencing of episodic or progressive deformation are preserved in a few locations at the intersection of major fold hinges such as on Timew Island and

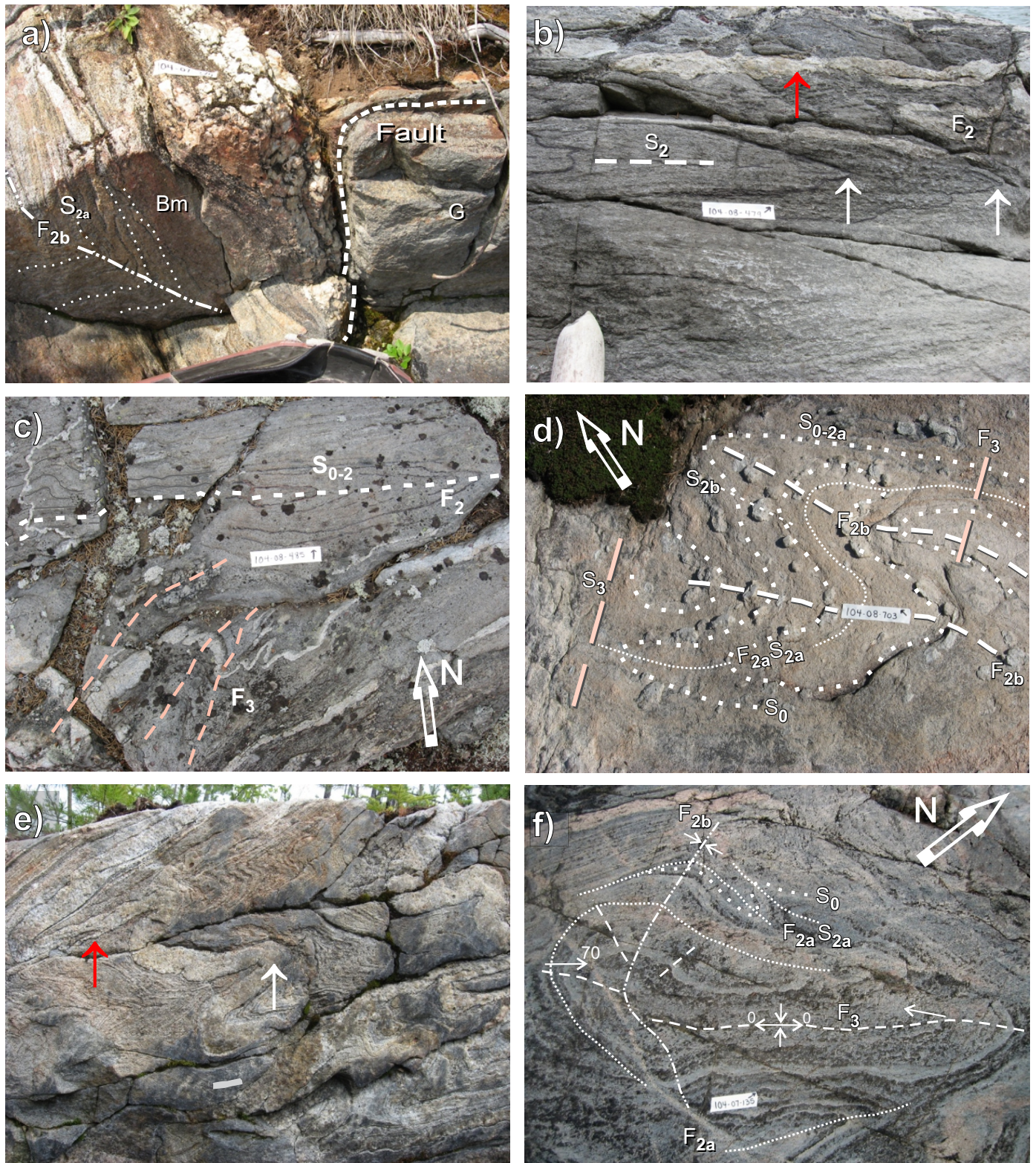


**Figure 24:** Minor structures at Notigi Lake: **a)** sheared contact between Burntwood group (Bm) and Granville complex (G), interpreted as a thrust, folded in late  $D_2$  because it affects gneissosity ( $S_{2a}$ ) and in a north-dipping axial plane ( $F_{2b}$ ); **b)** early recumbent fold in bedding (outlined in black marker) of Sickle group hornblende-biotite meta-arenite, with white arrows at bed closures; axial-planar  $S_2$  foliation dipping gently northeast; granite vein parallel to  $S_2$  (red arrow) but also folded ( $F_2$ ); **c)** early isocline ( $F_2$ ) in bedding (outlined in black marker) with axial surface trace (white dashed line); a set of  $F_3$  folds in bedding and granite vein (axial surfaces traces in pink) terminating against  $F_2$  structure; **d)**  $F_{20}$  double-plunging isoclines in bedding (heavy dots,  $S_0$ ) with axial-planar  $S_{20}$  foliation (with flattened faserkiesel) in Sickle group sillimanite-biotite gneiss;  $F_{20}$  structures refolded by  $F_{2b}$  with weak axial-planar  $S_{2b}$  (above white dashes); open  $F_3$  folds and  $S_3$  overprinting all; **e)** inclined folds in the Burntwood group gneissosity and granitoid veins with segments that are folded (white arrow) and others that are axial planar (red arrow), as seen on a steep rock face nearly perpendicular to plunge; **f)**  $F_2$ - $F_3$  interference structures in hornblende-bearing gneiss of the Sickle group, in the hinge zone of a major anticline; note similar map pattern. Tapes are all approximately 12 cm long.

in the southwestern part of Notigi Lake (Murphy and Zwanzig, 2019a). Foliation parallel to bedding and affected by apparently late  $F_2$  folds must have formed during high-grade metamorphism after the development of quartz-sillimanite knots (faserkiesel, Figure 24d). These, and refolded folds, generally double-plunging isoclines, are identified as  $S_{2a}$  and  $F_{2a}$ . They are best seen where early and late hinge zones cross and strain is relatively low. Biotite- and amphibole alignment in folded foliation at the deep structural level, further indicate a synmetamorphic development of  $S_{2a}$  and weaker  $S_{2b}$  foliations with associated folds (Figure 24d). The northwest-trending foliation ( $S_{2a-b}$ ) was overprinted by northeast-trending  $S_3$  schistosity and fracture cleavage (Figure 24d). Folds in mesoscopic layering and thinner gneissosity are ubiquitous in the high-grade rocks. Thin granitoid sheets and veins have portions that are folded and portions that are axial planar to the abundant folds (Figure 24e). Originally these folds were possibly recumbent, but are now seen as inclined on rock faces where the Rat River empties into Notigi Lake. Folding must have occurred during late  $D_2$  after migmatization but during the injection of thicker late veins. Some minor interference structures (Figure 24f) are similar to the map-scale pattern at Notigi Lake. They include repeated  $F_{2a}$  folds, commonly isoclines that were refolded along an  $F_{2b}$  axial surface, and refolded, in turn, in a tight northeast-trending  $F_3$  fold. Because the dip changed across the  $F_2$  folds, the  $F_3$  plunge varies in orientation and locally reverses along the  $F_3$  folds. This forms elongate basins, domes and sheath-like folds. The  $F_3$  structures consist of multiple folds often restricted to earlier planar  $F_2$  fold limbs.

An elongate northeast-trending minor-scale basin with narrowing in the middle, at a slight upward bulge, resulted in the structure shown in Figure 24f. Major and minor  $F_3$  folds, which can dominate the map pattern, have a distinctive flexural style in some areas (Figure 25a) but are highly appressed and progressively rotated in the core and sheared limbs of tight  $F_3$  folds (Figure 25b). These domains produced some elasticas, in which the hinge area is wider than the combined limb areas (Figure 25b).

High-strain domains also feature sheath-like folds, especially where early folds were inverted, for example the west-northwest-plunging domal isocline on the north side of the larger Notigi structure (SF in Figure 26). This structural style suggests progressive transposition of most  $D_1$  and  $D_2$  structures. Notably, during the progressive strain, the typically flexural  $F_3$  folds may have been converted to flow folds or sheath folds. The  $F_2$  isoclines with sharp hinges, however, are deformed in  $F_3$  folds like ordinary layers, as in the northeastern Notigi culmination (e.g.,  $F_{2a}$  isocline at B' and D', Figure 26). The  $F_{2b}$  hinge zones, on the other hand, would have acted as competent bodies and resisted the  $F_3$  folding and flattening, thus preserving earlier structures locally.

The  $S_3$  foliation is apparent in younger granitoid rocks like unit Lgg, in which it is identified by its straight northeast strike (Figure 25c, d) and steep dip. The youngest surfaces are north-

erly trending, spaced cleavage ( $S_4$ ) and perpendicular fracture cleavage ( $S_4'$ ) that do not significantly affect the older structures (Figure 25c). Much of  $S_2$ , especially in the limbs of tight northeast-trending folds, has been rotated or transposed into the composite  $S_{2-3}$  foliation formed by rotation of, and compression across  $S_2$ . Although the relative age of foliation cannot be clearly assigned at most local sites, crosscutting features, such as early, peak-metamorphic leucosome (with diffuse contacts, no selvages and in apparent equilibrium with the host mineral assemblage), suggest late development or transposition into northeast-trending foliation (Figure 25d). Faserkiesel can also act as local, relative-age indicators (see above). These knots of quartz-sillimanite or plagioclase-sillimanite formed as spheres by the reactions

- muscovite+plagioclase+quartz→K-Na-feldspar +sillimanite+H<sub>2</sub>O or
- muscovite+plagioclase+quartz+H<sub>2</sub>O→sillimanite+melt

occurring mainly in arkosic arenite (Zwanzig and Bailes, 2010). The reactions did not consume all quartz or all plagioclase in contact with sillimanite in the faserkiesel. Flattened faserkiesel are an indication of strain and development of foliation after the above reactions took place. The presence of faserkiesel in leucosome, and their orientation at an angle to the local foliation, indicates that the rock in Figure 25d had formed leucosome and undergone strain before the  $S_3$  foliation was formed. Where the  $F_3$  folds are open to moderately close,  $S_2$  is recognized by its high angle to  $F_3$  and a lower angle to  $F_0$  (Figure 25e).

Typical deep-level major structures such as at Notigi Lake arose in  $F_3$ - $F_2$  interference. The Notigi structure consists of a northeastern and a smaller southwestern culmination separated by a saddle (Figure 26). Its polyphase origin has been modelled (below).

### 6.2.1 Large recumbent/inclined folds and structural interleaving ( $D_2$ )

The isoclinal Timew Island syncline (outer  $F_{2a}$  syncline in Ksb, Kb in the Notigi structure) developed  $S_2$  foliation parallel to transposed bedding ( $S_{0-2}$  in DRI2021014, Figure 1). The fold wraps around the northeastern Notigi culmination, but between Timew Island and the east side of the culmination (US, Figure 26), the core units (Kb, Ksb) of the syncline lie above the erosion surface, and only Kh is exposed.

In subarea 1, on the west side of the culmination, a plunge concentration ( $\pi_3$ ) at 67° toward north-northwest is indicated by a well-developed girdle of poles to all layering and foliations (Figure 26). This is the local plunge of the of the en-échelon-fold packet that forms the part of the  $F_3$  culmination in subarea 1. The  $F_2$  lineations and fold axes lie near a small circle with a 70° radius and a steeply plunging axis ( $\pi_3'$  in stereoplot, sub-area 1). The local  $F_2$  fold axes (brown asterisks) have retained a shallow plunge in  $F_3$  hinge areas but are folded about the steep  $F_3$  axis ( $\pi_3'$ ).

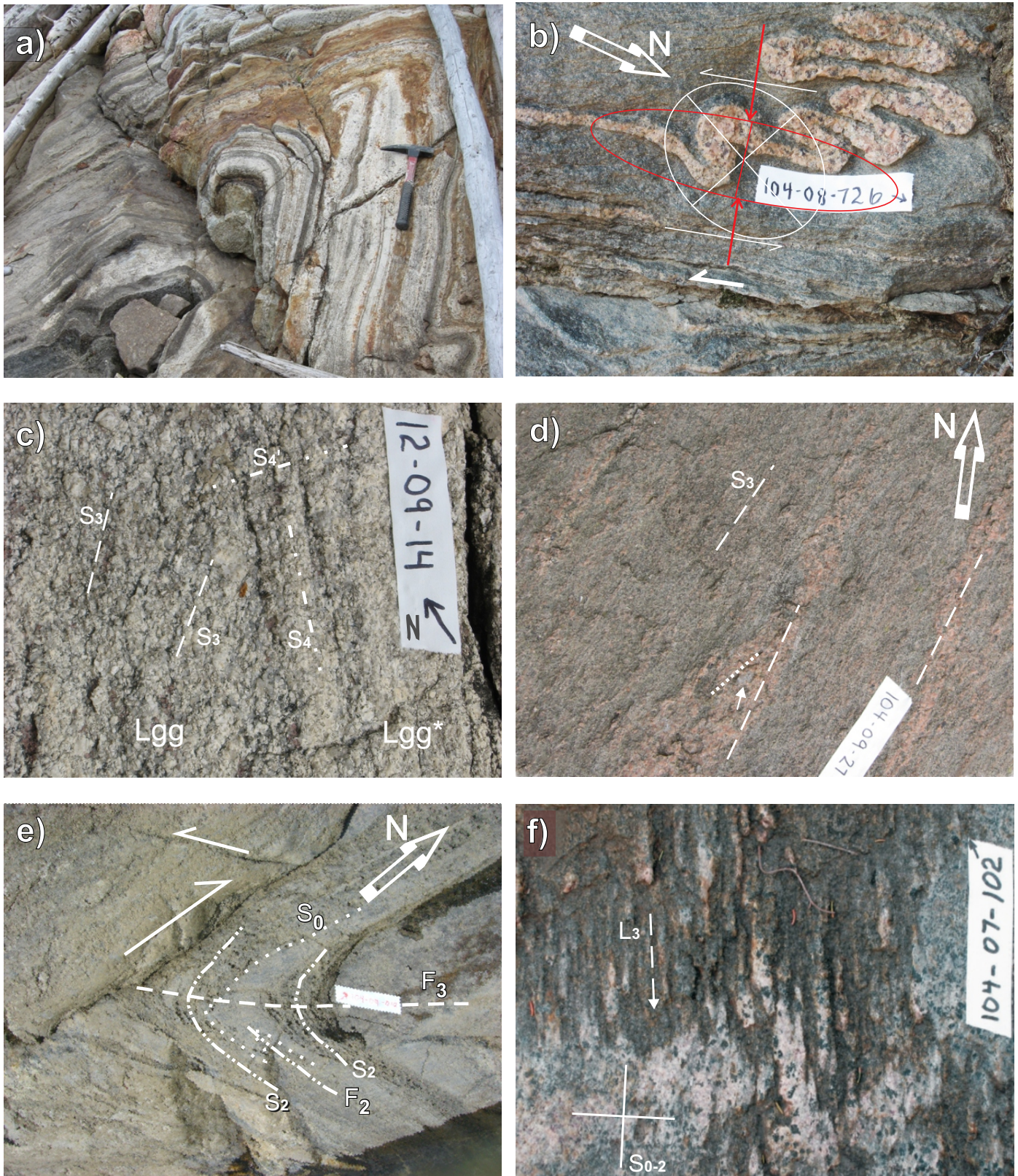


**Figure 25:** Structures at Notigi Lake with interpretations: **a)**  $F_3$  fold with a flexural style in Granville complex calcisilicate and sulphidic pelite; **b)** ptygmatic fold in granite vein (above tape) and sinistral shear bands (thick arrow); structure can be reproduced graphically using a small component of sinistral shear (thin arrows) and a major component of compression (red); ellipses are sectional, showing minimum strain; **c)**  $S_3$  foliation and  $S_4$  spaced cleavage with perpendicular fracture cleavage in granodiorite (Lgg) and leucogranodiorite (Lgg\*); **d)**  $S_3$  foliation in Sickie group (Ksb) and in granite leucosome with faserkiesel (at arrow) flattened in  $D_2$  and rotated toward  $S_3$  (long axis along dotted line); **e)**  $F_3$  fold in bedding ( $S_0$ ), in  $F_2$  fold and in  $S_2$  at angle to  $S_0$ ; **f)** crenulation surface of ( $S_{0-2}$ ) forming rodding and amphibole alignment. This  $L_3$  intersection-lineation is useful in establishing the local plunge that helps to determine the shape of the  $S_{0-2}$  layering and foliation that were crossfolded in  $D_3$ . Tapes are 12 cm long.



Subarea 2 shows an  $F_3$  plunge of about  $20^\circ$  trending north-east. A scattering of poles to early planes outside the main  $F_3$  girdle has a weak concentration along a northeast-trending great circle with a shallow northwest-plunging axis ( $\pi_2'$ ), accompanied by  $L_2$  lineations. The lineations and  $\pi_2'$  lie on a small circle  $50^\circ$  from  $\pi_3$ . Such a noncylindrical distribution is typical of linear structures curved over flexural folds in the KD (Zwanzig, 1999). As in subarea 1, these structures must be remnants of the  $F_2$  folds.

On the southwest side of the culmination (at A') the plunge is steeply south. Farther southeast, near B', the plunge is gently north as units are wrapped under the culmination. The nearby north-plunging synform is interpreted to be a result of  $D_{3-4}$  compression. The changes in plunge are interpreted to be the result of the superposition of the  $F_3$  fold-packet on shallow  $F_{2b}$  fold limbs in the northeast (upper limb) and south (lower limb) as well as the intervening steep part (the  $F_{2b}$  hinge area). The outward dips in the east and northwest (DRI2021014, Figure 1) confirm that the whole structure is a culmination and that the  $F_{2b}$  fold was a gently inclined (nearly recumbent) antiform. Thus the culmination was formed by  $F_{2b}$ - $F_3$  interference. The large  $F_{2a}$  isoclines were refolded much like simple layering. An  $F_{2b}$  synform southwest of the main culmination is shown as extending from D'' (Figure 26) northwest across the saddle (S). In the southwest the Granville complex may be in an anticline, or younging reverses at the Burntwood megathrust. The presence of the tectonized Granville complex along the boundary between the Burntwood and Sickie groups at Notigi Lake and in surrounding areas is a further indication that it lies at the sole of a large nappe, probably as part of the Russell nappe carried southeast on the Burntwood megathrust. The proposed Burntwood megathrust separates narrow, discontinuously mapped amphibolite (Gtb, Gg) and its stratigraphically overlying Sickie group from the Burntwood group. And so, the Granville complex is likely missing in the northeast half of the Notigi culmination because the thrust cuts stratigraphically up section from C' to D' (Figure 26). Dips, plunge and younging commonly change across the fault. Possible younger ( $D_2$ ) splay faults may join the main fault at C'' and farther northeast.

A thin amphibolite unit with gabbro and quartz diorite of uncertain origin extends from Timew Island north into the mainland and, from there, northeast apparently into unit Gtb along the Notigi granite (Murphy and Zwanzig, 2019c). On Timew Island, gabbro is overlain and underlain by units of the Sickie group. The base of the lowest sill is sheared and highly metasomatized to mafic garnet-biotite schist. This is interpreted as another possible  $D_1$  thrust fault within the Granville complex and the unconformably overlying lower Sickie group. The presence of quartz-rich beds in unit Ksb on the island and unit Kse to the north, typical of the Sickie group base, supports the suggestion of a low stratigraphic position. This exposure of a panel of the lowest unit of the Sickie group and a sliver of the Granville complex (G) in the core of the  $F_{2a}$  syncline would have placed these units at a high structural level in an early thrust

stack. The proposed thrust must cut up section on the island, where the sills are lost and the thrust panels can no longer be distinguished. North of Timew Island the proposed thrust and amphibolite are folded in the  $F_{2a}$  syncline.

Rodding ( $L_3$ ) has formed from crenulation where  $S_{0-2}$  is intersected at high angles by  $S_3$  (Figure 25f). This lineation tracks the changes in  $F_3$  plunge and reflects the changes in the dip of the  $F_2$  folded surfaces. The changes in  $L_3$  orientation and  $F_3$  plunge are used to approximate the original shape of a major  $F_{2b}$  inclined antiform. Northeast of Timew Island, where the  $F_3$  plunge reverses, is the crest of what was the original  $F_{2b}$  fold. This provides the isolated exposures of the Burntwood group, the granodiorite and most likely the  $F_{2b}$  axial surface in the core of the culmination (Figure 26). Where the local plunge changes its trend from northeast to northwest-southeast and steepens to south-southwest, between A''' and A' is the approximate site of the hinge of the  $F_{2b}$  fold with the deepest exposure north of P. The upright part of the  $F_{2a}$  syncline on Timew Island along with the inverted part to the northeast are consistent with the emergence of the  $F_{2b}$  axial surface northeast of P. Other deep-level exposures lie close to line C-C'' and trend northwest to provide the orientation of the hinge zone of the  $F_{2b}$  antiform. This geometry establishes the  $D_{2b}$  vergence toward the southwest. The  $F_{2b}$  fold is seen as refolded by  $F_3$  structures, and the exact location of the folded axial surface at ground level is uncertain. It may be exposed as far northeast as P'. Shallow to moderately northwest- and southeast-plunging folds and  $L_2$  lineations are preserved close to  $F_3$  hinges along the central crest of the Notigi culmination.

Results of the structural analysis are illustrated in a three-dimensional diagram in Figure 27a based on down-plunge projections (Figure 27b, c) along the stereographic girdle axes,  $\pi_3$  (Figure 26). The diagrams show the presence of the large refolded Timew Island syncline, cored in the upper unit of the Sickie group (Ksb) that closes at B\*, south of Timew Island, in Notigi Lake, as proposed by Zwanzig and Murphy (2009) but called  $F_1$ . This early fold is however most likely the same age as the northerly overturning and north-verging  $F_2$  folds at Granville Lake. The syncline extends around the culmination and over it (Figure 27a) into stacked isoclinal folds, a synclinorium, exposed on the east side of the culmination (Figure 27c). At B\* the plunge is  $31^\circ$  toward  $67^\circ$ NW and at US  $20^\circ$  toward  $35^\circ$ NE. This  $90^\circ$  bend of the  $F_{2a}$  hinge (in a past saddle above the erosion surface) is shown schematically in Figure 27a. The northerly vergence of  $F_{2a}$  in the Notigi structure is confirmed by the hinge of the syncline in the south, its upright orientation on Timew Island and at US, yet its inverted orientation on the northwest side of the culmination.

A downward view of the southeast half of the culmination is similar to a vertical projection unfolding this limb along the central  $F_3$  hinge but without removing other  $F_3$  and earlier folds (Figure 27d). The northeast- and southwest-plunging lineations are shown with their true plunge as dip lines. These match the adjacent contacts in the projection also and show the  $F_{2b}$  ver-

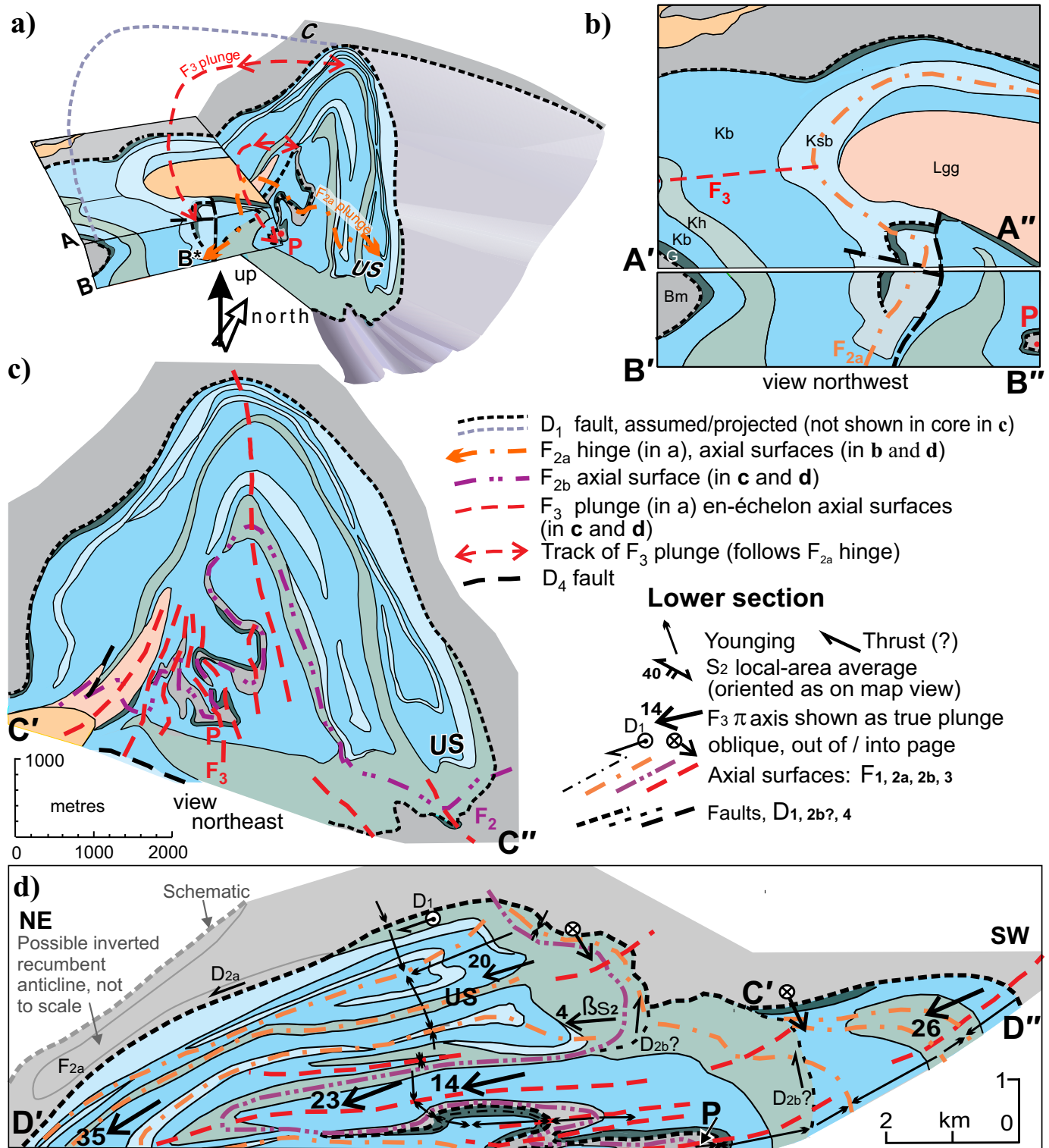


**Figure 27:** Three-dimensional geometry of the main Notigi culmination shown as **a)** perspective diagram viewed to the north and slightly downward, constructed from **b)** and **c)**, down-plunge structure sections (panels A', B' and C'), each with a different plunge as calculated using stereographic analysis. **b), c)** The three corresponding sectional cuts (panels A', B' and C') are perpendicular to the mean local plunge (stereoplote π axis). The panels are joined at point P. Panels A' and B' are cut approximately parallel to the mean F<sub>3</sub> fold axis in the northeast and perpendicular to parts of the folded F<sub>2</sub> fold hinge. They show the F<sub>2a</sub> syncline, which closes sillimanite-bearing gneiss (Ksb) in panel B'. Panel C' is perpendicular to the mean F<sub>3</sub> fold axis where it is only slightly curved in the northeast. The complex pattern of the F<sub>2a</sub> axial surface in the core of the structure in C' resulted from fold-interference or sheath folding. The simplified hairpin curve enveloping the F<sub>3</sub> fold axis shown in a) overprinted the F<sub>2b</sub> fold. The folded surface (violet) on the right front in a) represents the outer repetition of the D<sub>1</sub> Burntwood megathrust. The figure is adapted from Zwanzig and Murphy (2009) and the unit legend is as in Figure 26. **d)** Longitudinal down-dip section, viewed toward southeast, with map view rotated to lie in the F<sub>3</sub> axial plane, parallel to plunge, but without removing F<sub>3</sub> folds. The plunge of F<sub>3</sub> axes/lines became an F<sub>2</sub> dip.

gence as southwest. There also appears to be renewed southwest stacking of folds and possible faults.  $D_{2b}$  imbrications are suggested to have merged with the overturned  $D_1$  fault acting as roof. An unmapped  $F_{2a}$  antiform closing northeast toward  $D'$ , above a reactivated thrust ( $D_{2a}$ ), should be present paired with the  $F_{2a}$  synclines at US under the thrust. This achieved the early large-scale structural inversion. The  $F_{2a}$  antiform could not be mapped because of the uniformity of the Burntwood greywacke-migmatite (Bm) and lack of sufficient outcrop or possible erosion of the upright limb. Its presence is implied by the inversion of the Bm-G-K contacts at Notigi Lake, and the regionally inverted section. The  $F_{2a}$  synclines in the Sickie group close on the south side of the Notigi structure (Figure 26) and may not extend much farther under the Burntwood group at depth. On the northwest side of the Notigi structure, however, the Sickie group extends far under the Burntwood group and reappears northwest of the  $F_3$  synforms ( $C^*-C$  in Figure 26).

The structural culmination at Notigi Lake also contains the Notigi composite pluton with an interpreted igneous age of  $1862 \pm 6$  Ma of its eastern body (Section 5.1.3). It is mantled by Sickie group rocks and locally by thin mafic tectonite of the Granville complex. The Sickie group surrounding the composite pluton is interpreted as continuous at depth with the Sickie group that mantles the Rat granite (gn) to the northwest (Figure 28a). This geometry is supported by the presence of the  $F_3$  synforms between the domal intrusions and the poorly preserved but similar stratigraphy in the two areas, as illustrated in the regional structural model (Figure 28a).

The hinge of the  $F_{2b}$  antiform in the culmination is also interpreted to extend northwest where it joins the domal shape of the Rat granite. The  $F_{2b}$  hinge zone, marked approximately on Figure 26, is intruded by leucogranite (Llg) in shapes that resemble large folded sills. Such granitoid and pegmatite intrusions are common in  $F_3$  synformal and basal areas that approach the top of the KD migmatite zone, in this area also crossing an  $F_2$  hinge. The overall structure is probably more tightly refolded by  $F_3$  and more deeply eroded than shown in the simplified Figure 28a. The regional structural model suggests that the Notigi monzogranite, like the Rat granite, could represent part of a granitoid, arc-derived, mobilized basement to the Sickie group.

The results of the 3-D analysis (Figures 27, 28b) can be compared to the development of incipient sheath folds (Alsop and Carreras, 2007). Although the present crustal geometry at Notigi Lake is interpreted to be the result of fold interference, the reconstructed  $F_{2b}$  folds share characteristics with incipient sheath folds (Stage 1 in Alsop and Carreras, 2007). Similarities include a start as buckle folds and highly attenuated limbs with down-plunge mineral lineations marking a stretching and transport direction (e.g., Figure 25f). A diagram illustrating the general shape of the  $F_{2b}$  structures, restored as they may have appeared before  $D_3$ , is included as Figure 28b. It suggests an original northwest strike and a ca.  $40^\circ$  dip toward northeast for the  $F_{2b}$  axial plane, and a  $50^\circ$  inter-limb angle. Compared with

statistics on such close structures (Alsop and Carreras, 2007), the short- to long-limb ratio is about 1:6, and hinges are cylindrical or curve less than  $30^\circ$ . This is consistent with a short, moderately northeast-dipping lower limb of the northeastern  $F_{2b}$  antiform with a narrow synform and tight second culmination nearby to the southwest (S and D in Figure 28b). The figure shows progressive hinge curvature as indicated on the south margin of the culmination. The relatively thick, moderately overturned short limb is consistent with the presence of  $F_2$  lower-order folds and thrusts ( $D''-P$ , Figure 26). The overall fold-style is important for kinematics because folding with axial surfaces dipping close to  $45^\circ$  represent horizontal transport of upper layers, as does the hinge curvature and limb-rotation at depth. It is consistent with the tight curvature of the  $F_{2b}$  fold axes in the final style of folding that includes sheath-fold-like structures.

Farther to the south, at Wapisi Lake, very different units are in structural culminations. They are the Wuskwatim Lake sequence, its Archean basement and, most prominently, plutons of the FLPS (qm). Culminations of these pre-Burntwood rocks in the Northeast Kiseynew subdomain extend from Atik Lake east to Footprint Lake and southeast to Wuskwatim Lake; and from there, south beyond Tullibee Lake to the TNB (Figure 1). East-west-trending trains contain quartz monzonite (qm) "domes". Some of these culminations contain unit gx granite or Archean gneiss (Ag, Ai) underlying or interleaved with the Wuskwatim Lake sequence (Murphy and Zwanzig, 2019c). Most of these discontinuous belts are parallel to the  $D_2$  structures in the Kiseynew north flank and were refolded by the  $F_3$  major folds (see below). Their structural style and attitude is similar to the Notigi culminations and consistent with an early interpretation (Zwanzig et al., 2006) of the Mel zone (location in Figure 17) in the TNB, northeast of Wuskwatim Lake.

### 6.2.2 Deepest level: Wuskwatim Lake area

As at Notigi Lake, the outward northwest- and southeast-dipping foliation ( $S_{2-3}$ ) at the sides of Wuskwatim Lake and shallow northeast- and south-dipping foliation at the ends of the lake frame a culmination. This exposes the Wuskwatim Lake sequence (W) and its Archean basement gneiss (Ag, Ai). The steepening dip farther south suggest the presence of a major south-verging, inclined  $F_2$  antiform and its nearby axial trace (Figure 29a). The trace is interpreted to extend northwest into the culmination along the Burntwood River where W and Ag are also exposed. This geometry and history suggest that the older rocks became structurally interleaved with the Burntwood group during  $D_2$  folding. En-échélon culminations were formed at the intersection of  $F_2$  and  $F_3$  antiforms.

At this structural level the  $F_2$  folds formed under amphibolite- and transitional granulite-facies metamorphic conditions for an extended  $D_2$  deformation (Zwanzig, 1999). They represent subhorizontal ductile flow of the basement, cover and early plutons during the formation of large inclined folds with

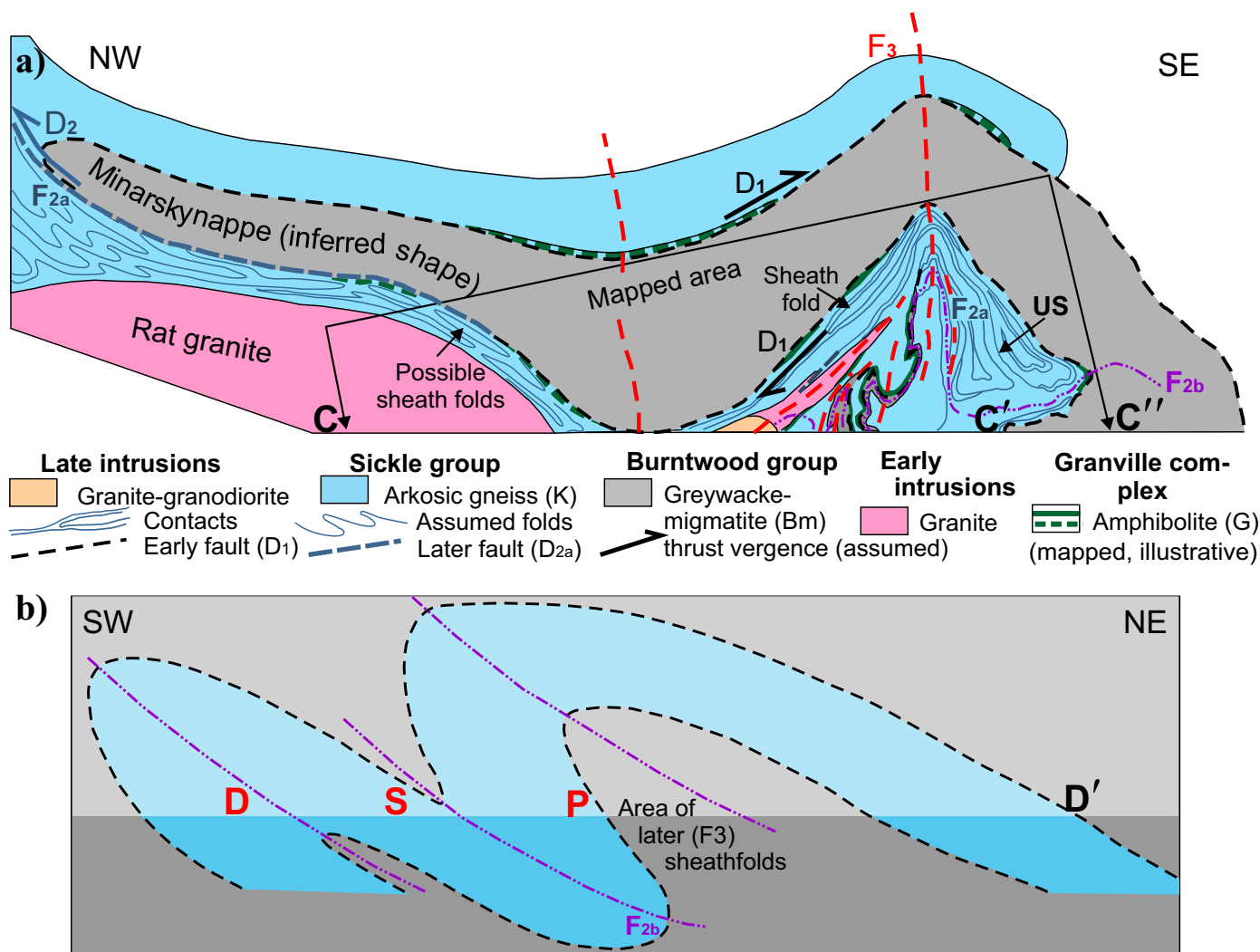


**Figure 28:** Regionally modelled structure sections and deformation stages, Misingagu–Notigi lakes: **a)** simplified projection is viewed to northeast, down plunge, but outside the mapped area has an assumed shape; the assumptions are that the Burntwood group (Bm) contact is a  $D_1$  southeast-verging thrust; the Sickle group (K) lies unconformably on Granville complex (G) and provides stratigraphic younging. An asymmetric dome (Rat granite) and upright  $F_3$  antiforms (at Notigi Lake) expose the inversion of the Bm/G+K contact at the scale of a fold nappe (Minarski nappe). The  $D_1$  thrust relation is not destroyed but G may be in widely separated boudins. Features in a) are a northwest vergence (Minarski nappe) as shown by the southeast-closing isoclinal synclinorium at US. Folding of high-grade foliation after crystallization of sillimanite, and reversal of vergence requires a  $D_2$  age for the Minarski nappe. **b)** Folding along variably plunging axes, shallowly northeast, steepening to southwest and returning to shallowly northeast, requires superposition by a second, nearly recumbent (inclined) antiform ( $F_{2b}$ , reconstructed in b) that is southwest-verging and also formed at near-peak metamorphic  $D_2$  conditions.  $F_3$  upright structures have refolded the superposed nappes to squeezing units G and B into the core and apparently turning them into thin sheets of box-shaped sheathfolds. Shear-strain along the  $D_2$  thrust and along the reactivated  $D_1$  thrust may have stretched and rotated adjacent folds and produced sheath folds. The  $F_3$  antiforms are developed in en-échelon segments (multiple projected  $F_3$  axes in a) superposed on originally subplanar  $F_{2b}$  fold limbs with different dips. Some  $F_3$  folds die out at the  $F_{2b}$  hinge because of the mechanical constraints posed by the hinge of close, flexure folds. Diagram b) viewed northwest is a reconstructed section using variations in  $F_3$  plunge and preserved  $F_2$  dips from 3-D analysis (Figure 27) to illustrate the deduced vertical profile of the  $F_{2b}$  anticlines that are the first stage in forming culminations. The approximate location of the restored  $F_{2b}$  profile is D–D', as in Figure 26. The near 45° dip, northwest-plunging  $L_3$  lineations (below P) and the curvature of axial surfaces indicate southwest, upper-layer, crustal-scale transport and lower-layer shear. Melt-assisted, mid-crustal,  $D_{2b}$  flow toward SW is inferred (see text).

structurally inverted lower limbs. They have a southwest vergence and are interpreted to have formed within, under and in front of a southward penetrating crustal wedge of LRD-type granitoid rocks into the KD. A series of en-échelon–domal culminations of the Archean gneiss (Ag, Ai) and its Paleoproterozoic cover rocks (W) occur in  $F_3$  cross folds (Figure 29a, b). They are revealed by positive aeromagnetic anomalies and shown to exist by Percival et al. (2006). The anomalies allowed rocks

with variable magnetite content to be traced even beneath water, swamp, muskeg and thick bush. Peak magnetic signatures are assumed to lie near the upper, dipping contact of magnetic units, where the vertical section is deep but just below the surface.

The best exposures providing stratigraphy and structure are along the shore lines of the widened Burntwood River, north of Wuskwatim Lake. With the help of the aeromagnetic map of

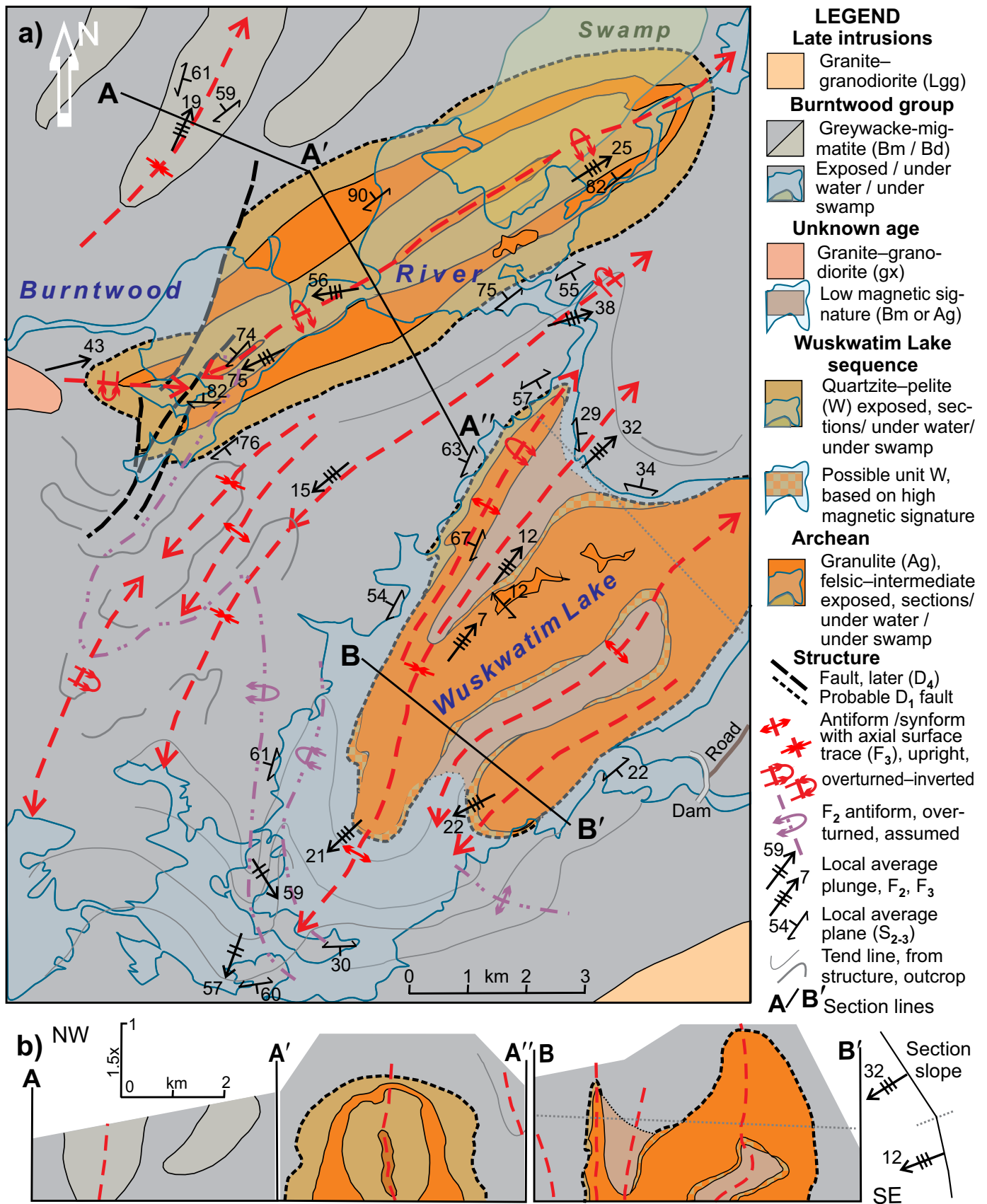


**Figure 29:** Interpretive structure map and sections, Wuskwatim Lake include **a)** the structural patterns beneath lakes and swamp as interpreted from aeromagnetic maps (Kiss and Coyle, 2008) and surrounding foliation trends. Structural features are local averages with plunge from stereoplots; trend lines are from field data and airphotos;  $D_1$  fault is inferred from Granville and Notigi lakes. **b)** Sections are perpendicular to local plunge. B–B' uses 7–12° below dotted line, 32° above, to match  $F_3$  axis curve. Major culminations are separated and bordered by synforms. The section buried below Burntwood group northwest of A'' probably connects the “domes”. Lake level predates minor flooding (except forebay).

Kiss and Coyle (2008) a close oval structure was identified as a double-plunging culmination (Figure 29a). The highest magnetic anomalies mark unit *Wi* and allow the Wuskwatim Lake sequence to be traced where it is poorly exposed or covered (Murphy and Zwanzig, 2019d). The oval structure has a shallow northeast plunge and a steep southwest plunge, similar to the Notigi structures. The oval structure may represent a dome with a central depression forming an upright M-shaped structure as in Figure GS-8-4b in Percival et al. (2006). As mapped along the Burntwood River this would require an M-shape both along and across the structure—a dimple on a dome. Preferred in this report is the presence of a refolded  $F_2$  recumbent fold (Figure GS-8-4c in Percival et al., 2006). It is interpreted herein as refolded in an upright  $F_3$  antiform with a structural culmination in the southwest. The plunge returns to moderately east-northeast beyond the structure in the southwest. The  $F_3$  fold overprinted on a southwest-verging  $F_{2b}$  antiform is like the better-exposed structure at Notigi Lake. On the Burntwood River the 43°NE plunge in the west represents the lower limb of the  $F_{2b}$  antiform that determined the changes in plunge of the crossing  $F_3$  antiform. This interference structure contains interleaved units *Ag* and *W*, interpreted to form  $F_{2a}$  isoclinal anticlines cored in unit *Ag*. Contacts are exposed in the northeast and southwest of the structure and interpreted as an unconformity between *Ag* and *W* (Section 3.2.1). Outcrops on an island near the southwest closure of the structure and the magnetic pattern to the northeast suggest an additional deeper layer of *Ag* in the core of the  $F_3$  anticline (Figure 29). The inner contact of the ovoid surface of the sheet of *Ag* is not exposed however, and a thrust cannot be ruled out there. The outer contact of the Wuskwatim Lake sequence, which is with the Burntwood group, is most likely a major thrust fault, consistent with the interpretation in Burnham et al. (2009) in the TNB as in Figure GS-14-5 in Zwanzig and Böhm (2002), and as structures interpreted at Granville and Notigi lakes in this report.

Lithologically similar granulite-facies orthogneiss as on the Burntwood River is well exposed on two islands in Wuskwatim Lake (Figure 29a; Zwanzig et al., 2019). The units in this “dome” and along the Burntwood River are interpreted as connected at depth below intervening synforms, and probably continue northwest to Threepoint Lake and beyond in a large  $F_2$  structure that was deformed by the  $F_3$  crossfolds. A moderate positive aeromagnetic anomaly beneath Wuskwatim Lake also corresponds to the presence of granulite-facies Archean basement gneiss (*Ag*, *Ai*). This is generally under the lake except for the two islands in the middle (Figure 29a). Subhorizontal  $S_2$  foliation and  $L_3$  lineation characterize the crest of the structure. Lineations curve into a gentle northeast plunge to the north and moderate to steep southerly plunge to the south. Thus, lineations follow an asymmetric dome or a refolded, nearly recumbent  $F_2$  fold. The central anomaly of units *Ag* and *Ai* is separated by a stronger positive anomaly from the surrounding magnetically quiet background of the Burntwood group

paragneiss. The strong positive anomaly is identified as resulting from sulphide-facies iron formation, *Wi*(su), of the Wuskwatim Lake sequence in exposures on the northwest shore of the lake. Thus, Wuskwatim Lake is interpreted as underlain by Archean gneiss with a thin or partial mantle of *W*. Internal belts of positive magnetic anomalies may be belts of unit *W* with bordering Burntwood group in the magnetic lows or, more simply, unit *Ag* with phases of different magnetite contents (as implied by Zwanzig et al., 2019). Evidence that the Wuskwatim Lake structure is an  $F_{2b}$ - $F_3$  interference structure having  $F_{2b}$  as a south verging inclined fold lies in the southeast-plunging fold axes ( $F_3$ ) in the Burntwood group on the south end of Wuskwatim Lake (Figure 29a). This implies that the full structure lies below the present level of erosion, as also indicated by the magnetic pattern. The exposed part of the structure therefore resembles a dome. A connection at depth between the structures at Wuskwatim Lake and the Burntwood River, is supported by the presence of the major synform-antiform-synform triplet between the two structures. A unit of felsic gneiss (mapped as unit *Gc*, which it resembles) occurs locally adjacent to the Burntwood group on each side of the synformal structure.

Trends in the gneissosity southwest of the Wuskwatim Lake culmination outline large  $F_{2b}$  folds with axial surfaces curved southeast toward the  $F_3$  Wuskwatim Lake antiform. There, they died out, and a single open  $F_{2b}$  fold appears on the  $F_3$  southeast limb. This arrangement suggests that an earlier fold existed with which the  $F_3$  hinge came to coincide. This style of folds that terminate against older structures is expected in superposed buckle folds (Skjærnaa, 1975). The early fold is interpreted to have been part of the regional  $D_1$  nappe, so that all stages of deformation were involved in producing the culmination.

South of Wuskwatim Lake a southwest-trending chain of large granitoid bodies with FLPS components includes a culmination with a Burntwood group core. The chain occupies an anticlinal ridge that extends into younger granites. Northwest of Wuskwatim lake FLPS intrusions, remnants of the Wuskwatim Lake sequence and local basement gneiss extend to an area north of the Highrock Lake batholith (Figure 1). The local abundance of the FLPS, and younger granites with Archean isotope chemistry mark the wide extent of the Archean basement rocks and Wuskwatim Lake sequence at depth. In this southeastern part of the study area, these rocks are seen in refolded sheet-like structures, exposed in culminations but greater thicknesses of *Ag* may occur at depth.

Whereas the bodies of the FLPS at Threepoint and Wapisiu lakes have partial mantles or extensions of unit *W*, other bodies appear to be completely surrounded by Burntwood group migmatite or have an intervening sheet of younger granite. All these structural culminations are interpreted to have developed on  $F_3$  anticlinal crossfolds. Bodies as at Footprint and Threepoint lakes are various granitoid plutons in a chain that extends south-southwest, parallel to  $F_3$ , in a long antiformal

ridge across the central KD to the Flin Flon domain (Figure 1). Given the poor exposure of the less competent unit W, the FLPS intrusions look like they have intruded the (younger) Burntwood group even where short attenuated segments of unit W sidewalls are exposed. The large antiform-shaped intrusion with unit gx at Threepoint Lake, also consists partly of unit qm, now flooded (Baldwin et al., 1979). Pink leucogranite within the body has  $\epsilon_{Nd}$  of  $-5.5$ , and must be highly contaminated by this and/or unit W. The intrusion has east-west extensions of unit W and a mantle of highly magnetic rock like the FLPS (Zwanzig et al., 2019).

The FLPS body on the southwest end of Wapisi Lake has a partial mantle of unit W and internal and bordering sheets of pink leucogranite (Llg) with  $T_{CR}$  of 2.8 Ga, similar to the FLPS. Where observed at Wapisi Lake, the mantling paragneiss (W) has been attenuated to less than 10 m thick. Negative  $\epsilon_{Nd}$  values indicate that sheets of leucogranite (Llg) surrounding the pluton have assimilated Archean material and may have assisted FLPS doming or “emplacement” into the overlying Burntwood group. Such melt-enhanced deformation (“melt-enhanced diffusion creep”, Dell’Angelo and Tullis, 1988) is considered to have occurred in the KD. Structures within the FLPS (Figure 8a) are consistent with such a process. The most potassic sheets (gx, Llg) at the margins and within the FLPS pluton at Wapisi Lake may be margin phases of unit qm. Alternatively, partial melting of qm

may have taken place. Relatively well-preserved Burntwood group gneiss (Bg), having remnant bedding and intrusions of Lgg with sharp contacts in structural basins, suggests that the older rocks rose and translated in “domes” toward the cooler roof zone of the Kiseynew migmatite complex along with the younger melts.

## 7. Regional and THO-wide correlation and tectonic model

Tracing lithotectonic successions and intrusive suites along the length of the KD north flank and the Northeast Kiseynew subdomain points to a common tectonic evolution for the Wuskwatim–Granville lakes corridor, much like the rest of the western Trans-Hudson internides and the THO across Canada (Table 5).

During the evolution of the THO from Saskatchewan to Baffin Island, five or six tectonic episodes are proposed to have occurred in the western internides until final convergence of the three surrounding Archean cratons into Laurentia (Table 5). These episodes define more than 200 m.y. of tectonic history shared in Manitoba and Saskatchewan and with the THO at large. This history involved ocean-floor and arc magmatism as well as syn- to postcollisional intrusion, each episode coeval or overlapping in age throughout the W-THO. This history has been divided into orogenies in a Wilson cycle that started with rifting and ended with the amalgamation of Laurentia, the

**Table 5:** Tectonic history of the western Trans-Hudson orogen with Canada-wide correlation.

<sup>1</sup> Manitoba–Saskatchewan				<sup>2</sup> Saskatchewan–Manitoba– <sup>3</sup> Quebec–Baffin Island		
Episode	Date (Ma)	Duration (m.y.)	Deformation	Episode	Date (Ma)	Orogeny
Continental rifting	2075			Continental rifting	2075	
Opening of Manikewan ocean, onset/TNB sediments	1975			Opening of Manikewan ocean, onset/Watts group <sup>3</sup>	2000	
Subduction, early-arc magmatism onset	1920			Meta Incognita shelf <sup>3</sup>	2010–1900	
Arc-rift– & back-arc–volcanism				Early-arc magmatism	1920	
Onset (Flin Flon east)	1905			Hearne/Rae craton amalgamation	1920 to 1890	Snowbird
(Levesque Bay)	>1900					
(West of File Lake)	>1886					
Early-arc magmatism, end; arc amalgamation	1880			Flin Flon–Glennie collage amalgamation; Hearne craton/La Ronge domain collision	1980	Reindeer
Hearne/La Ronge–Lynn Lake collision, subduction flip; Lynn Lake gabbro; tonalite	1876 to 1874		Lynn Lake D <sub>1</sub>	Meta Incognita/Rae craton <sup>3</sup> collision	to	Foxe <sup>3</sup>
Middle successor-arc magmatism, onset/end	1865 to 1850			Middle successor-arc magmatism: Flin Flon, La Ronge, Rottenstone, Lynn Lake, Southern Indian, Wathaman–Chipewyan domains	1865 to	Wathaman
Kiseynew turbidite sedimentation	1850 to 1835		Southern Indian Lake D <sub>2</sub>	Hearne craton/Southern Indian domain collision?	1845	
Continental sedimentation & late-arc magmatism; Flin Flon–Glennie/Sask craton/Superior craton collisions	1845 to		Kiseynew D <sub>1</sub>	Sask craton/Flin Flon–Glennie complex collision	to	<sup>1</sup> Saskatchewan
Ocean closure; delamination; Early nappe emplacement; Metamorphism, KD migmatization, nappe emplacement	1830 to 1790			THO internides/Superior craton collision	1830 to 1800	Trans-Hudson
Continental transpression TNB metamorphism, uplift	1780 to 1765					

Manikewan ocean (200)

Neomanikewan ocean (70)

Postcollision (I) Successor-arc magmatism (45)

Successor–back-arc extension

Early-arc magmatism (40)

Final early arc-rifting, earlier arc-rifting

Chipewyan excursion?

Bimodal ultramafic-mafic/fesic magmatism, TNB & KD margin (15)

Deformation (65)

Virgine

SE

NW

SW

NW

<sup>1</sup>This report; <sup>2</sup>,<sup>3</sup>Corrigan et al. (2009); <sup>4</sup>Also komatiite in final rifting at Superior margin; <sup>5</sup>Kramer et al. (2009).

core of North America (Corrigan et al., 2005). Zircon ages of early arc, arc-rift, back-arc and successor-arc magmatism in the Wuskwatim–Granville lakes corridor, fall into the time-span of the same episodes as in the THO across the entire Canadian Shield. In Manitoba they fit into the histories of the Lynn Lake–Rusty Lake belts (LRD) as well as the Southern Indian and Flin Flon domains (Figure 30a–d).

### 7.1 Early arc–back-arc magmatism

In summary, the geological mapping, geochemistry, structural analysis and compilation of published data along the Kiskeynew north flank are consistent with the interpretation that the main element of the newly defined Granville complex is dominantly amphibolite derived from back-arc-basin basalt (Tod Lake basalt) formed during early arc magmatism that

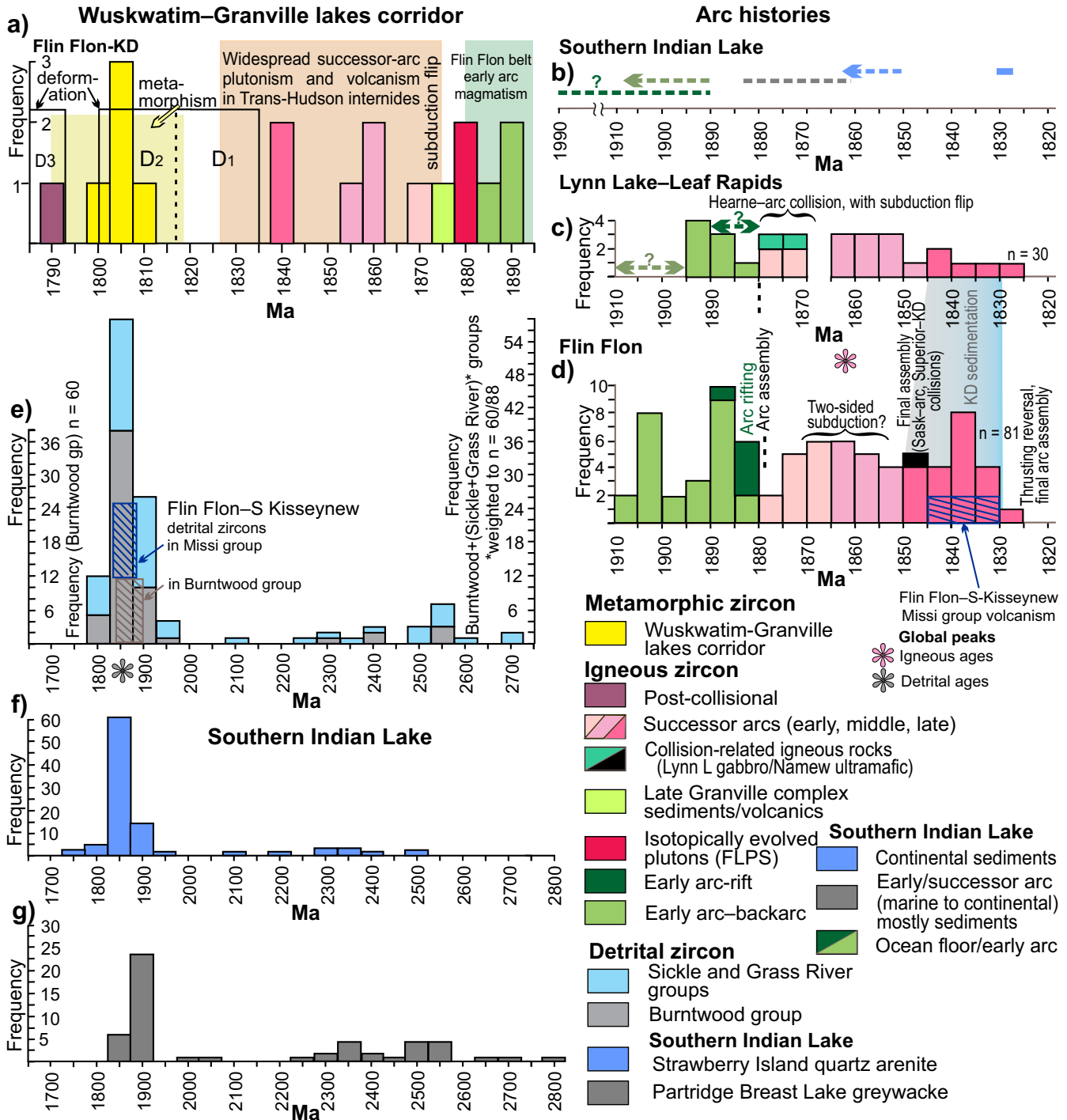


**Figure 30:** U-Pb zircon-age frequency plots of the Wuskwatim–Granville lakes corridor and surrounding areas of the THO: **a)** igneous and metamorphic ages in the Wuskwatim–Granville lakes corridor with shaded fields of similar episodes in adjacent domains; **b)** ocean-floor to arc-related igneous and sedimentary rocks of the Southern Indian Lake domain; **c)** igneous rocks of the Lynn Lake belt and KD north flank; **d)** igneous rocks of the Flin Flon domain; **e)** detrital-zircon ages of the Sickle/Grass River and Burntwood groups with fields from the Flin Flon and southern Kiskeynew domains; **f, g)** detrital-zircon ages in the Southern Indian domain. Data references in Tables 3 to 5 and text.

occurred to the northwest. Lesser units are ocean-island basalt (Pickereel Narrows amphibolite) and prominent OIB-related ultramafic rocks. The volcanic rocks are intruded by diabase sills and underlain by gabbro. They contain thin pelagic sediments near the top in a partial supra-subduction-zone ophiolite with contributions from a mantle plume (Section 4.4.4). Younger, mostly immature sediments formed a structural base, and the Sickie group of mainly nonmarine sediments lies unconformably on top. The volcanic succession, which extends west to the southwest end of the Lynn Lake belt, is part of the generally ca. 1.9 Ga Wasekwan collage/group (Zwanzig et al., 1999a) and correlated with the Levesque Bay assemblage in Saskatchewan, also dated as ca. 1.9 Ga (Section 2.2). It may also correlate with amphibolite along the TNB margin, geochemically and isotopically like the Tod Lake basalt. This also has local overlying chert and iron formation and is unconformably overlain by the Sickie-like Grass River group. Nearby amphibolite (upper part of Ospwagan group?) is older than 1891 Ma intrusions (Zwanzig et al., 2003, Percival et al., 2004).

The position of remnants of an early back-arc between the La Ronge–Lynn Lake arc deposits and the Kiseynew turbidite-basin deposits, which extend to the TNB, implies an early history of subduction of an oceanic plate (Manikewan ocean) under the La Ronge, Lynn Lake and Rusty Lake belts, and leading the Hearne craton. For lack of definitive arc-volcanic rocks on the Hearne margin, early subduction is suggested to have been entirely under the La Ronge–Lynn Lake–Rusty Lake belts (Figure 1, inset). Corrigan et al. (2005, 2009) based this interpretation on the closing of a Manikewan seaway and collision of Hearne craton with the arc terranes, which occurred between 1880 and 1865 Ma. It triggered a subduction flip and the onset of the successor-arc magmatism with subduction from the KD side (Corrigan and Rayner, 2002).

A similar history of early arc and back-arc magmatism occurred in the Flin Flon domain, with early subduction directed away from the Sask craton (e.g., Ansdell et al., 1995). Arc-rift- and back-arc-basins-basalts, assemblages that formed along the Flin Flon domain margin with the KD also have a similar history of evolution with ages of rocks like those in the Wuskwatim–Granville lakes corridor (Figure 30a–d). The record of arc and back-arc magmatism started by 1904 Ma in the central Flin Flon domain (Manitoba Geological Survey, 2018) and earlier in its southwest and, according to the detrital and igneous zircon records (Corrigan et al., 2009) also earlier in the La Ronge belt. In the latter part of the early arc development, arc rifting became prominent (Syme et al., 1999). Some back-arc/intra-arc basins closed during an early amalgamation of arc segments to form the Amisk and Wasekwan collages. Following the oceanic-arc assembly was the change to successor-arc magmatism about 1.87–1.88 Ga in the Flin Flon domain (Lucas et al., 1996) and Lynn Lake belt (Figure 30). The successor-arc magmatism, mainly preserved as plutons intruding the early arc deposits, started ca. 1876 Ma in the south (Whalen and Hunt, 1994) as well as about 1870–1876 Ma in the north.

Remapping along the Wuskwatim–Granville Lakes transect has favoured the interpretation of early back-arc-basin-volcanic rocks present in the Granville complex, originally lying distant from the Hearne craton, between the La Ronge–Lynn Lake belts and the Superior craton. This paleogeography resulted from the subduction of the Manikewan-ocean slab leading a Hearne-craton plate (Corrigan et al., 2005, 2009) to form a sizable back-arc sea (Neomanikewan ocean, Figure 31a) behind the arc(s). The tectonic model is supported by the presence of the Leveque Bay–Granville Lake suture, along which the slab of the back-arc sea was subducted to produce the abundant successor-arc magmatism to its northwest (Figure 31b). Zwanzig and Bailes (2010) first proposed that the early arc terrane formed a single belt that extended southwest (present coordinates) not only along the Lynn Lake–La Ronge belts but onward to include the Flin Flon–Glennie complex, continuing past Snow Lake. This conclusion was based on the remarkably similar tectonic history of these areas and evidence of oroclinal bending and crustal scale overturning with the emplacement of multiple nappes during collision tectonics (Zwanzig, 1999; Zwanzig and Bailes, 2010). Kiseynew-wide nappe tectonics during the convergence of the surrounding cratons is consistent with the interleaving, in the northeast, of the juvenile Burntwood group with Archean basement gneiss and its cover of the Wuskwatim Lake sequence. The great lateral extent of the back-arc volcanic rocks and the presence of the Wuskwatim Lake sequence have economic significance (Section 8).

## 7.2 Successor-arc magmatism

The results of the geological work along the Kiseynew north flank is consistent with the interpretation that the Levesque Bay–Granville Lake suture zone was active during the ~1870–1830 Ma successor-arc magmatism to its northwest (Section 3.2.2; Figure 31b). The disrupted units in rocks dated as ca. 1874 Ma in the sedimentary panel that forms the southern belt of the Granville complex (Section 6.1.2) suggest deposition at a steep marine margin. This environment is interpreted as the inner slope of a trench because it overlies the suture dipping toward domains with abundant successor-arc magmatism during and after 1874 Ma. The whole structural zone with an apparent megafault (Burntwood megathrust) at the base of the Granville complex, and with the fold-thrust stack in the Burntwood group to the south, is considered to have formed above and in front of the subduction zone. This extended 200 km into Saskatchewan and an equal distance east to the TNB. It may have stretched onward to northern Quebec and Baffin Island (Corrigan et al., 2009).

The common early arcuate paleogeography of the internides of the W-THO (Manitoba–Saskatchewan) also includes the La Ronge belt as proposed by Zwanzig and Bailes (2010) and the Southern Indian domain (Martins et al., 2019) as summarized in Table 5. Zwanzig and Bailes (2010) suggested that the new subduction zone was established having a Neomanikewan slab of the back-arc seaway subducting under the

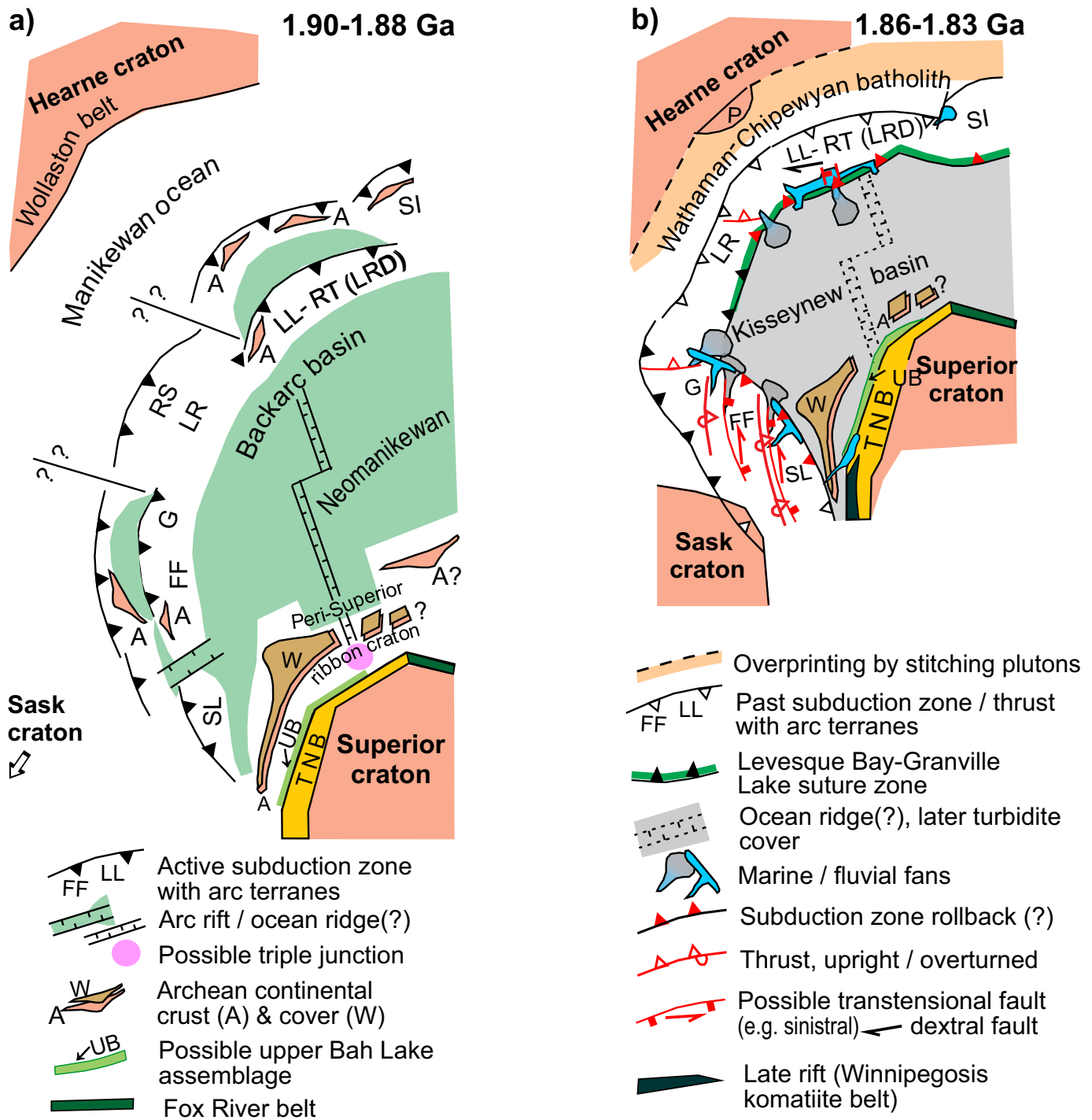


**Figure 31:** Scale-free tectonic model of W-THO internides and surrounding Archean cratons, Manitoba and Saskatchewan, from 1890 to 1830 Ma, shows selected stages of paleogeographic evolution in which all greenstone belts were part of a single volcanic arc or a number of contiguous arcs. **a)** Early subduction polarity in the La Ronge–Leaf Rapids (Lynn Lake–Rusty Lake, LRD) arc– and back–arc–basin domains is after Corrigan et al. (2005); the early evolution of a large back-arc sea is after Zwanzig and Bailes (2010) and this report. **b)** The ca. 1.87–1.88 Ga subduction flip is inferred to be in response to collision with the Hearne craton, causing the termination of early arc magmatism and the subsequent onset of 1865–1830 Ma successor-arc magmatism toward the La Ronge–LRD and forming the arc–craton–stitching Wathaman–Chipewyan batholith domains. Late successor-arc magmatism (1.85–1.83 Ga) was by continued subduction away from the TNB, producing arc-volcanic and -plutonic rocks from Snow Lake to the LRD. Abundant sediments (Burntwood, Sickle, Missi and related groups) covered the floor of the Neomanikewan ocean at the onset of continental collision. Subduction rollback and slab-failure probably caused KD closure. Abbreviations: A, Archean; FF, Central Flin Flon domain; G, Glennie domain; LL, Lynn Lake belt; LRD, Leaf Rapids domain; LR, La Ronge belt; P, Peter Lake, RS, Rottenstone domains; RT, Rusty Lake belt; SI, Southern Indian domain; SL, Snow Lake belt; TNB, Thompson nickel belt; UB, Upper Bah Lake assemblage?; W, Wuskwatim Lake sequence. The figure is modified from Zwanzig and Bailes (2010).

Flin Flon–Glennie complex as well as under the La Ronge-to-Rusty Lake belts and onward under the Rottenstone–Southern Indian and Wathaman–Chipewyan domains. This would have required a more open arcuate volcanic terrane than the present geography suggests (Figure 31). The continuous subduction zone in front was over 2000 km long (Corrigan et al., 2009) and preserved in Saskatchewan and Manitoba as the Levesque Bay–Granville Lake suture zone.

The collision of the Hearne craton with the La Ronge–Lynn Lake–Rusty Lake belts and the consequent subduction flip documented in the north, leading to the successor-arc magmatism, may have started two-sided subduction under components of the present Flin Flon–Glennie complex, which formed abundant plutons in the range of ages between 1876 and 1855 Ma (Figure 30d). This is also the main range of detrital-zircon ages in the Burntwood group on the north and east margins of the Flin Flon domain (Figure 14 in Zwanzig and Bailes, 2010). The low-SiO<sub>2</sub> igneous rocks, there, plot into the “Arc” domain in Nb/Y space, except the 1860 Ma Archie Lake tonalite, which may be a slab melt (adakite) and/or related to slab failure (Figure 15f). Subduction rollback during advanced stages of arc magmatism in the north and south may have started closure of the KD (Figure 31b). Three fault-bounded belts of Burntwood group turbidite extend across the Flin Flon–Glennie complex in Manitoba (Figure 1). Each separate disparate assemblages of arc, arc-rift, back-arc and successor-arc rocks. These belts indicate that the final amalgamation of the complex did not occur until after ca. 1.84 Ga. The presence of ~1835 Ma “stitching” plutons of sanukitoid to alkaline composition (Section 2.1) across the KD–TNB boundary indicates that such early terminal collision involved all components of the W-THO.

Seismic profiles show the present crustal structure after terminal continental collision. At the Flin Flon-belt–KD margins (Line 7a, b, Lucas et al., 1996; Clowes and Roy, 2020) between 5 and 10 km depths, and extending to ~16 km depth in the central Flin Flon domain, reflectors are similar to those in the stack of metasediments and granite in the KD but with a southerly apparent dip. This may be interpreted as the presence of an accretionary prism that had collected above a slab subducted under the Flin Flon domain from the side of the KD. The presence of Burntwood group at depth below the eastern part of the Flin Flon domain is evident in the side walls dragged up by the <1830 Ma Barron Lake pluton, and by greywacke migmatite in the core of the Reed Lake pluton/complex (Bailes, 1980a). Reflectors with an apparent dip to the north, above a detachment at 5 km depth are consistent with a history of structural inversion during advancing continental collision as proposed by Zwanzig and Bailes (2010). Surface mapping plus seismic reflectors indicate that rocks of the KD underlie and overlie a wedge of rocks continuous into the Flin Flon domain. The geometry of the reflectors are explained by the large-scale structural inversion observed at surface (Zwanzig, 1999) as well as the presence of the most distal sedimentary facies closest to the Flin Flon domain (Zwanzig and Bailes, 2010). The nappe

tectonics and crustal architecture are remarkably similar to those of the Wuskwatim–Granville lakes corridor but with the structural inversion toward the south (in present coordinates).

The sharp planar upper boundary of the highly reflective slab in the lower crust below the Wuskwatim–Granville lakes corridor (Figure 22d) is interpreted as a deep detachment at the top of the structural basement of the KD. This extends south under the Flin Flon domain (Clowes and Roy, 2020). The apparent detachment presently rises from a depth of 35 km under the Lynn Lake belt to 13 km under the southern exposure of the Flin Flon domain. The nature of the lower-crustal slab is proposed as arc-derived orthogneiss (Lucas et al., 1996) and has been used to model a collision between the Flin Flon and Lynn Lake belts. However, negative  $\epsilon_{Nd}$  values of some late (postcollisional) granite–quartz diorite indicate the presence of Archean rocks at depth. The origin of the unexposed reflective slab is therefore uncertain, and the detachment may be late and extensional (Zwanzig and Bailes (2010). It cast doubt on a direct collision between the Flin Flon and Leaf Rapids domains, particularly because the early KD basement (back-arc slab) was apparently subducted under the Flin Flon–Glennie complex during successor arc magmatism and sediment filling of the KD. Regardless of kinematic history and the origin of the lower crust, the entire upper crust from Flin Flon to Lynn Lake is interpreted as allochthonous, comprising nappes.

The Hearne–Lynn Lake belt collision was linked in time with the Ni-hosting ca. 1871 ±2 and 1870 ±6 Ma ultramafic–felsic Lynn Lake gabbro and the coeval granitoid Pool Lake intrusions (Figure 30c, d; Manitoba Geological Survey, 2018; Zwanzig et al., 1985). Similarly, the onset of late successor-arc magmatism south of the exposed part of the Flin Flon domain is linked in time to the 1847 ±6 Ma, Ni-hosting Namew Lake complex of mafic–ultramafic rocks under the Phanerozoic cover (Cumming and Krstić, 1991). Both appearances of mafic–ultramafic magma require high-percentage melting of the mantle such as can be provided by slab-breakoff or -tearing to allow hotter mantle to replace the sinking slab during arc-craton collision. In our model the process would be part of a rearrangement of the subducting plates. Volcanic and intrusive rocks of ≤1850 Ma successor-arc magmatism are concentrated along the north and east margins of the Flin Flon–Glennie complex with Missi-age plutons extending mostly across the Snow Lake end. This arrangement is interpreted to indicate a change in the relative direction of subduction of the Neomanikewan slab more under the Snow Lake segment of the complex, toward the Sask craton. Motion is interpreted to have become mainly dextral within the LRD, with less magmatism and its retreat to the KD boundary. Both north and south segments of contiguous subduction zones probably experienced slab rollback to account for extensional block faulting and basinal sedimentation (Figure 21b).

Niobium/yttrium plots of plutons on the Flin Flon domain north margin and in the Lynn Lake belt with middle and late successor-arc ages suggest that possible slab failure in the

W-THO occurred several times (Section 4.3.2), probably due to involvement of young oceanic lithosphere and high Paleoproterozoic mantle temperature. The change to late successor-arc magmatism involved the collision of Sask craton and the Glennie complex. This had occurred by 1845 Ma according to kinematic indicators and a dated dike (Ashton et al., 2005). The high-Nb/Y intrusions may indicate slab failure (Figure 15f). High-La/Yb rhyolite and intrusions of trondhjemite and granite (Figure 15e) occur on the outer margins of the volcanic terranes adjoining the KD in the north and south. These high-SiO<sub>2</sub> melts with deep Nb and Ti troughs on primitive-mantle-normalized plots (Figure 15e) may also indicate slab failure. Their multi-element plots mimic those of the FLPS (Figure 15c). Slab failure must have occurred near the KD margins of both northern and southern volcanic terranes. Such an event during Sask collision is interpreted to have triggered the uplift and erosion of the sediment source for the Missi, Grass River, and western equivalent groups (Figure 31b). These and the Sickle group developed in continental intra-arc- and forearc-basin-environments such as described by Pavlis et al. (2019).

### **7.3 *Syncollisional sedimentation: Partridge Breast, Granville complex (southern belt), Burntwood, Missi, Grass River, Sickle groups***

The onset of abundant immature clastic sedimentation appears to have signalled the collisions with the cratons surrounding the internides of the W-THO along with changes in the subduction geometry. In the Southern Indian domain immature sediments (e.g., Partridge Breast Lake greywacke) were deposited early and with major Neoproterozoic-age peaks (Figures 18h, 19a, 30b, g; Martins et al., 2019), as were continental sediments (Figure 30b, f). The former covered a period of forearc and syncollisional marine sedimentation leading to and during the ca. 1880–1870 Ma collision with the Hearne craton. These sediments are preserved in the Rottenstone and Southern Indian domains.

An approximate age of deposition of 1874 for the felsic volcanogenic unit at Granville Lake (Corrigan and Rayner, pers. comm., 2008) supported by a minimum age of 1867 ±3 Ma (Corrigan et al., 2001) of the deposition of correlative rocks in Saskatchewan lies in the range of the 1880–1870 Ma collision between Hearne craton and the THO internides. The ~1874 Ma sediments were deposited in the southern belt of the Granville complex, and very similar, likely correlative rocks (Fox Road turbidite; Gilbert et al., 1980) in the Lynn Lake belt. Likewise coarse-grained proximal turbidite was deposited or thrust into the KD at Kamuchawie Lake (Zwanzig and Wielezyski, 1975). Erosion caused by uplift of the arc after collision and slab break-off and/or slab rollback would have provided the ca. 1874 Ma sediments. This early sedimentation was followed by <1865 Ma, postcollisional, continental sedimentation in the Southern Indian domain, with the same peaks of detrital-zircon ages and same arc provenance as the Burntwood and Sickle groups to the south (Figure 30e, f).

About 1850 to 1830 Ma was the main sedimentation in the successor arc and marginal basins, interpreted to mark continental collision with Sask craton in the southwest during continuing arc magmatism. Comparing probability plots and overlaid frequency plots of the detrital zircons of the Burntwood and Sickle groups and the continental sediments in the Southern Indian domain provides insight into the regional tectonics and the age distribution of the source terranes. The detrital zircons of the post-1850 Ma sediments represent sources from the nearby arc-back-arc terrane. Most detrital ages fall between 1890 and 1830 Ma (Figure 21a) and correspond to the age range of early-arc to late successor-arc magmatism (Figure 30). Peak ages of the detrital-zircon distribution for the Burntwood and Sickle groups are only 15 m.y. apart at Lynn, Granville, Wheatcroft and Setting lakes. The peaks all range from 1870 to 1845 Ma (Figure 21a). Mainly granitoid rocks yielding those ages must have been exposed in local uplifts and provided abundant, relatively large zircon grains amenable to dating. A small peak at 1915 Ma may represent the earliest local arc magmatism (Figure 21b). The minor peaks between ca. 2.3 and 2.6 Ga suggests a presence and uplift of the Hearne craton margin or similar rocks available for erosion. These peaks are most prominent in young northern units. A minor frequency peak at ca. 1833 Ma provides a possible local maximum age of deposition in the Sickle group near Lynn Lake. Deposition and/or exposure of source rocks apparently diminished considerably about 1845–1830 Ma (Figure 21b, c). Analyses giving a minor age-peak of 1800 Ma from a sample from Granville Lake are metamorphic (Figure 21c).

Because the depositional ages of megaunit Gs and the Burntwood and Sickle groups are important in dating the times of uplift and high sediment flux during collision of arc segments with cratons as well as during terminal continental collision, the maximum and probable depositional ages of the successions are crucial in helping to establish the tectonic history of the W-THO. Cawood et al. (2012) have matched igneous- and detrital-zircon ages from numerous studies in various tectonic settings and determined that, where synsedimentary magmatic activity occurs, the youngest group of detrital-zircon grains may approximate the time of sediment accumulation. Herriott et al. (2019) have made a comparison with LA-MC-ICPMS and chemical abrasion-thermal ionization mass spectrometry detrital-zircon ages of Jurassic forearc strata in Alaska. The precision TIMS maximum depositional ages of sets of the youngest detrital zircons are only 1–4 ±1 m.y. younger than the peak laser-ablation ages of Dickinson and Gehrels (2009) of six members of the Alaskan forearc succession. These TIMS ages are also 5–10 m.y. older than the youngest single grains dated by laser-ablation and warrant caution in using such ages. The similar environment of megaunit Gs, the Burntwood and Sickle groups (i.e., trench and forearc deposits), is consistent with erosion and deposition during arc magmatism, and therefore relevant to ages of sedimentation and its tectonic cause.

Part of a massive database of zircon ages from global orogens active between 1.9 and 1.7 Ga (Trans-Hudson–New Quebec orogens in Laurentia, and belts in Siberia and Congo with four lesser belts, all involving the early assembly of supercontinent Nuna; Condie and Puetz, 2019) provides some confirmation for the smaller datasets in Manitoba. The global belts feature elevated igneous- and detrital-zircon ages between 1900 and 1825 Ma with an igneous peak at 1862 Ma and a detrital peak at 1865 Ma (Figure 30). A peak age for large igneous provinces (LIP–plumes) lies at 1880 Ma. Smaller peaks of younger ages of igneous and detrital zircons range from 1780 to 1760 Ma. In this database of Condie and Puetz (2019), the THO is the largest orogen and our Manitoba data fit well into the global data. A match between respective global peak ages and those of an apparently widespread LIP, the range of detrital ages in the KD, peak ages of successor-arc granitoid magmatism in the surrounding domains, and the age of late deformation lend credence to our limited age data for the timing of these events.

Deposition of the upper part of the Burntwood group and of the Sickie group at Granville Lake is suggested as 1845–1830 Ma by the steepest part on the young side of the detrital-zircon–age distribution curve (Figure 21). This was related to the rapidly diminishing age of the sediment supply at that time, and with the above suggested 2–5 m.y. error range. The age of 1830 Ma of enderbite intruding the Burntwood group and older rocks (Gordon et al., 1990; Ashton et al., 1999), and the similar inferred age of Blacktrout diorite sills intruding the Sickie group is the minimum age of preserved sediment deposition in the W-THO. This was probably the start of inversion of the KD due to the thrusting within, its contraction during ongoing collision and mantle dynamics below. The lack of preserved sediments deposited from 1850–1829 Ma detritus in the Southern Indian domain (Figure 30b) suggests uplift and erosion there, providing sediments to the LRD and KD. This corresponds to the suggested age of ca. 1843 Ma for the  $D_2$  deformation at Southern Indian Lake (Kremer et al., 2009). Latest orogenic (continental back-arc?) sedimentation (1832–1829 Ma Whyne Bay assemblage of Martins et al., 2019) terminated along with the Sickie group sedimentation. The full dataset from the tectonic domains, including the Flin Flon domain as compiled by Zwanzig and Bailes (2010), supports the concept of a single early arc that segmented, re-amalgamated and had a reversal in subduction polarity. Arc segments are interpreted to have rotated independently and converged toward the shrinking KD during late arc-magmatism and continental collision (Figure 31 and see Figure 44 in Zwanzig and Bailes, 2010).

#### 7.4 *Syncollisional periods of deformation*

Like sedimentation and the formation of basins, the various stages of deformation in the W-THO progressed inward from the cratons to the arc terranes and into the KD. All components including the arc segments are interpreted to have

been mobile and converged toward the KD and so determined the direction of thrusting and fold vergence. This included the ca. 1886 Ma recumbent folding in the Flin Flon domain (Zwanzig and Bailes, 2010) and the progression of local  $D_1$  from the Southern Indian domain (Martins et al., 2019), >1870 Ma deformation, before Pool Lake granitoid intrusion in the Lynn Lake belt (Beaumont-Smith and Böhm, 2002) to the post-Burntwood  $D_1$ – $D_2$  in the KD. The low-angle unconformities of the Sickie group on the Granville complex, and of the Missi group on the back-arc volcanics on the north margin of the Flin Flon domain (Zwanzig and Bailes, 2010) indicate that only tilting and/or in-sequence, thin-skin thrusting reached the back-arc volcanics that formed the basement of the KD before deposition of the Sickie and Missi groups.

The early deformation ( $D_1$ ) along the Wuskwatim–Granville lakes corridor, as seen south of Granville Lake, involved folding and thrusting of the Burntwood group. Apparently, this occurred ca. 1845–1830 Ma, during latest successor-arc magmatism before full lithification and final sedimentation (Section 5.1.5). The Burntwood turbidite sequence was overthrust by the Granville complex from the northwest, all along the Levesque Bay–Granville Lake suture zone, with the proposed Burntwood megathrust at the sole of the complex—the base of the Russell nappe. To the north, in the Southern Indian domain,  $D_2$  deformation, also on a northeast trend, is reported to have occurred ca. 1843 Ma (Kremer et al., 2009). Orogenic uplift, basin inversion and erosion in the Southern Indian domain probably took place during the local detrital-zircon–age gap between 1850 and 1830 Ma (Figure 30b). In the Lynn Lake belt the onset of upright folding and dextral transposition (also  $D_2$  there) is estimated as ca. 1835 Ma (Table 4; Beaumont-Smith and Böhm, 2002). Apparently,  $D_2$  in the northwest fell into the same age range as  $D_1$  in the KD. At Lynn Lake, east-west dextral shearing is consistent with the south-east shortening in the KD. This stage may have included clockwise rotation of the Lynn Lake belt at an oroclinal hinge to the west and so impinging on the KD. The widespread  $D_1$ – $D_2$  orogenic period in the internides of the W-THO may have been the result of continued underthrusting of the Sask craton below the Flin Flon–Glennie complex, underway by 1845 Ma (Ashton et al., 2005) and under the KD with the Hearne craton as backstop. A strong increase in the volume of late successor-arc magmatism from La Ronge toward Snow Lake and Wekusko Lake suggests that, in the south, the area of subducted Neomanikewan slab increased from west to east. This may have been brought about by counterclockwise rotation of the Flin Flon–Glennie complex with sinistral shear zones on the north margin and a dextral shear zone on the south margin of the Flin Flon domain (Zwanzig and Bailes, 2010). The Euler pole of rotation would have lain at the junction of the Flin Flon–Glennie complex and the La Ronge belt, where the Missi-age volcanism ended. The bend from the north trend to the west trend along the north margin of the Flin Flon domain margin has been attributed to oroclinal bending by Zwanzig and Bailes

(2010). An inward rotation of the volcanic belts under extension is consistent with the development of the Sickle and Missi intra-arc and forearc basins (Figure 31).

The rotational partial closing of the KD and the multiple stages of nappe emplacement are accredited to convergence and subsequent collisions with the Hearne, Sask and Superior cratons along with their amalgamation of fringing arc domains. The largely juvenile arc units and derived sedimentary rocks extend 200 km over the Sask craton (Lewry et al., 1994). They were overthrust from the north and west. This stack of megaunits was mapped in Saskatchewan (Lewry et al., 1990) as four sheets (nappes), from the top down:

- i) La Ronge belt metavolcanic and intrusive rocks
- ii) Sickle and Burntwood groups
- iii) gneissic intrusions with lesser supracrustal rocks
- iv) gneissic intrusions

The stack of megaunits lie above thick mylonite gneiss forming the roof of the Sask craton. The crustal architecture (Lewry et al., 1994), and the kinematic indicators in the mylonite gneiss are consistent with southerly verging nappe-tectonics in the KD (Ashton et al., 2005). This includes the KD north flank, where transport with a southerly component was later reversed and then restored. Unfolding the  $F_{2a}$  backfold in the Russell nappe (Section 6.1.2) indicates up to 100 km southeast thrusting of the Granville complex and its Sickle group cover into the Kiskeynew basin. Notably, unfolding the  $F_{2b}$  nappe moves the overturned, lower contact of the Sickle group lying stratigraphically on the Burntwood group, to the south of the Russell Lake structure, most distal and farthest into the KD. Thus, the facies changes in the lower Sickle group to more distal can be restored to the southeast. Northeast-trending, northwest-dipping isoclinal cores in the Sickle group occur northeast of Russell Lake, and a culmination to the south occurs at McKnight Lake (Figure 1). These have a unique basal unit of magnetite-bearing pelitic gneiss rich in cordierite, and grading up into pyrite-bearing garnetiferous meta-arenite (metagreywacke of Lenton, 1981). Unfolding the  $F_{2a}$  backfold affecting the Russell nappe restores this deeper-basin deposit farther into the KD. Similarly-inverted nappes with upward- and downward-younging Burntwood and Missi group successions were also restored from proximal to distal facies by unfolding multiple nappes at the KD south flank (Zwanzig and Bailes, 2010). The seismic profiles in Lewry et al. (1994) show reflectors dipping away from the northward-concave margin of the Sask craton under its Paleoproterozoic allochthons. The overall vergence of the nappes, including the volcanic terranes, is toward the culmination of the structurally buried Sask craton. Consequently, the Sask craton is a key element in the crustal architecture and history of the W-THO. The Levesque Bay–Granville Lake suture zone is the root zone of the  $F_1$  and  $F_{2b}$  nappes, and, with the Sask craton, determined the final crustal architecture and overall southwest vergence in Manitoba.

In conclusion, the changes in the directions of fold-and-thrust vergence (tectonic transport direction) are interpreted to mark major phases of deformation or progressive deformation in different thermotectonic environments, including structural level. These phases required changes in the structural slope in surface topography driven by belts of crustal thickening and uplift. Apparently, deformation and sedimentation shifted from upper to lower plates during collision and the continued convergence of Hearne craton with the THO internides—from the Rottenstone–Southern Indian domains to the LRD and onward to the KD. The latter domain experienced uplift and inversion leading to diverging tectonic transport during high-grade metamorphism. The return of southerly transport is thought to be the result of mantle dynamics that caused uplift and/or traction. This may have been the result of lithospheric-mantle delamination and slab breakoff or flat-slab rollback (e.g., Kusky et al., 2014). The late  $D_2$  southwest vergence is thought to be a result of the LRD, driven by mantle forces from the north, to overthrusting the margin of Superior craton and thickened the KD crust. Closure with disappearance of the KD-ocean floor is interpreted to have involved crustal-scale rotations, clockwise in the north and counter-clockwise in the south, leaving oroclines at the bends in the orogen in Saskatchewan. Remnants of this ophiolite are preserved in the Leveque Bay–Granville Lake suture zone. The return to north-west compression during  $D_3$  produced the northeast-trending structures and must have produced the crustal bulge near the TNB in a narrow fan structure with a westward reversal in dip from steeply northwest to southeast. This would have exposed the highest-grade metamorphic rocks and deepest crustal units, much of the FLPS and related granites with Archean Nd-model ages. The  $D_3$ – $D_4$  structures, which formed about 20 m.y. after the end of  $D_2$ , were probably due to far-field forces during the onset of the Yavapai orogeny southwest of the Superior craton (Table 5; Whitmeyer and Karlstrom, 2007).

## 8. Economic considerations

Previous geological work in the KD along the north flank did not establish the extent of the Granville complex containing mafic volcanic rock with gold potential. Most of the widespread thin amphibolite unit was considered to have a sedimentary rather than volcanic origin. Neither was the Wuskwatim Lake sequence recognized or explored for its nickel potential. Hydrothermal alteration on the LRD margin and its Kiskeynew inliers was not associated with arc magmatism nor explored for base-metal potential. The entire KD, particularly the north flank and Northeast Kiskeynew subdomain, is underexplored and most of the area is currently available for staking.

Trace-showings of gold and sedimentary copper on the north flank of the KD are shown in Figure 17. A possible nickel potential is in the occurrence of the Wuskwatim Lake sequence. An important inference of the proposed related tectonic history of all the volcanoplutonic belts surrounding the KD is the potential for new discoveries of base- and pre-

cious-metal deposits in hitherto unmined areas but that host a paleotectonic environment similar to that in areas with past discoveries. Particular types of deposits are restricted to particular tectonic environments. It is therefore suggested that the tectonic environments mapped out in this and previous MGS reports can serve to focus exploration to areas of manageable size and complexity.

### **8.1 Historical mineral exploration**

Historical, systematic mineral-exploration work along the north flank of the KD began in 1960–1966 with targeted airborne electromagnetic surveys by Canadian Nickel Co. Ltd and included geological mapping at Granville Lake by Barry (1965), and Barry and Gait (1966). Work by the MGS during the Burntwood Project (in the north by Frohlinger, 1971; Kendrick et al., 1979; Campbell, 1972) resulted with the publication of the first complete set of maps of the KD (Baldwin et al., 1979). A history of exploration was included in McRitchie et al., 1979. Open assessment files from the 1930s to the 1990s, however, indicate several nickel, copper, lead, zinc, silver and gold occurrences, as well as sulphide showings and gossans along the north flank. Airborne surveys were commissioned by the department of Manitoba Mines and Natural Resources in 1968, and the department of Manitoba Mineral Resources conducted ground horizontal loop electromagnetic and magnetic surveys and diamond drilling. Early MGS reports concentrated mostly on mapping in the Leaf Rapids and Southern Indian domains but extended into the KD north flank to Notigi and Osik lakes (Elphick, 1972; Schledewitz, 1972). Areas of economic interest were documented in Mineral Deposit Series reports (Ferreira, 1993a, b; Ferreira and Baldwin, 1997).

### **8.2 Kiseynew domain north flank**

The main mineral potential in the Kiseynew north flank includes gold in the Granville Lake complex. Malachite staining occurs in the Sickie group, north of Timew Island, on Notigi Lake (Murphy and Zwanzig, 2019a), and stratiform copper mineralization had been documented at Kadeniuk Lake (Baldwin, 1980), suggesting some potential for this type of deposit in the Sickie group.

#### **8.2.1 Granville complex: gold**

A historical gold showing (Figure 17; Barry, 1965; Richardson et al., 1996) is hosted by or lies directly north of sulphide-facies iron formation at the top of a narrow belt of amphibolite (Gt, Gtb) herein assigned to the Granville complex on the north shore of Wheatcroft Lake (UTM 6230425N, 393450E), south of Granville Lake. Another gold showing, the Caimito occurrence, described as a quartz-vein type (Location 25 in Ferreira, 1993a), is in the Granville complex, near its type area on Laurie Lake (UTM 6274222N, 324581E). It lies at a small fault near the contact between the Sickie group and amphibolite with sediment layers including chert (Tod Lake basalt and pelagic cover).

In the Wuskwatim–Granville lakes corridor, however, the Granville complex requires additional exploration for gold. The rocks of the Granville complex can be traced by the magnetic signature associated with iron formation (Gi). The associated published maps (Murphy and Zwanzig, 2019a–c; Zwanzig, 2019; Zwanzig et al., 2019) which show these units, as well as the previously recorded stratabound sulphide showings and gossans, can serve as a first-order exploration guide. Work on the Reykjanes ridge in proximity to the Icelandic plume has shown gold enrichment in plume-enriched oceanic crust (Webber et al., 2013). These authors suggested that Atlantic MORB with its deep mantle component and elevated trace enrichments can act as a primary source of gold, with up to 13 times normal concentration (median value of 0.34 ppb Au) to potentially develop gold deposits by secondary concentration during orogeny. The plume-enriched mafic–ultramafic megacrysts (Gt, Gu) in the Granville complex are locally arsenic enriched. The high-Mg amphibolite (Gu) derived from OIB-like rocks may be a primary source for further concentration of gold during fluid flux in fault zones. Splay faults to the Burntwood megathrust are a possible exploration target. Most basaltic samples have up to 5 ppm As. Eight out of 16 samples with high Mg or altered samples with elevated Cr, a proxy for MgO, have As contents of 70–2000 ppm, considered to be due to alteration. Unit Gu ultramafic fragmental rocks on the south side of Granville Lake are also highly enriched in As (820–1990 ppm). The only sampled normal-Mg basalt with elevated As lies on strike with the Wheatcroft Lake gold occurrence, 2.4 km to its east. Although slightly elevated in MgO (7–10%), Cr is high (430–850 ppm) in three samples from Wheatcroft Lake, suggesting alteration. Unit Gu ultramafic fragmental rocks apparently formed an As anomaly with local flakes of gold in till extending south across the KD (Kaszycki et al., 1988). The common association of Au with As, coupled with the Au showing, suggests that the Granville complex may be an interesting exploration target with a potential for a gold metalotect more than 200 km long.

From Lasthope Lake down its north-south arm, the eastern Sickie sub-basin (Figure 5b) has been interpreted as bounded by syndepositional faults (Section 3.2.6) covered by conglomerate wedges, intruded by Blacktrout diorite (Lqd; Section 3.2.7.3) and locally reactivated in younger faults. Before  $D_1$  thrusting, the diorite must have had access to deep mantle. Particularly, any shear zones associated with unit Lqd and the base of the Sickie group may be further exploration targets. Blacktrout diorite is currently under being explored for gold (Joshua Bailey, Exiro Minerals, pers. comm., 2019).

### **8.3 Northeast Kiseynew subdomain**

#### **8.3.1 Wuskwatim Lake sequence: nickel**

The stratigraphy of the Wuskwatim Lake sequence in the Northeast Kiseynew subdomain is potentially correlative to the lower part of the Ospwagan group, in the TNB, suggesting that possible magmatic nickel-sulphide deposits exist in the KD

(Figure 32a). The geochemistry (Figure 11d, f), detrital-zircon ages (Figure 32b) and  $\epsilon_{Nd}$  (Figure 12c, d) of the Wuskwatim Lake sequence are similar to those in the Ospwagan group. However, small detrital-zircon peaks between 2.25 and 2.45 Ga as well as older than 3.1 Ga occur in the Wuskwatim Lake sequence comparable to those in some Southern Indian gneiss units (Figure 32b, c). These ages are rare or absent in the zircons of the Ospwagan group. The Wuskwatim Lake sequence may have some provenance from the Hearne craton, a local exotic basement such as Sask craton, or the Assean Lake crustal complex (Figure 32c; Bohm et al., 2003). The source of Ospwagan group detritus is assumed to be entirely from the Superior craton whose margin was intruded by the Molson dikes, which are coeval with the ultramafic bodies associated with the Thompson nickel deposits. Nevertheless, there is little doubt that the Wuskwatim Lake sequence comprised early Paleoproterozoic pericontinental sediments with a 2.7 Ga detrital-zircon peak and sulphide-facies iron formation like the Ospwagan group, and that Archean basement gneiss (Ag) is very similar to the basement gneiss in the TNB (Section 5.1.1). The apparent structural truncation of the stratigraphic sequence by the Burntwood group above interlayered semipelite, pelite and iron formation is also seen in the Mel zone at the north end of the TNB (Zwanzig and Böhm, 2002). Mafic sills occur in the Wuskwatim Lake sequence (Section 3.2.1, e.g., Figure 3b), but whether these are related to the ca. 1883 Ma Molson dikes and have the associated ultramafic intrusions as in the TNB is unknown.

con peak and sulphide-facies iron formation like the Ospwagan group, and that Archean basement gneiss (Ag) is very similar to the basement gneiss in the TNB (Section 5.1.1). The apparent structural truncation of the stratigraphic sequence by the Burntwood group above interlayered semipelite, pelite and iron formation is also seen in the Mel zone at the north end of the TNB (Zwanzig and Böhm, 2002). Mafic sills occur in the Wuskwatim Lake sequence (Section 3.2.1, e.g., Figure 3b), but whether these are related to the ca. 1883 Ma Molson dikes and have the associated ultramafic intrusions as in the TNB is unknown.

### 8.3.2 Potential mineral occurrences: IOCG, REE

Although the FLPS intrusions have not been explored for iron oxide-copper-gold (IOCG) systems, they have chemical and likely tectonic affinity to intrusions associated with such systems. The characteristics of crossing the alkaline-subalka-

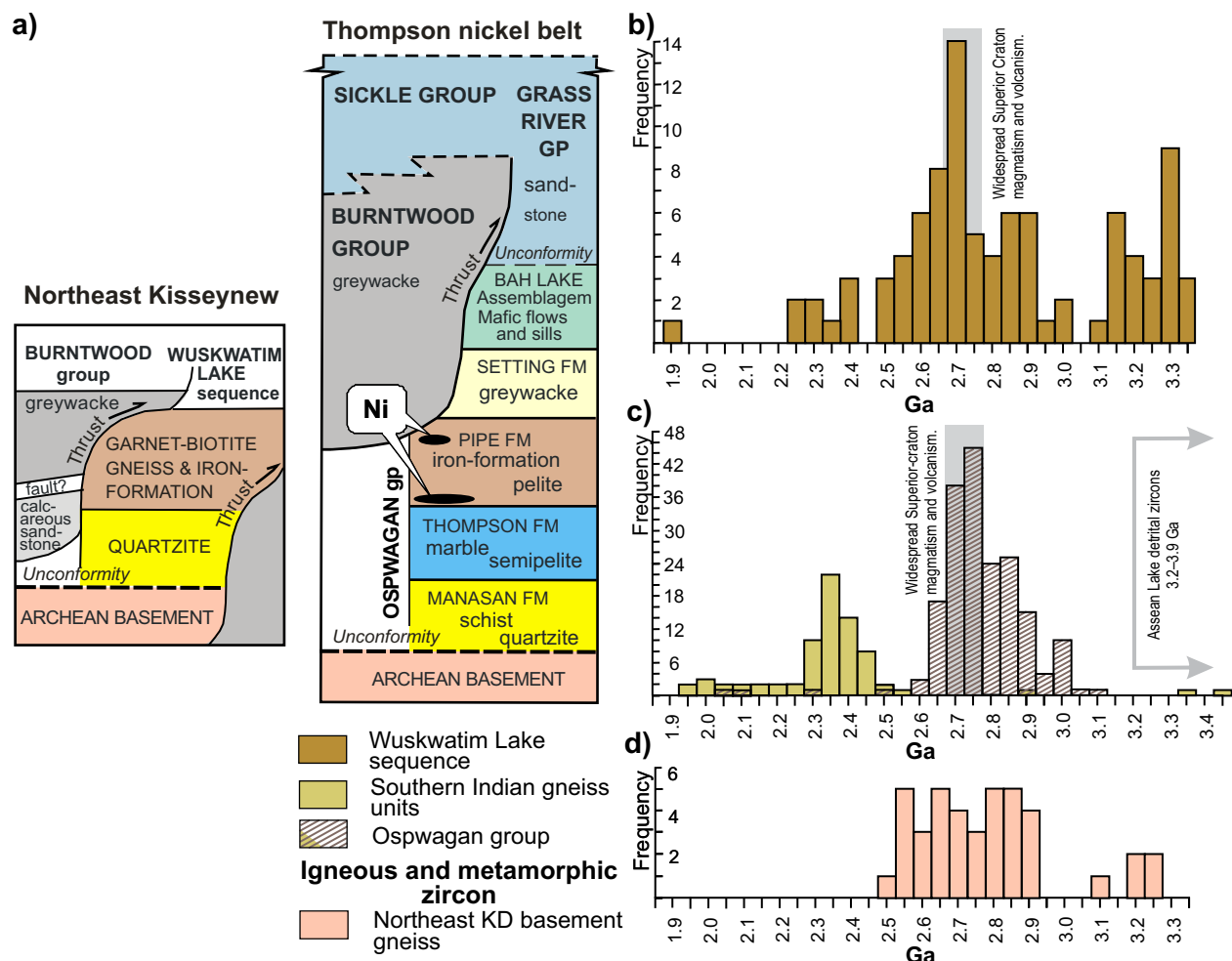


**Figure 32:** Possible correlation between the Wuskwatim Lake sequence (W) and the Ospwagan group (O): **a)** stratigraphic unit correlation (shown by the same colours). Unit thicknesses are not to scale and the thrust relationship with the Burntwood group is assumed because of truncations and widely differing origins of the groups. Internal stratigraphy of the Sickle and Grass River groups are similar but not shown. The fault truncation at the top of W is similar to a truncation in O in the northernmost TNB (e.g., Mel zone), but the absence of marble requires a facies change, probably to deeper-water pelite (garnet-biotite gneiss). Ultramafic bodies in the Pipe Formation are associated with the Thompson nickel deposits; **b-d)** U-Pb zircon-age-frequency plots comparing **b)** detrital-zircon populations of the Wuskwatim Lake sequence with **c)** detrital zircons in the Ospwagan group, and Southern Indian paragneiss; and **d)** basement gneiss of the Wuskwatim Lake sequence; with data from Böhm et al. (2007) and Martins et al. (2019). Abbreviation: FM, formation.

line boundary at similar contents of  $\text{SiO}_2$  (Figure 15a), highly fractionated REE, elevated Th and Ba and depleted Nb (Figure 15c) are comparable to the Late Cretaceous Divrigi intrusion, which hosts one of the largest iron oxide-copper (gold?) deposits in Turkey (Kuşçu et al., 2013). The Divrigi system is postcollisional and postdates continental arc magmatism by 5 m.y. If the 1890–1885 Ma calcalkaline granite–granodiorite along the TNB margin are indeed volcanic-arc–back-arc intrusions, the ca. 1880 Ma FLPS may be analogous to the Turkish intrusions. The FLPS intrusions have positive magnetic signatures (Murphy and Zwanzig, 2019d), which would facilitate exploration.

Syenite complexes throughout the central KD, such as at Burntwood and McCallum lakes (McRitchie, 1987), have potential for rare-earth element (REE) enrichments. MGS studies of metasomatized syenite intrusive complexes at Brezden Lake (Martins et al., 2012) and Burntwood Lake (Martins et al., 2011) indicate significant potential for REE enrichments, with only minimal previous exploration.

### 8.3.3 Archean basement: possible diamond potential

Archean crust in the Northeast Kiseynew subdomain is indicated by Archean inliers (Ag, Ai), their cover sequence (W), and FLPS intrusions. Evidence of underlying Archean subcontinental lithosphere, at least at 1.88 Ga, is indicated by the geochemistry and highly negative  $\epsilon_{\text{Nd}}$  values of the FLPS (Section 4.3.1; Whalen et al., 2008). The full extent of Archean crust and its sublithospheric mantle underlying the mainly juvenile Paleoproterozoic rocks in the KD is not known. It may be more widespread than the suggested boundary of the Northeast Kiseynew subdomain. If the Archean crust in the KD is not a direct part of the Superior craton (Section 8.3.1), it is likely a ribbon fragment of Sask craton, which may have become attached early in the history of the THO internal zone, before the intrusion of the ca. 1880 Ma FLPS plutons, which extend across the TNB boundary. Such an early collision puts the record of an early ( $D_1$ ) deformation in the TNB before the ca. 1885 Ma intrusion of the Molson dikes (Bleeker, 1990). The presence of tonalite gneiss on the KD east margin with a possible age of 1890 Ma would support early convergent tectonics (Section 5.1.3). Sask craton is the site of two kimberlite occurrences discovered as part of an exploration drilling program by North Arrow Minerals Inc. at the Pikoo Diamond Project in central eastern Saskatchewan.

The presence of Archean crust and possibly its thick subcontinental mantle raises the feasibility of diamond pipes in the KD. The structural culminations of the Northeast Kiseynew subdomain and widely scattered negative  $\epsilon_{\text{Nd}}$  values in volcanic and intrusive rocks in the THO internal zone in Manitoba and Saskatchewan are consistent with a diamond potential. Small but strong “bullseye” magnetic anomalies in the Lynn Lake belt (P. Lenton, pers. comm., 2016) may be considered as possible diamond pipes and warrant exploration.

## 8.4 Regional economic implications

Present and past mines and economic mineral deposits are shown in Lawley et al. (2020) and selections in Figure 33. These are restricted to the arc-, arc-rift- and back-arc–volcanic rocks, and ultramafic-bearing intrusions, all in the domains surrounding the KD.

### 8.4.1 Leaf Rapids domain

Near the southwest end of the Lynn Lake belt, south of Dunphy Lake, the extracted Fox mine volcanogenic massive sulphide (VMS) deposit occurred in arc tholeiite in fault contact with the Tod Lake (back-arc) basalt as well as Sickle group arkosic arenite. Feldspathic metagreywacke (Fox Road greywacke; Gilbert et al., 1980) with thick beds containing various types of cobbles and blocks, similar to unit Gsa in the Granville complex also appears to be in fault contact with the Fox Mine succession. The transition between E-MORB and arc-tholeiite northeast of the mine may represent a target of further exploration for VMS deposits as well as for gold. Such transitions occur at the Rainbow zone (Figure 33a) in the northern extent of the Lynn Lake belt and in the southwest part of the belt (Zwanzig et al., 1999b).

In the southwestern Rusty Lake belt (Ruttan block of Baldwin, 1981, 1988) the Ruttan VMS deposit formed in volcanoclastic rocks with intercalated basalt overlain by sedimentary mass-flow deposits and greywacke (Baldwin, 1988). The epiclastic deposits overlying flows and breccia probably represent the final stage of arc extension and intra-arc basin formation that followed the all-important synvolcanic faulting that may have focussed metal-bearing hydrothermal fluids in the clastic rocks. Consequently, careful stratigraphic mapping coupled with geochemistry should form an early stage in VMS exploration, whereas structural mapping is required for gold exploration.

Despite extensive past exploration, further work may be required at the arc- and MORB-like basalt transition in the “Northern belt” of the Lynn Lake belt (Gilbert et al., 1980; Zwanzig et al., 1999a, b). Syme et al. (1999) have shown in the Flin Flon domain that the volcanic arc deposits are the hosts to base metals, particularly associated with arc extension or rifting.

### 8.4.2 Flin Flon–Lynn Lake connection

The abundant VMS deposits (Figure 33c) in the well-explored Flin Flon domain may serve as an analogue for the other, apparently contiguous, greenstone belts in the W-THO, particularly the Lynn Lake and Rusty Lake belts (i.e., the LRD). This report interprets that the volcanic rocks in the LRD formed in similar types and ages of tectonic environments as those at Flin Flon and Snow Lake. The similar timing of the volcanism and tectonic events has led to the conclusion by Zwanzig and Bailes (2010), supported herein, that they formed in a single arc or contiguous arc segments over a single subduction zone,

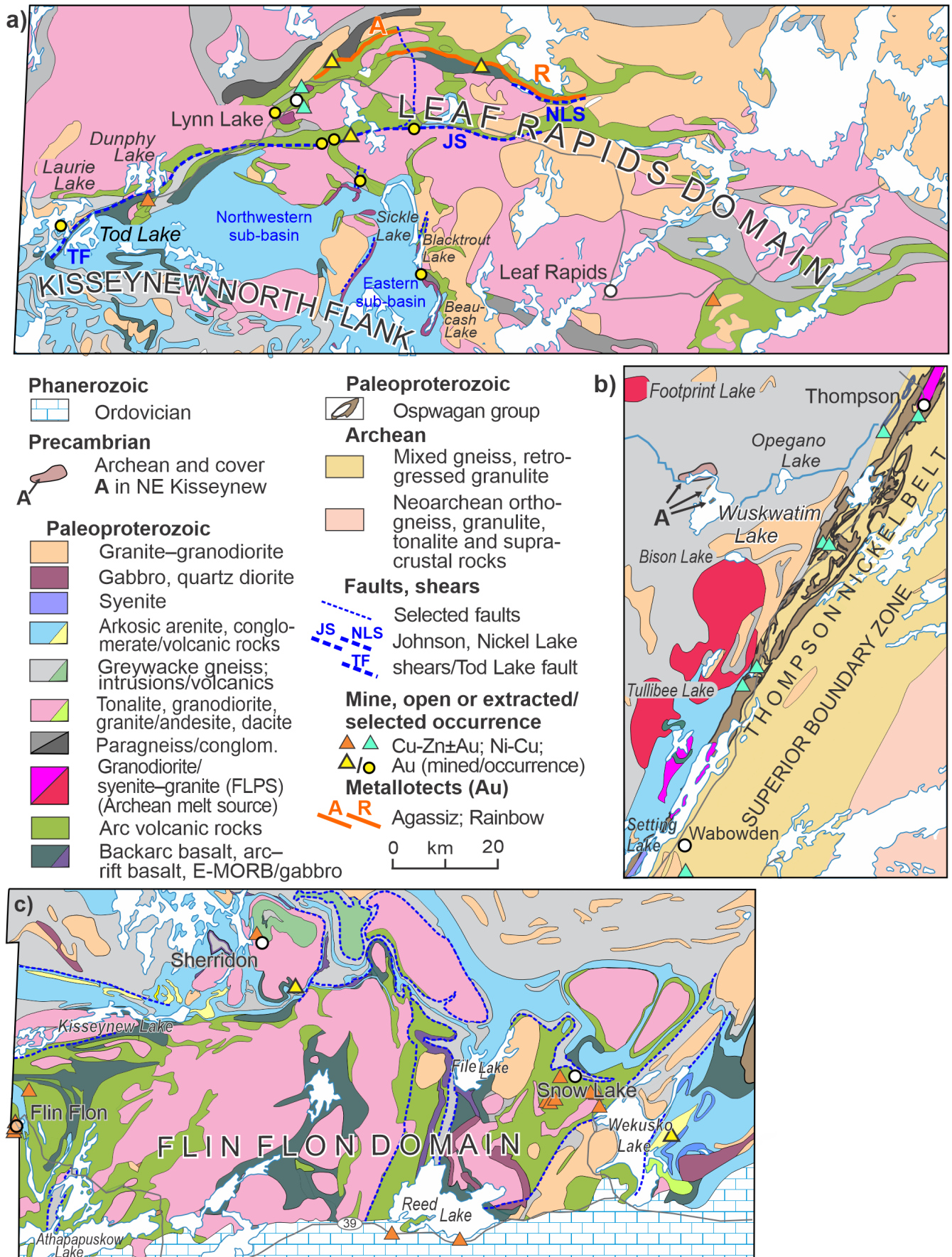


**Figure 33:** Mineral deposits in volcanic and sedimentary belts surrounding the Kisseynew domain in Manitoba: **a)** Lynn Lake and Rusty Lake belts; **b)** Thompson nickel belt; **c)** Flin Flon–Snow Lake belt. Main mineral deposits showing currently active mines and extracted deposits. Abbreviation: conglom., conglomerate.

and therefore may have a similar mineral potential. A major difference between the belts, however, is the crustal level of exposure indicated by lower metamorphic grades and fewer deep-level plutons in the Flin Flon domain compared to the La Ronge and Lynn Lake belts.

The tectonic origin of the volcanic rocks in the belts surrounding the KD can be considered important for mineral exploration. VMS deposits have been found to be restricted to arc-volcanic assemblages commonly developed during intra-arc extension (Syme et al., 1999). Many arc assemblages are in contact with arc-rift or back-arc assemblages or may extend into the latter along strike. Conversely, the several extracted gold deposits in the Lynn Lake belt, occurring in long-lived shear zones and/or near the contact between arc tholeiite and E-MORB interpreted as arc-rift basalt and their faulted margins (Figure 33a; Zwanzig et al., 1999a, b), may serve as models for further gold exploration in the Flin Flon domain and the Granville complex.

Another possible environment for further gold exploration is the apparent syndepositional fault boundary between the east side of the north arm of the eastern Sickie sub-basin, with the upthrown volcano-plutonic rocks near Blacktrout Lake. This boundary is intruded by Blacktrout diorite (Lqd), a syncollisional unit that is transitional-to-alkaline, and its melts must have had access to deep fertile mantle. Late faults, mapped and probably unmapped, north of Granville Lake, on the east and west sides of the north arm of the eastern sub-basin (Figure 33a), with adjoining Blacktrout diorite dikes or sills, suggest long-lived activity in these zones. This environment possibly favoured deposition of gold in a number of places.

## Acknowledgments

The work leading to this report could not have been carried out effectively without the collaboration of J. Percival, J. Whalen, N. Rayner, D. Corrigan (GSC) and M. Growdon (Indiana University) or without the aeromagnetic surveys led by F. Kiss and M. Coyle (GSC). The authors enjoyed their help, comradeship, leadership and sometime criticism. Their work was financed under the Targeted Geoscience Initiative phases 1, 2 and 3 (TGI-1, -2 and -3). Our joint preliminary reports form an integral part of this report. We also acknowledge the full use of the MGS maps of Baldwin et al. (1979).

We thank several summer assistants for their help: G. Ashcroft, M. Smith, H. Slivinski, N. Ballantine, C. Currie and J. Mungall showed enthusiasm and capable field assistance in some exceptionally difficult terrain. Logistic field support was ably provided by N. Brandson and E. Anderson. C. Boe from Manitoba Hydro allowed our crews to reside at the Notigi hydro station. We thank Darcy Linklater from the Nisichawayasihk Cree Nation (Nelson House) for taking us to and leasing us his cottage. We appreciated the opportunity to give a slide show at the Nelson House school. We also enjoyed the visit from community members of Granville Lake. Thanks also go to A. Bailles, C. Böhm and S. Anderson for constructive comments through-

out this project. Thorough editing by S. Anderson has led to major revisions and additions to sections of this report, and subsequently, to upgrading it using more current work (e.g., Martins et al., 2019) and further literature review. Very appreciated are the attention to detail provided for our maps and figures by P. Lenton, L. Chackowsky, M. Timcoe and B. Lenton, and the editing comments of C. Couëslan. Final editing by T. Martins, C. Couëslan and C.O. Böhm is most appreciated. Many thanks to C. Stefano for his professional layout and production of this report.

## References

- Aldanmaz, E., Pearce, J.A., Thirlwall, M.F. and Mitchell, J.G. 2000: Petrogenetic evolution of late Cenozoic, post-collision volcanism in western Anatolia, Turkey; *Journal of Volcanology and Geothermal research*, v. 102, p. 67–95, URL <[https://doi.org/10.1016/S0377-0273\(00\)00182-7](https://doi.org/10.1016/S0377-0273(00)00182-7)>.
- Alsop, G.I. and Carreras, J. 2007: The structural evolution of sheath folds: a case study from Cap de Creus; *Journal of Structural Geology*, v. 29, p. 1915–1930, URL <<https://doi.org/10.1016/j.jsg.2007.09.010>>.
- Ansdell, K.M. 2005: Tectonic evolution of the Manitoba–Saskatchewan segment of the Paleoproterozoic Trans-Hudson Orogen, Canada; *Canadian Journal of Earth Sciences*, v. 42, p. 741–759, URL <<https://doi.org/10.1139/e05-035>>.
- Ansdell, K.M. and Yang, H. 1995: Detrital zircons in the McLennan Group meta-arkoses and MacLean Lake Belt, western Trans-Hudson Orogen; in LITHOPROBE Trans-Hudson Orogen Transect, Z. Hajnal and J. Lewry (ed.); LITHOPROBE Secretariat, University of British Columbia, LITHOPROBE Report no. 48, p. 190–197.
- Ansdell, K.M., Heaman, L.M., Machado, N., Stern, R.A., Corrigan, D., Bickford, P., Annesley, I.R., Böhm, C.O., Zwanzig, H.V., Bailles, A.H., Syme, E.C., Corkery, M.T., Ashton, K.E., Maxeiner, R.O., Yeo, G.M. and Delaney, G.D. 2005: Correlation chart of the evolution of the Trans-Hudson Orogen — Manitoba–Saskatchewan segment; *Canadian Journal of Earth Sciences*, v. 42, p. 761, URL <<https://doi.org/10.1139/e05-004>>.
- Ansdell, K.M., Lucas, S.B., Connors, K. and Stern, R.A. 1995: Kiseynew metasedimentary gneiss belt, Trans-Hudson orogen (Canada): back-arc origin and collisional inversion; *Geology*, v. 23, p. 1039–1043, URL <[https://doi.org/10.1130/0091-7613\(1995\)023<1039:KMGBTH>2.3.CO;2](https://doi.org/10.1130/0091-7613(1995)023<1039:KMGBTH>2.3.CO;2)>.
- Anderson, S.D. 2008: Lithochemical database, Sm-Nd isotopic data and U-Pb geochronological data for the Rice Lake area, Rice Lake greenstone belt, Manitoba (parts of NTS 52L13, 52M4); Manitoba Science, Technology, Energy and Mines, Manitoba Geological Survey, Data Repository Item DRI2008002, Microsoft® Excel® file, URL <<https://www.manitoba.ca/iem/info/libmin/DRI2008002.xls>> [September 2021].
- Ashton, K.E., Heaman, L.M., Lewry, J.F., Hartlaub, R.P. and Shi, R. 1999: Age and origin of the Jan Lake Complex: a glimpse at the buried Archean craton of the Trans-Hudson Orogen; *Canadian Journal of Earth Sciences*, v. 36, p. 185–208, URL <<https://doi.org/10.1139/e98-038>>.
- Ashton, K.E., Lewry, J.F., Heaman, L.M., Hartlaub, R.P., Stauffer, M.R. and Tran, H.T. 2005: The Pelican Thrust Zone: basal detachment between the Archean Sask Craton and Paleoproterozoic Flin Flon–Glennie Complex, western Trans-Hudson Orogen; *Canadian Journal of Earth Sciences*, v. 42, p. 685–706, URL <<https://doi.org/10.1139/e04-035>>.

- Bailes, A.H. 1980a: Geology of the File Lake area; Manitoba Energy and Mines, Mineral Resources Division, Geological Report GR78-1, 134 p., URL <<https://www.manitoba.ca/iem/info/libmin/GR78-1.zip>> [September 2021].
- Bailes, A.H. 1980b: Origin of early Proterozoic volcanoclastic turbidites, south margin of the Kisseynew sedimentary gneiss belt, File Lake, Manitoba; *Precambrian Research*, v. 12, p. 197–225, URL <[https://doi.org/10.1016/0301-9268\(80\)90029-7](https://doi.org/10.1016/0301-9268(80)90029-7)>.
- Baldwin, D.A. 1980: Disseminated stratiform base metal mineralization along the contact zone of the Burntwood River metamorphic suite and the Sickie Group; Manitoba Department of Energy and Mines, Mineral Resources Division, Economic Geology Report ER79-5, 20 p., URL <<https://www.manitoba.ca/iem/info/libmin/ER79-5.zip>> [September 2021].
- Baldwin, D.A. 1981: Mineral deposits in the Ruttan Lake, Karsakuwigamak Lake, Muskayk Lake areas, Manitoba (Parts of NTS 64B/5, 6, 11 and 12); Manitoba Department of Energy and Mines, Mineral Resources Division, Open File Report OF81-4, 59 p., URL <<https://www.manitoba.ca/iem/info/libmin/OF81-4.zip>> [September 2021].
- Baldwin, D.A. 1988: Geology of the southern part of the Rusty Lake volcanic belt; Manitoba Energy and Mines, Minerals Division, Geological Report GR86-1, 90 p. plus 1 map at 1:50 000 scale, URL <<https://www.manitoba.ca/iem/info/libmin/GR86-1.zip>> [September 2021].
- Baldwin, D.A., Frohlinger, T.G., Kendrick, G., McRitchie, W.D. and Zwanzig, H.V. 1979: Geology of the Nelson House and Pukatawagan region (Burntwood Project); Manitoba Department of Mines, Natural Resources and Environment, Mineral Resources Division, Geological Maps 78-3-1 to 78-3-22.
- Baldwin, D.A., Syme, E.C., Zwanzig, H.V., Gordon, T.M., Hunt, P.A. and Stevens, R.D. 1987: U-Pb zircon ages from the Lynn Lake and Rusty Lake metavolcanic belts, Manitoba: two ages of Proterozoic magmatism; *Canadian Journal of Earth Sciences*, v. 24, p. 1053–1063, URL <<https://doi.org/10.1139/e87-101>>.
- Barker, F., Peterman, Z.E., Henderson, W.T. and Hildreth, R.E. 1974: Rubidium-strontium dating of the trondhjemite of Rio Brazos, New Mexico and of the Kroenke Granodiorite, Colorado; *Journal of Research of the U.S. Geological Survey*, v. 2, p. 705–709.
- Barry, G.S. 1965: Geology of the Trophy Lake area (east half); Manitoba Mines and Natural Resources, Mines Branch, Publication 63-3, 47 p. plus 1 map at 1:63 360 scale.
- Barry, G.S. and Gait, R.I. 1966: Geology of the Suwannee Lake area; Manitoba Mines and Natural Resources, Mines Branch, Publication 64-2, 46 p. plus 1 map at 1:63 360 scale.
- Beaumont-Smith, C.J. and Böhm, C.O. 2002: Structural analysis and geochronological studies in the Lynn Lake greenstone belt and its gold-bearing shear zones (NTS 64C10, 11, 12, 14, 15 and 16), Manitoba; *in* Report of Activities 2002, Manitoba Industry, Trade and Mines, Manitoba Geological Survey, p. 159–170, URL <<https://www.manitoba.ca/iem/geo/field/roa02pdfs/GS-19.pdf>> [September 2021].
- Beaumont-Smith, C.J. and Böhm, C.O. 2003: Tectonic evolution and gold metallogeny of the Lynn Lake greenstone belt, Manitoba (NTS 64C10, 11, 12, 14, 15 and 16); *in* Report of Activities 2003, Manitoba Industry, Economic Development and Mines, Manitoba Geological Survey, p. 39–49, URL <<https://www.manitoba.ca/iem/geo/field/roa03pdfs/GS-06.pdf>> [September 2021].
- Beaumont-Smith, C.J. and Böhm, C.O. 2004: Structural analysis of the Lynn Lake greenstone belt, Manitoba (NTS 64C10, 11, 12, 14, 15 and 16); *in* Report of Activities 2004, Manitoba Industry, Economic Development and Mines, Manitoba Geological Survey, p. 55–68, URL <<https://www.manitoba.ca/iem/geo/field/roa04pdfs/GS-06.pdf>> [September 2021].
- Beaumont-Smith, C.J., Machado, N. and Peck, D.C. 2006: New uranium-lead geochronology results from the Lynn Lake greenstone belt, Manitoba (NTS 64C11–16); Manitoba Science, Technology, Energy and Mines, Manitoba Geological Survey, Geoscientific Paper GP2006-1, 11 p., URL <<https://www.manitoba.ca/iem/info/libmin/GP2006-1.pdf>> [September 2021].
- Bleeker, W. 1990: New structural-metamorphic constraints on Early Proterozoic oblique collision along the Thompson nickel belt, Manitoba, Canada; *in* The Early Proterozoic Trans-Hudson Orogen of North America, J.F. Lewry and M.R. Stauffer (ed.), Geological Association of Canada, Special Paper 37, p. 57–73.
- Böhm, C.O., Heaman, L.M., Stern, R.A., Corkery, M.T. and Creaser, R.A. 2003: Nature of assean lake ancient crust, Manitoba: a combined SHRIMP-ID-TIMS U-Pb geochronology and Sm-Nd isotope study; *Precambrian Research*, v. 126, p. 55–94.
- Böhm, C.O., Zwanzig, H.V. and Creaser, R.A. 2007: Sm-Nd isotope technique as an exploration tool: delineating the northern extension of the Thompson nickel belt, Manitoba, Canada; *Economic Geology*, v. 102, p. 1217–1231, URL <<https://doi.org/10.2113/gsecongeo.102.7.1217>>.
- Burnham, O.M., Halden, N., Layton-Matthews, D., Leshner, C.M., Liwanag, J., Heaman, L., Hulbert, L., Machado, N., Michalak, D., Pacey, M., Peck, D.C., Potrel, A., Theyer, P., Toope, K. and Zwanzig, H. 2009: CAMIRO project 97E-02, Thompson Nickel Belt: final report March 2002, revised and updated 2003; Manitoba Science, Technology, Energy and Mines, Manitoba Geological Survey, Open File OF2008-11, 434 p. plus appendices and GIS shape files for use with ArcInfo®, URL <<https://www.manitoba.ca/iem/info/libmin/OF2008-11.zip>> [September 2021].
- Cameron, H.D.M. 1981: Granville Lake Project (parts of 64C/1, 2, 7 and 8); *in* Report of Field Activities 1981, Manitoba Department of Energy and Mines; Mineral Resources Division, p. 22–23.
- Campbell, F.H.A. 1972: Stratigraphic and structural studies in the Granville Lake-Lynn Lake region; Manitoba Mines, Resources and Environmental Management, Mines Branch, Publication 71-2A, 40 p. plus 1 map at 1:50 000 scale.
- Cawood, P.A. and Hawkesworth, C.J. 2014: Earth's middle age; *Geology*, v. 42, p. 503–506, URL <<https://doi.org/10.1130/G35402.1>>.
- Cawood, P.A., Hawkesworth, C.J. and Dhuime, B. 2012: Detrital zircon record and tectonic setting; *Geology*, v. 40, p. 875–878, URL <<https://doi.org/10.1130/G32945.1>>.
- Clowes, R.M. and Roy, B. 2020: Crustal structure of the metasedimentary Kisseynew domain and bounding volcanic-plutonic domains, Trans-Hudson orogen, Canada; *Canadian Journal of Earth Sciences*, v. 58, p. 268–285, URL <<https://doi.org/10.1139/cjes-2020-0062>>.
- Condie, K.C. and Puetz, S.J. 2019: Time series analysis of mantle cycles Part II: The geologic record in zircons, large igneous provinces and mantle lithosphere; *Geoscience Frontiers*, v. 10, p. 1327–1336, URL <<https://doi.org/10.1016/j.gsf.2019.03.005>>.
- Corfu, F. and Davis, D.W. 1992: A U-Pb geochronological framework for the western Superior Province, Ontario; *in* Geology of Ontario, P.C. Thurston, H.R. Williams, R.H. Sutcliffe and G.M. Stott (ed.), Ontario Geological Survey, Special Volume 4, p. 1335–1346.
- Corkery, M.T. and Lenton, P.G. 1990: Geology of the lower Churchill River region; Manitoba Energy and Mines, Geological Services, Geological Report GR85-1, 7 maps at 1:100 000 scale and 2 maps at 1:250 000 scale.
- Corrigan, D. and Rayner, N. 2002: Churchill River–Southern Indian Lake Targeted Geoscience Initiative (NTS 64B, 64C, 64G, 64H), Manitoba: update and new findings; *in* Report of Activities 2002, Manitoba Industry, Trade and Mines, Manitoba Geological Survey, p. 144–158, URL <<https://www.manitoba.ca/iem/geo/field/roa02pdfs/GS-18.pdf>> [September 2021].

- Corrigan, D., Maxeiner, R.O. and Harper, C.T. 2001a: Preliminary U-Pb results from the La Ronge–Lynn Lake Bridge Project; *in* Summary of Investigations 2001, v. 2, Saskatchewan Geological Survey, Saskatchewan Energy and Mines, Miscellaneous Report 2001-4.2, p. 111–115.
- Corrigan, D., Therriault, A. and Rayner, N.M. 2001b: Preliminary results from the Churchill River–Southern Indian Lake Targeted Geoscience Initiative; *in* Report of Activities 2001, Manitoba Industry, Trade and Mines, Manitoba Geological Survey, p. 94–107, URL <<https://www.manitoba.ca/iem/geo/field/roa01pdfs/01gs-14.pdf>> [September 2021].
- Corrigan, D., Hajnal, Z., Németh, B. and Lucas, S.B. 2005: Tectonic framework of a Paleoproterozoic arc-continent to continent-continent collisional zone, Trans-Hudson Orogen, from geological and seismic reflection studies; *Canadian Journal of Earth Sciences*, v. 42, p. 421–434, URL <<https://doi.org/10.1139/e05-025>>.
- Corrigan, D., Pehrsson, S., Wodicka, N. and de Kemp, E. 2009: The Palaeoproterozoic Trans-Hudson Orogen: a prototype of modern accretionary processes; *in* Ancient Orogens and Modern Analogues, J.B. Murphy, J.D. Keppie and A.J. Hynes (ed.), Geological Society of London, Special Publications, v. 327, p. 457–479, URL <<https://doi.org/10.1144/SP327.19>>.
- Couëslan, C.G. 2016: Whole-rock litho-geochemistry, Sm-Nd isotope geochemistry, and U-Pb zircon geochronology for samples from the Paint and Phillips lakes area, Manitoba (parts of NTS 63O1, 8, 9, 63P5, 12); Manitoba Growth Enterprise and Trade, Manitoba Geological Survey, Data Repository Item DRI2016001, Microsoft® Excel® file, URL <<https://www.manitoba.ca/iem/info/libmin/DRI2016001.xlsx>> [September 2021].
- Couëslan, C.G. and Pattison, D.R.M. 2012: Low-pressure regional amphibolite-facies to granulite-facies metamorphism of the Paleoproterozoic Thompson Nickel Belt, Manitoba; *Canadian Journal of Earth Sciences*, v. 49, p. 1117–1153, URL <<https://doi.org/10.1139/e2012-029>>.
- Coyle, M. and Kiss, F. 2006: First vertical derivative of the magnetic field, Wuskwatim Lake aeromagnetic survey, Manitoba, Wuskwatim Lake (NTS 63O/10), Manitoba: Geological Survey of Canada, Open File 5145, Manitoba Industry, Economic Development and Mines, Manitoba Geological Survey, Open File Report OF2006-24, scale 1:50 000, URL <<https://www.manitoba.ca/iem/info/libmin/OF2006-24.pdf>> [September 2021].
- Cruciani, G., Franceschelli, M., Elter, F.M., Puxeddu, M. and Utzeri, D. 2008: Petrogenesis of Al–silicate-bearing trondhjemitic migmatites from NE Sardinia, Italy; *Lithos*, v. 102, p. 554–574, URL <<https://doi.org/10.1016/j.lithos.2007.07.023>>.
- Cumming, G.L. and Krstić, D. 1991: Geochronology at the Namew Lake Ni–Cu deposit, Flin Flon area, Manitoba, Canada: a Pb/Pb study of whole rocks and ore minerals; *Canadian Journal of Earth Sciences*, v. 28, p. 1328–1339, URL <<https://doi.org/10.1139/e91-116>>.
- David, J., Bailes, A.H. and Machado, N. 1996: Evolution of the Snow Lake portion of the Palaeoproterozoic Flin Flon and Kisseynew belts, Trans-Hudson Orogen, Manitoba, Canada; *Precambrian Research*, v. 80, p. 107–124, URL <[https://doi.org/10.1016/S0301-9268\(96\)00008-3](https://doi.org/10.1016/S0301-9268(96)00008-3)>.
- Dell'Angelo, L.N. and Tullis, J. 1988: Experimental deformation of partially melted granitic aggregates; *Journal of Metamorphic Geology*, v. 6, p. 495–515, URL <<https://doi.org/10.1111/j.1525-1314.1988.tb00436.x>>.
- Dickinson, W.R. and Gehrels, G.E. 2009: Use of U–Pb ages of detrital zircons to infer maximum depositional ages of strata: a test against a Colorado Plateau Mesozoic database; *Earth and Planetary Science Letters*, v. 288, p. 115–125, URL <<https://doi.org/10.1016/j.epsl.2009.09.013>>.
- DiLabio, R.N.W. and Kaszycki, C.A. 1988: An ultramafic dispersal train and associated gold anomaly in till near Osik Lake, Manitoba; *in* Current Research, Part C, Geological Survey of Canada, Paper 88-1C, p. 67–71, URL <<https://doi.org/10.4095/122617>>.
- Elphick, S.C. 1972: Geology of the Mynarski-Notigi lakes area; Manitoba Department of Mines, Resources and Environmental Management, Mines Branch, Publication 71-2C, 48 p. plus 2 maps at 1:50 000 scale.
- Ferreira, K.J. 1993a: Mineral deposits and occurrences in the Laurie Lake area, NTS 64C/12; Mineral Deposit Series Report No. 9, Manitoba Energy and Mines, Geological Services, 101 p. plus 1 map at 1:50 000 scale, URL <<https://www.manitoba.ca/iem/info/libmin/MDS9.zip>> [September 2021].
- Ferreira, K.J. 1993b: Mineral deposits and occurrences in the Sickie Lake area, NTS 64C/10; Mineral Deposit Series Report No. 23, Manitoba Energy and Mines, Geological Services, 28 p. plus 1 map at 1:50 000 scale, URL <<https://www.manitoba.ca/iem/info/libmin/MDS23.zip>> [September 2021].
- Ferreira, K.J. and Baldwin D.A. 1997: Mineral deposits and occurrences in the Cockeram Lake area, NTS 64C/15; Mineral Deposit Series Report No. 8, Manitoba Energy and Mines, Geological Services, 154 p. plus 1 map at 1:50 000 scale, URL <<https://www.manitoba.ca/iem/info/libmin/MDS8.zip>> [September 2021].
- Fornelli, A., Piccarreta, G., Del Moro, A. and Acquafredda, P. 2002: Multi-stage melting in the lower crust of the Serre (southern Italy); *Journal of Petrology*, v. 43, p. 2191–2217, URL <<https://doi.org/10.1093/petrology/43.12.2191>>.
- Frohlinger, T.G. 1971: Hall Lake-Wapisiu Lake area (63O-13, 63O-14 and parts of 63O-10, 11, 12 and 15); *in* Summary of Geological Field Work 1971, Manitoba Department of Mines, Resources and Environmental Management, Mines Branch, Geological Paper GP6/71, p. 35–43, URL <<https://www.manitoba.ca/iem/info/libmin/GP71-6.pdf>> [September 2021].
- Furnes, H., Dilek, Y. and Pedersen, R.B. 2012: Structure, geochemistry, and tectonic evolution of trench-distal backarc oceanic crust in the western Norwegian Caledonides, Solund-Stavfjord ophiolite (Norway); *Geological Society of America Bulletin*, v. 124, no. 7-8, p. 1027–1047, URL <<https://doi.org/10.1130/B30561.1>>.
- Gagné, S. 2017: Sub-Phanerozoic geology of the Reed Lake area, Flin Flon belt, west-central Manitoba (parts of NTS 63K7, 8, 9, 10); Manitoba Growth, Enterprise and Trade, Manitoba Geological Survey, Preliminary Map PMAP2017-2, scale 1:30 000, URL <<https://www.manitoba.ca/iem/info/libmin/PMAP2017-2.pdf>> [September 2021].
- Gagné, S., Syme, E.C., Anderson, S.D. and Bailes, A.H. 2017: Geology of the exposed basement in the Reed Lake area, Flin Flon belt, west-central Manitoba (parts of NTS 63K9, 10, 15, 16); Manitoba Growth, Enterprise and Trade, Manitoba Geological Survey, Preliminary Map PMAP2017-1, scale 1:30 000, URL <<https://www.manitoba.ca/iem/info/libmin/PMAP2017-2.pdf>> [September 2021].
- Gapais, D., Potrel, A., Machado, N. and Hallot, E. 2005: Kinematics of long-lasting Paleoproterozoic transpression within the Thompson Nickel Belt, Manitoba, Canada; *Tectonics*, v. 24, 16 p., URL <<https://doi.org/10.1029/2004TC001700>>.
- Gilbert, H.P., Syme, E.C. and Zwanzig, H.V. 1980: Geology of the metavolcanic and volcanoclastic metasedimentary rocks in the Lynn Lake area; Manitoba Energy and Mines, Mineral Resources Division, Geological Paper GP80-1, 118 p., URL <<https://www.manitoba.ca/iem/info/libmin/GP80-1.zip>> [September 2021].
- Goldstein, S.L., O’Nions, R.K. and Hamilton, P.J. 1984: A Sm-Nd isotopic study of atmospheric dusts and particulates from major river systems; *Earth and Planetary Science Letters*, v. 70, p. 221–236; URL <[https://doi.org/10.1016/0012-821X\(84\)90007-4](https://doi.org/10.1016/0012-821X(84)90007-4)>.

- Gordon, T.M., Hunt, P.A., Bailes, A.H. and Syme, E.C. 1990: U-Pb ages from the Flin Flon and Kiseynew belts, Manitoba: chronology of crust formation at an early Proterozoic accretionary margin; *in* The Early Proterozoic Trans-Hudson Orogen of North America, J.F. Lewry and M.R. Stauffer (ed.), Geological Association of Canada, Special Paper 37, p. 177–199.
- Green, A.C., Hajnal, Z. and Weber, W. 1985: An evolutionary model of the western Churchill province and western margin of the Superior province in Canada and the North-Central United States; *Tectonophysics*, v. 116, p. 281–322, URL <[https://doi.org/10.1016/0040-1951\(85\)90212-4](https://doi.org/10.1016/0040-1951(85)90212-4)>.
- Growdon, M.L., Wintsch, R.P., Percival, J. and Rayner, N. 2009: Time scales of lower crustal granulite facies metamorphism during the Trans-Hudson Orogen, northern Manitoba; Geological Society of America, Annual Meeting, October 18, 2009, Portland, Oregon, Program with Abstracts, v. 41, p. 357.
- Hamilton, M.A. and Bleeker, W. 2002: SHRIMP U-Pb geochronology of the Ospwagan group: provenance and depositional age constraints of a Paleoproterozoic rift sequence, SE externalides of the Trans-Hudson Orogen (abstract); Geological Association of Canada–Mineralogical Association of Canada, Joint Annual Meeting, Saskatoon, Saskatchewan, Program with Abstracts, v. 27, p. 44.
- Heaman, L.M., Peck, D. and Toope, K. 2009: Timing and geochemistry of 1.88 Ga Molson Igneous Events, Manitoba: insights into the formation of a craton-scale magmatic and metallogenic province; *Precambrian Research*, v. 172, p. 143–162, URL <<https://doi.org/10.1016/j.precamres.2009.03.015>>.
- Herriott, T.M., Crowley, J.L., Schmitz, M.D., Wartes, M.A. and Gillis, R.J. 2019: Exploring the law of detrital zircon: LA-ICP-MS and CA-TIMS geochronology of Jurassic forearc strata, Cook Inlet, Alaska, USA; *Geology*, v. 47, p. 1044–1048, URL <<https://doi.org/10.1130/G46312.1>>.
- Hildebrand, R.S. and Whalen J.B. 2014: Arc and slab-failure magmatism in Cordilleran batholiths II – the Cretaceous peninsular ranges batholith of southern and Baja California; *Geoscience Canada*, v. 41, p. 399–458, URL <<https://doi.org/10.12789/geocanj.2014.41.059>>.
- Hulbert, L.J., Hamilton, M.A., Horan, M.F. and Scoates, R.F.J. 2005: U-Pb zircon and Re-Os isotope geochronology of mineralized ultramafic intrusions and associated nickel ores from the Thompson nickel belt, Manitoba, Canada; *Economic Geology*, v. 100, p. 29–41, URL <<https://doi.org/10.2113/100.1.0029>>.
- Hunt, P.A. and Zwanzig, H.V. 1993: U-Pb ages of intrusion, metamorphism and deformation in the Batty Lake area, Kiseynew gneiss belt, Manitoba; *in* Report of Activities 1993, Manitoba Energy and Mines, Geological Services, p. 34–37.
- Kaszycki, C.A., Suttner, W. and DiLabio, R.N.W. 1988: Gold and arsenic in till, Wheatcroft Lake dispersal train, Manitoba; *in* Current Research, Part C, Geological Survey of Canada, Paper 88-1C, p. 341–351, URL <<https://doi.org/10.4095/122648>>.
- Kendrick, G., Frohlinger, T.G. and Baldwin, D.A. 1979: Wuskwatim Lake, Manitoba; Manitoba Mines, Natural Resources and Environment, Mineral Resources Division, Map 78-3-18, scale 1:50 000.
- Kiss, F. and Coyle, M. 2008: Residual total magnetic field, Kiseynew-north aeromagnetic survey, Wapisu Lake/Hall Lake (NTS 63-O/14 and part of 63-O/13), Manitoba; Geological Survey of Canada, Open File 5786 and Manitoba Science, Technology, Energy and Mines, Manitoba Geological Survey, Open File OF2008-2, scale 1:50 000, URL <<https://www.manitoba.ca/iem/info/libmin/OF2008-2.pdf>> [September 2021].
- Kremer, P.D., Rayner, N. and Corkery, M.T. 2009: New results from geological mapping in the west-central and northeastern portions of Southern Indian Lake, Manitoba (parts of NTS 64G1, 2, 8, 64H4, 5); *in* Report of Activities 2009, Manitoba Innovation, Energy and Mines, Manitoba Geological Survey, p. 94–107, URL <<https://www.manitoba.ca/iem/geo/field/roa09pdfs/GS-9.pdf>> [September 2021].
- Kuşcu, I., Tosdal, R.M., Gencalioglu-Kuşcu, G., Friedman, R. and Ullrich, T.D. 2013: Late Cretaceous to middle Eocene magmatism and metallogeny of a portion of the southeastern Anatolian orogenic belt, east-central Turkey; *Economic Geology*, v. 108, p. 641–666, URL <<https://doi.org/10.2113/econgeo.108.4.641>>.
- Kusky, T.M., Windley, B.F., Wang, L., Wang, Z., Li, X. and Zhu, P. 2014; Flat slab subduction, trench suction, and craton destruction: Comparison of the North China, Wyoming, and Brazilian cratons; *Tectonophysics*, v. 630, p. 208–221, URL <<https://doi.org/10.1016/j.tecto.2014.05.028>>.
- Lawley, C.J.M., Yang, X.M., Selby, D., Davis, W., Zhang, S., Petts, D.C. and Jackson, S.E. 2020: Sedimentary basin controls on orogenic gold deposits: New constraints from U-Pb detrital zircon and Re-Os sulphide geochronology, Lynn Lake greenstone belt, Canada; *Ore Geology Reviews*, v. 26, art. 103790, URL <<https://doi.org/10.1016/j.oregeorev.2020.103790>>.
- Lenton, P.G. 1981: Geology of the McKnight-McCallum lakes area; Manitoba Department of Energy and Mines, Mineral Resources Division, Geological Report GR79-1, 39 p., URL <<https://www.manitoba.ca/iem/info/libmin/GR79-1.zip>> [September 2021].
- Lenton, P.G. and Corkery, M.T. 1981: The lower Churchill River project (interim report); Manitoba Department of Energy and Mines, Mineral Resources Division, Open File Report OF81-3, 23 p., URL <<https://www.manitoba.ca/iem/info/libmin/OF81-3.pdf>> [September 2021].
- Lewry, J.F. and Collerson, K.D. 1990: The Trans-Hudson Orogen: extent, subdivisions and problems; *in* The Early Proterozoic Trans-Hudson Orogen of North America, J.F. Lewry and M.R. Stauffer (ed.), Geological Association of Canada, Special Paper 37, p. 1–14.
- Lewry, J.F., Thomas, D.J., Macdonald, R. and Chiarenzelli, J. 1990: Structural relations in accreted terranes of the Trans-Hudson Orogen, Saskatchewan: telescoping in a collisional regime?; *in* The Early Proterozoic Trans-Hudson Orogen of North America, J.F. Lewry and M.R. Stauffer (ed.), Geological Association of Canada, Special Paper 37, p. 75–94.
- Lewry, J., Hajnal, Z., Green, A., Lucas, S.B., White, D., Stauffer, M., Ashton, K., Weber, W. and Clowes, R. 1994: Structure of a Paleoproterozoic continent-continent collision zone: a LITHOPROBE seismic reflection profile across the Trans-Hudson Orogen, Canada; *Tectonophysics*, v. 232, no. 1–4, p. 143–160, URL <[https://doi.org/10.1016/0040-1951\(94\)90081-7](https://doi.org/10.1016/0040-1951(94)90081-7)>.
- Lucas, S.B., Stern, R.A., Syme, E.C., Reilly, B.A. and Thomas, D.J. 1996: Intraoceanic tectonics and the development of continental crust: 1.92–1.84 Ga evolution of the Flin Flon Belt, Canada; *Geological Society of America Bulletin*, v. 108, p. 602–629, URL <[https://doi.org/10.1130/0016-7606\(1996\)108<0602:ITATDO>2.3.CO;2](https://doi.org/10.1130/0016-7606(1996)108<0602:ITATDO>2.3.CO;2)>.
- Ludwig, K.R. 2003: User’s manual for Isoplot 3.00: a geochronological toolkit for Microsoft Excel; Berkeley Geochronological Center, Special Publication 4, 71 p.
- Machado, N., Zwanzig, H. and Parent, M. 1999: U-Pb ages of plutonism, sedimentation, and metamorphism of the Paleoproterozoic Kiseynew metasedimentary belt, Trans-Hudson Orogen (Manitoba, Canada); *Canadian Journal of Earth Sciences*, v. 36, p. 1829–1842, URL <<https://doi.org/10.1139/E99-012>>.

- Manitoba Geological Survey 2018: Manitoba geochronology database; Manitoba Growth, Enterprise and Trade, Manitoba Geological Survey, version 1.8, URL <[https://www.manitoba.ca/iem/info/libmin/mbgeochron\\_version\\_1\\_8.zip](https://www.manitoba.ca/iem/info/libmin/mbgeochron_version_1_8.zip)> [September 2021].
- Martins, T. and Couëslan, C.G. 2019: Geological investigations in the Russell–McCallum lakes area, northwestern Manitoba (parts of NTS 64C3–6); *in* Report of Activities 2019, Manitoba Agriculture and Resource Development, Manitoba Geological Survey, p. 30–41, URL <<https://www.manitoba.ca/iem/geo/field/roa19pdfs/GS2019-3.pdf>> [September 2021].
- Martins, T., Couëslan, C.G. and Böhm, C.O. 2011: The Burntwood Lake alkali-feldspar syenite revisited, west-central Manitoba (part of NTS 63N8); *in* Report of Activities 2011, Manitoba Innovation, Energy and Mines, Manitoba Geological Survey, p. 79–85, URL <<https://www.manitoba.ca/iem/geo/field/roa11pdfs/GS-8.pdf>> [September 2021].
- Martins, T., Couëslan, C.G. and Böhm, C.O. 2012: Rare metals scoping study of the Brezden Lake intrusive complex, western Manitoba (part of NTS 64C4); *in* Report of Activities 2012, Manitoba Innovation, Energy and Mines, Manitoba Geological Survey, p. 115–123, URL <<https://www.manitoba.ca/iem/geo/field/roa12pdfs/GS-10.pdf>> [September 2021].
- Martins, T., Kremer, P.D., Corrigan, D. and Rayner, N. 2019: Geology of the Southern Indian Lake area, north-central Manitoba (parts of NTS 64G1, 2, 7–10, 64H3–6); Manitoba Growth, Enterprise and Trade, Manitoba Geological Survey, Geoscientific Report GR2019-1, 51 p. and 4 maps at 1:50 000 scale, URL <<https://www.manitoba.ca/iem/info/libmin/GR2019-1.zip>> [September 2021].
- McKenzie, N.R., Hughes, N.C., Gill, B.J. and Myrow, P.M. 2014: Plate tectonic influences on Neoproterozoic–early Paleozoic climate and animal evolution; *Geology*, v. 42, p. 127–130, URL <<https://doi.org/10.1130/G34962.1>>.
- McRitchie, W.D. 1987: Burntwood Lake Syenite (63N/8, 9, 10); Manitoba Energy and Mines; Minerals Division, Preliminary Map 1987K-5, scale 1:5 000.
- McRitchie, W.D., Peters, J. and Frohlinger, T.G. 1979: History of exploration and geological work in the Nelson House-Pukatawagan region (Burntwood project); Manitoba Mines, Natural Resources and Environment, Mineral Resources Division, Geological Report GR78-3 (part II), 40 p. plus 2 figures, URL <<https://www.manitoba.ca/iem/info/libmin/GR78-3.zip>> [September 2021].
- Meyer, M.T., Bickford, M.E. and Lewry, J.F. 1992. The Wathaman batholith: An Early Proterozoic continental arc in the Trans-Hudson orogenic belt, Canada; *Geological Society of America Bulletin*, v. 104, p. 1073–1085, URL <[https://doi.org/10.1130/0016-7606\(1992\)104<1073:TWBAEP>2.3.CO;2](https://doi.org/10.1130/0016-7606(1992)104<1073:TWBAEP>2.3.CO;2)>.
- Milligan, G.C. 1960: Geology of the Lynn Lake district; Manitoba Mines and Natural Resources, Mines Branch, Publication PUB57-1, 317 p. plus 16 maps, URL <<https://www.manitoba.ca/iem/info/libmin/PUB57-1.zip>> [September 2021].
- Murphy, L.A. 2008: Update on geological investigations of the Notigi Lake area, Manitoba (parts of NTS 63O14, 64B3); *in* Report of Activities 2008, Manitoba Science, Technology, Energy and Mines, Manitoba Geological Survey, p. 53–65, URL <<https://www.manitoba.ca/iem/geo/field/roa08pdfs/GS-5.pdf>> [September 2021].
- Murphy, L.A. and Zwanzig, H.V. 2007a: Preliminary stratigraphy and structure of the Notigi Lake area, Manitoba (parts of NTS 63O14, 64B3); *in* Report of Activities 2007, Manitoba Science, Technology, Energy and Mines, Manitoba Geological Survey, p. 51–62, URL <<https://www.manitoba.ca/iem/geo/field/roa07pdfs/GS-5.pdf>> [September 2021].
- Murphy, L.A. and Zwanzig, H.V. 2007b: Unique amphibolite–iron formation assemblage in the Kawawayak Lake area, Manitoba (part of NTS 63O15); *in* Report of Activities 2007, Manitoba Science, Technology, Energy and Mines, Manitoba Geological Survey, p. 63–70, URL <<https://www.manitoba.ca/iem/geo/field/roa07pdfs/GS-6.pdf>> [September 2021].
- Murphy, L.A. and Zwanzig, H.V. 2008: Revised geology of Notigi Lake, Manitoba (parts of NTS 63O14 and 64B3); Manitoba Science, Technology, Energy and Mines, Manitoba Geological Survey, Preliminary Map PMAP2008-2, scale 1:20 000, URL <<https://www.manitoba.ca/iem/info/libmin/PMAP2008-2.pdf>> [September 2021].
- Murphy, L.A. and Zwanzig, H.V. 2009: Geology of the Notigi–Wapisi lakes area, Northeast Kisseynew subdomain, Manitoba (parts of NTS 63O14 and 64B3); Manitoba Innovation, Energy and Mines, Manitoba Geological Survey, Preliminary Map PMAP2009-5, scale 1:20 000, URL <<https://www.manitoba.ca/iem/info/libmin/PMAP2009-5.pdf>> [September 2021].
- Murphy, L.A. and Zwanzig, H.V. 2019a: Geology and structure of the Notigi Lake area, Manitoba (parts of NTS 63O14, 64B3); Manitoba Growth, Enterprise and Trade, Manitoba Geological Survey, Geoscientific Map MAP 2019-3, scale 1:25 000, URL <<https://www.manitoba.ca/iem/info/libmin/MAP2019-3.pdf>> [September 2021].
- Murphy, L.A. and Zwanzig, H.V. 2019b: Geology of the Kawawayak Lake area, Manitoba (part of NTS 63O15) Manitoba Growth, Enterprise and Trade, Manitoba Geological Survey, Geoscientific Map MAP2019-4, scale 1: 10 000, URL <<https://www.manitoba.ca/iem/info/libmin/MAP2019-4.pdf>> [September 2021].
- Murphy, L.A. and Zwanzig, H.V. 2019c: Geology of the Notigi–Footprint lakes area, Manitoba (parts of NTS 63O10, 11, 14, 15); Manitoba Growth, Enterprise and Trade, Manitoba Geological Survey, Geoscientific Map MAP2019-2, scale 1:50 000, URL <<https://www.manitoba.ca/iem/info/libmin/MAP2019-2.pdf>> [September 2021].
- Murphy, L.A. and Zwanzig, H.V. 2019d: Notigi–Tullibee lakes aeromagnetic map: residual total field with shaded relief; Manitoba Growth, Enterprise and Trade, Manitoba Geological Survey, Geoscientific Map MAP2019-6, scale 1:50 000, URL <<https://www.manitoba.ca/iem/info/libmin/MAP2019-6.pdf>> [September 2021].
- Murphy, L.A., Zwanzig, H.V. and Rayner, N. 2009: Geology of the Notigi–Wapisi lakes area, Kisseynew Domain, Manitoba (parts of NTS 63O14, 64B3); *in* Report of Activities 2009, Manitoba Innovation, Energy and Mines, Manitoba Geological Survey, p. 69–84, URL <<https://www.manitoba.ca/iem/geo/field/roa09pdfs/GS-7.pdf>> [September 2021].
- Parent, M., Machado, N. and Zwanzig, H. 1999: Comportement du système U-Pb dans la monazite et chronologie de la déformation et du métamorphisme des métasédiments du domaine de Kisseynew, orogène trans-hudsonien (Manitoba, Canada); *Canadian Journal of Earth Sciences*, v. 36, p. 1843–1857, URL <<https://doi.org/10.1139/e99-051>>.
- Pavlis, T.L., Amato, J.M., Trop, J.M., Ridgway, K.D., Roeske, S.M. and Gehrels, G.E. 2019: Subduction polarity in ancient arcs: a call to integrate geology and geophysics to decipher the Mesozoic tectonic history of the northern Cordillera of North America; *GSA Today*, v. 29, p. 4–10, URL <<https://doi.org/10.1130/GSATG402A.1>>.

- Pearce, J.A. 1983: Role of the sub-continental lithosphere in magma genesis at active continental margins; *in* Continental basalts and mantle xenoliths, C.J. Hawkesworth and M.J. Norry (ed.), p. 230–249.
- Pearce, J.A. and Peate, D.W. 1995: Tectonic implications of the composition of volcanic ARC magmas; *Annual Review of Earth and Planetary Sciences*, v. 23, p. 251–285, URL <<https://doi.org/10.1146/annurev.ea.23.050195.001343>>.
- Pearce, J.A., Harris, N.B.W. and Tindle A.G. 1984: Trace element discrimination diagrams for the tectonic interpretation of granitic rocks; *Journal of Petrology*, v. 25, p. 956–983, URL <<https://doi.org/10.1093/petrology/25.4.956>>.
- Percival, J.A., Whalen, J.B. and Rayner, N. 2004: Pikwitonei–Snow Lake, Manitoba transect (parts of NTS 63J, 63O and 63P), Trans-Hudson Orogen–Superior Margin Metallotect Project: initial geological, isotopic and SHRIMP U–Pb results; *in* Report of Activities 2004, Manitoba Industry, Economic Development and Mines, Manitoba Geological Survey, p. 120–134, URL <<https://www.manitoba.ca/iem/geo/field/roa04pdfs/GS-11.pdf>> [September 2021].
- Percival, J.A., Whalen, J.B. and Rayner, N. 2005: Pikwitonei–Snow Lake Manitoba transect (parts of NTS 63J, 63O and 63P), Trans-Hudson Orogen–Superior Margin Metallotect Project: new results and tectonic interpretation; *in* Report of Activities 2005, Manitoba Industry, Economic Development and Mines, Manitoba Geological Survey, p. 69–91, URL <<https://www.manitoba.ca/iem/geo/field/roa05pdfs/GS-09.pdf>> [September 2021].
- Percival, J.A., Zwanzig, H.V. and Rayner, N. 2006: New tectonostratigraphic framework for the northeastern Kiseynew Domain, Manitoba (parts of NTS 63O); *in* Report of Activities 2006, Manitoba Science, Technology, Energy and Mines, Manitoba Geological Survey, p. 74–84, URL <<https://www.manitoba.ca/iem/geo/field/roa06pdfs/GS-08.pdf>> [September 2021].
- Percival, J.A., Rayner, N., Growdon, M.L., Whalen, J.B. and Zwanzig, H.V. 2007: New field and geochronological results for the Osik–Atik–Footprint lakes area, Manitoba (NTS 63O13, 14, 15, 64B2, 3); *in* Report of Activities 2007, Manitoba Science, Technology, Energy and Mines, Manitoba Geological Survey, p. 71–81, URL <<https://www.manitoba.ca/iem/geo/field/roa07pdfs/GS-7.pdf>> [September 2021].
- Ramsay, J.G. and Huber, M.I. 1987: The techniques of modern structural geology, volume 2: folds and fractures; Academic Press, Elsevier Science Ltd., San Diego, California, 391 p.
- Rayner, N. 2009: Geochronological data of the Notigi–Wapisu lakes area, Kiseynew Domain, Manitoba (parts of NTS 63O14, 64B3); Manitoba Innovation, Energy and Mines, Manitoba Geological Survey, Data Repository Item DRI2009005, Microsoft® Excel® file, URL <<https://www.manitoba.ca/iem/info/libmin/DRI2009005.xls>> [September 2021].
- Rayner, N. and Corrigan, D. 2004: Uranium–lead geochronological results from the Churchill River–Southern Indian Lake transect, northern Manitoba; *in* Current Research 2004-F1, Geological Survey of Canada, 14 p., URL <<https://doi.org/10.4095/214975>>.
- Rayner, N. and Percival, J.A. 2007: Uranium–lead geochronology of basement units in the Wuskwatim–Tullibee lakes area, north-eastern Kiseynew Domain, Manitoba (NTS 63O); *in* Report of Activities 2007, Manitoba Science, Technology, Energy and Mines, Manitoba Geological Survey, p. 82–90, URL <<https://www.manitoba.ca/iem/geo/field/roa07pdfs/GS-8.pdf>> [September 2021].
- Richards, J.P. 2003: Tectono-magmatic precursors for porphyry Cu–(Mo–Au) deposit formation; *Economic Geology*, v. 98, p. 1515–1533, URL <<https://doi.org/10.2113/gsecongeo.98.8.1515>>.
- Richardson, D.J. and Ostry, G. (revised by Weber, W. and Fogwill, D.) 1996: Gold deposits of Manitoba; Manitoba Energy and Mines, Economic Geology Report ER86-1 (2nd edition), 114 p., URL <<https://www.manitoba.ca/iem/info/libmin/ER86-1.zip>> [September 2021].
- Sawyer, E.W. and Barnes, S.-J. 1988: Temporal and compositional differences between subsolidus and anatectic migmatite leucosome from the Quetico metasedimentary belt, Canada; *Journal of Metamorphic Geology*, v. 6, p. 437–450.
- Schledewitz, D.C.P. 1972: Geology of the Rat Lake area; Manitoba Department of Mines, Resources and Environmental Management, Mines Branch, Publication 71-2B, 57 p. plus 4 maps at 1:50 000 scale, URL <<https://www.manitoba.ca/iem/info/libmin/PUB71-2B.zip>> [September 2021].
- Simonetti, A., Heaman, L.M., Hartlaub, R.P., Creaser, R.A., MacHattie, T.G. and Böhm, C. 2005: U–Pb zircon dating by laser ablation-MC-ICP-MS using a new multiple ion counting Faraday collector array; *Journal of Analytical Atomic Spectrometry*, v. 20, p. 677–686, URL <<https://doi.org/10.1039/B504465K>>.
- Skjerna, L. 1975: Experiments on superimposed buckle folding; *Tectonophysics*, v. 27, p. 255–270, URL <[https://doi.org/10.1016/0040-1951\(75\)90020-7](https://doi.org/10.1016/0040-1951(75)90020-7)>.
- Stauffer, M.R. 1984: Manikewan: an early proterozoic ocean in central Canada, its igneous history and orogenic closure; *Precambrian Research*, v. 25, p. 257–281, URL <[https://doi.org/10.1016/0301-9268\(84\)90036-6](https://doi.org/10.1016/0301-9268(84)90036-6)>.
- Stern, R.A. 1997: The GSC sensitive high resolution ion microprobe (SHRIMP): analytical techniques of zircon U–Th–Pb age determinations and performance evaluation; Geological Survey of Canada, Radiogenic age and isotopic studies, Report 10, p. 1–31, URL <<https://doi.org/10.4095/209089>>.
- Stern, R.A. and Amelin, Y. 2003: Assessment of errors in SIMS zircon U–Pb geochronology using a natural zircon standard and NIST SRM 610 glass; *Chemical Geology*, v. 197, p. 111–142, URL <[https://doi.org/10.1016/S0009-2541\(02\)00320-0](https://doi.org/10.1016/S0009-2541(02)00320-0)>.
- Stern, R.A., Syme, E.C. and Lucas, S.B. 1995: Geochemistry of 1.9 Ga MORB- and OIB-like basalts from the Amisk collage, Flin Flon Belt, Canada: Evidence for an intra-oceanic origin; *Geochimica et Cosmochimica Acta*, v. 59, p. 3131–3154, URL <[https://doi.org/10.1016/0016-7037\(95\)00202-B](https://doi.org/10.1016/0016-7037(95)00202-B)>.
- Sun, S.-s. 1982: Chemical composition and origin of the earth's primitive mantle; *Geochimica et Cosmochimica Acta*, v. 46, p. 179–192, URL <[https://doi.org/10.1016/0016-7037\(82\)90245-9](https://doi.org/10.1016/0016-7037(82)90245-9)>.
- Sun, S.-s. and McDonough, W.F. 1989: Chemical and isotopic systematics of oceanic basalts: implication for mantle composition and processes; Geological Society of London, Special Publications, v. 42, p. 313–345, URL <<http://dx.doi.org/10.1144/GSL.SP.1989.042.01.19>>.
- Syme, E.C. 1977: Sickle Lake–Hughes Lake area; *in* Report of Field Activities 1977, Manitoba Department of Mines, Resources and Environmental Management, Mineral Resources Division, p. 31–36.
- Syme, E.C., Lucas, S.B., Bailes, A.H. and Stern, R.A. 1999: Contrasting arc and MORB-like assemblages in the Paleoproterozoic Flin Flon Belt, Manitoba, and the role of intra-arc extension in localizing volcanic-hosted massive sulphide deposits; *in* Canadian Journal of Earth Sciences, v. 36, p. 1767–1788, URL <<https://doi.org/10.1139/e98-084>>.
- Turek, A., Woodhead, J. and Zwanzig H.V. 2000: U–Pb age of the gabro and other plutons at Lynn Lake (part of NTS 64C); *in* Report of Activities 2000, Manitoba Industry, Trade and Mines, Manitoba Geological Survey, p. 97–104, URL <<https://www.manitoba.ca/iem/geo/field/roa00pdfs/00gs-18.pdf>> [September 2021].

- Vanderhaeghe, O. 2001: Melt segregation, pervasive melt migration and magma mobility in the continental crust: the structural record from pores to orogens; *Physics and Chemistry of the Earth, Part A: Solid Earth and Geodesy*, v. 26, p. 213–223, URL <[https://doi.org/10.1016/S1464-1895\(01\)00048-5](https://doi.org/10.1016/S1464-1895(01)00048-5)>.
- Webber, A.P., Roberts, S., Taylor, R.N. and Pitcairn, I.K. 2013: Golden plumes: Substantial gold enrichment of oceanic crust during ridge-plume interaction; *Geology*, v. 41, no. 1, p. 87–90, URL <<https://doi.org/10.1130/G33301.1>>.
- Whalen, J.B. and Hildebrand, R.S. 2019: Trace element discrimination of arc, slab failure, and A-type granitic rocks; *Lithos*, v. 348–349; art. 105179, URL <<https://doi.org/10.1016/j.lithos.2019.105179>>.
- Whalen, J.B. and Hunt, P.A. 1994: Geochronological study of granitoid rocks in the Elbow Lake map area, Manitoba: a portion of the Flin Flon Domain of the Trans Hudson Orogen; *in Radiogenic Age and Isotopic Studies: Report 8*, Geological Survey of Canada, Current Research 1994-F, p. 87–96, URL <<https://doi.org/10.4095/195174>>.
- Whalen, J.B., Syme, E.C. and Stern, R.A. 1999: Geochemical and Nd isotopic evolution of Paleoproterozoic arc-type magmatism in the Flin Flon Belt, Trans-Hudson Orogen, Canada; *Canadian Journal of Earth Sciences*, v. 36, p. 227–250, URL <<https://doi.org/10.1139/e98-026>>.
- Whalen, J.B., Zwanzig, H.V., Percival, J.A. and Rayner, N. 2008: Geochemistry of an alkaline, ca. 1885 Ma K-feldspar–porphyritic, monzonitic to syenogranitic suite, northeastern Kiseynew Domain, Manitoba (parts of NTS 63O); *in Report of Activities 2008*, Manitoba Science, Technology, Energy and Mines, Manitoba Geological Survey, p. 66–78, URL <<https://www.manitoba.ca/iem/geo/field/roa08pdfs/GS-6.pdf>> [September 2021].
- White, D.J., Jones, A.G., Lucas, S.B. and Hajnal, Z. 1999: Tectonic evolution of the Superior Boundary Zone from coincident seismic reflection and magnetotelluric profiles; *Tectonics*, v. 18, p. 430–451, URL <<https://doi.org/10.1029/1999TC900002>>.
- White, D.J., Zwanzig, H.V. and Hajnal, Z. 2000: Crustal suture preserved in the Paleoproterozoic Trans-Hudson orogen, Canada; *Geology*, v. 28, p. 527–530, URL <[https://doi.org/10.1130/0091-7613\(2000\)28<527:CSPITP>2.0.CO;2](https://doi.org/10.1130/0091-7613(2000)28<527:CSPITP>2.0.CO;2)>.
- Whitmeyer, S.J. and Karlstrom, K.E. 2007: Tectonic model for the Proterozoic growth of North America; *Geosphere*, v. 3, p. 220–259, URL <<https://doi.org/10.1130/GES00055.1>>.
- Williams, H.M., Turner, S.P., Pearce, J.A., Kelley, S.P. and Harris, N.B.W. 2004: Nature of the source regions for post-collisional, potassic magmatism in southern and northern Tibet from geochemical variations and Inverse Trace Element Modelling; *Journal of Petrology*, v. 45, p. 555–607, URL <<https://doi.org/10.1093/petrology/egg094>>.
- Zwanzig, H.V. 1979: Sickle Lake; *in Report of Field Activities 1979*, Manitoba Department of Mines, Natural Resources and Environment, Mineral Resources Division, p. 13–15.
- Zwanzig, H.V. 1981: Beaucage Lake; *in Report of Field Activities 1981*, Manitoba Department of Energy and Mines; Mineral Resources Division, p. 13–16.
- Zwanzig, H.V. 1990: Kiseynew gneiss belt in Manitoba: stratigraphy, structure, and tectonic evolution; *in The Early Proterozoic Trans-Hudson Orogen of North America*, J.F. Lewry and M.R. Stauffer (ed.), Geological Association of Canada, Special Paper 37, p. 95–120.
- Zwanzig, H.V. 1999: Structure and stratigraphy of the south flank of the Kiseynew Domain in the Trans-Hudson Orogen, Manitoba: implications for 1.845–1.77 Ga collision tectonics; *in NATMAP Shield Margin Project, Volume 2*, Canadian Journal of Earth Sciences, v. 36, no. 11, p. 1859–1880, URL <<https://doi.org/10.1139/e99-042>>.
- Zwanzig, H.V. 2000a: Geochemistry and tectonic framework of the Kiseynew Domain-Lynn Lake belt boundary (part of NTS 63P/13); *in Report of Activities 2000*, Manitoba Industry, Trade and Mines, Manitoba Geological Survey, p. 91–96, URL <<https://www.manitoba.ca/iem/geo/field/roa00pdfs/00gs-17.pdf>> [September 2021].
- Zwanzig, H.V. 2000b: Mystery Lake high-strain zones: sinistral and dextral, east-side-up displacements, Thompson Nickel Belt; *in Report of Activities 2000*, Manitoba Industry, Trade and Mines, Manitoba Geological Survey, p. 18–23, URL <<https://www.manitoba.ca/iem/geo/field/roa00pdfs/00gs-5.pdf>> [September 2021].
- Zwanzig, H.V. 2005: Geochemistry, Sm-Nd isotope data and age constraints of the Bah Lake assemblage, Thompson Nickel Belt and Kiseynew Domain margin: relation to Thompson-type ultramafic bodies and a tectonic model (NTS 63J, O and P); *in Report of Activities 2005*, Manitoba Industry, Economic Development and Mines, Manitoba Geological Survey, p. 40–53, URL <<https://www.manitoba.ca/iem/geo/field/roa05pdfs/GS-06.pdf>> [September 2021].
- Zwanzig, H.V. 2008: Correlation of lithological assemblages flanking the Kiseynew Domain, Manitoba (parts of NTS 63N, 63O, 64B, 64C): proposal for tectonic/metallogenic subdomains; *in Report of Activities 2008*, Manitoba Science, Technology, Energy and Mines, Manitoba Geological Survey, p. 38–52, URL <<https://www.manitoba.ca/iem/geo/field/roa08pdfs/GS-4.pdf>> [September 2021].
- Zwanzig, H.V. 2019: Geology of the southern Granville Lake area, Manitoba (parts of NTS 64C1, 2, 7); Manitoba Growth, Enterprise and Trade, Manitoba Geological Survey, Geoscientific Map MAP2019-1, scale 1:20 000, URL <<https://www.manitoba.ca/iem/info/libmin/MAP2019-1.pdf>> [September 2021].
- Zwanzig, H.V. and Bailes, A.H. 2010: Geology and geochemical evolution of the northern Flin Flon and southern Kiseynew domains, Kissinging-File Lake areas, Manitoba (parts of NTS 63K, N); Manitoba Growth, Enterprise and Trade, Manitoba Geological Survey, Geoscientific Report GR2010-1, 134 p., URL <<https://www.manitoba.ca/iem/info/libmin/GR2010-1.zip>> [September 2021].
- Zwanzig, H.V. and Böhm, C.O. 2002: Tectonostratigraphy, Sm-Nd isotope and U-Pb age data of the Thompson Nickel Belt and Kiseynew north and east margins (NTS 63J, 63O, 63P, 64A, 64B), Manitoba; *in Report of Activities 2002*, Manitoba Industry, Trade and Mines, Manitoba Geological Survey, p. 102–114, URL <<https://www.manitoba.ca/iem/geo/field/roa02pdfs/GS-14.pdf>> [September 2021].
- Zwanzig, H.V. and Cameron, H.D.M. 1981: Granville Lake project; *in Report of Field Activities 1981*, Manitoba Department of Energy and Mines; Mineral Resources Division, p. 17–24.
- Zwanzig, H.V. and Cameron, H.D.M. 2002: Geology of southern Granville Lake (parts of NTS 64C1, 2 and 7); Manitoba Industry, Trade and Mines, Manitoba Geological Survey, Preliminary Map PMAP2002-3, scale 1:20 000, URL <<https://www.manitoba.ca/iem/info/libmin/PMP2002-3.pdf>> [September 2021].
- Zwanzig, H.V. and Corrigan, D. 2005: Extension tectonics in Trans-Hudson internal zone: from rifted arcs to syncollisional basins (abstract); Geological Association of Canada–Mineralogical Association of Canada–Canadian Society of Petroleum Geologists–Canadian Society of Soil Science, Joint Meeting 2005, Halifax, Nova Scotia, May 15, 2005, Abstracts v. 30, p. 219.

- Zwanzig, H.V. and Murphy, L.A. 2009: Geometry and history of the Notigi Lake structure (parts of NTS 63O14 and 63B3); *in* Report of Activities 2009, Manitoba Innovation, Energy and Mines, Manitoba Geological Survey, p. 85–93, URL <<https://www.manitoba.ca/iem/geo/field/roa09pdfs/GS-8.pdf>> [September 2021].
- Zwanzig, H.V. and Wielezynski, P. 1975: Geology of the Kamuchawie Lake area; *in* Summary of Geological Fieldwork 1975, Manitoba Mines, Resources and Environmental Management, Mineral Resources Division, Geological Paper GP2/75, p. 12–15.
- Zwanzig, H.V., Böhm, C.O., Protrel, A. and Machado, N. 2003: Field relations, U-Pb zircon ages and Nd model ages of granitoid intrusions along the Thompson Nickel Belt–Kisseynew Domain boundary, Setting Lake area (NTS 63J15 and 63O2); *in* Report of Activities 2003, Manitoba Industry, Economic Development and Mines, Manitoba Geological Survey, p. 118–129, URL <<https://www.manitoba.ca/iem/geo/field/roa03pdfs/GS-16.pdf>> [September 2021].
- Zwanzig, H.V., Macek, J.J. and McGregor, C.R. 2007: Lithostratigraphy and geochemistry of the high-grade metasedimentary rocks in the Thompson nickel belt and adjacent Kisseynew domain, Manitoba: implications for nickel exploration; *Economic Geology*, v. 102, p. 1197–1216, URL <<https://doi.org/10.2113/gsecongeo.102.7.1197>>.
- Zwanzig, H.V., Murphy, L., Percival, J.A., Whalen, J.B. and Rayner, N. 2006: Thompson Nickel Belt-type units in the northeastern Kisseynew Domain, Manitoba (parts of NTS 63O); *in* Report of Activities 2006, Manitoba Science, Technology, Energy and Mines, Manitoba Geological Survey, p. 85–103, URL <<https://www.manitoba.ca/iem/geo/field/roa06pdfs/GS-09.pdf>> [September 2021].
- Zwanzig, H.V., Parker, J.S.D., Schledewitz, D.C.P. and Van Schmus, W.R. 1985: Lynn Lake regional compilation and geochronology; *in* Report of Field Activities 1985, Manitoba Energy and Mines, Geological Services/Mines Branch, p. 6–8, URL <<https://www.manitoba.ca/iem/geo/field/RFA1985.pdf>> [September 2021].
- Zwanzig, H.V., Syme, E.C. and Gilbert, H.P. 1999a: Updated trace element geochemistry of ca. 1.9 Ga metavolcanic rocks in the Paleoproterozoic Lynn Lake belt; Manitoba Industry, Trade and Mines, Geological Services, Open File Report OF99-13, 46 p., URL <<https://www.manitoba.ca/iem/info/libmin/OF99-13.zip>> [September 2021].
- Zwanzig, H.V., Syme E.C. and Gilbert, H.P. 1999b: Geochemical units in the Lynn Lake Belt with sample locations; Manitoba Industry, Trade and Mines, Geological Services, Open File Report OF99-13, Map OF99-13-1, scale 1:100 000, URL <<https://www.manitoba.ca/iem/info/libmin/OF99-13.zip>> [September 2021].
- Zwanzig, H.V., Percival, J.A., Murphy, L.A. and Growdon, M.L. 2019: Geology of the Wuskwatim–Threepoint lakes area, Manitoba (parts of NTS 63O10, 11); Manitoba Growth, Enterprise and Trade, Manitoba Geological Survey, Geoscientific Map MAP2019-5, scale 1:50 000, URL <<https://www.manitoba.ca/iem/info/libmin/MAP2019-5.pdf>> [September 2021].